Report Title

"Integrated Geologic-Engineering Model for Reef and Carbonate Shoal Reservoirs Associated with Paleohighs: Upper Jurassic Smackover Formation, Northeastern Gulf of Mexico"

Type of Report

Technical Progress Report for Year 3

Reporting Period Start Date

September 1, 2002

Reporting Period End Date

August 31, 2003

Principal Author

Ernest A. Mancini (205/348-4319)
Department of Geological Sciences
Box 870338
202 Bevill Building
University of Alabama
Tuscaloosa, AL 35487-0338

Date Report was Issued

September 25, 2003

DOE Award Number

DE-FC26-00BC15303

Name and Address of Participants

Ernest A. Mancini Dept. of Geological Sciences Box 870338 Tuscaloosa, AL 35487-0338	Bruce S. Hart Earth & Planetary Sciences McGill University 3450 University St. Montreal, Quebec H3A 2A7 CANADA	Thomas Blasingame Dept. of Petroleum Engineering Texas A&M University College Station, TX 77843-3116
Robert D. Schneeflock, Jr. Paramount Petroleum Co., Inc. 230 Christopher Cove Ridgeland, MS 39157	Richard K. Strahan Strago Petroleum Corporation 811 Dallas St., Suite 1407 Houston, TX 77002	Roger M. Chapman Longleaf Energy Group, Inc. 319 Belleville Ave. Brewton, AL 36427

Disclaimer

ABSTRACT

The University of Alabama in cooperation with Texas A&M University, McGill University, Longleaf Energy Group, Strago Petroleum Corporation, and Paramount Petroleum Company are undertaking an integrated, interdisciplinary geoscientific and engineering research project. The project is designed to characterize and model reservoir architecture, pore systems and rock-fluid interactions at the pore to field scale in Upper Jurassic Smackover reef and carbonate shoal reservoirs associated with varying degrees of relief on pre-Mesozoic basement paleohighs in the northeastern Gulf of Mexico. The project effort includes the prediction of fluid flow in carbonate reservoirs through reservoir simulation modeling that utilizes geologic reservoir characterization and modeling and the prediction of carbonate reservoir architecture, heterogeneity and quality through seismic imaging.

The primary objective of the project is to increase the profitability, producibility and efficiency of recovery of oil from existing and undiscovered Upper Jurassic fields characterized by reef and carbonate shoals associated with pre-Mesozoic basement paleohighs.

The principal research effort for Year 3 of the project has been reservoir characterization, 3-D modeling, testing of the geologic-engineering model, and technology transfer. This effort has included six tasks: 1) the study of seismic attributes, 2) petrophysical characterization, 3) data integration, 4) the building of the geologic-engineering model, 5) the testing of the geologic-engineering model and 6) technology transfer. This work was scheduled for completion in Year 3.

Progress on the project is as follows: geoscientific reservoir characterization is completed. The architecture, porosity types and heterogeneity of the reef and shoal reservoirs at Appleton and Vocation Fields have been characterized using geological and geophysical data. The study of

rock-fluid interactions has been completed. Observations regarding the diagenetic processes influencing pore system development and heterogeneity in these reef and shoal reservoirs have been made. Petrophysical and engineering property characterization has been completed. Porosity and permeability data at Appleton and Vocation Fields have been analyzed, and well performance analysis has been conducted. Data integration is up to date, in that, the geological, geophysical, petrophysical and engineering data collected to date for Appleton and Vocation Fields have been compiled into a fieldwide digital database. 3-D geologic modeling of the structures and reservoirs at Appleton and Vocation Fields has been completed. The models represent an integration of geological, petrophysical and seismic data. 3-D reservoir simulation of the reservoirs at Appleton and Vocation Fields has been completed. The 3-D geologic models served as the framework for the simulations. The geologic-engineering models of the Appleton and Vocation Field reservoirs have been developed. These models are being tested. The geophysical interpretation for the paleotopographic feature being tested has been made, and the study of the data resulting from drilling of a well on this paleohigh is in progress. Numerous presentations on reservoir characterization and modeling at Appleton and Vocation Fields have been made at professional meetings and conferences and a short course on microbial reservoir characterization and modeling based on these fields has been prepared.

Table of Contents

INTRODUCTION

The University of Alabama in cooperation with Texas A&M University, McGill University, Longleaf Energy Group, Strago Petroleum Corporation, and Paramount Petroleum Company is undertaking an integrated, interdisciplinary geoscientific and engineering research project. The project is designed to characterize and model reservoir architecture, pore systems and rock-fluid interactions at the pore to field scale in Upper Jurassic Smackover reef and carbonate shoal reservoirs associated with varying degrees of relief on pre-Mesozoic basement paleohighs in the northeastern Gulf of Mexico. The project effort includes the prediction of fluid flow in carbonate reservoirs through reservoir simulation modeling that utilizes geologic reservoir characterization and modeling and the prediction of carbonate reservoir architecture, heterogeneity and quality through seismic imaging.

The Upper Jurassic Smackover Formation is one of the most productive hydrocarbon reservoirs in the northeastern Gulf of Mexico. Production from Smackover carbonates totals 1 billion barrels of oil and 4 trillion cubic feet of natural gas. The production is from three plays: 1) basement ridge play, 2) regional peripheral fault play, and 3) salt anticline play. Unfortunately, much of the oil in the Smackover fields in these plays remains unrecovered because of a poor understanding of the rock and fluid characteristics that affects the understanding of reservoir architecture, heterogeneity, quality, fluid flow and producibility. This scenario is compounded because of inadequate techniques for reservoir detection and the characterization of rock-fluid interactions, as well as imperfect models for fluid flow prediction. This poor understanding is particularly illustrated for the case with Smackover fields in the basement ridge play where independent producers dominate the development and management of these fields. These producers do not have the financial resources and/or staff expertise to

substantially improve the understanding of the geoscientific and engineering factors affecting the producibility of Smackover carbonate reservoirs, which makes research and application of new technologies for reef-shoal reservoirs all that more important and urgent. The research results from studying the fields identified for this project will be of direct benefit to these producers.

This interdisciplinary project is a 3-year effort to characterize, model and simulate fluid flow in carbonate reservoirs and consists of 3 phases and 11 tasks. Phase 1 (1 year) of the project involves geoscientific reservoir characterization, rock-fluid interactions, petrophysical and engineering property characterization, and data integration. Phase 2 (1.5 years) includes geologic modeling and reservoir simulation. Phase 3 (0.5 year) involves building the geologic-engineering model, testing the geologic-engineering model, and applying the geologic-engineering model.

The principal goal of this project is to assist independent producers in increasing oil producibility from reef and shoal reservoirs associated with pre-Mesozoic paleotopographic features through an interdisciplinary geoscientific and engineering characterization and modeling of carbonate reservoir architecture, heterogeneity, quality and fluid flow from the pore to field scale.

The objectives of the project are as follows:

1. Evaluate the geological, geophysical, petrophysical and engineering properties of reef-shoal reservoirs and their associated fluids, in particular, the Appleton and Vocation Fields.
2. Construct a digital database of integrated geoscience and engineering data taken from reef-shoal carbonate reservoirs associated with basement paleohighs.
3. Develop a geologic-engineering model(s) for improving reservoir detection, reservoir characterization, flowspace imaging, flow simulation, and performance prediction for

reef-shoal carbonate reservoirs based on a systematic study of Appleton and Vocation Fields.

4. Validate and apply the geologic-engineering model(s) on a prospective Smackover reservoir through an iterative interdisciplinary approach, where adjustments of properties and concepts will be made to improve the model(s).

This project has direct and significant economic benefits because the Smackover is a prolific hydrocarbon reservoir in the northeastern Gulf of Mexico. Smackover reefs represent an underdeveloped reservoir, and the basement ridge play in which these reefs are associated represents an underexplored play, Initial estimations indicate the original oil resource target available in this play from the 40 fields that have been discovered and developed approximates at least 160 million barrels. Any newly discovered fields are expected to have an average of 4 million barrels of oil. The combined estimated reserves of the Smackover fields (Appleton and Vocation Fields) proposed for study in this project total 9 million barrels of oil. Successful completion of the project should lead to increased oil producibility from Appleton and Vocation Fields and from Smackover reservoirs in general. Production of these domestic resources will serve to reduce U.S. dependence on foreign oil supplies.

Completion of the project will contribute significantly to the understanding of: the geologic factors controlling reef and shoal development on paleohighs, carbonate reservoir architecture and heterogeneity at the pore to field scale, generalized rock-fluid interactions and alterations in carbonate reservoirs, the geological and geophysical attributes important to geologic modeling of reef-shoal carbonate reservoirs, the critical factors affecting fluid flow in carbonate reservoirs, particularly with regard to reservoir simulation and the analysis of well performance, the elements important to the development of a carbonate geologic-engineering model, and the

geological, geophysical, and/or petrophysical properties important to improved carbonate reservoir detection, characterization, imaging and flow prediction.

EXECUTIVE SUMMARY

The University of Alabama in cooperation with Texas A&M University, McGill University, Longleaf Energy Group, Strago Petroleum Corporation, and Paramount Petroleum Company are undertaking an integrated, interdisciplinary geoscientific and engineering research project. The project is designed to characterize and model reservoir architecture, pore systems and rock-fluid interactions at the pore to field scale in Upper Jurassic Smackover reef and carbonate shoal reservoirs associated with varying degrees of relief on pre-Mesozoic basement paleohighs in the northeastern Gulf of Mexico. The project effort includes the prediction of fluid flow in carbonate reservoirs through reservoir simulation modeling which utilizes geologic reservoir characterization and modeling and the prediction of carbonate reservoir architecture, heterogeneity and quality through seismic imaging.

The primary objective of the project is to increase the profitability, producibility and efficiency of recovery of oil from existing and undiscovered Upper Jurassic fields characterized by reef and carbonate shoals associated with pre-Mesozoic basement paleohighs.

The principal research effort for Year 3 of the project has been reservoir characterization, 3-D modeling, testing of the geologic-engineering model, and technology transfer. This effort has included six tasks: 1) study of seismic attributes, 2) petrophysical characterization, 3) data integration, 4) building the geologic-engineering model, 5) the testing of the geologic-engineering model, and 6) technology transfer.

Progress on the project is as follows: Geoscientific reservoir characterization is completed. The architecture, porosity types and heterogeneity of the reef and shoal reservoirs at Appleton

and Vocation Fields have been characterized using geological and geophysical data. All available whole cores have been described and thin sections from these cores have been studied. Depositional facies were determined from the core descriptions and well logs. The thin sections studied represent the depositional facies identified. The core data and well log signatures have been integrated and calibrated on graphic logs. The well log and seismic data have been tied through the generation of synthetic seismograms. The well log, core, and seismic data have been entered into a digital database. Structural maps on top of the basement, reef, and Smackover/Buckner have been constructed. An isopach map of the Smackover interval has been prepared, and thickness maps of the Smackover facies have been prepared. Cross sections have been constructed to illustrate facies changes across these fields. Maps have been prepared using the 3-D seismic data that Longleaf and Strago contributed to the project to illustrate the structural configuration of the basement surface, the reef surface, and Buckner/Smackover surface. Seismic forward modeling and attribute-based characterization has been completed for Appleton and Vocation Fields. Petrographic analysis has been completed and a paragenetic sequence for the Smackover in these fields has been prepared.

The study of rock-fluid interactions is completed. Thin sections (379) have been studied from 11 cores from Appleton Field to determine the impact of cementation, compaction, dolomitization, dissolution and neomorphism has had on the reef and shoal reservoirs in this field. Thin sections (237) have been studied from 11 cores from Vocation Field to determine the paragenetic sequence for the reservoir lithologies in this field. An additional 73 thin sections have been prepared and studied for the shoal and reef lithofacies in Vocation Field to identify the diagenetic processes that played a significant role in the development of the pore systems in the reservoirs at Vocation Field. The petrographic analysis and pore system studies have been

completed. A paragenetic sequence for the Smackover carbonates at Appleton and Vocation Fields has been prepared.

Petrophysical and engineering property characterization is completed. Petrophysical and engineering property data have been gathered and tabulated for Appleton and Vocation Fields. These data include oil, gas and water production, fluid property (PVT) analyses and porosity and permeability information. Porosity and permeability characteristics of Smackover facies have been analyzed for each well using porosity histograms, permeability histograms and porosity versus depth plots. Log porosity versus core porosity and porosity versus permeability cross plots for wells in the fields have been prepared.

Well performance studies through type curve and decline curve analyses have been completed for the wells in Appleton and Vocation Fields, and the original oil in place and recoverable oil remaining for the fields has been calculated.

3-D geologic modeling of the structure and reservoirs at Appleton and Vocation Fields has been completed. The models represent an integration of geological, petrophysical and seismic data.

3-D reservoir simulations of the reservoirs at Appleton and Vocation Fields have been completed. The 3-D geologic models served as framework for these simulations.

Data integration is up to date, in that, geological, geophysical, petrophysical and engineering data collected to date for Appleton and Vocation Fields have been compiled into a fieldwide digital database for development of the geologic-engineering model for the reef and carbonate shoal reservoirs for each of these fields.

The geologic-engineering models of the Appleton and Vocation Field reservoirs have been developed. These models are being tested. The geophysical interpretation for the

paleotopographic feature being tested has been made, and the study of the data resulting from the drilling of a well on this paleohigh is in progress.

Numerous presentations on reservoir characterization and modeling at Appleton and Vocation Fields have been made at professional meetings and conferences and a short course on microbial reservoir characterization and modeling based on these fields has been prepared.

EXPERIMENTAL

The principal research effort for Year 3 of the project has been 1) reservoir characterization, including the study of seismic attributes and petrophysical characterization, 2) 3-D modeling, including the building of the geologic-engineering model, 3) testing of the geologic-engineering model and 4) technology transfer (Table 1).

Table 1. Milestone Chart.

Tasks	Project Year/Quarter									
	2000		2001				2002			2003
	3 4	1 2	3 4	1 2	3 4	1 2	3 4	1 2		
Reservoir Characterization (Phase 1)										
Task 1—Geoscientific Reservoir Characterization	xxxxxx	xxx								
Task 2—Rock-Fluid Interactions	xxxxxx	xxx								
Task 3—Petrophysical Engineering Characterization	xxxxxx	xxx								
Task 4—Data Integration		xxx								
3-D Modeling (Phase 2)										
Task 5—3-D Geologic Model			xxxxxx							
Task 6—3-D Reservoir Simulation Model					xxxxxx					
Task 7—Geologic-Engineering Model							xxxxxx			
Testing and Applying Model (Phase 3)										
Task 8—Testing Geologic-Engineering Model										xxxxxx
Task 9—Applying Geologic-Engineering Model										xxxxxx
Technological Transfer										
Task 10—Workshops					xx					xx
Technical Reports										
Task 11—Quarterly, Topical and Annual Reports	x	x x	x x		x x		x x		x x	

xxxxx—Work Planned

Work Accomplished in Year 3

Task 1—Reservoir Characterization (Seismic Attributes).--3-D seismic-based analyses of the Smackover Formation at Appleton and Vocation Fields has been done by Tebo and Hart

of McGill University. The work on Appleton Field described below is from Tebo's thesis at McGill University and a paper submitted in May 2003 for publication in the Journal of Sedimentary Research by Tebo and Hart. Results of the study of the Vocation Field are also included. The objective has been to integrate well logs and attributes derived from seismic data to generate porosity volumes that predict the 3-dimensional distribution of that property for the Smackover Formation in and around Appleton and Vocation Fields.

Introduction

One of a sedimentary geologist's primary roles is to predict the occurrence and distribution of subsurface physical properties. These predictions might be needed for applied (e.g., exploiting aquifers or hydrocarbon reservoirs), or for fundamental purposes (e.g., developing depositional models). The data used may include core, wireline logs, outcrop analogs, seismic data, etc. Several approaches have been developed and applied but each has limitations.

Facies models and sequence stratigraphic concepts are commonly used to guide subsurface mapping work that is based on analysis of wireline logs, core and/or seismic data. In both cases however ambiguities or limitations often remain about: a) the exact 3-D geometries of the lithofacies of interest, especially when data are sparse, b) relationships between depositional facies and physical properties of interest (e.g., is porosity distribution more a function of depositional environment or diagenesis, and c) the three-dimensional distribution of properties of interest (results are often presented as 2-D maps or cross-sections). As a result, the products of facies modeling or sequence stratigraphic analyses may not be adequate or suitable for use by others (e.g., petroleum engineers, hydrogeologists) who require robust quantitative predictions of the 3-D distribution of subsurface physical properties.

Geostatistical methods help to overcome some of these limitations. The application of geostatistics in sedimentary geology serves a dual purpose: 1) to construct realistic 2-D or 3-D geologic models that closely depict the heterogeneity of physical property distribution, and 2) to predict and quantify the uncertainty in the physical property prediction (Dubrule 1998). The usefulness of this method for defining the spatial distribution of physical properties is dependent on several factors, both geologic and statistical, which may influence the outcome of the prediction (Dubrule 1998; Hirsche *et al.* 1998).

Seismic attribute studies represent a relatively new approach that has been developed and applied in the oil industry. This approach seeks to find empirical correlations between seismic attributes and log-derived physical properties (e.g., porosity, lithology, bed thickness) through methods such as multivariate linear regression (MLR) and artificial or probabilistic neural networks (ANN/PNN; Schultz *et al.* 1994 a & b; Russell *et al.* 1997; Hampson *et al.* 2001). Seismic attributes are derivatives or mathematical transforms of a basic seismic measurement and include amplitude, frequency, phase and other measures (Taner *et al.* 1979; Brown 1996; Chen and Sidney 1997). Some of these correlations have an obvious rock physics basis (e.g., tuning effects or changes in acoustic impedance; Robertson and Nogami 1984; Brown 1996), whereas the physical basis for other relationships is more poorly understood. Accordingly, some authors have advocated statistical approaches to correlate seismic attributes with physical properties measured by logs (Schultz *et al.* 1994a; Hampson *et al.* 2001). Criticisms of purely statistical approaches were offered by Hart (1999, 2002), and Mukerji *et al.* (2001) amongst others.

There are two main types of seismic attribute studies. Horizon or interval-based methods use attributes that are extracted or averaged along or between interpreted seismic horizons. These

attributes are then correlated to log-derived properties (e.g., average porosity, net thickness) to produce a map (e.g., Schultz *et al.* 1994a). Volume-based studies look for correlations between attributes and log properties on a sample-by-sample basis over a window that is defined by two seismic horizons (Hampson *et al.* 2001). This type of study produces a physical property volume, and thus better defines changes in physical properties and their corresponding geometries in 3-D space. The latter method is particularly useful for property prediction in thick and complex stratigraphic sequences where lateral and vertical facies changes are frequent.

In this paper, we use a case study to illustrate the use of volume-based 3-D seismic attributes studies to directly image rock physical properties (porosity) in Jurassic carbonate buildups of the Smackover Formation in southwestern Alabama (Fig. 1and 2). We compare and contrast our results with those of produced by conventional geologic analysis (Mancini *et al.* 1999) and a horizon-based attribute study (Hart and Balch 2000). We show that volume-based attribute studies can provide robust, quantitative predictions of the 3-D distribution of subsurface physical properties, and furthermore, that these results may be used to gain insights into fundamental processes of interest to sedimentary geologists.

Geological Overview of Appleton Field

Aspects of the tectonic and depositional history of the study area were summarized by Mancini (2002; Fig. 2). “Basement” in this area consists of deformed metamorphic and igneous rocks of the Appalachian chain. Siliciclastic sediments of the Norphlet Formation were deposited in topographically low areas during the Mid- to Late Jurassic. Late Jurassic (Oxfordian) transgression led to the deposition of Smackover carbonates, first in paleotopographic lows

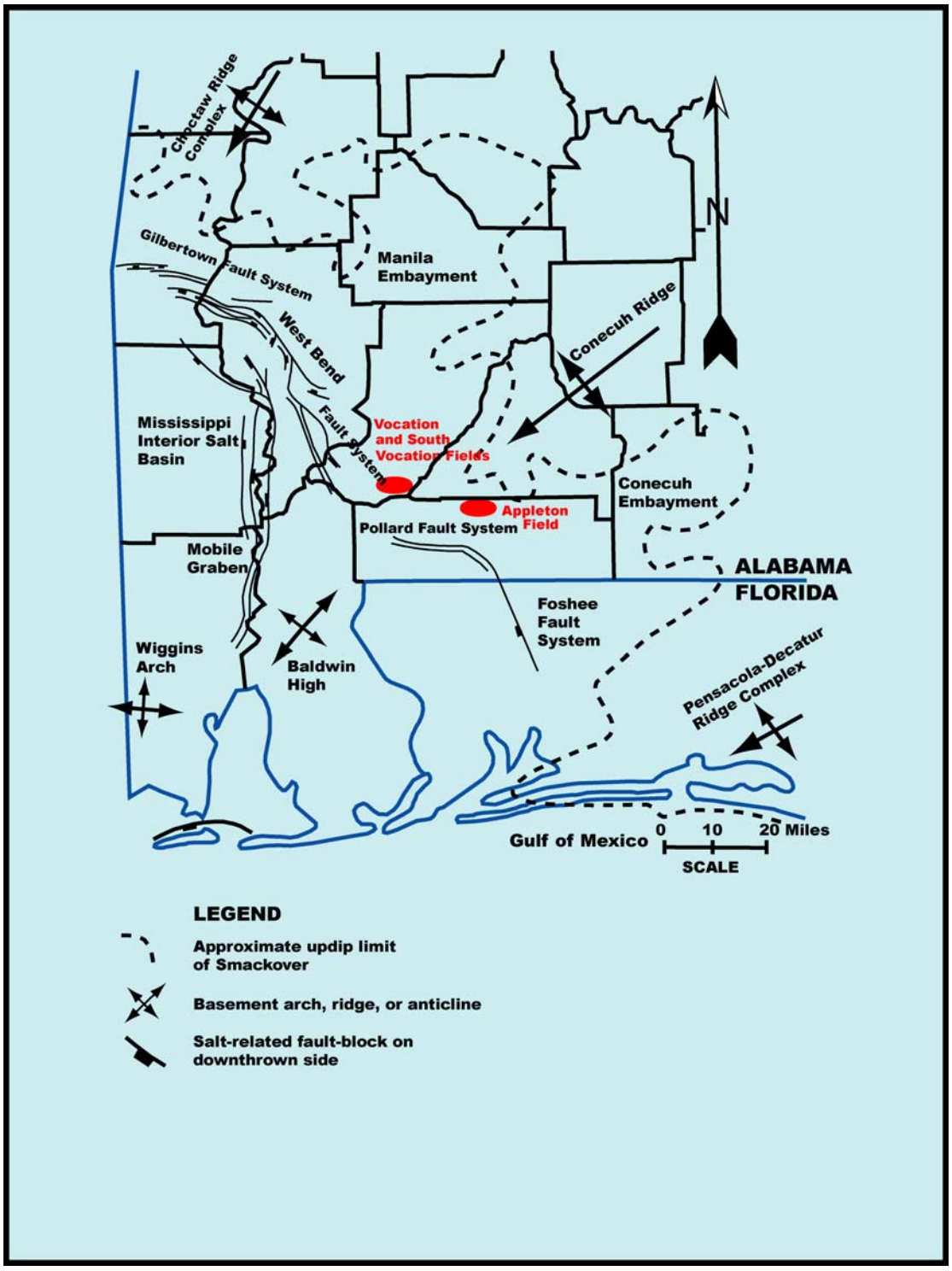

Figure 1: Location map of study area showing existing structural controls at time of Smackover deposition. Adapted from Mancini (2002).

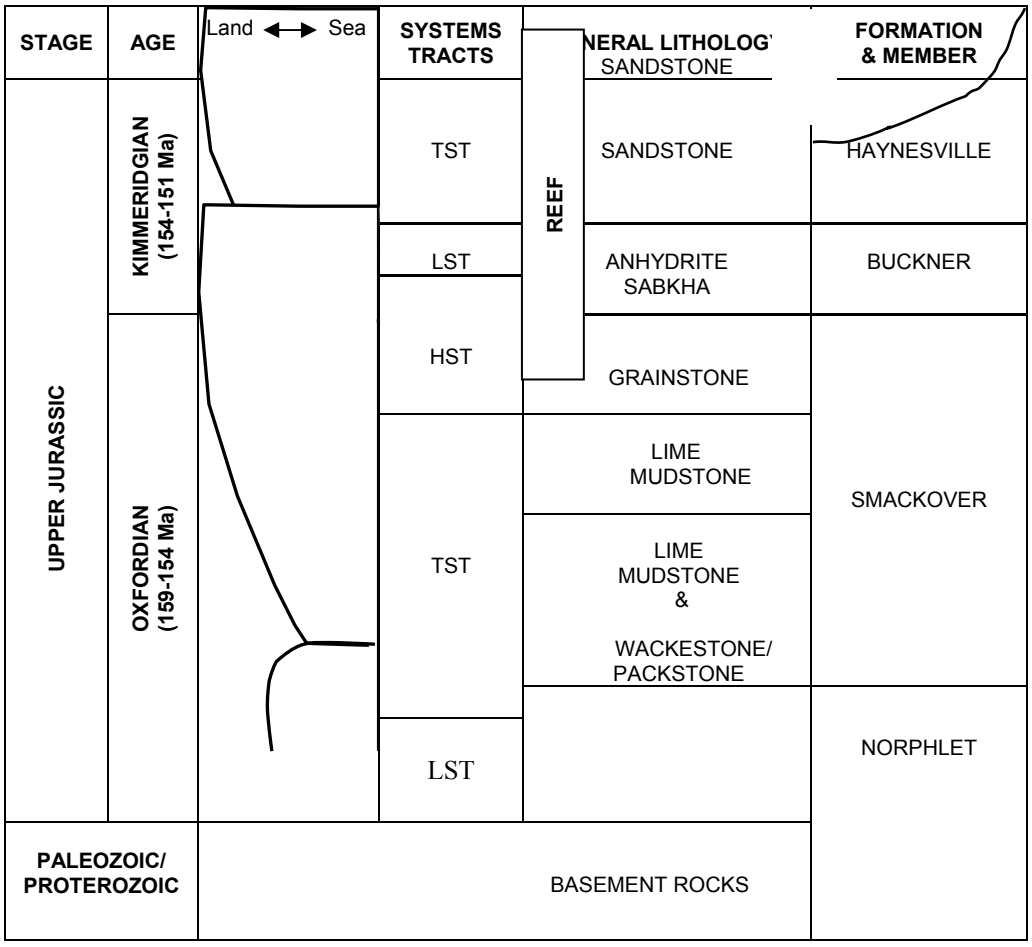

Figure 2: Lithostratigraphic and sequence stratigraphic interpretation for Appleton Field, SW Alabama. Adapted from Parcell (2000).

(Lower Smackover) but eventually over paleotopographic highs as well (Middle Smackover Member). Together the Lower (which is absent at Appleton Field) and Middle Smackover members form the transgressive systems tract (Mancini *et al.* 1990). Microbial patch reefs of the Middle Smackover formed on paleotopographic highs. They consist of boundstone (bafflestone in the deeper water reef front, and bindstone on the shallower reef crest). These facies constitute the best reservoirs at Appleton Field (Benson *et al.* 1996, 1997; Mancini *et al.* 2000). Off-structure, reef deposits grade into peloidal packstone and wackestone typical of deeper water, low energy sub-tidal environments.

Slowing of sea level rise allowed the Smackover reefs to grow to sea level, accrete laterally and prograde seawards, changing the system from one dominated by aggradation to one of progradation. Subsequent fall in sea level led to increased energy levels, limited growth and eventually exposure and subsequent death of reef organisms. Characteristic on-structure facies include high-energy ooid grainstones, that are flanked seaward by sub-wave base peloidal wackestone or packstone facies, and landward by lagoonal peloid packstone, where they occur in deeper water, and by peloid/oncoidal packstone where they occur in shallow water (Saller and Moore 1986; Benson *et al.* 1996). Sea level was relatively stable during this time (Late Oxfordian), with short-term fluctuations producing shallowing upward parasequences (Benson *et al.* 1997).

The Buckner Anhydrite Member of the Haynesville Formation caps the Smackover sediments and is interpreted as being deposited in a salina or sabkha environment (Benson *et al.* 1997). The Upper Smackover unit and Buckner anhydrite member of the Haynesville Formation together characterize the late highstand to early lowstand system tract (Fig. 2, Mancini *et al.* 1990). Transgression led to siliciclastic deposition of the overlying Haynesville Formation.

Database

The primary database consisted of 11 wells with logs and a 3-D seismic volume. We used six of these wells with sonic logs for the attribute study. These logs were used to generate synthetic seismograms that were then employed to tie log and seismic data. Seismic data consisted of an approximately 5 x 3.5 km grid of post-stack time-migrated 3-D volume (Fig. 3), with a 4 ms sample rate, a bin spacing of 165 x 165 ft (~50 x 50 m), and a 4 second two-way travel time (TWT) trace length. Supplementary data in the form of production data and core analyses (Parcell 2000; Mancini 2002) were also used to help guide the interpretations.

Methodology

We established a stratigraphic framework for the study through log analysis and construction of log cross-sections (Fig. 4). The geology was then tied to the seismic data by generating synthetic seismograms and 2-D seismic models (cf Tebo 2003; Fig. 5). The well-tying procedure was critical in the analysis because it ensured that both data types were imaging and comparing the same stratigraphic interval. These stratigraphic picks were then mapped in the 3-D seismic volume, and the seismic horizons so defined were used for geologic interpretation and to constrain the attribute analysis.

We used a volume-based seismic attribute study as described by Russell *et al.* (1997) and Hampson *et al.* (2001) due to the thickness (80-230ft/24-70m) and expected stratigraphic complexity of this interval. We sought to predict porosity, as measured by the density porosity log, because of its direct relation to depositional facies at the Appleton Field (Benson 1988; Benson *et al.* 1996) and because it is an important variable controlling hydrocarbon production. The window of analysis was defined by the top and base of the Smackover Formation. The choice of which attribute(s) to generate and use was determined by the capabilities of the

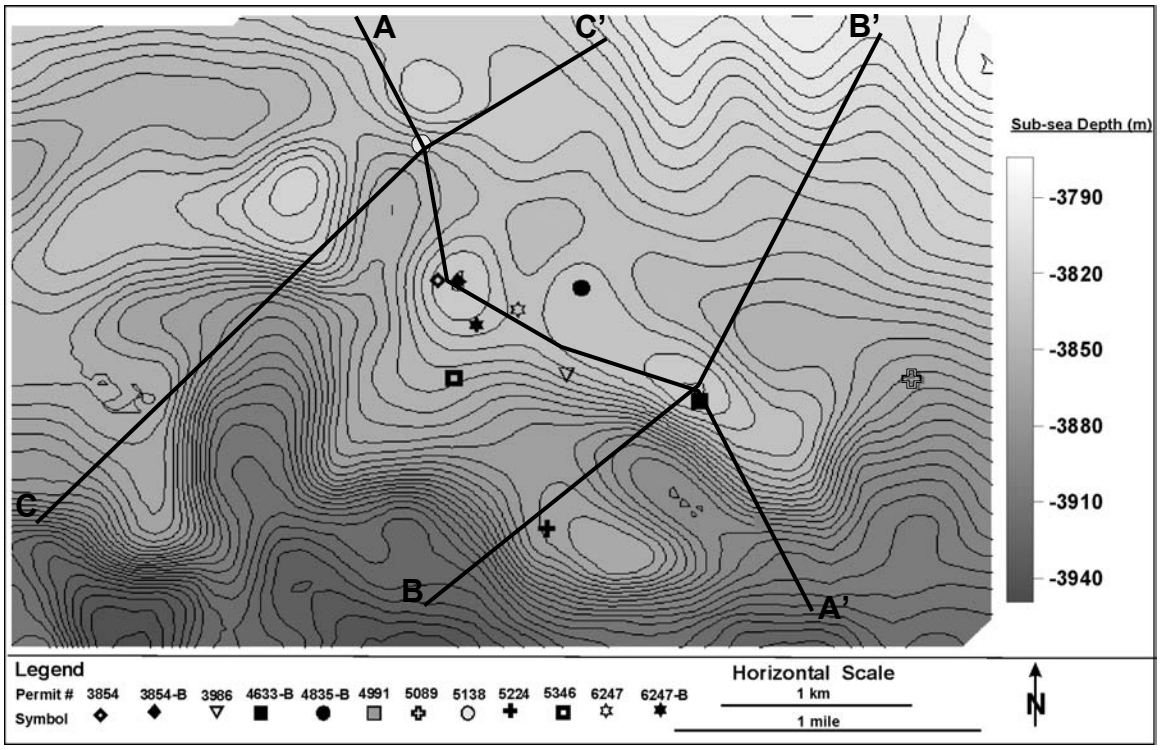

Figure 3: Seismic grid showing the aerial coverage of current survey area and well locations. Transects A-A', B-B', C-C' are shown in Figures 7, 11, 12 & 14.

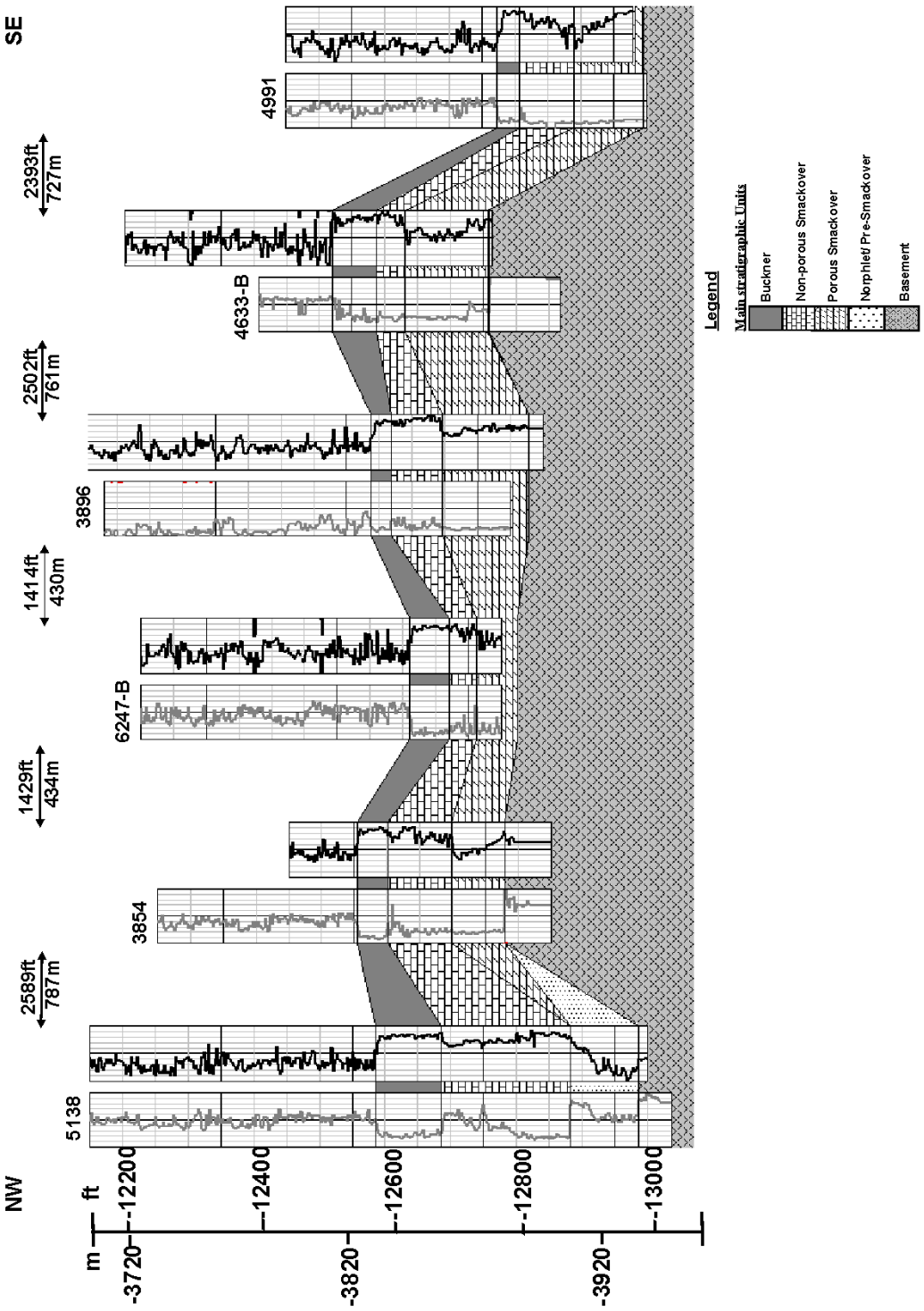

Figure 4: NW-SE well-to-well cross-section showing major stratigraphic units and their relationships. Cross-section was obtained along strike of paleohighs (A-A' transect of Fig. 3). Note that the eastern paleohigh at well 4633-B is structurally higher than that in the west beneath well 3854. Grey curve = gamma ray, black curve = sonic.

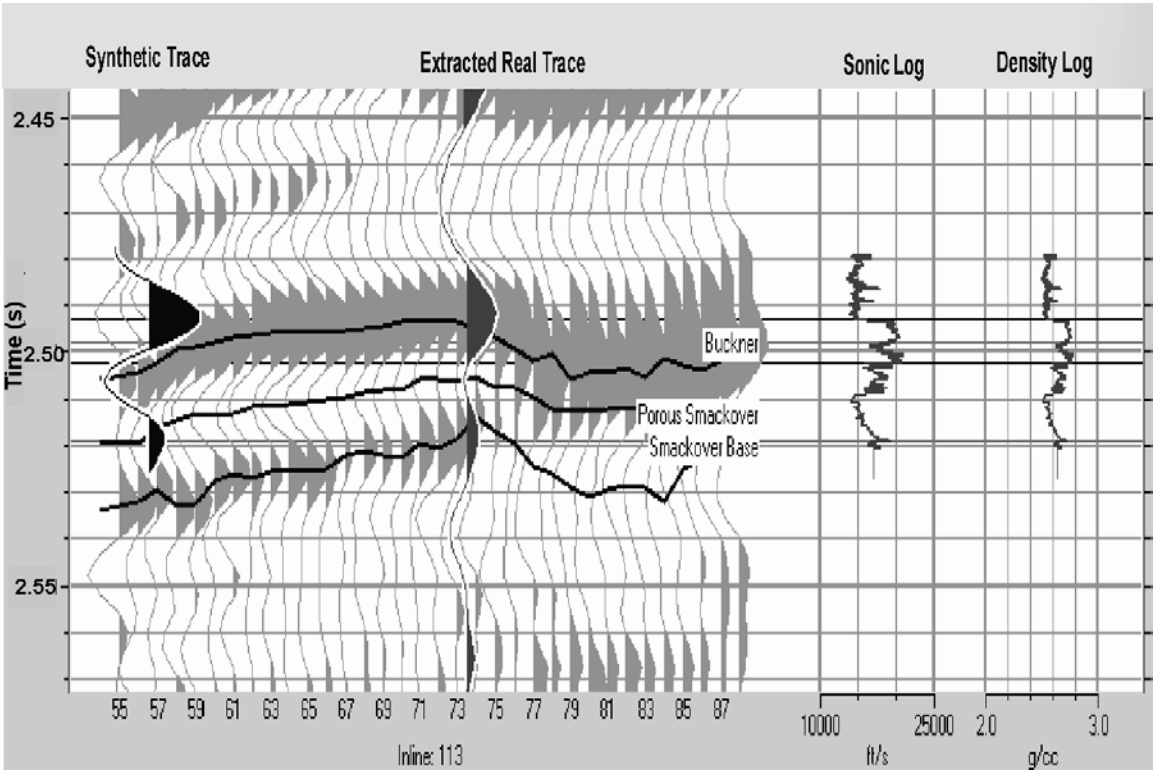

Figure 5: Example of synthetic seismogram (well 4633-B) used for tying well data to seismic. Black curve = log synthetic, grey = seismic trace extracted along wellbore at well location.

software, which offered 18 attributes that were extracted over the analysis window. Although not considered a "true" attribute by some authors (Schultz *et al.* 1994a), we also included inversion results (acoustic impedance derived from seismic data) as an attribute.

We sought to predict porosity in 3-dimensions. This was done by obtaining a statistical relationship between the best set of predicting attributes and porosity using a probabilistic neural network (PNN). The relationship has the form:

$$P_{PNN}(z) = \frac{[P_1 e^{(-d^2_1/\sigma^2)} + P_2 e^{(-d^2_2/\sigma^2)} + P_3 e^{(-d^2_3/\sigma^2)}]}{[e^{(-d^2_1/\sigma^2)} + e^{(-d^2_2/\sigma^2)} + e^{(-d^2_3/\sigma^2)}]} \quad (1)$$

where: P_{PNN} = predicted porosity at each sample using probabilistic neural network, $P_{1\text{-}3}$ = actual porosity value, d^2_1 = distance between input point and the training data $[(X_1 - X_0)^2 + (Y_i - Y_0)^2]$ as measured in the multidimensional space spanned by the attributes, and σ is a scalar.

Application of this relationship led to the generation of a porosity volume from the seismic data volume. In essence, the method replaces each seismic trace within the analysis window by a porosity curve. This result is different to that obtained from a horizon-based attribute analysis, whereby an average porosity value might be produced at each trace location to generate a map (e.g., Hart and Balch 2000).

We derived and evaluated the porosity volume using quantitative and qualitative methods described by Hampson *et al.* (2001) and Hart (1999, 2002). In particular, and as described fully below, we examined the statistical significance of the results, their geologic plausibility, and the physical basis for relationships between attributes and porosity.

Results And Interpretation

Based on velocity and density contrasts, Hart and Balch (2000) defined the following six units at Appleton Field: a) metamorphic and igneous rocks of "Basement", b) siliciclastics of the Norphlet Formation, c) lower, porous dolomites of the Smackover that are restricted to the flanks and crests of basement structures (broadly corresponding to the Middle Smackover), d) generally non-porous Smackover dolomites that overlie the porous zone on-structure but form the entire thickness of the Smackover off-structure (Upper Smackover on-structure, Middle and Upper Smackover off-structure), e) Buckner Anhydrite, and f) siliciclastics of the Haynesville Formation (Fig. 6).

Seismically, the top of the Buckner and top of the Smackover are imaged as a single high amplitude peak (Fig. 7). This is because of both the relative thinness of the Buckner Anhydrite and low acoustic impedance contrast between these two units. The top of the porous Smackover is imaged as a trough that is only locally developed. The base of the Smackover Formation changes character from a peak, where relatively low acoustic impedance porous dolomites overlies basement, to a trough, where relatively high acoustic impedance tight dolomites overlie siliciclastics of the Norphlet Formation, within the study area.

Mapping indicates that five main structural culminations occur in and around the Appleton Field, with four of these (Figs. 3 and 8) being present during Smackover deposition. Their NW-SE orientation is parallel to structural paleostrike and perpendicular to the direction of transgression. The Porous Smackover is thickest on the southward flanks and thinner on the crests of paleohighs (Fig. 4). We attribute this pattern to greater accommodation space and increasing water depth resulting from rising sea levels during Smackover deposition. The

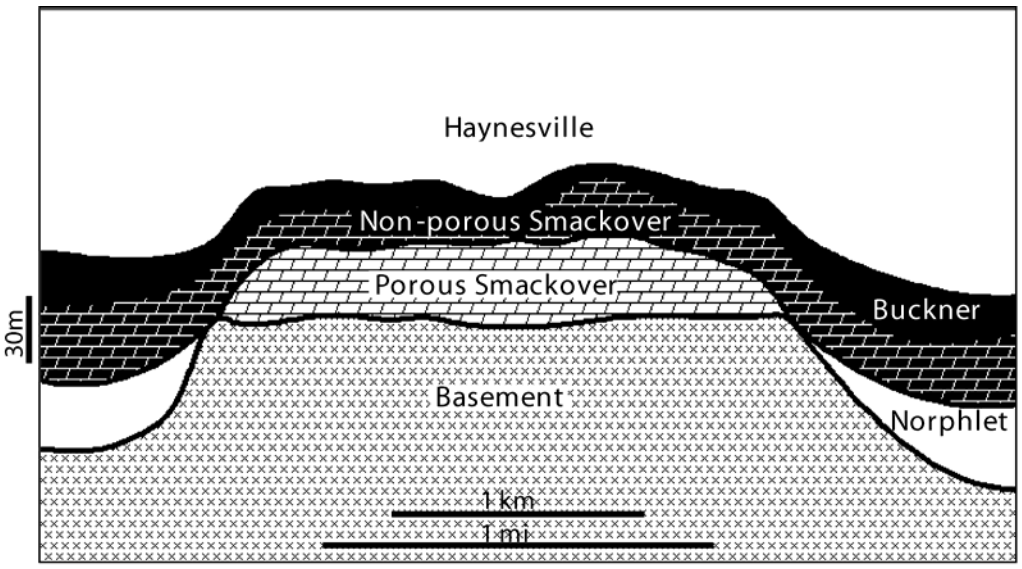

Figure 6: Geologic model depicting the relationship of the main stratigraphic units at Appleton Field (from Hart and Balch, 2000).

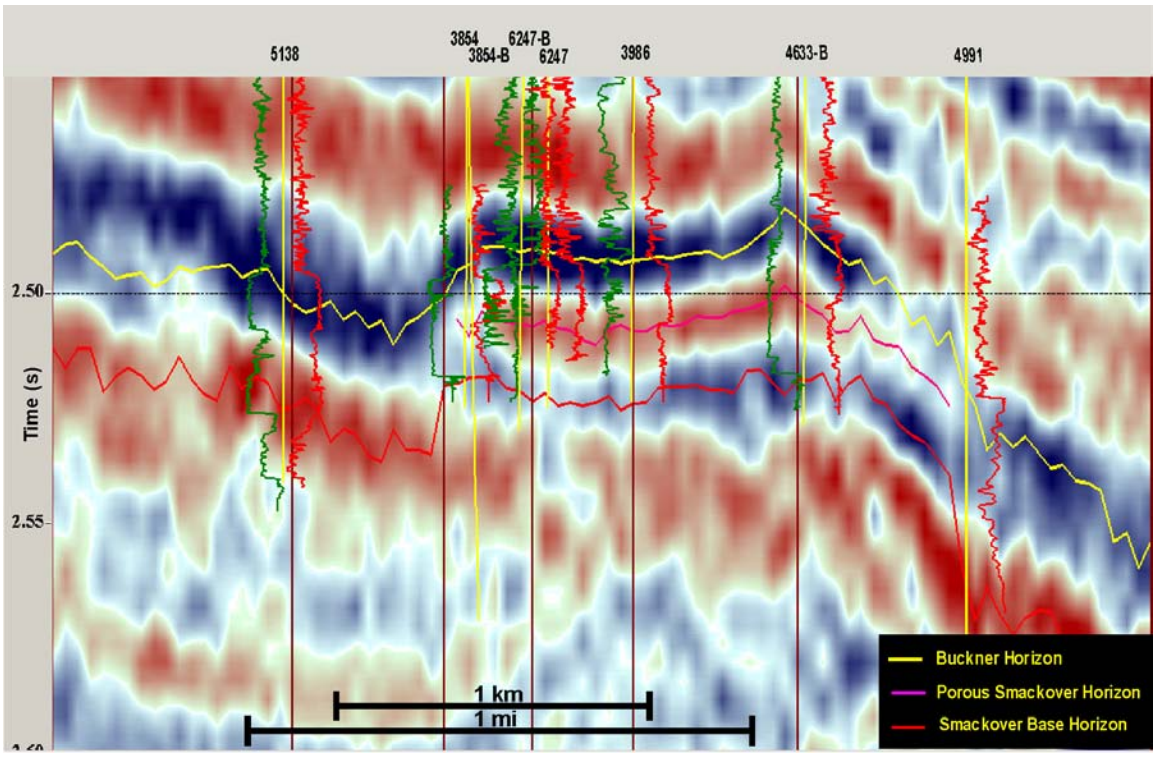
5138
3854
3854-B
6247-B
6247
3986
4633-B
4991
2.50
Time (s)
2.55
1 km
1 mi
Buckner Horizon
Porous Smackover Horizon
Smackover Base Horizon

(a)

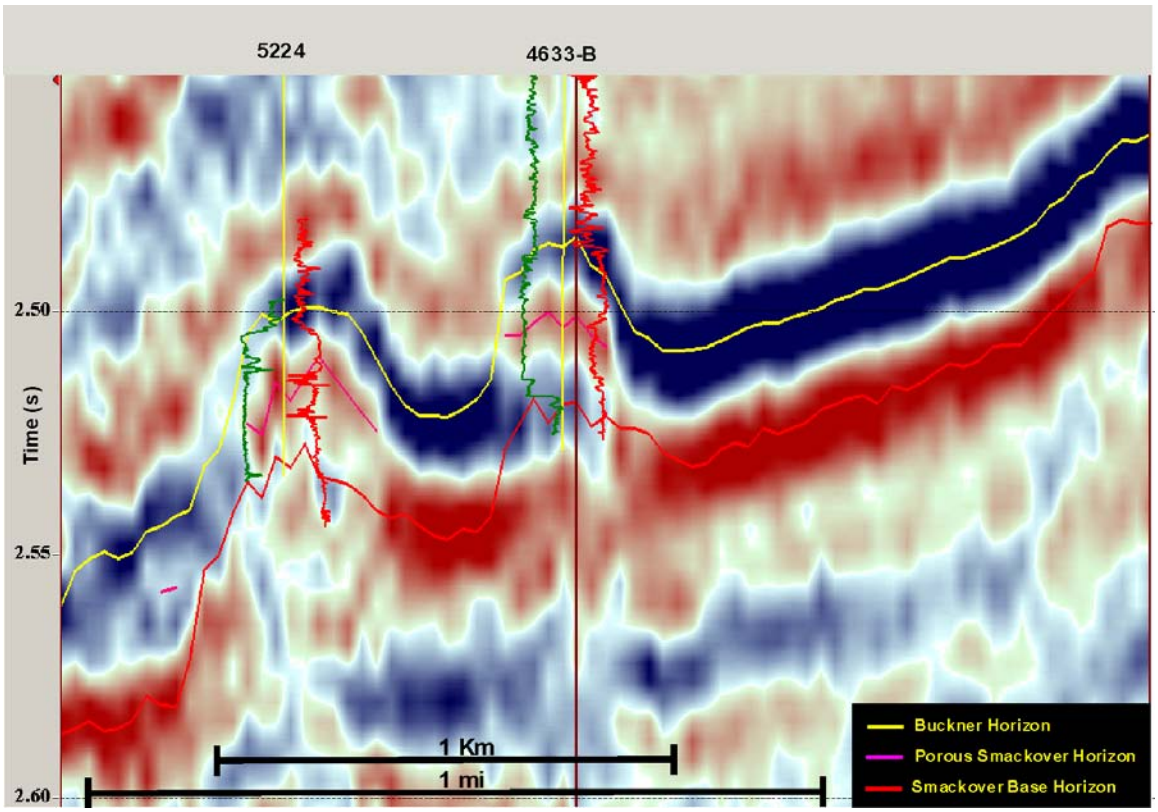
5224
4633-B
2.50
Time (s)
2.55
2.60
1 Km
1 mi
Buckner Horizon
Porous Smackover Horizon
Smackover Base Horizon

(b)

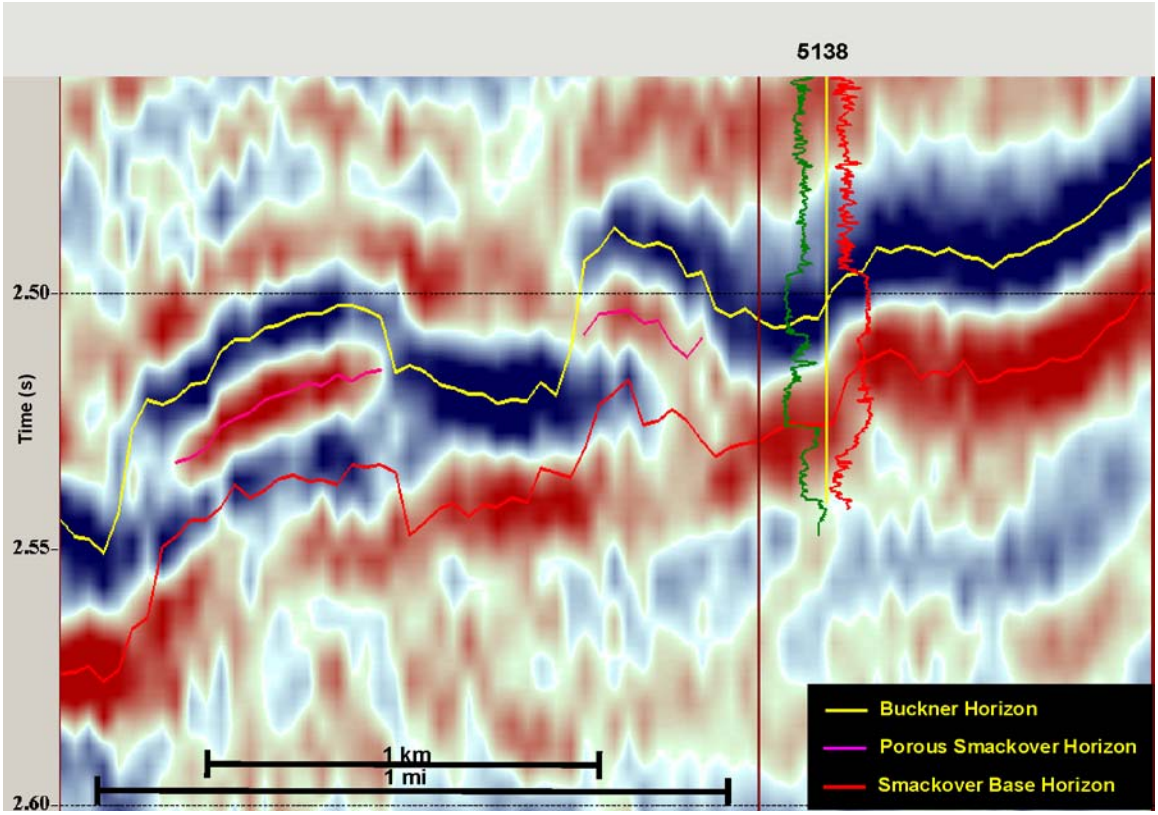

(c)

Figure 7: Transects showing seismic data across Appleton Field; note location of the porous Smackover on paleostructure. (a) NW-SE transect parallel to strike (A-A' in Fig. 3), and shows horizon picks ans seismic character of the mapped formations (red = trough, blue = peak); (b) & (c) dip sections (B-B', C-C' in Fig. 3) across Appleton Field.

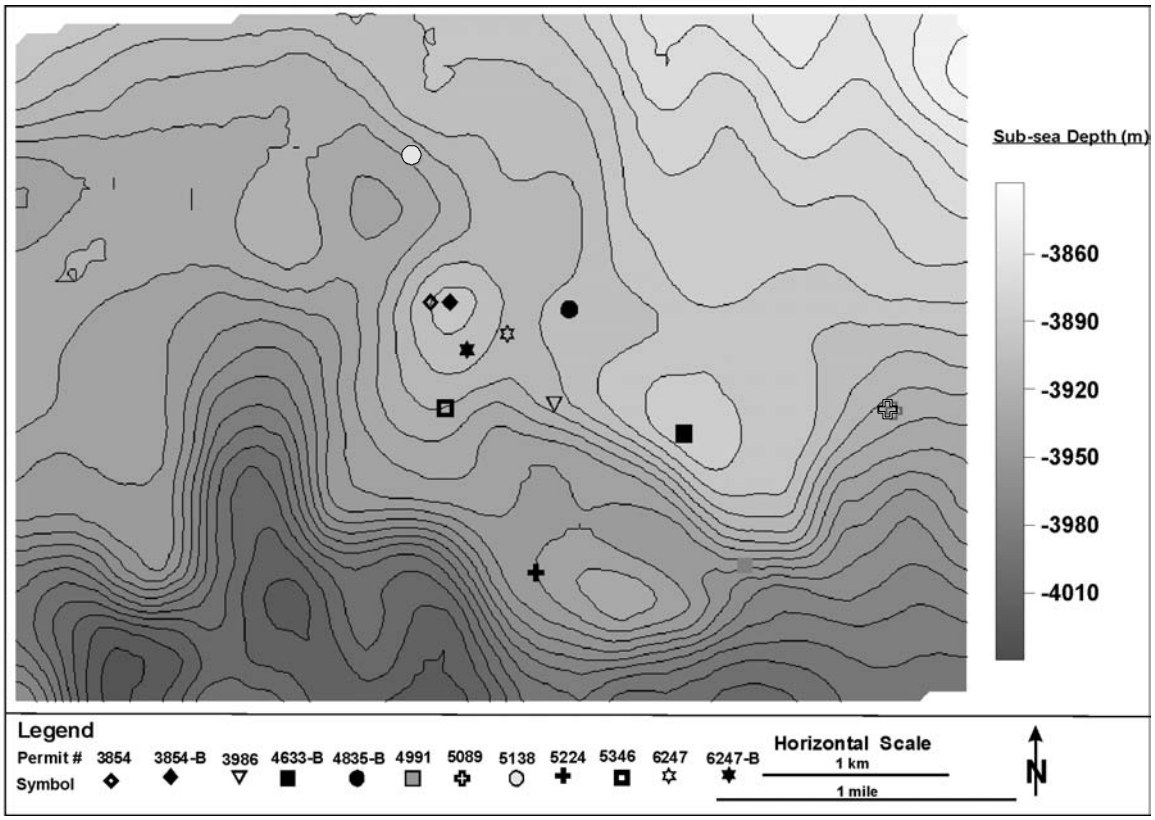

Figure 8: Structure map (depth sub-sea) of the base of the Smackover Formation. This shows main pre-existing structural culminations that controlled facies deposition, three at the Appleton Field in the east, and one to the NW. The structural high to the SW had no closure prior to Smackover deposition.

combination of paleostructure, steep seaward slope and eustatic sea level rise provided optimal conditions (e.g., temperature, salinity, substrate, etc.) for reef growth.

Step-wise linear regression and validation testing (Hampson *et al.* 2001) indicated that four of the nineteen attributes represent the optimum combination of attributes required to predict porosity (Fig. 9). These four attributes are:

1. Derivative. Overall, this was the best single-predicting attribute, with a correlation coefficient of 73%. Chen and Sidney (1997) defined derivative as the difference between the seismic trace amplitude of one sample and the preceding sample. Calculated as such, derivative shows the onset and variation of energy for the Porous Smackover unit (Fig. 10a).

Forward modeling (described by Tebo, 2003) demonstrated that areas with highest porosity, and consequently greater acoustic impedance contrast with overlying and underlying rocks, had the most positive derivative. At Appleton Field, porosity is strongly related to depositional facies (Benson 1988) and therefore variations in derivative are indicative of facies changes.

2. Derivative Reflection Strength (DRS). This is the rate of change of reflection strength over time (Fig. 10b). Reflection strength is amplitude independent of phase, and it shows the location of maximum energy within an event, which may be different from that of the maximum amplitude (Taner *et al.* 1979; Fig. 10c). Reflection strength as an attribute loses vertical resolution, which is captured more effectively by its derivative. The derivative of reflection strength is therefore most useful in characterizing vertical interfaces and discontinuities resulting from stratigraphic (facies), lithologic, or fluid changes.

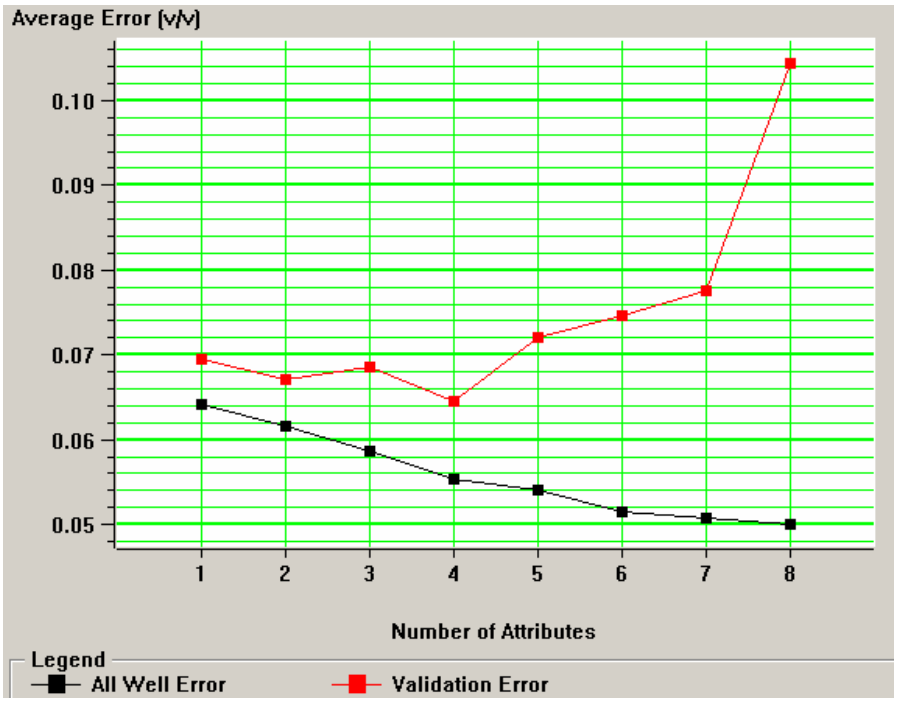

Figure 9: Validation plot, showing the optimum number of attributes to use in predicting porosity from density porosity logs using stepwise multilinear regression. This optimum number of attributes is reached when the validation error (red curve) associated with adding a new attribute to the predicting relationship fails to decrease convincingly. The black curve shows the training error. The training error generally decreases with an increase in number of attributes. See Hampton *et al.* (2001) for a full description and justification of this method.

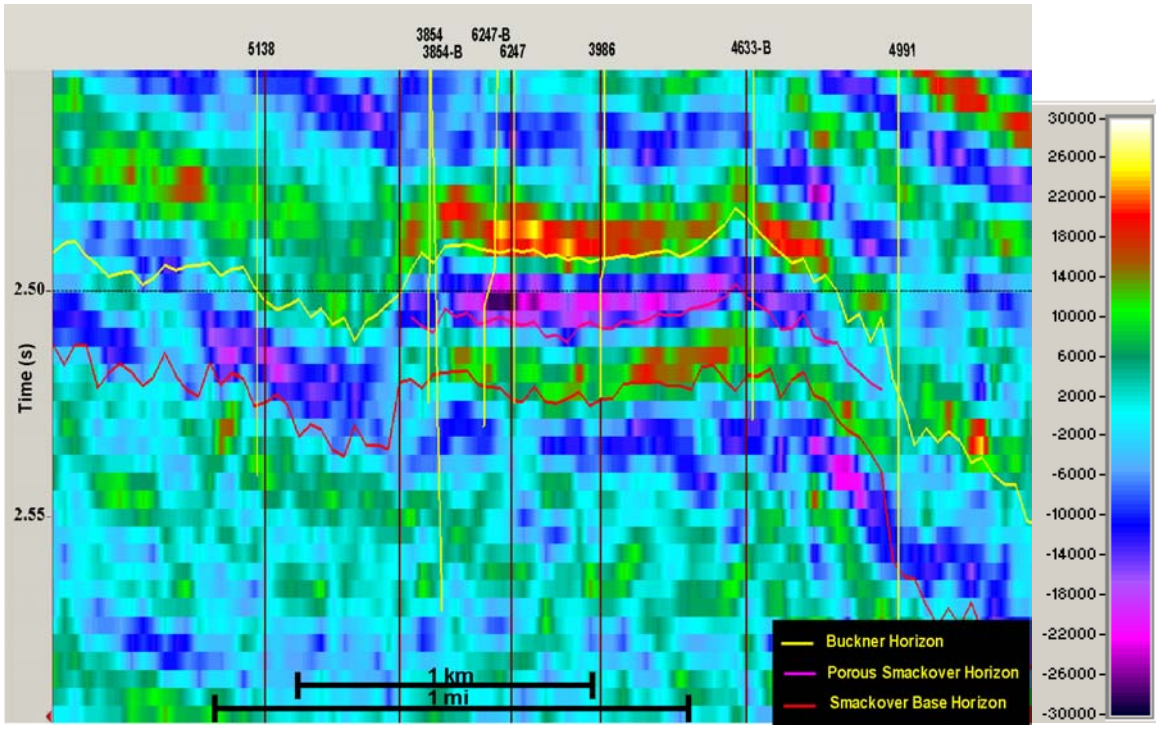
5138
3854
3854-B
6247-B
6247
3986
4633-B
4991
2.50
2.55
Time (s)
1 km
1 mi
Buckner Horizon
Porous Smackover Horizon
Smackover Base Horizon
30000
26000
22000
18000
14000
10000
6000
2000
-2000
-6000
-10000
-14000
-18000
-22000
-26000
-30000

(a)

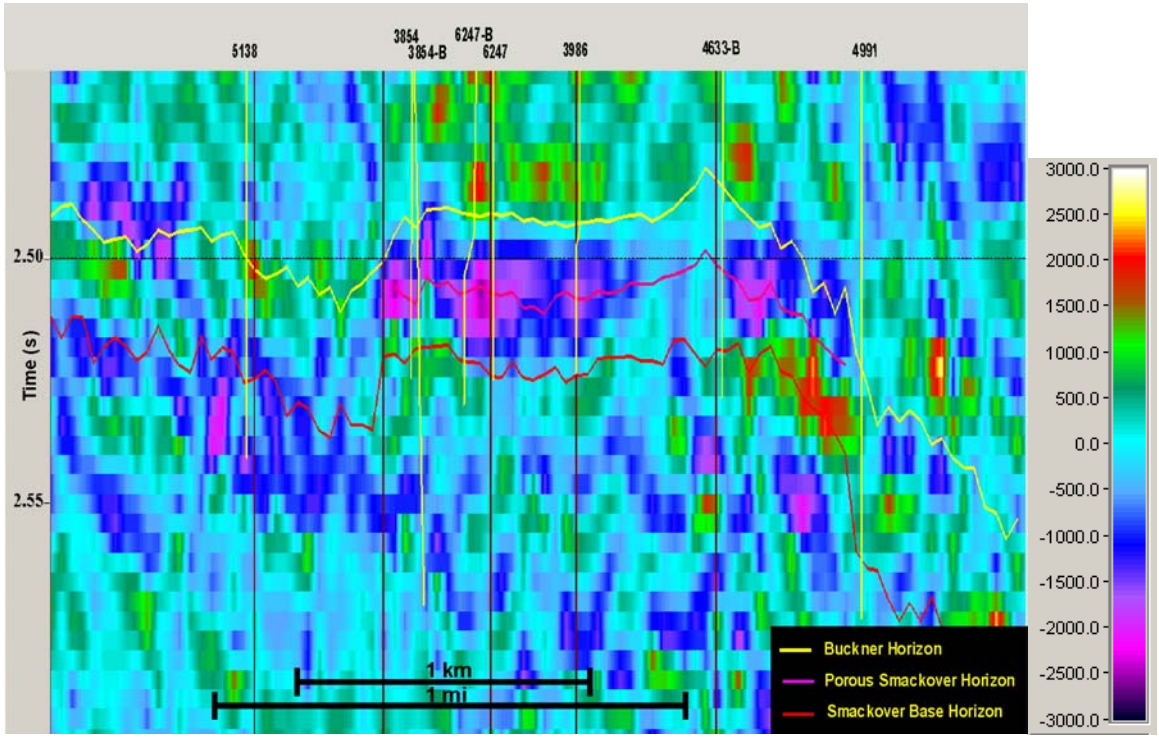
5138
3854
3854-B
6247-B
6247
3986
4633-B
4991
2.50
2.55
Time (s)
1 km
1 mi
Buckner Horizon
Porous Smackover Horizon
Smackover Base Horizon
3000.0
2500.0
2000.0
1500.0
1000.0
500.0
0.0
-500.0
-1000.0
-1500.0
-2000.0
-2500.0
-3000.0

(b)

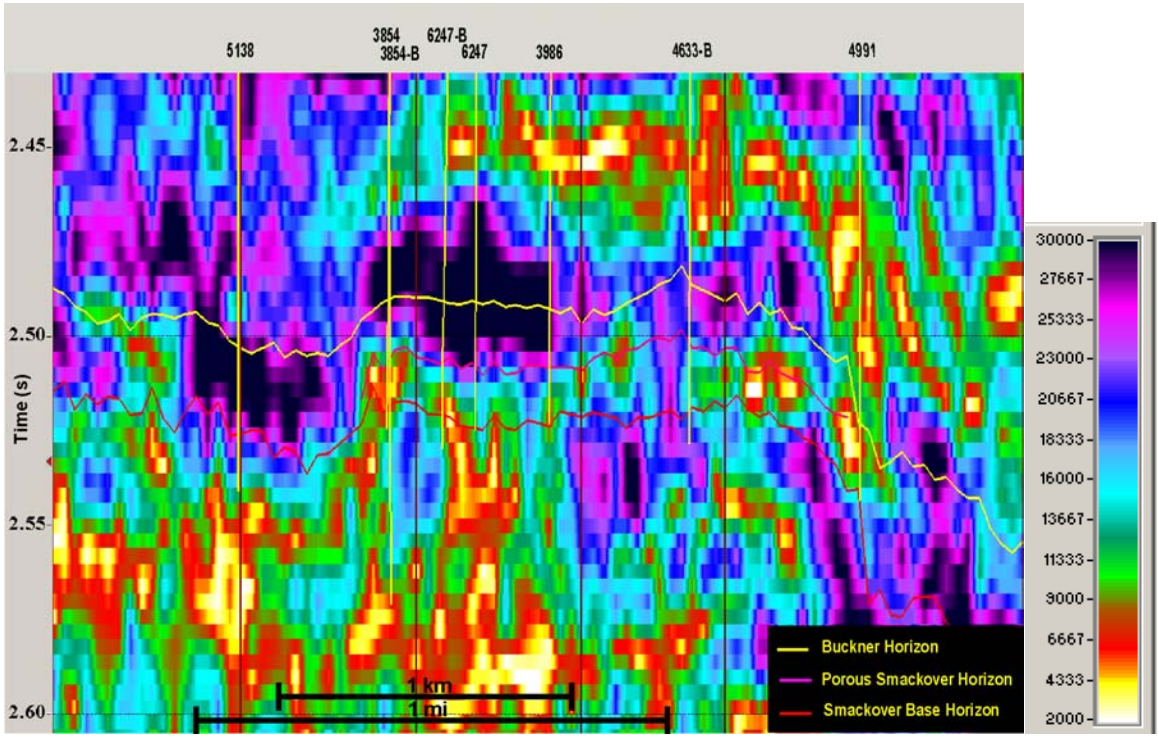

(c)

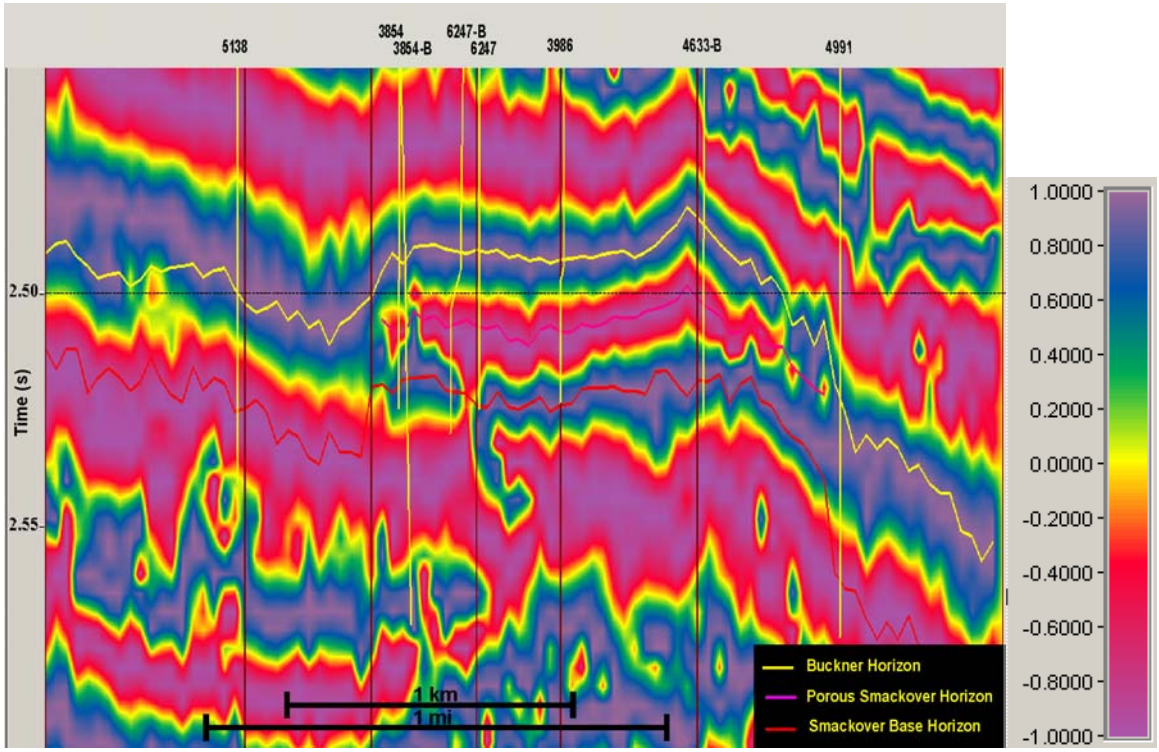

(d)

Figure 10: NW-SE transects through attribute volumes corresponding to Figure 7a. These show the physical relationship between the predicting attributes and porosity within the porous interval. (a) Derivative (b) Derivative of reflection strength (c) Reflection strength (this attribute is shown to illustrate the importance of its derivative (b) in imaging vertical changes) (d) Cosine instantaneous phase. See Figure 3 for location of transects.

Tebo (2003) showed that major changes observed in DRS resulted primarily from thickness variation of the porous unit, while acoustic impedance contrast had little effect. Figures 10b and 10c show transects through DRS and reflection strength (RS) volumes respectively. High porosity areas were seen to have higher values in DRS and lower values in RS volumes (both denoted in hot colors to enhance similarities). Lateral variations in DRS observed within the porous interval show discontinuity in porosity distribution.

3. Cosine Instantaneous Phase. This attribute is derived from instantaneous phase. Because cosine instantaneous phase avoids the 180^{o} phase discontinuity that occurs with instantaneous phase, it generates a better and smoother display of phase variations. Instantaneous phase is phase independent of amplitude, and emphasizes the continuity of reflection events (Taner *et al.* 1979). Within the Smackover interval, changes in cosine instantaneous phase correlated in magnitude and sign to the corresponding amplitude changes of the various stratigraphic units (Fig. 10d). No criteria could be identified from this attribute volume nor from model results that might directly relate to changes in porosity within the porous interval. However, on the whole, this attribute defined precisely the lateral extent and stratigraphic configuration of the porous unit.
4. 1/Smoothed Inversion Results. We used a model-based inversion over a 700 ms window that included the interval of interest. Full details are provided in Tebo (2003). In a general way, seismic inversion attempts to derive an acoustic impedance volume from the seismic data by removing the embedded seismic wavelet. Acoustic impedance in the Smackover is inversely proportional to porosity (i.e., high porosity equals relatively low velocity and density; Fig. 11). Because well data are used directly in the inversion process to generate the acoustic impedance volume, the results need to be smoothed

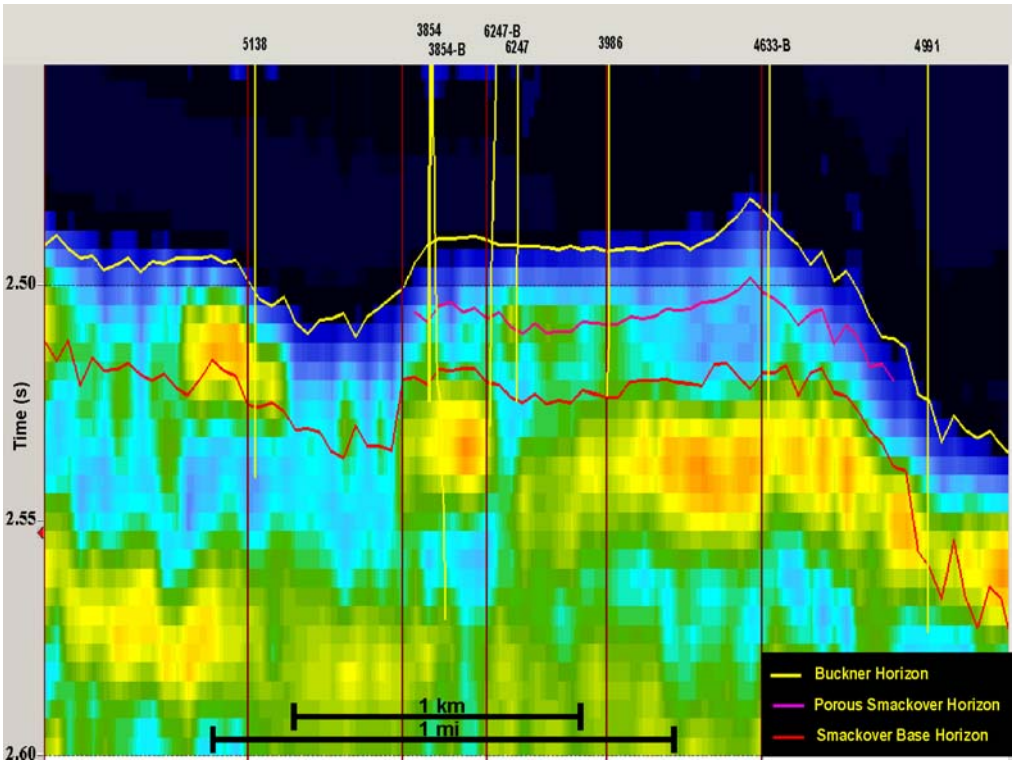
5138
3854
3854-B
6247-B
6247
3986
4633-B
4991
2.50
Time (s)
2.55
2.60
1 km
1 mi
Buckner Horizon
Porous Smackover Horizon
Smackover Base Horizon

(a)

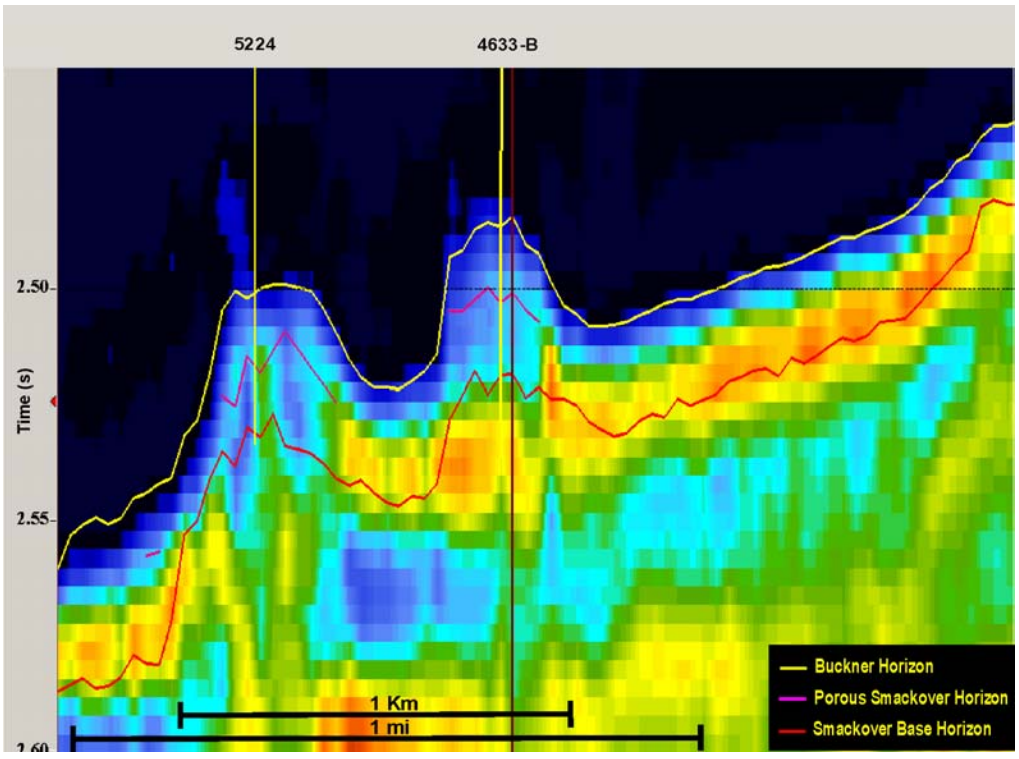
5224
4633-B
2.50
Time (s)
2.55
1 Km
1 mi
Buckner Horizon
Porous Smackover Horizon
Smackover Base Horizon

(b)

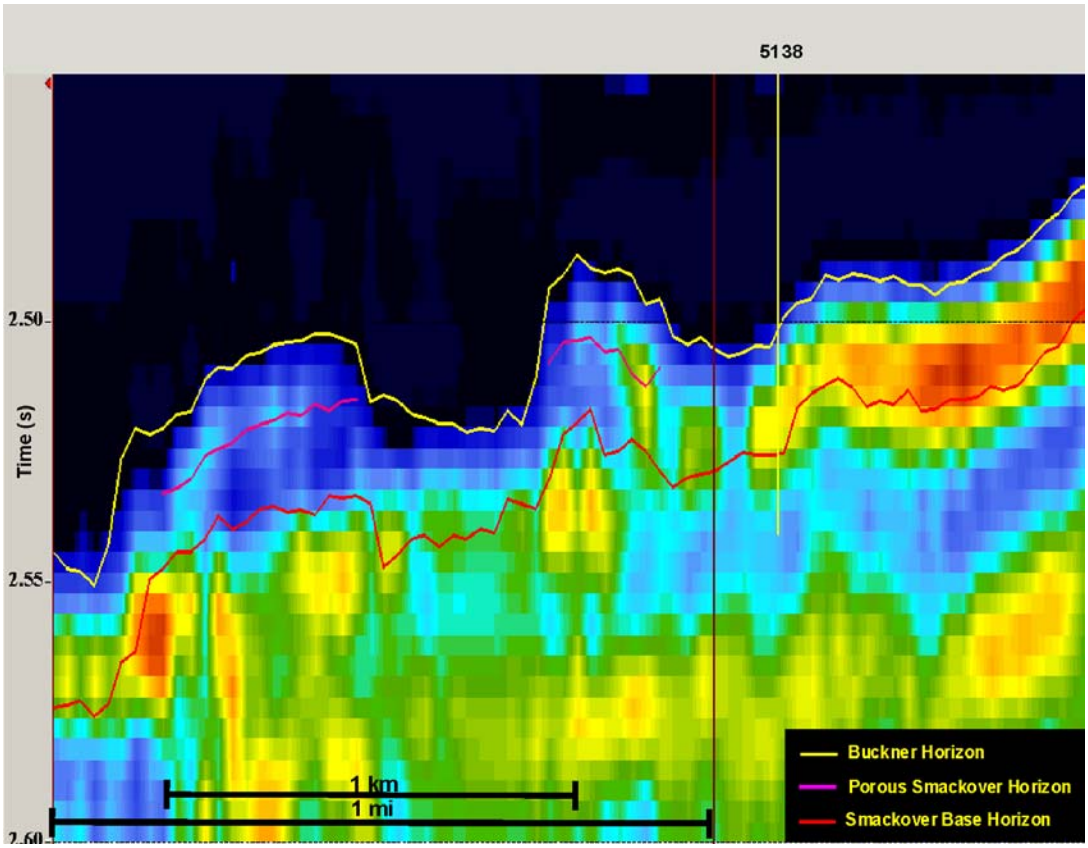

(c)

Figure 11: Transects, corresponding to those shown in Figure 7, showing the acoustic impedence structure of the Smackover Formation. Impedences are generally lower in the porous Smackover and the Norphlet Formation. (a) Strike section, (b) & (c) Dip sections. Units = ft/s*g/cc. See Figure 3 for location of transects.

before inversion results may be used as an attribute. Otherwise, statistical correlations between the inversion results and well data might be suspect.

The PNN-trained relationship with four attributes provided a correlation of 93%, with RMS error of 1.7%. Figure 12 shows that the PNN is able to capture subtle trends in the porosity log. The predictive equation for PNN derived from the analysis was applied to the seismic data to create a porosity volume.

Examination of the porosity volume shows that, like the thickness of the porous interval, porosity is generally higher on the forereef flanks than the crests of paleohighs, although there are other restricted areas (e.g., the highest point of the crests) of high porosity (Fig. 13). Slices through the Smackover interval of the PNN volume highlight this trend (Fig. 14). We generated a porosity thickness (Øh) map for the Smackover Formation to better examine the relationship between porosity development and paleostructure. We used a 12% porosity cut-off as the porosity indicator (12% porosity is the lower limit for production in the Appleton Field), and then calculated the cumulative thickness (in time) of porosity for the Smackover Formation. We then multiplied this value by the average velocity (ft/s) for the Smackover to get thickness (ft). This thickness map (Fig. 15) clearly shows better development of porosity on the forereef flanks than on the crests of structures. This result is geologically realistic given the facies types and their growth forms described from core studies (Table 2).

Tebo (2003) also used multivariate linear regression (MLR) to generate a porosity volume. That result had a lower correlation coefficient (81%) than the PNN and was less geologically reasonable. Leiphart and Hart (2001) noted similar results in their study. This is because the PNN better captures non-linear relationships between attributes and physical properties than the MLR.

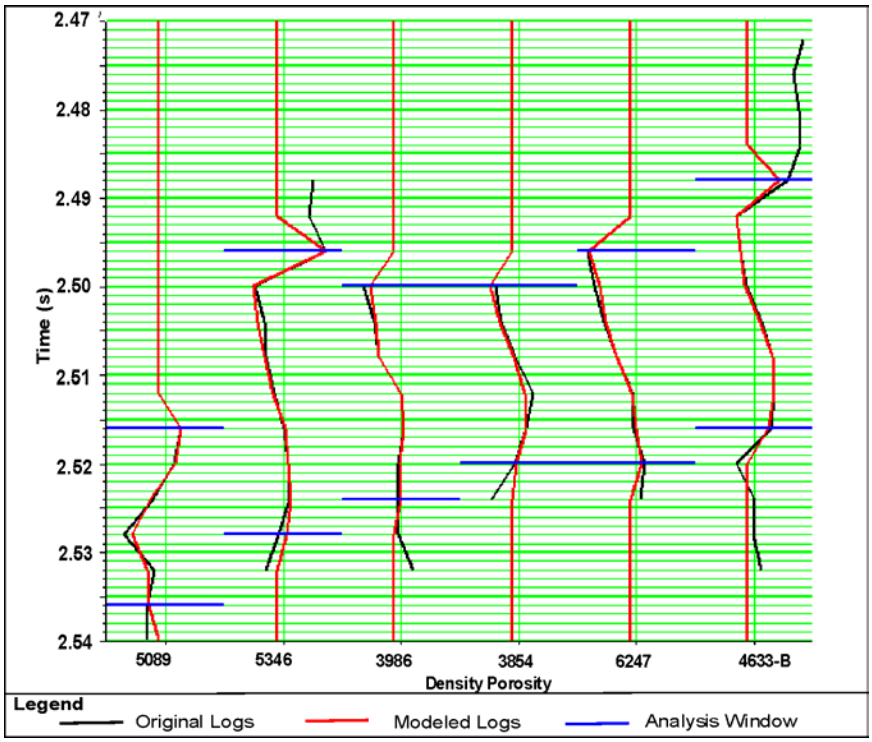
2.47
2.48
2.49
2.50
2.51
2.52
2.53
2.54
Time (s)
5089
5346
3986
3854
6247
4633-B
Density Porosity
Legend
Original Logs
Modeled Logs
Analysis Window

(a)

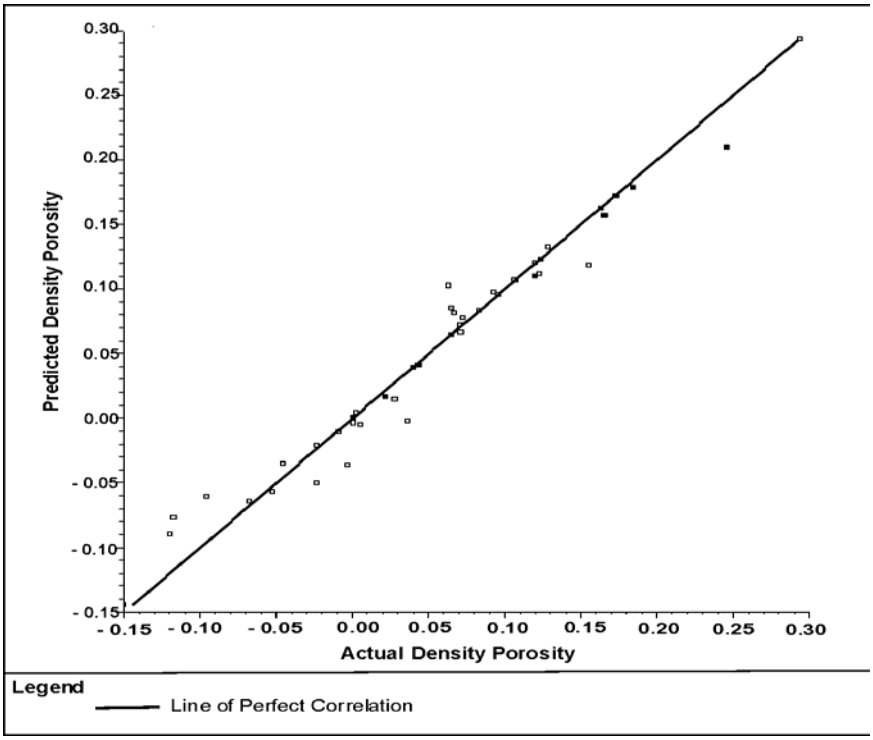
0.30
0.25
0.20
0.15
0.10
0.05
0.00
- 0.05
- 0.10
- 0.15
Predicted Density Porosity
- 0.15
- 0.10
- 0.05
0.00
0.05
0.10
0.15
0.20
0.25
0.30
Actual Density Porosity
Legend
Line of Perfect Correlation

(b)

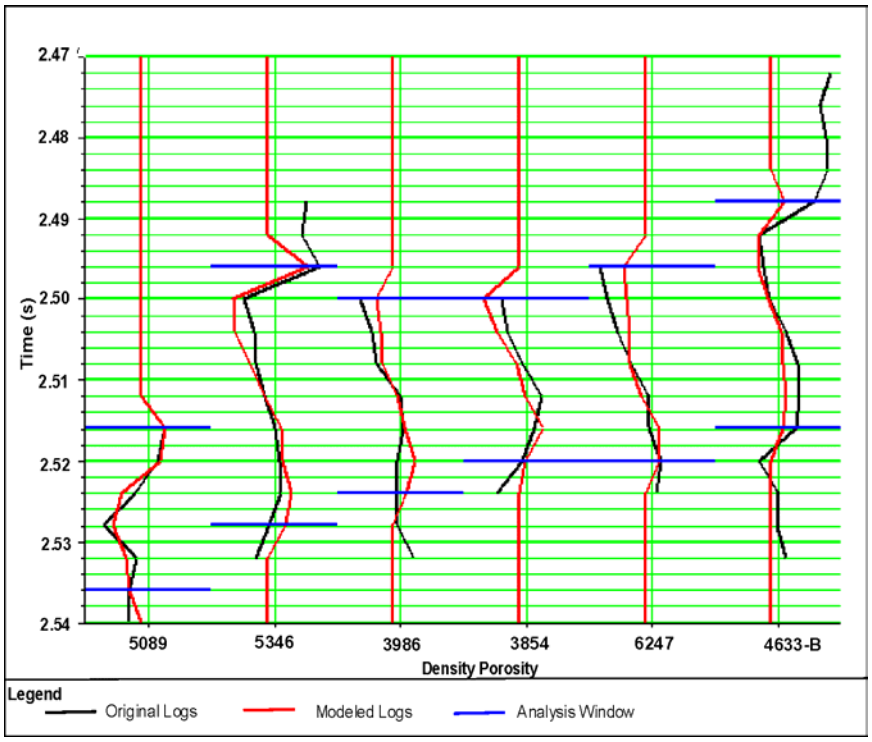

(c)

Figure 12: Visual correlation of actual and modeled/predicted porosity using PNN. (a) On application of multiattribute equation. Note how good the PNN-derived relationship is in modeling subtle changes in porosity within the Smackover Formation. (b) On crossplotting actual vs. predicted porosity values. (c) This figure shows how accurately the porosity at each well can be modeled using the PNN-derived empirical relationship, when that well is excluded from the analysis. Porosity increases to the right of the curve.

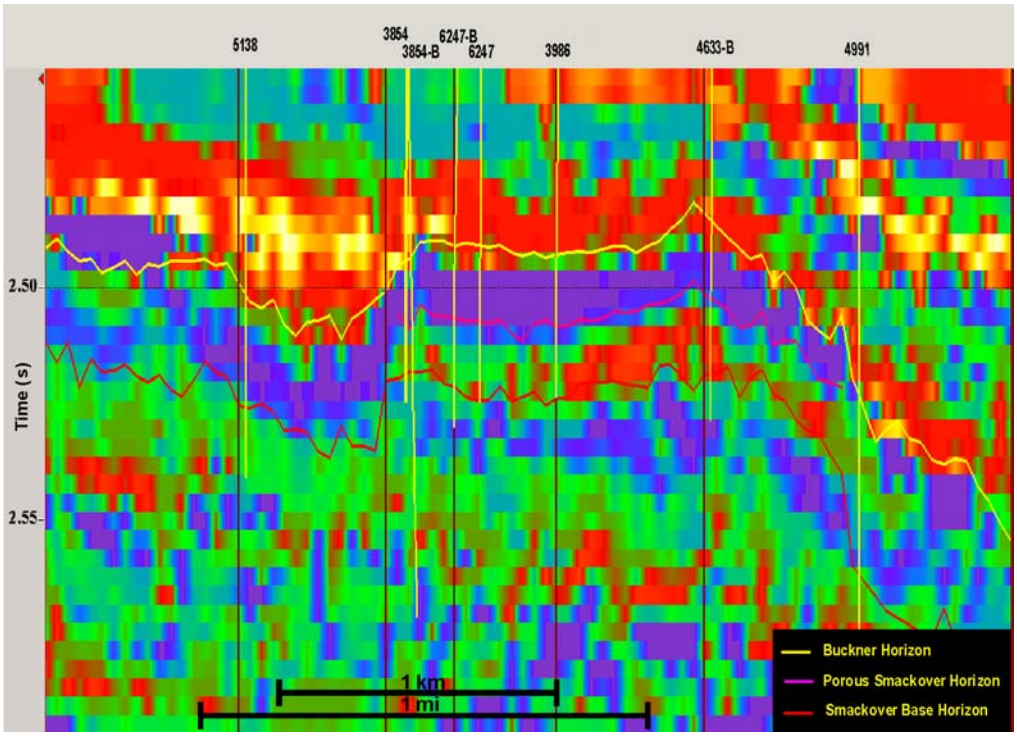
5138
3854
3854-B
6247-B
6247
3986
4633-B
4991
2.50
Time (s)
2.55
1 km
1 mi
Buckner Horizon
Porous Smackover Horizon
Smackover Base Horizon

(a)

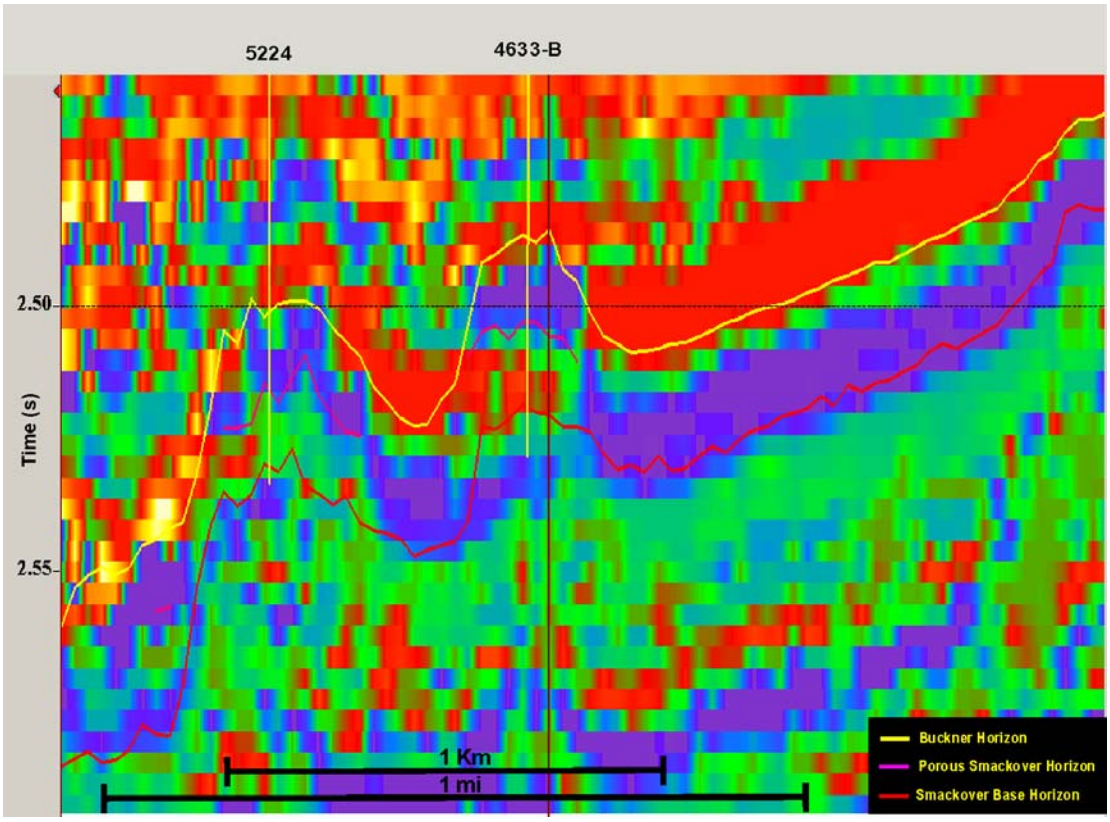
5224
4633-B
2.50
Time (s)
2.55
1 Km
1 mi
Buckner Horizon
Porous Smackover Horizon
Smackover Base Horizon

(b)

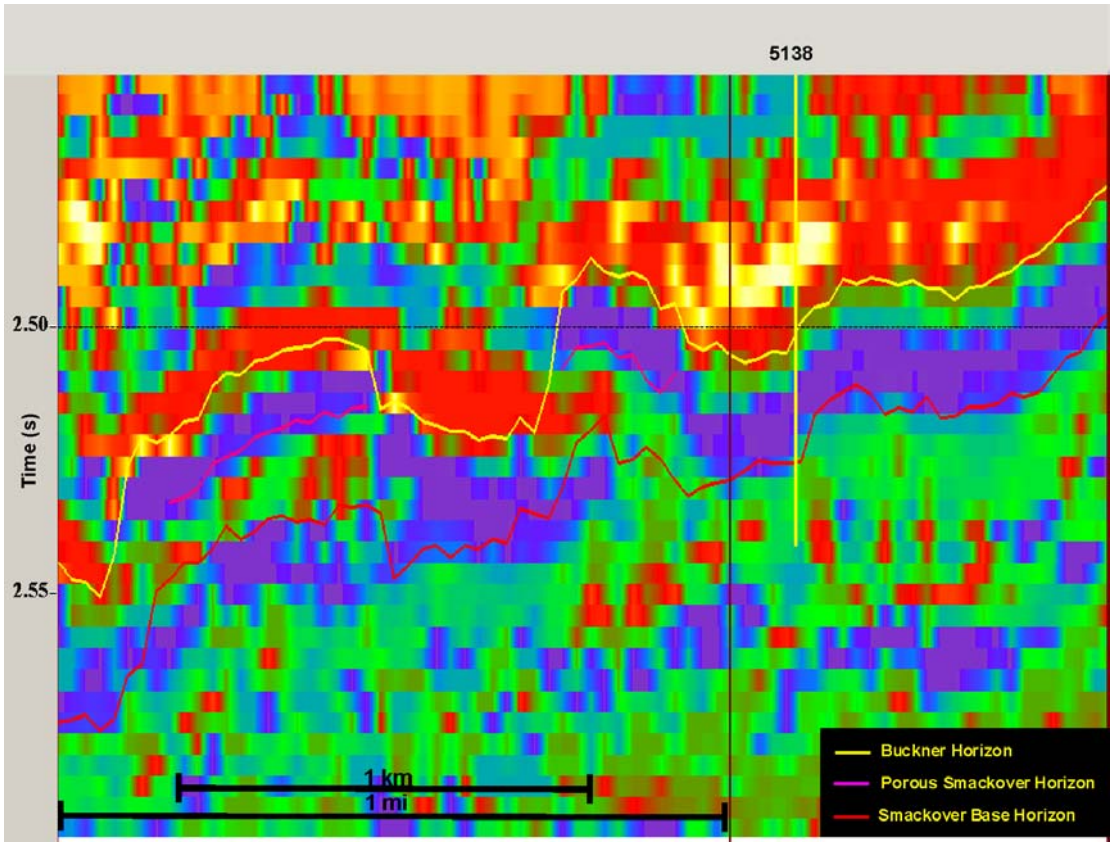

(c)

Figure 13: Strike (a) and dip sections (b & c) through the PNN porosity volume. All sections show that higher porosities (hot colors) are best developed on the seaward flanks of structure. See Figure 3 for location of transects.

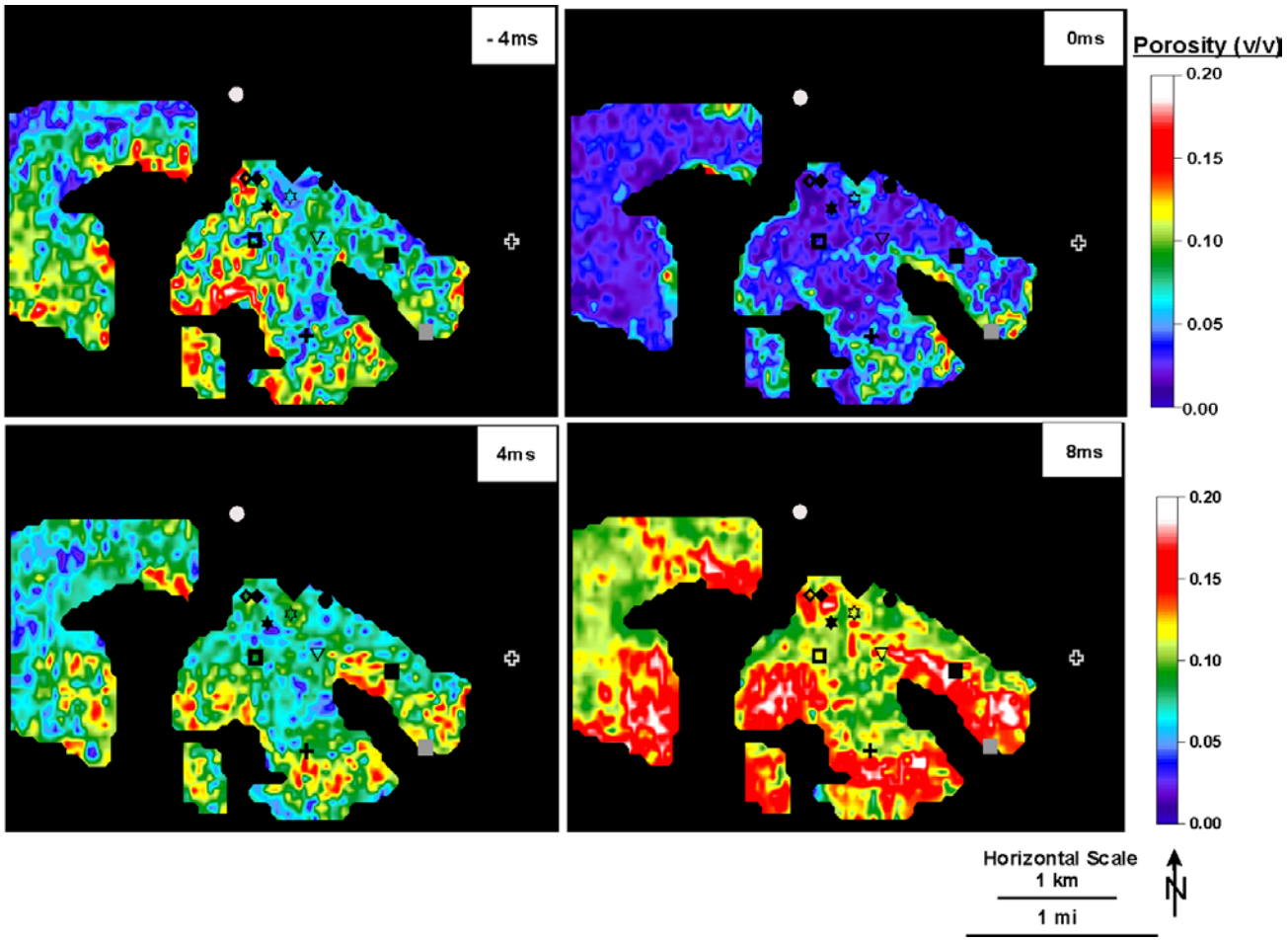

Figure 14: Slices through the porosity volume (porosity values are in decimals (v/v) i.e., volume of voids/total volume of rock, and not percentages), starting 4 ms above the porous Smackover pick. Porosity at -4ms above this pick was attributed to shoal grainstone facies, which constitute the other major reservoir facies in the Appleton Field. Note the overall association of higher porosities (hot colors) with the southern (paleoseaward) flanks of structure, which we attribute primarily to changes in facies type and growth form. Well symbols are indicated in Figure 3 and 8.

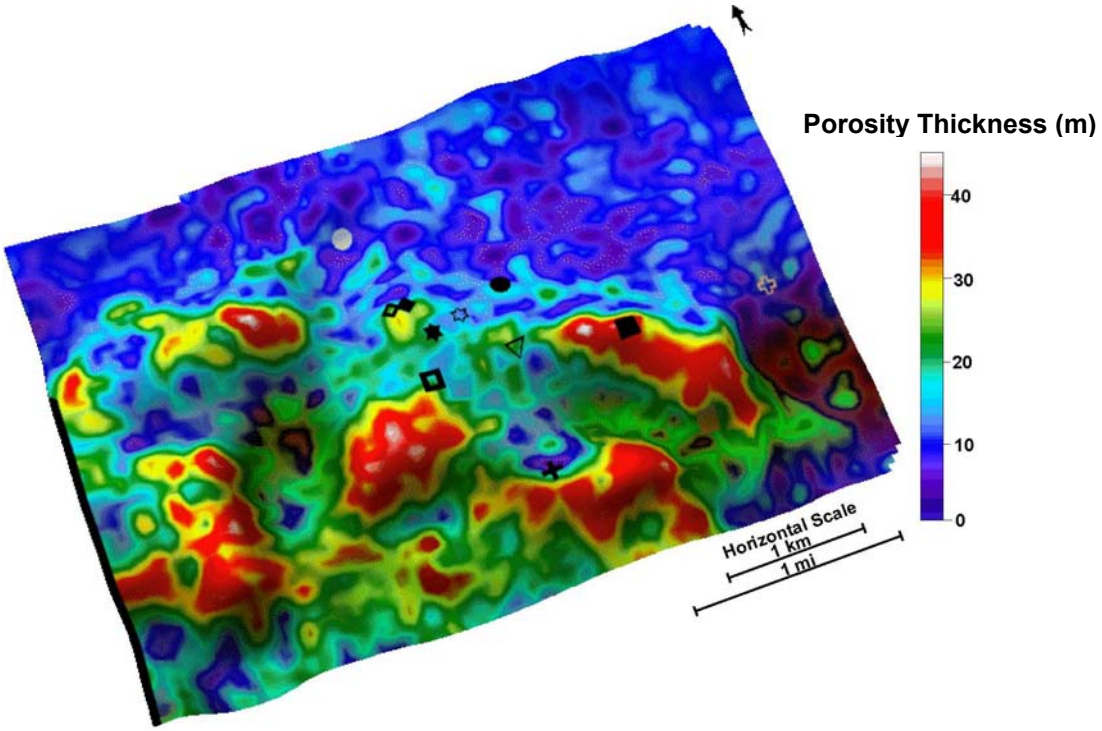

Figure 15: Porosity thickness map of the Smackover Formation overlain on the Buckner/Smackover structure map for better display. Note the overall porosity thickness (hot colors) on the southern flanks of structure. Observed differences in the distribution of porosity are mainly a result of the non-linear relationship between the predicting attributes and the seismic data. Well symbols are indicated in Figures 3 and 8.

Table 2: Reef type, depositional fabric/growth forms, and their reservoir characteristics observed at the Appleton Field, SW Alabama. (Modified from Parcell, 2000).

Reef	Depositional	Reservoir characteristics at
Type I	Layered thrombolites (higher energy)	Good reservoir, lateral permeability
Type II	Reticulate/Chaotic thrombolites (moderate energy)	Good reservoir, lateral-vertical permeability
Type III	Dendroid thrombolites (lower energy)	Best reservoir, vertical permeability
Type IV	Isolated stromatolitic crusts (moderate energy)	Poor reservoir, low permeability
Type V	Oncoidal packstone/ Grainstone (higher energy)	Poor reservoir, low permeability (better if primary fabric is not occluded)

Discussion

The results presented in this paper are consistent with carbonate sedimentologic and sequence stratigraphic principles. Preferential development of reservoir facies on paleohighs at Appleton Field and similar areas has been attributed to the favorable substrate provided by these features, relative fluctuations of sea level, and carbonate productivity (Kopaska-Merkel *et al.* 1994; Benson *et al.* 1996). Fluctuations in relative sea level interacted with paleobathymetry and other environmental factors to control the growth form, fabric and, ultimately, diagenetic alteration of the carbonate deposits. At Appleton, these changes have been described from core and logs studies by Benson *et al.* (1996), Parcell (2000), and Mancini and Parcell (2001). The buildups at Appleton Field are mainly thrombolitic[1] (Parcell 2000; Mancini and Parcell 2001). The preferential development of porosity in the forereef environment in this field was attributed to the low background sedimentation and low to moderate energy levels, which enhanced the proliferation of deeper water dendroid thrombolites (Leinfelder 1993, 1996; Parcell 2000; Mancini and Parcell 2001). The high accommodation potential of the forereef environment permitted these buildups to attain thicknesses in excess of 30m. Just as conventional 3-D seismic data permit more accurate mapping of structural and stratigraphic features than may be undertaken using log and/or core information alone (Brown 1996, Hart 2000), we believe that the 3-D seismic attribute-based porosity prediction more accurately portrays the 3-D distribution of dendroid thrombolites and other porous facies than the results of previous studies. This interpretation is based on previous studies of diagenesis at Appleton Field, which suggested that dolomitization was responsible for porosity preservation and enhancement, rather than

widespread development or obliteration (Saller and Moore 1986; Prather 1992; Kopaska-Merkel *et al.* 1994; Haywick *et al.* 2000).

We focus the remainder of the discussion on two aspects of the results: a) comparison of the results with those of previous studies at Appleton Field, and b) attribute studies as tools for studying sedimentary successions.

Several previous studies have examined porosity development at Appleton Field, and related porosity to depositional history. Differences between these studies and the results lie in the choice of analytical methods used and the nature (e.g., quantitative or qualitative) of the results.

Hart and Balch (2000) used a horizon-based attribute study to predict porosity thickness at Appleton Field. Their results suggested that the porous Smackover unit was best developed on the crests rather than the flanks of the paleohighs (Fig. 16a). They suggested that porosity development on the southern flanks of structure might be related to forereef talus deposits. Although some evidence points to the limited existence of talus deposits (e.g., oncoids, which are characteristic to talus deposits have been observed in cores from the Appleton Field and other Upper Jurassic reef-dominated fields; Jansa *et al.* 1989, Pratt *et al.* 1992, Pratt 1995, Parcell 2000), the results suggest that talus-derived porosity is not a major contributor to porosity development in this field. Transects through the porosity volume (e.g., Figs. 13a-c) depict porous units on the forereef flanks of structures that are disproportionately thick, compared to the thickness of porous reef crest units, for reef front talus deposits. Instead the results are more compatible with models that relate preferential porosity development to thrombolite facies at Appleton Field.

The results presented in this paper have a stronger statistical basis than those presented by Hart and Balch (2000) and, perhaps equally important, are 3-D rather than 2-D in nature. The 3-D

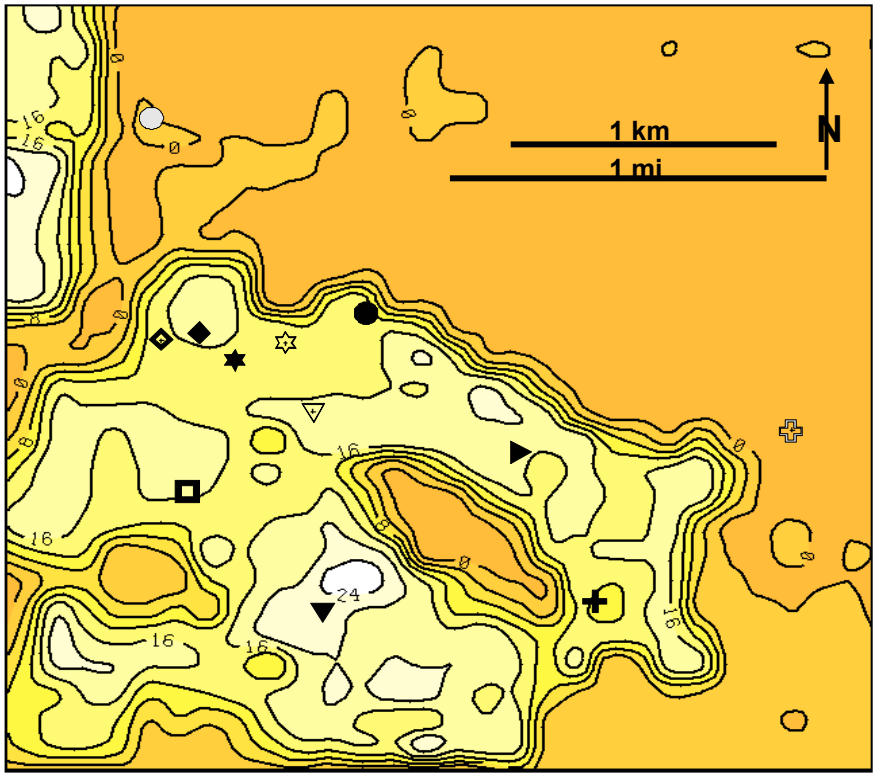

(a)

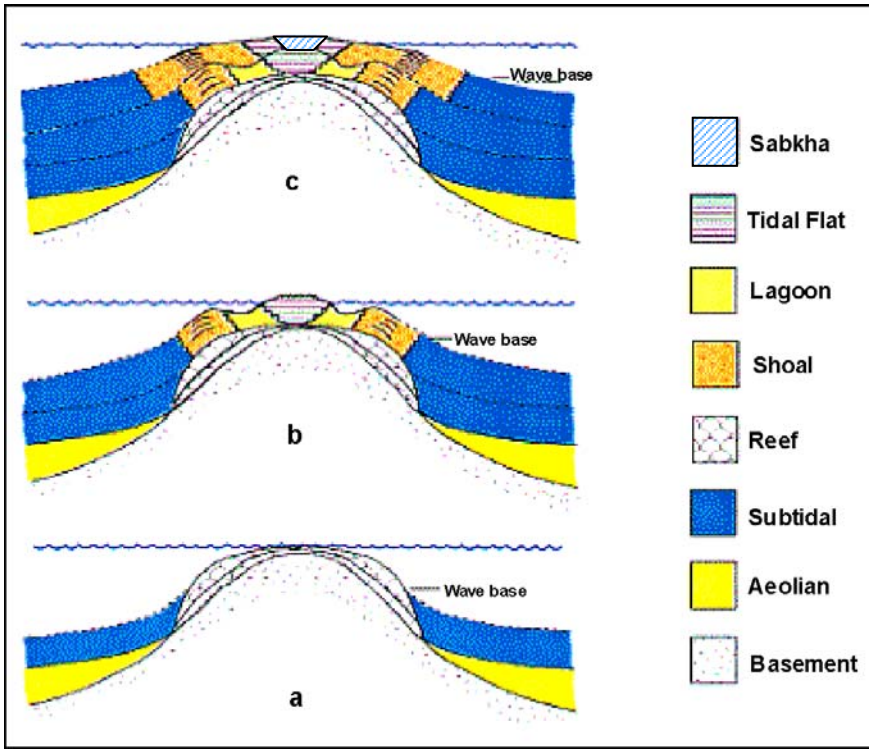

(b)

Figure 16: Existing models for the Appleton field. (a) Model of Hart and Balch (2000) depicting porosity distribution in the porous unit of the Smackover Formation, Appleton Field. Map created using a horizon-based seismic attribute study. (b) Model by Mancini *et al,* 1999. This illustrates facies distribution as a function of water depth on the basement paleohigh.

porosity volume may be viewed in ways (e.g., Figs. 13 and 14) that facilitate geological analysis of the results, thereby improving the quality and robustness of the interpretation.

Mancini *et al.* (1999, 2000) suggested that the distribution of facies was dependent on the height of the paleohighs (Fig. 16b) and associated paleowater depth at Appleton Field. Their model is mainly conceptual and not unique to their study area. As such, it does not provide a detailed guide to facies heterogeneity in the Smackover at Appleton Field. The result has the advantage of quantitatively portraying 3-D porosity changes, hence large-scale reservoir heterogeneities, in the area (Figs. 13-15). As such, the result is of greater utility to those who might be interested in understanding fluid flow in this reservoir.

Attribute studies such as the one presented in this paper have several advantages over other methods (e.g., facies models, sequence stratigraphy, geostatistics, etc.) for defining the distribution of stratigraphic features and rock properties in three dimensions. The lateral continuity of a 3-D seismic volume generally allows formation tops and other features of contrast (e.g., reef margins, channels) to be more accurately mapped than may be done using wireline logs, core or 2-D seismic (Brown 1996, Hart 2000). Seismic attribute studies, and especially volume-based studies such as ours, integrate the high degree of lateral resolution from a 3-D seismic survey with the relatively better (compared to seismic data) vertical resolution of wireline logs. The result is a quantitative output that: a) is of greater utility for applied studies than facies maps, cross-section or conceptual models, b) has well-defined statistical properties (correlation with input, average error, etc.), and c) typically shows greater geologic "reality" than purely geostatistically based methods.

Several authors have presented workflows and precautions to be taken when working with seismic attribute studies (e.g. Schultz *et al.*1994a, Kalkomey 1997, Hampson *et al.* 2001, Hart

1999, 2002) and a full discussion of these aspects cannot be presented here. Instead, we emphasize the following selected points:

a) Data quality and quality control at all aspects of the interpretation process (e.g., horizon picking) are essential. In the case, we could only use six of the eleven wells for which we had logs. This is because the rest could not be adequately tied to the seismic data because of poor log quality and/or seismic data quality problems at the well location.

b) The use of a volume-based as opposed to a horizon-based method increases sample size, and hence the statistical basis of the analysis. As was observed during the multiattribute analysis, the sample size was substantially increased from six (one sample per well) to forty-three (an average of six samples per well). Hence, this method is most appropriate in areas of limited well control (Russell *et al.* 1997; Hampson *et al.* 2001).

c) Although the degree of statistical correlation between input and output variables, and between attributes and physical properties, is important, high correlation coefficients alone are not sufficient for accepting the results of an attribute study. The results must also be examined to determine whether they are geologically logical and whether they are supported by other data types (e.g. engineering data). The physical basis for the relationships between attributes and physical properties also needs to be established. Seismic modeling (Tebo, 2003) helped us to understand the meaning of the attributes employed in this study.

d) Seismic attribute studies do not eliminate the need for conventional geologic analyses. Instead, they are best thought of as a means of building upon those studies. For example, although we can use seismic attributes to image porosity at Appleton Field; it

is only through the integration of the results with previous geological analyses that we can understand the relative importance depositional facies and diagenesis in the creation of that porosity.

Other studies have shown how seismic attribute studies can provide useful information for sedimentary geologists. Studies by Raeuchle *et al.* (1997), Gastaldi *et al.* (1997), Leiphart and Hart (2001), Carr *et al.* (2001) and others have used images derived from seismic attribute studies to define the geometry and distribution of stratigraphic features. Attribute studies have also been used to image diagenetic trends (Pearson and Hart, *in press*). We suggest that this method could be adapted for use in geotechnical studies (e.g., mapping mechanical properties), hydrogeology (aquifers, aquicludes), mining (stratiform deposits, placers), and other domains of interest to sedimentary geologists.

Conclusions

- The main objective was to show how seismic attribute studies may be used to predict subsurface physical properties thereby providing sedimentary geologists with insights that might otherwise be unobtainable. We have demonstrated this approach using a volume-based attribute study of stratigraphically complex carbonate buildups of the Smackover Formation in SW Alabama. Given the limited number and extent of wells, hard constraints provided by seismic and log-based mapping of the top and base of the formation were necessary to guide porosity distribution away from boreholes. The integration of various data and analytical methods in the analysis, (e.g., geophysics, geostatistics, geology) made the results more robust. Transects, slices, and thickness maps generated from the PNN-derived porosity volume depict geologically meaningful porosity distribution away from existing well control.

- Porosity was found to be generally greater and thicker on the forereef flanks than the crest of paleobasement highs. This result is geologically reasonable because this area affords greater accommodation and optimal conditions for reef growth. The predicted porosity distribution is also consistent with known facies types of the porous interval, their growth forms and reservoir characteristics, derived from previous studies of core and outcrop analogs. Thus, the predicted porosity volume also fits the sedimentologic and stratigraphic framework for the Appleton Field established by core and log analyses (Mancini, 2002). The results thus strongly suggest that porosity development is controlled mainly by primary depositional facies at Appleton Field, even though these facies have been pervasively dolomitized.
- Improved knowledge of the controls on thrombolite deposition and the seismic expression of thrombolite buildups gained from this study can be applied to other situations where thrombolitic facies are encountered. These include other Smackover carbonate buildups of the basement ridge play or other Upper Jurassic carbonate buildups of the northern Tethyan ocean (e.g., Atlantic Upper Jurassic carbonate play (Jansa *et al.* 1989), Portugal (Leinfelder 1993; Parcell 2000), etc.).
- Although this is not the only porosity model derived for the Appleton Field, it is the first to be based on a volume-based seismic attribute study. This volume model offers greater flexibility in data display and for defining vertical and lateral heterogeneity, than a 2-D map obtained from horizon-based attribute studies. Because the results are quantitative, they may be used directly in reservoir management work, unlike conceptual models developed previously.

•Although seismic attribute studies have significant advantages over other methods, they are best thought of as complementary or building upon conventional geologic analyses, not replacing them.

Vocation Field

This work was undertaken to predict the distribution of porosity at Vocation Field by integrating attributes derived from a 3-D seismic volume with log-derived physical properties. The purpose was twofold: 1) to generate a data-based porosity volume using Hampson-Russell's Emerge software that could be used in reservoir modeling, and b) to use the results to gain insights into the geologic controls on porosity development at Vocation Field.

Database

Twenty-two wells with a varied suite of logs, along with their coordinates and deviation surveys were available for analysis (Fig. 17, Table 3). Fourteen of these wells had both the sonic log (needed to generate synthetic seismograms) and the porosity (density and neutron) logs. Logs were edited for spikes or other problems. The 3-D seismic data used in this study covered a 5.2 x 4.9 km (3.2 x 3.0 mi) grid, of which a 4.3 km^2 (2.7 mi^2) grid was used for analysis. The seismic data had a bin spacing of 110 x 110 ft (~33 x 33 m) and a trace length of 3 s two-way travel time (TWT). Also available for comparison and interpretation were core descriptions and production information for some of the wells. No checkshot surveys were available.

Methodology

Given the lack of checkshot information, wells needed to be tied to seismic data using the log and seismic picks provided to us. We used the following procedure to generate synthetic seismograms:

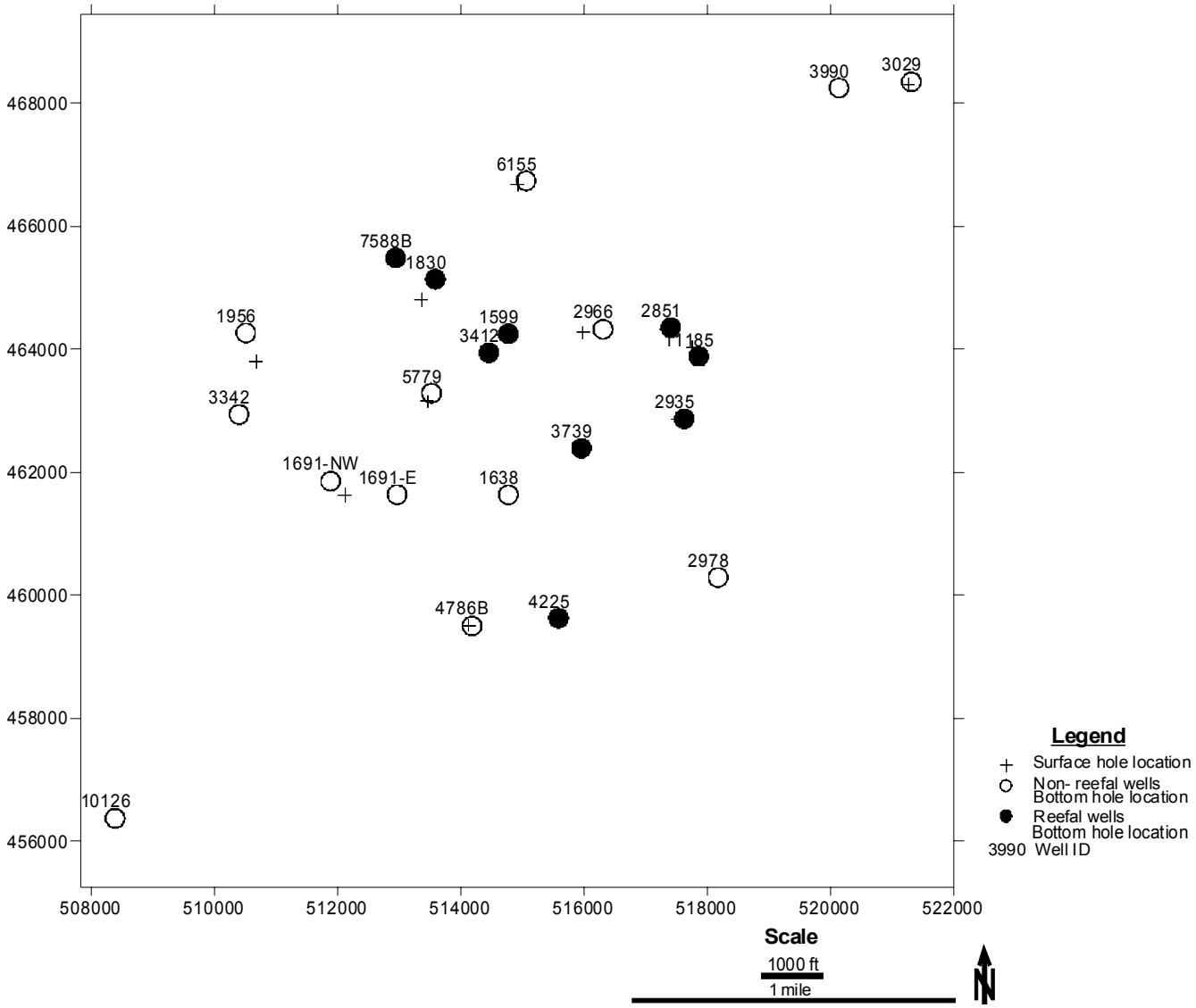

Figure 17: Well locations at Vocation Field. Wells classified based on presence or absence of reef facies.

Table 3: Cross section of logs available for the Vocation Field.

Permit #	GR	NPHI	DPHI	DT	ILM	ILD	SP	SFL	CALI	RHOB	LLS
10126	X	X	X	X	X	X	X	X	0	0	0
11185	X	X	X	X	X	X	X	X	0	0	0
1599	X	X	X	X	X	X	X	X	0	0	0
1638	X	X	X	X	X	X	X	X	0	0	0
1691-NW	X	X	X	0	X	X	X	X	0	0	0
1691-E	X	X	X	0	X	X	X	X	0	0	0
1830	X	X	X	0	X	X	X	X	0	0	0
1956	X	X	X	0	X	X	X	0	0	0	X
2851	X	X	X	X	X	X	X	0	0	0	X
2935	X	X	X	X	X	X	X	X	0	0	0
2966	X	X	X	X	X	X	X	X	0	0	0
2978	X	X	X	X	X	X	X	X	0	0	0
3029	X	X	X	X	X	X	X	X	0	0	0
3342	X	X	X	0	X	X	X	X	0	0	0
3412	X	X	X	X	X	X	X	X	0	0	0
3739	X	X	X	0	X	X	X	X	0	0	0
3990	X	X	X	X	X	X	X	X	0	0	0
4225	X	X	X	0	X	X	X	X	0	0	0
4786B	X	X	X	X	X	X	X	X	0	0	0
5779	X	X	X	X	X	X	X	X	0	0	0
6155	X	X	X	X	X	X	X	X	0	0	0
7588B	X	X	X	0	X	X	X	X	0	0	0
X = curve, 0 = No curve											

•Statistical wavelet extraction: We needed to use a wavelet that matched the frequency content of the seismic data. To generate this wavelet, we used the following parameters:

•Time window: A window length of 600ms (2300 – 2900ms), twice the length of the wavelet was used.

•Seismic data: A subset of the seismic data, 130 inlines by 130 crosslines, was used to minimize the influence of bad data particularly noticeable at survey edges but large enough to improve statistics of the extracted wavelet.

A wavelet with a dominant frequency of ~35Hz (Fig. 18) was generated.

•The statistical wavelet was convolved with the well-derived reflectivity series to create synthetic seismograms for wells with sonic logs. The synthetics were then compared to the seismic data at well locations. A series of constant phase rotations was applied to this wavelet and each time the resulting synthetic trace was correlated to the seismic. The synthetic with the best overall correlation, determined by the correlation coefficient, was chosen. The phase at which this occurs was assumed to be identical to the incident wavelet (Fig. 19).

Of the total 22 wells, 14 had all logs needed for this study. Of that number, it was possible to generate synthetics that adequately tied (correlation coefficient > 0.75) with the seismic data for only 6 wells. We cite the following potential reasons for these problems:

•Incorrect horizon picks: We identified slight discrepancies in the seismic and log picks provided to us. We were able to correct some log picks but kept the seismic picks for consistency with the U. of A. database. We suspect that lateral variations in seismic phase might be responsible for some of the problems in maintaining consistent seismic picks

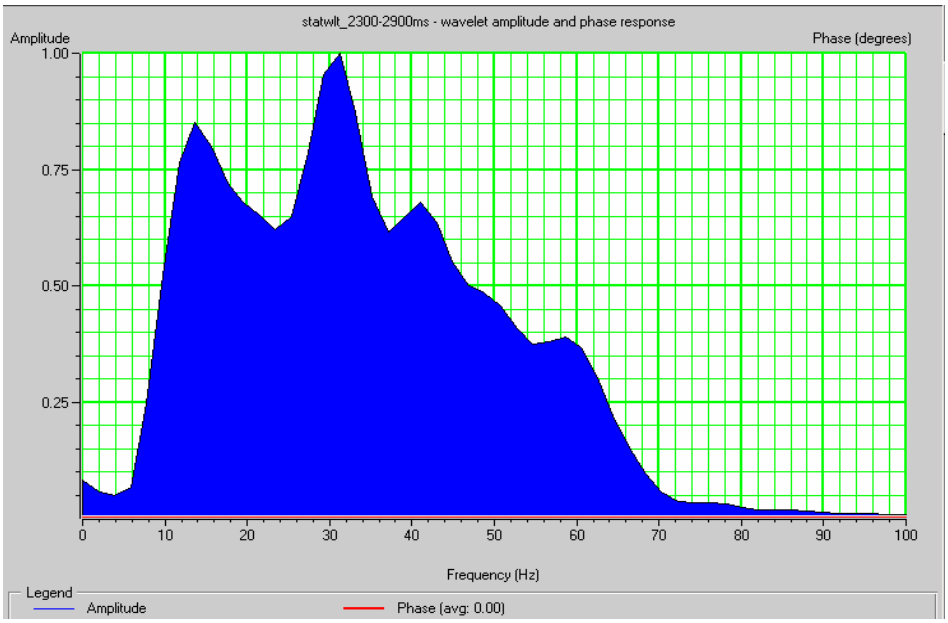

(a)

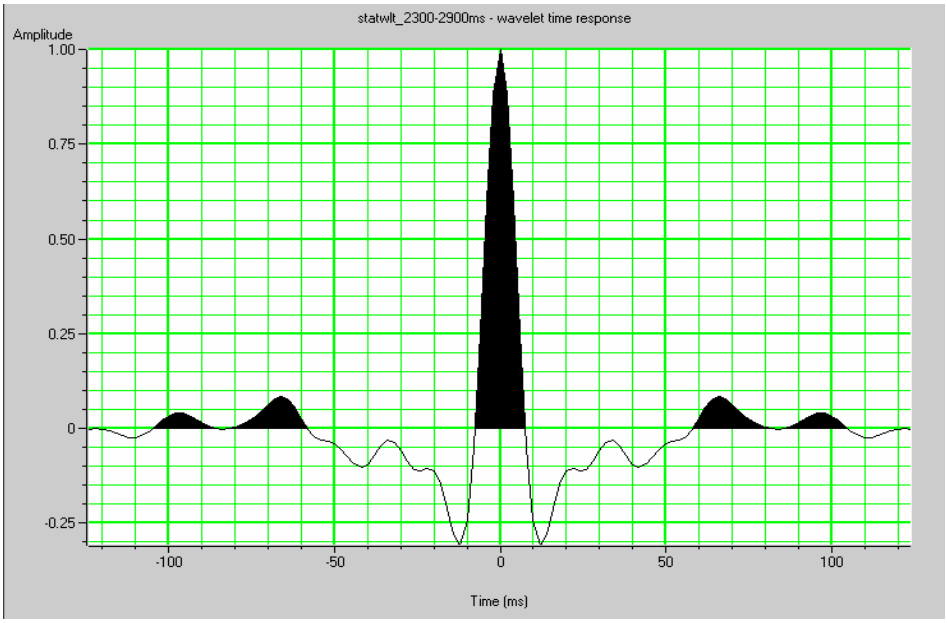

(b)

Figure 18: Estimated (statistical) seismic wavelet: (a) amplitude spectrum showing the range of frequencies embedded in the wavelet, dominant frequency range is between 25-35 Hz, (b) wavelet shape in time domain.

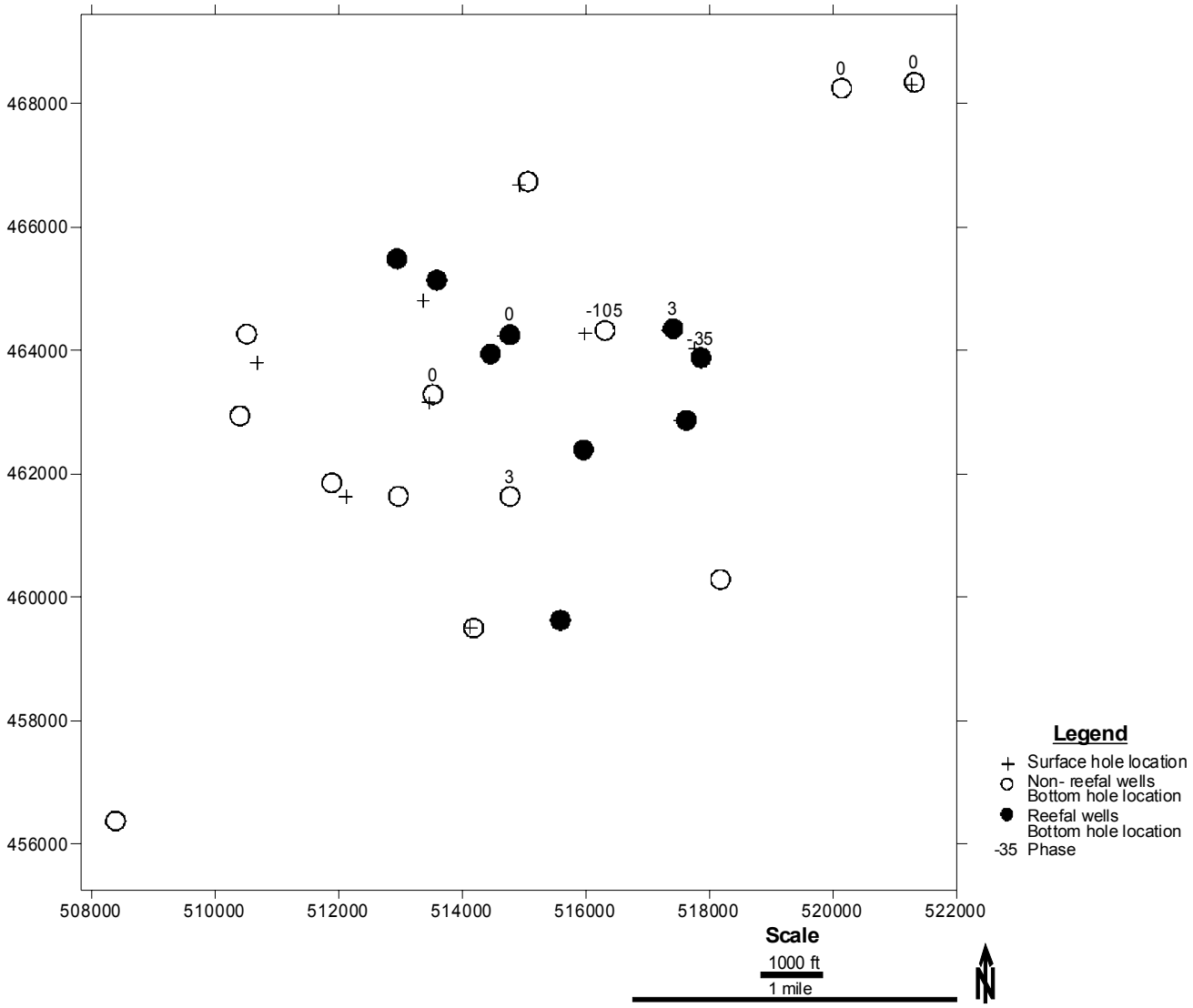

Figure 19: Seismic grid showing phase rotation necessary to obtain a statistically significant synthetic tie. Note phase variation in the east, which could be attributed to structural changes in that area. Wells with excessive phase rotations were not included in subsequent attribute analyses.

(e.g., Well 2966). Wells that required extreme phase changes in the source wavelet for the synthetic seismograms compared to the others (e.g., Wells 2966, 11185) were not used for the Emerge attribute analysis.

- Log length: Most of the digital logs provided to us within and around the Vocation Field have a limited vertical extent. Most extend only a few feet above and below the Smackover Formation (e.g. Wells 2851, 5779, 10126) while some started below (e.g., Well 6155), or were not logged to the end of this formation (e.g., Wells 1638, 2966, 3412, 3990). For this reason, adequate synthetic seismograms could not be generated due to the lack of velocity information above and below the formation, (Fig. 20, Table 4). Ideally, longer digital logs would be available for analysis.
- Seismic data quality: The overall quality of the available seismic data was somewhat poor in areas. Noisy data would prevent us from obtaining adequate well ties between logs and seismic data.

The six calibrated wells with the predicted property logs were trained with 23 attribute volumes, including the original seismic trace, that were derived by the Hampson-Russell software. We chose to predict apparent porosity (the average of neutron and density porosity) because it provided a better approximation of porosity (compared to core measurements) at Vocation Field than neutron, density or sonic porosity alone (See Table 5).

A volume-based method (Hampson *et al.*, 2001; see fuller description of the methodology in Section 2.5) was adopted due to the thickness (0-440ft/0-134m) and stratigraphic complexity (rapid facies changes) of this interval. For this study, we evaluated multivariate linear regression and three types of neural networks. The three neural networks we trained are:

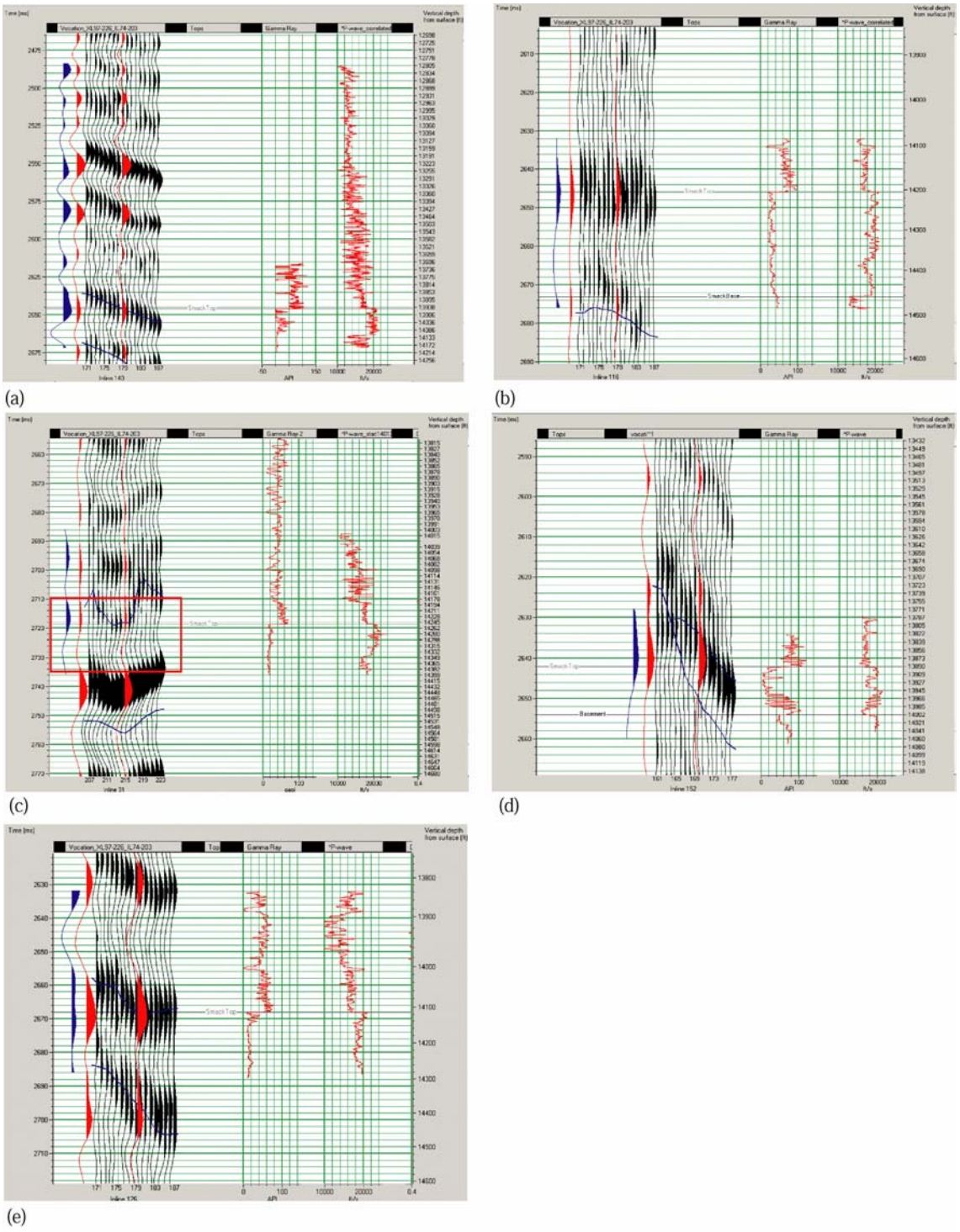

Figure 20: Synthetic seismograms of selected wells showing good ties: a) 1638, b) 2851, c) 3990, d) 5779, e) 2966. The synthetic for 2966 was generated using a -105° phase-rotated wavelet, judged to be an excessive amount. Blue wiggle = synthetic, red wiggle = seismic trace extracted along the wellbore.

Table 4: Summary statistics of available data and synthetic calibration for the Vocation Field.

Permit #	DT Logs	Reefal Facies	Cored	Well Status	Hole Type	Synthetic	Correlation Coefficient	Wavelet Phase
10126	yes	no	no	na	straight	no	-	-
11185	yes	yes	yes	producing	deviated	yes	0.5674	-35
1599	yes	yes	yes	temp plugged- oil	deviated	yes	0.6695	0
1638	yes	no	no	na	straight	yes	0.7939	3
2851	yes	yes	yes	abandoned -oil	deviated	yes	0.8408	3
2935	yes	yes	yes	abandoned -oil	deviated	no	could not tie	-
2966	yes	no	yes	na	deviated	yes	0.8857	-105
2978	yes	no	no	na	straight	no	could not tie	-
3029	yes	no	no	na	deviated	yes	0.748	0
3412	yes	yes	yes	abandoned -oil	straight	no	-	-
3990	yes	no	yes	na	straight	yes	0.8782	0
4786B	yes	no	no	na	deviated	no	-	-
5779	yes	no	yes	abandoned -oil	deviated	yes	0.9618	0
6155	yes	no	no	na	deviated	no	-	-
1691-NW	no	no	yes	na	deviated	no	-	-
1691-E	no	no	no	na	deviated	no	-	-
1830	no	yes	no	abandoned -oil	deviated	no	-	-
1956	no	no	no	na	deviated	no	-	-
3342	no	no	no	na	straight	no	-	-
3739	no	yes	yes	abandoned -oil	straight	no	-	-
4225	no	yes	no	abandoned -oil	deviated	no	-	-
7588B	no	yes	yes	na	deviated	no	-	-

Table 5: Comparison of porosity measured by different porosity logs. PHID = Density porosity, PHIN = Neutron porosity, PHIA = Apparent porosity ([PHID + PHIN]/2).

Permit #	PHIDmax	PHINmax	PHIAmax	PHIDavg	PHINavg	PHIAavg	Coremax	Coreavg	Misc
10126	0.222	0.162	0.112	0.047	0.077	0.023			
11185	0.182	0.226	0.184	0.039	0.133	0.086	0.130	0.061	
1599	0.387	0.324	0.169	0.084	0.115	0.055	0.350	0.109	No base
1638	0.038	0.100	0.061	-0.044	0.041	-0.002			
1691-E	0.088	0.151	0.118	-0.054	0.033	-0.011			
1691-NW	0.055	0.223	0.139	-0.026	0.141	0.058			
1830	0.101	0.232	0.159	-0.002	0.105	0.052	0.250	0.105	
1956	0.157	0.293	0.221	-0.006	0.068	??			
2851	0.185	0.204	0.187	0.008	0.113	0.060	0.250	0.106	
2935	0.137	0.259	0.198	0.012	0.146	0.079	0.200	0.091	
2966	0.14	0.217	0.163	-0.015	0.157	0.071			No base
2978	0.283	0.274	0.277	0.010	0.139	0.075			
3029	0.166	0.281	0.207	0.006	0.110	0.058			
3342	0.126	0.259	0.192	0.006	0.088	0.047			
3412	0.281	0.187	0.190	-0.009	0.068	0.039	0.175	0.052	No base
3739	0.160	0.233	0.179	0.061	0.155	0.108	0.150	0.062	No base
3990	0.121	0.191	0.144	0.030	0.144	0.087			No base
4225	0.112	0.236	0.174	-0.015	0.081	0.033	0.150	0.038	
4786B	x	x	x	X	X	X	x	X	No Smackover
5779	0.108	0.160	0.134	-0.019	0.067	0.024	0.225	0.059	
6155	0.174	0.263	0.199	0.036	0.141	0.088			
7588B	0.335	0.283	0.263	0.02	0.148	0.082			No base

- Probabilistic Neural Network (PNN) – Probabilistic Neural Networks are described in the section on Appleton Field (Section 2.5).
- Trend cascaded Probabilistic Neural Network (PNN) – This method is used to improve MLR prediction, and works best in data, such as Vocation Field, which have no significant trends within the analysis window. In this option, the network first performs linear regression using the attributes identified from the MLR analysis. This MLR-predicted log is smoothed, and a PNN is then used to predict the high frequency component (residual) of the logs that is not found in the smoothed MLR log. The final trend-cascaded log is the sum of the PNN residual and smoothed MLR logs. This is a new option for the Emerge software that was not available during the Appleton Field project.
- Multi-layer Feed Forward Network (MLFN) – The properties of this network are described in Masters (1994). The validity of this network is dependent on the number of nodes to use in the hidden layer and the number of iterations. The number of nodes, analogous to the degree of polynomial, is determined by the following method:

  Number of nodes = 2/3 x (Number of attributes x Operator length).

  The number of iterations basically controls computation time.

Results And Discussion

We used the top and base of the Smackover Formation to define the interval of interest (Fig. 21). The Buckner Anhydrite of the Haynesville Formation was used as the seismic proxy for the top of the Smackover Formation. Seismically this top was found to vary laterally in phase (see Figs. 19 & 20). This could be attributed to lateral changes in phase of the wavelet embedded in the seismic data, lateral changes in lithology or some other factor.

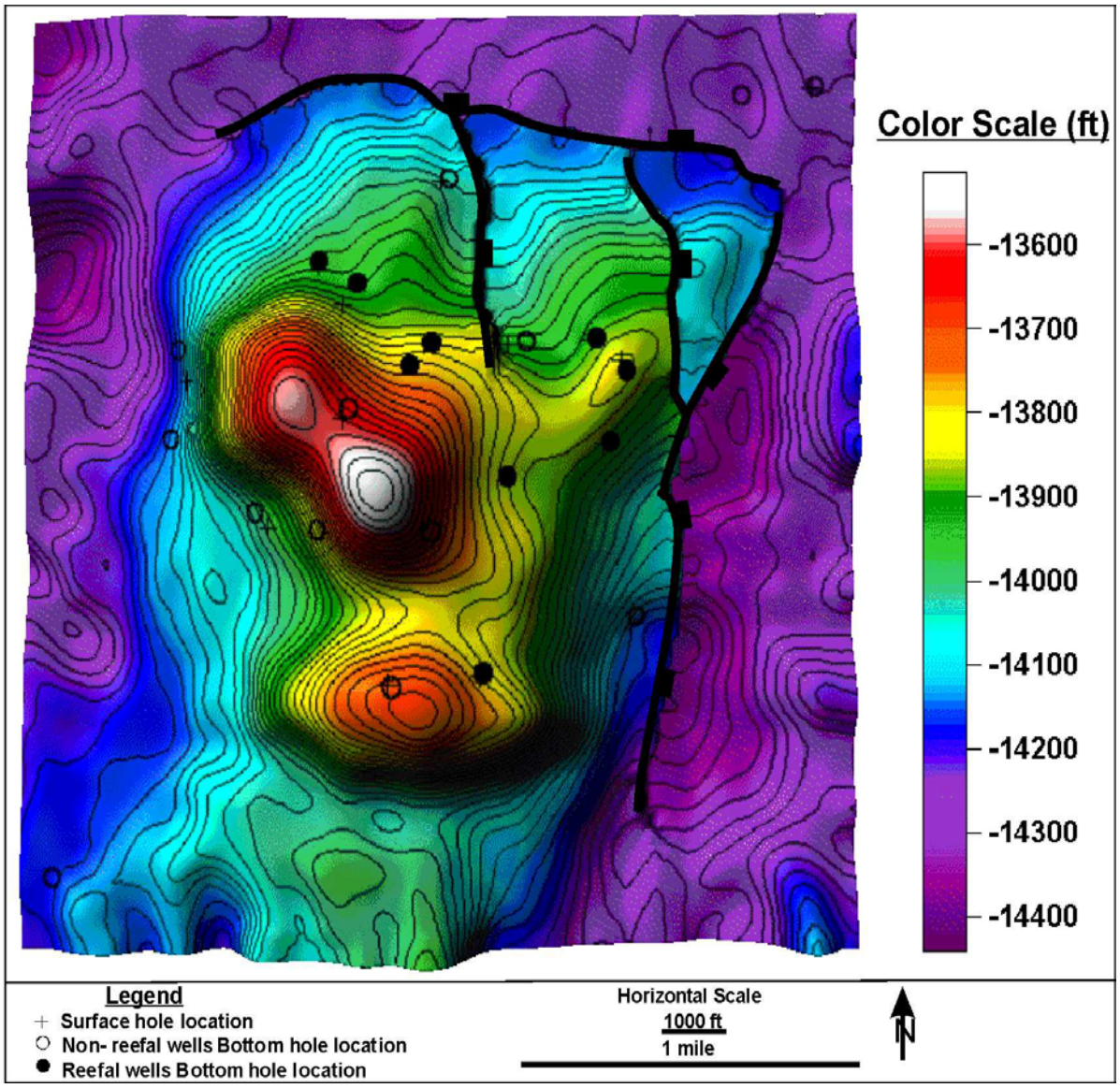

Figure 21: Depth-structure maps (sub-sea) from seismically interpreted horizons: a) Buckner/Smackover, b) Porous Smackover (reef), c) Smackover base. Thick black lines represent faults and their dip directions. Black areas in a) and b) show zones where Smackover carbonates did not develop over the crest of paleohighs. Note that the reflector corresponding to the top of the reef facies (21b) is not present throughout the survey area.

As was the case at Appleton Field, the phase of the base of the Smackover Formation in the Vocation dataset was dependent on the physical properties of the units underlying the Smackover Formation. This pick constituted a medium to high amplitude peak where the Smackover is underlain by the Basement, and a medium to high amplitude trough, when the formation is underlain by siliciclastics of the Norphlet Formation.

The best single predicting attribute was the integrated trace, with a correlation coefficient of 46% (Fig. 22). MLR results showed that 3 attributes were optimal in predicting apparent porosity (Fig. 23), these attributes were: integrated trace, time, and filter 25/30-30/35 (Tables 6 and 7).

- Integrated trace: This attribute is the integral of the seismic trace, which essentially is a band-limited (recursive) inversion, with low acoustic impedance being represented by negative numbers, and high acoustic impedance being represented by positive numbers. A crossplot of this attribute and apparent porosity of the trained wells reveals that higher porosity areas are associated with negative values of integrated trace, hence the relationship of high porosity and low acoustic impedance (Fig. 22b).
- Time: This mainly is a ramp function that adds a trend to the computed reservoir property, in this case apparent porosity. A crossplot of this attribute and porosity shows a positive correlation, which could be attributed to a relationship between structure and porosity development (Fig. 24).
- Filter 25/30 – 30/35Hz: This attribute is related to the spectral decomposition of the seismic wavelet. As observed for the amplitude spectrum of the wavelet computed over the interval of interest (Fig. 18), the majority of the spectrum falls within this given frequency range. This attribute is related to rock properties, specifically to mapping bed thickness, geologic

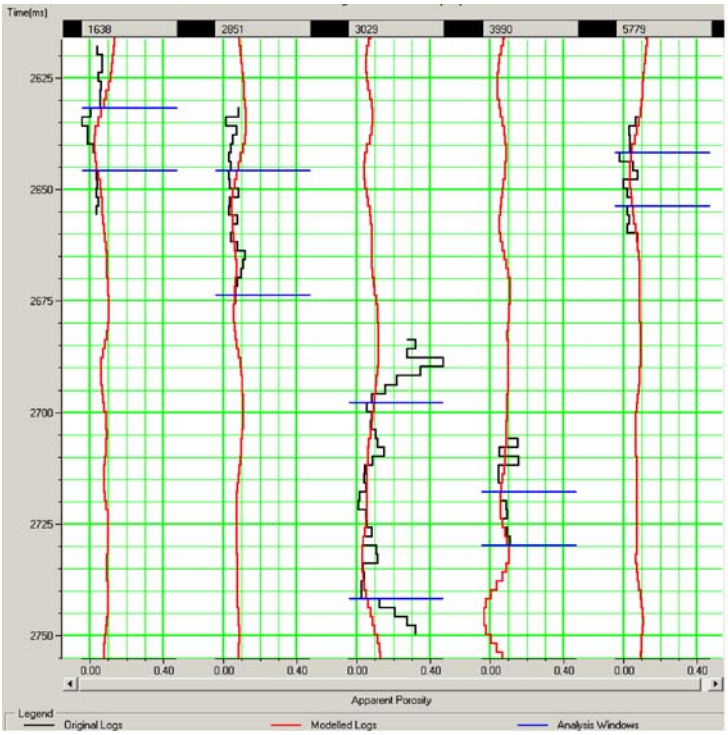

(a)

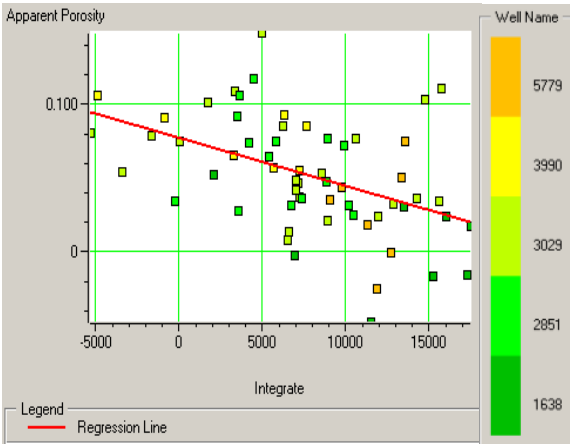

(b)

Figure 22: a) Comparison of modeled porosity logs (red curve) derived from the application of the best single-predicting attribute (integrated trace), and actual porosity logs (black curve). The blue lines across logs define the window for which this analysis is valid; b) Crossplot of actual porosity values from logs against integrated trace illustrates the negative relationship between this attribute and porosity. Higher porosities are associated with negative integrated trace values.

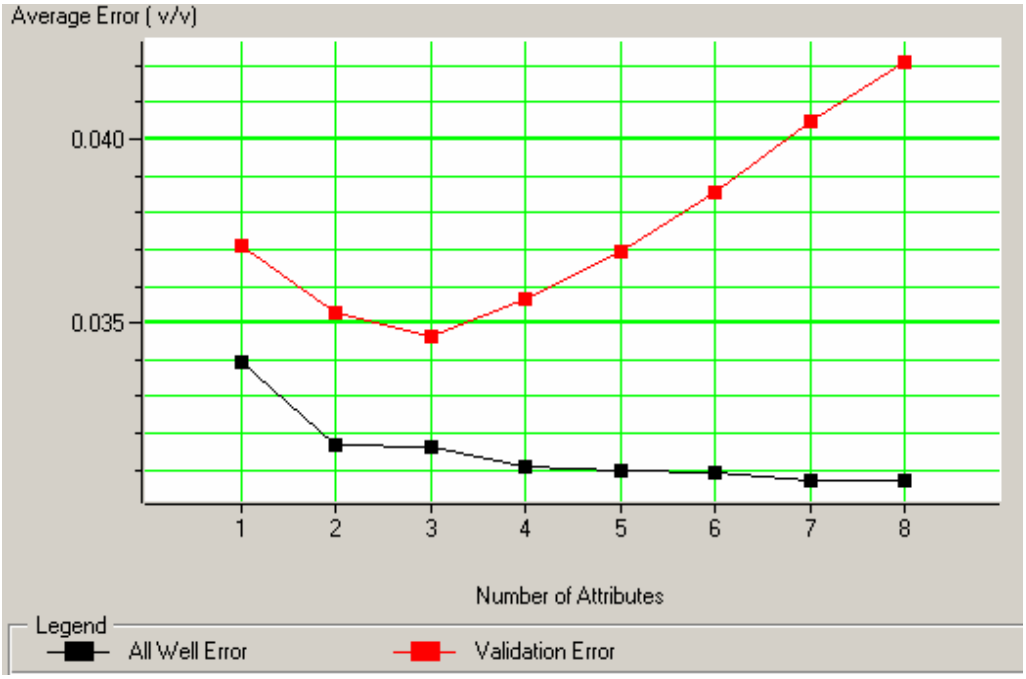

Figure 23: Validation plot, showing variation in all-well error and validation error in predicting porosity from apparent porosity logs using stepwise linear regression. The increase in validation error after the third attribute indicates that the optimum number of attributes to use is three. See Hampson *et al.* (2001) for a full description and justification of the method.

Table 6: Multiattribute list showing the best predicting 8 attributes, prediction error decreases with the addition of each attribute. Each added attribute consists the preceding set of attributes.

No. of attributes	Target	Final Attribute	Training Error	Validation Error
1	Apparent Porosity	Integrate	0.033962	0.037084
2	Apparent Porosity	Time	0.031673	0.035277
3	Apparent Porosity	Filter 25/30 – 35/40	0.031607	0.034657
4	Apparent Porosity	Instantaneous Phase	0.031104	0.035650
5	Apparent Porosity	Dominant Frequency	0.030976	0.036948
6	Apparent Porosity	Amplitude Weighted Phase	0.030954	0.038529
7	Apparent Porosity	Filter 55/60 – 65/70	0.030735	0.040484
8	Apparent Porosity	Second Derivative	0.030697	0.042113

Table 7: Attributes and their weights/sigmas contributed towards creating the empirical relationship (multiattribute transform) for porosity prediction using different analytical methods.

Attribute Name	Attribute Transform	MLR Weight	PNN_No Trend Sigmas	PNN_Trend Sigmas
Integrate	None	-2.79471e-006	0.267086659401869	0.0905277336448514
Time	None	0.000335289	0.525753681217157	1.37145498622836
Filter 25/30 – 35/40	None	-4.396e-010	0.554705532426393	0.269098355541889
Constant	-	-0.827684	0.704166667846342	0.462500001303852
Target Transform	None	0	-	-
Trend Length	-	1	-	-

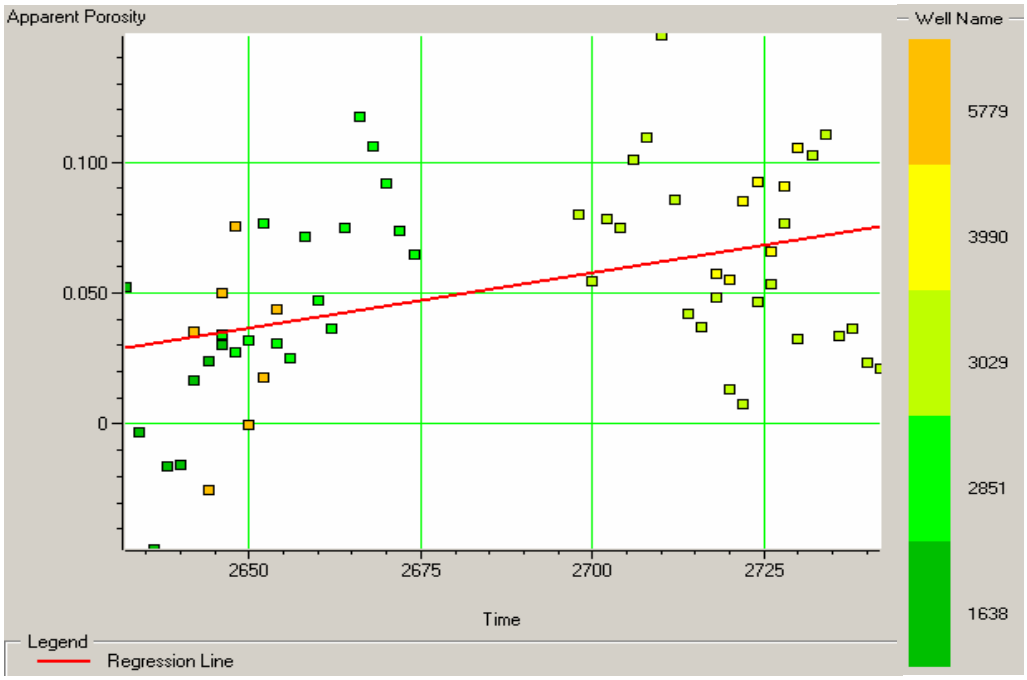

Figure 24: Crossplot of time vs. porosity indicates the presence and nature of relationship between these two variables. The trend indicates that higher porosity is generally found lower in the section.

discontinuities and/or absorption effects (Peyton *et al.*, 1998; Partyka *et al.*, 1999; Taner, 2001).

Applying the three-attribute transform obtained from the MLR increased the prediction coefficient to 56% (Fig. 25a & b). A 45% correlation shows how well this transform could be used to predict trained logs excluded from the analysis in the validation analysis (Fig. 25c).

Although the neural networks trained with MLR-derived attributes generally increased the statistical accuracy of the porosity prediction, the improvement was not uniform. The performance of each network was evaluated based on the correlation of predicted and actual porosity, their average error incurred upon application of the transform, the ability to predict porosity at each well excluded from the training dataset (cross correlation/validation), and visual correlation of predicted and actual porosity logs (Table 8; Figs. 26, 27 and 28). The "regular" (no trend-cascaded) PNN showed the least improvement, followed by the MLFN. The best (statistically and geologically) porosity prediction and resolution was produced by the trend cascaded PNN. This method also best modeled the higher frequency changes within the Smackover Formation in the trained wells (Fig. 27a).

Furthermore, comparison of PhiH (porosity thickness) maps calculated from all four porosity volumes (using a cut off of 8%) shows that the PNN trend-cascaded map best represents thickness distribution (Fig. 29). Below are some probable reasons for differences in predicted and actual porosity thickness:

- Resolution: From crossplots, histograms of predicted and actual porosity, and maximum porosity maps created for the Smackover Formation we observed that all methods do not predict the absolute range of porosity captured by logs (Figs. 25b, 26b, 27b, 28b, 30, & 31). This can be related, at least in part, to the resolution of the logs. Most high porosity

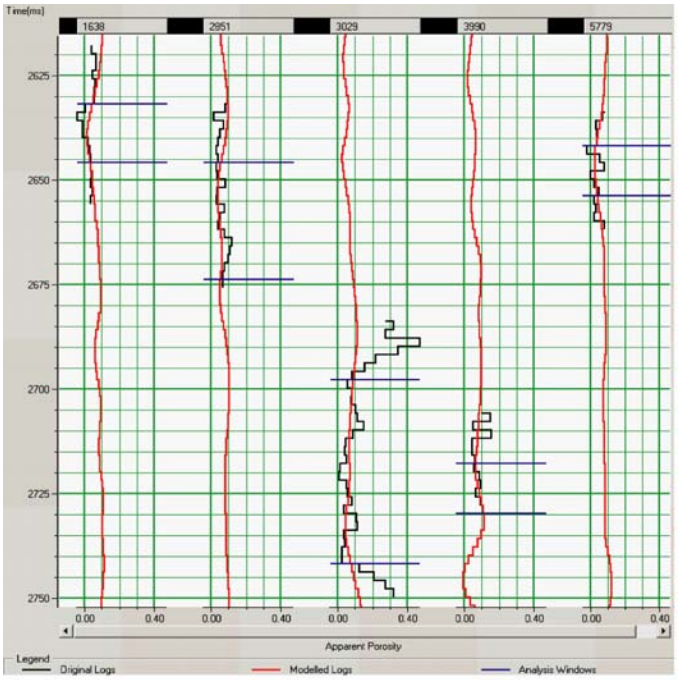

(a)

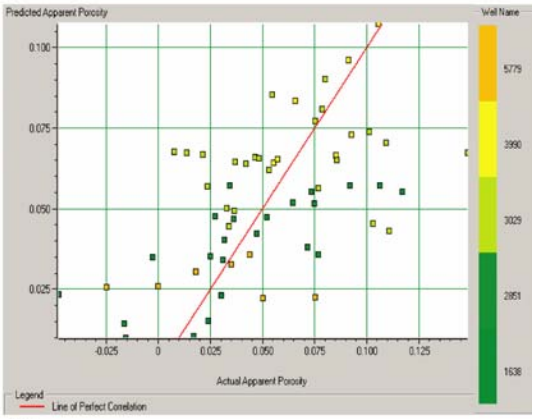

(b)

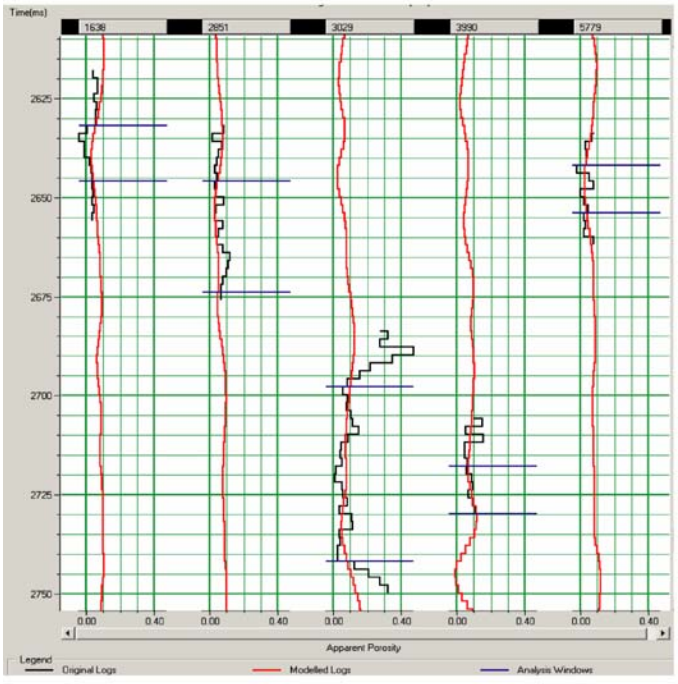

(c)

Figure 25: Visual correlation of actual and modeled porosity using MLR, a) on application of multiattribute equation, and b) on cross-plotting actual vs. predicted porosity values. Note the difference in range of actual and predicted porosity. c) Shows how accurately the porosity at each well can be modeled using the derived empirical relationship, when that well is excluded from the analysis. Porosity increases to the right of the curve.

Table 8: Table of correlation coefficients and average errors to evaluate performance of multiattribute transforms from the different analytical methods used in analysis. Best method determined by high correlation coefficients and correspondingly low average errors.

Analytical Method	Corr. Coeff. on Application	Average Error	Corr. Coeff. on validation	Average Error
Linear regression	0.46028	0.0339616	-	-
Multilinear regression	0.56333	0.0316073	0.44699	0.034657
No Trend PNN	0.72437	0.0270095	0.44425	0.034484
MLFN	0.73498	0.0259411	0.45239	0.037869
Trend PNN	0.87894	0.0189337	0.54557	0.033390

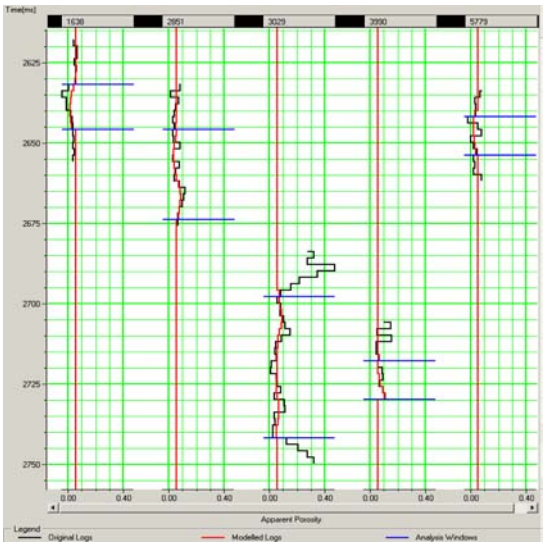

(a)

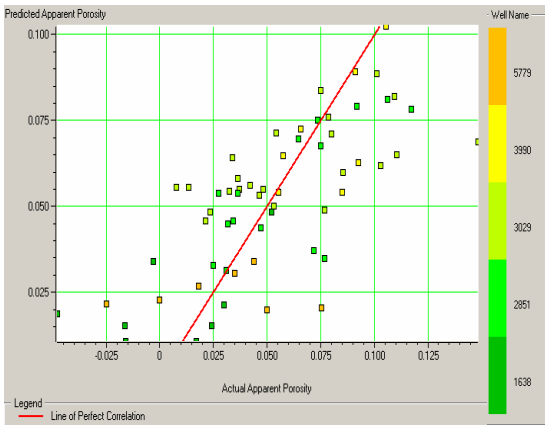

(b)

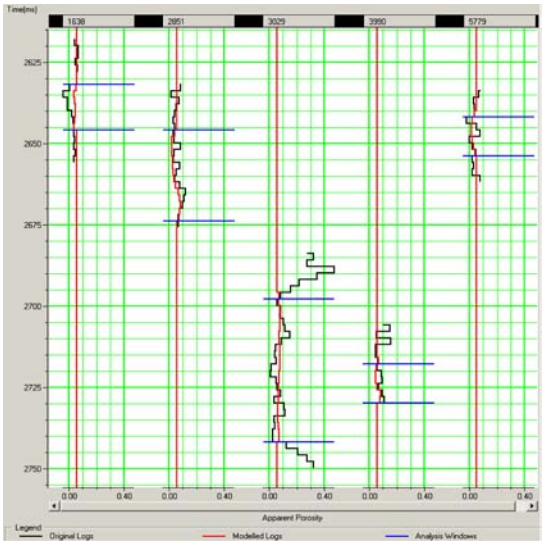

(c)

Figure 26: Visual correlation of actual and modeled porosity using a no trend-cascading PNN, a) on application of PNN results using all wells, and b) on cross-plotting actual vs. predicted porosity values. Also note the differences in range of actual and predicted porosity. c) Shows how accurately the porosity at each well can be modeled using the derived empirical relationship, when that well is excluded from the analysis. Porosity increases to the right of the curve.

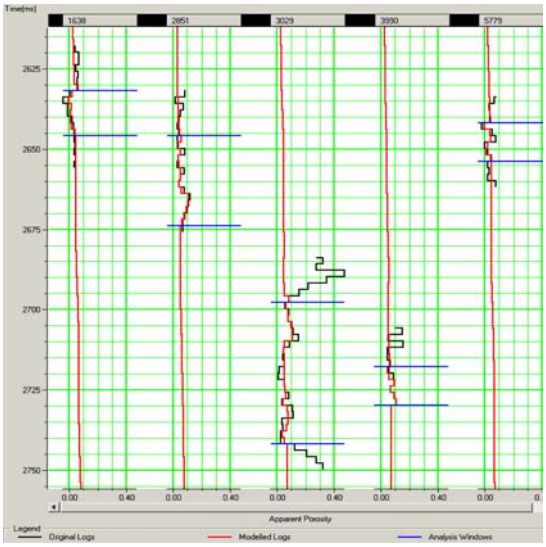

(a)

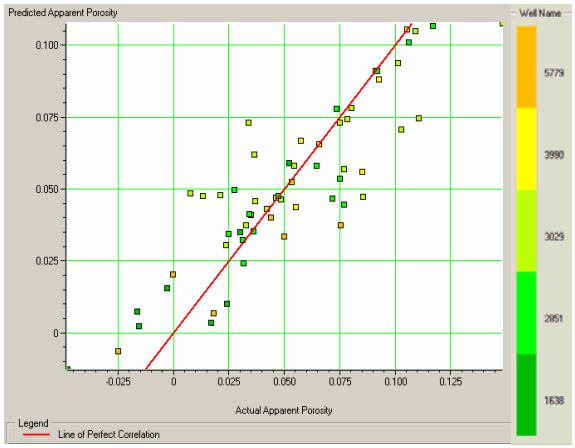

(b)

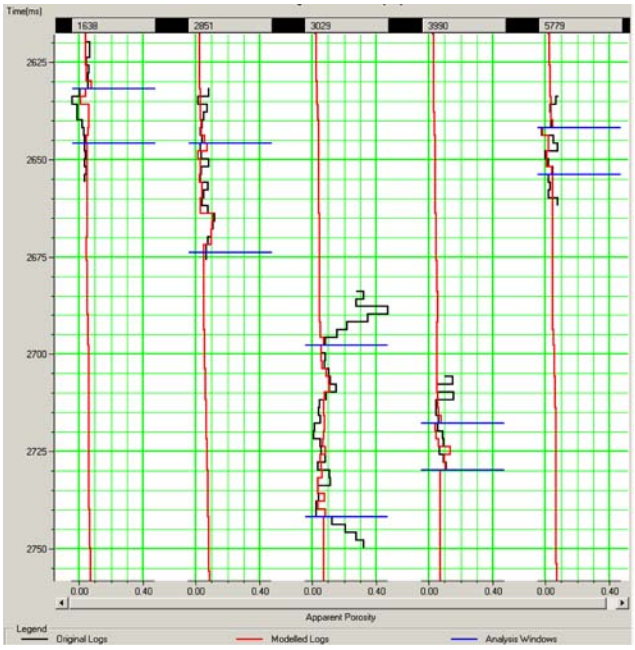

(c)

Figure 27: Visual correlation of actual and modeled porosity using the MLR trend-cascading PNN, a) on application of results using all wells, and b) on cross-plotting actual vs. predicted porosity values. Also note the difference in range of actual and predicted porosity. c) Shows the accuracy of porosity prediction at each well using the derived empirical relationship, when that well is excluded from the analysis. Porosity increases to the right of the curve. Note how ell this PNN-derived relationship captures subtle changes in porosity within the analysis window when compared to other methods.

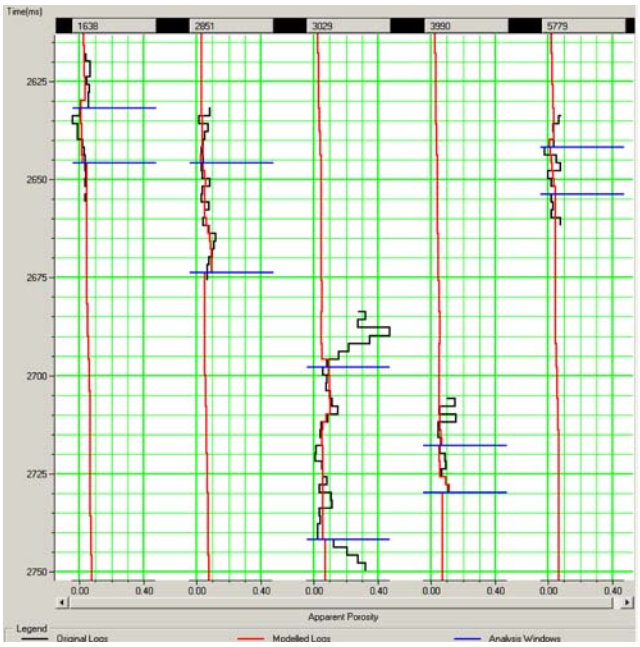

(a)

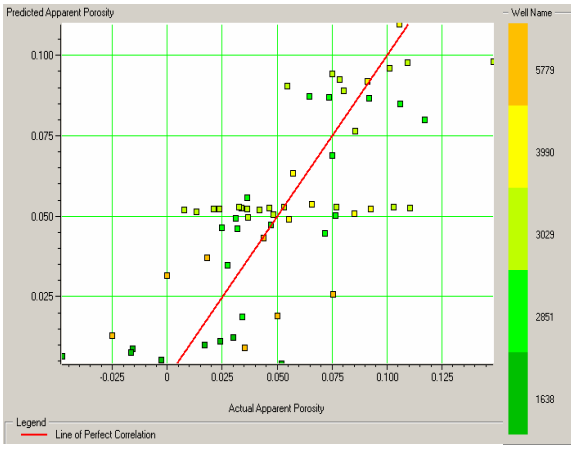

(b)

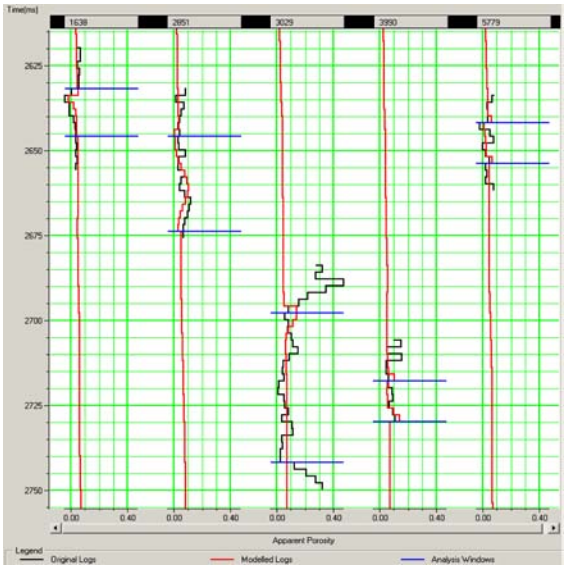

(c)

Figure 28: Visual correlation of actual and modeled porosity using MLFN. (a) on application of MLFN results using all wells, and b) on cross-plotting actual vs. predicted porosity values. Also note the difference in range of actual and predicted porosity. c) Shows how accurately the porosity at each well can be modeled using the derived empirical relationship, when that well is excluded from the analysis. Note how poorly the derived relationship models subtle changes in porosity within the analysis window, especially at well 3029. Porosity increases to the right of the curve.

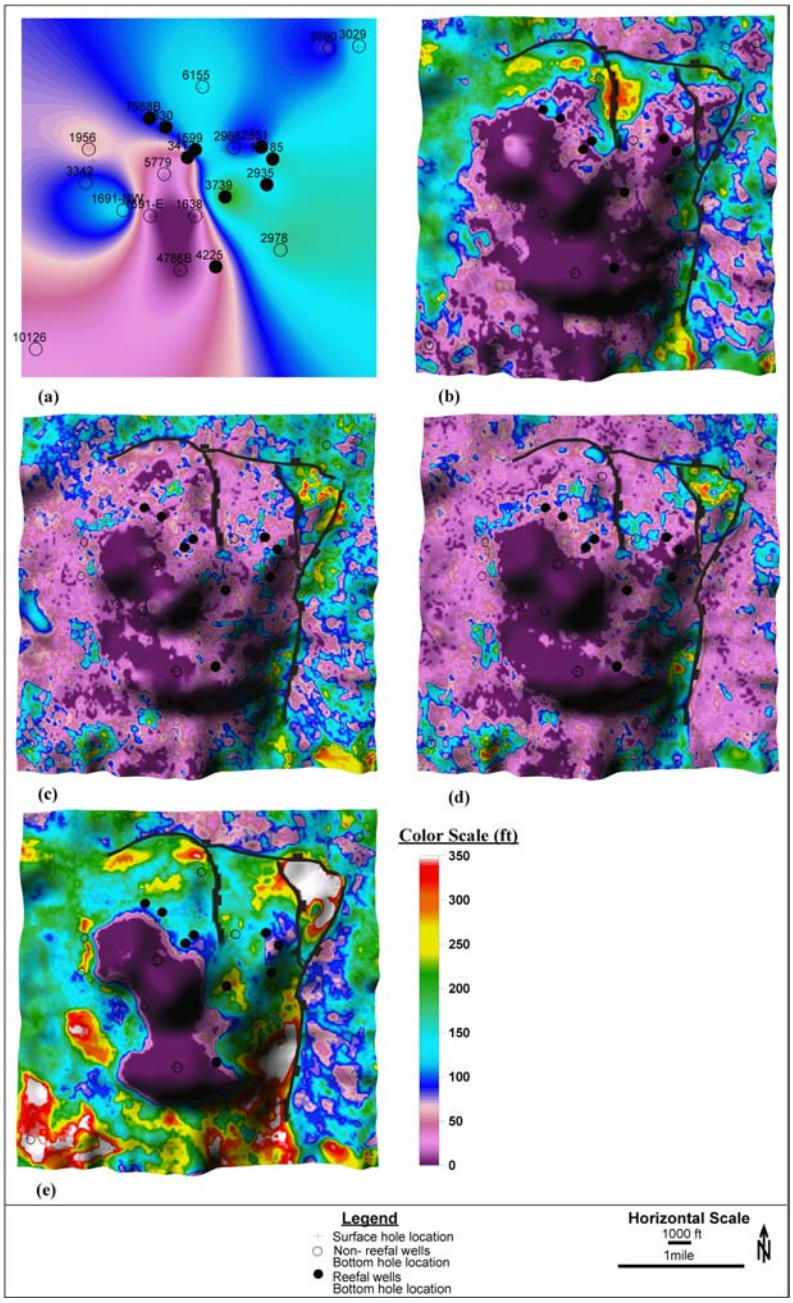

Figure 29: Porosity thickness map of the Smackover Formation overlain on the Buckner/Smackover depth-structure map for better display; a) based on contouring of wells only, b) MLR result, c) MLR trend-cascading PNN result, d) no trend cascaded PNN, and e) MLFN. Note the overall lack of porosity at the crests of structure, and thicker porosity to the flanks of structure and along faults. Also note the prediction of high/thick porosity zones associated with faults in eastern part of the study area. Observed differences in the distribution of porosity are mainly a result of the method used.

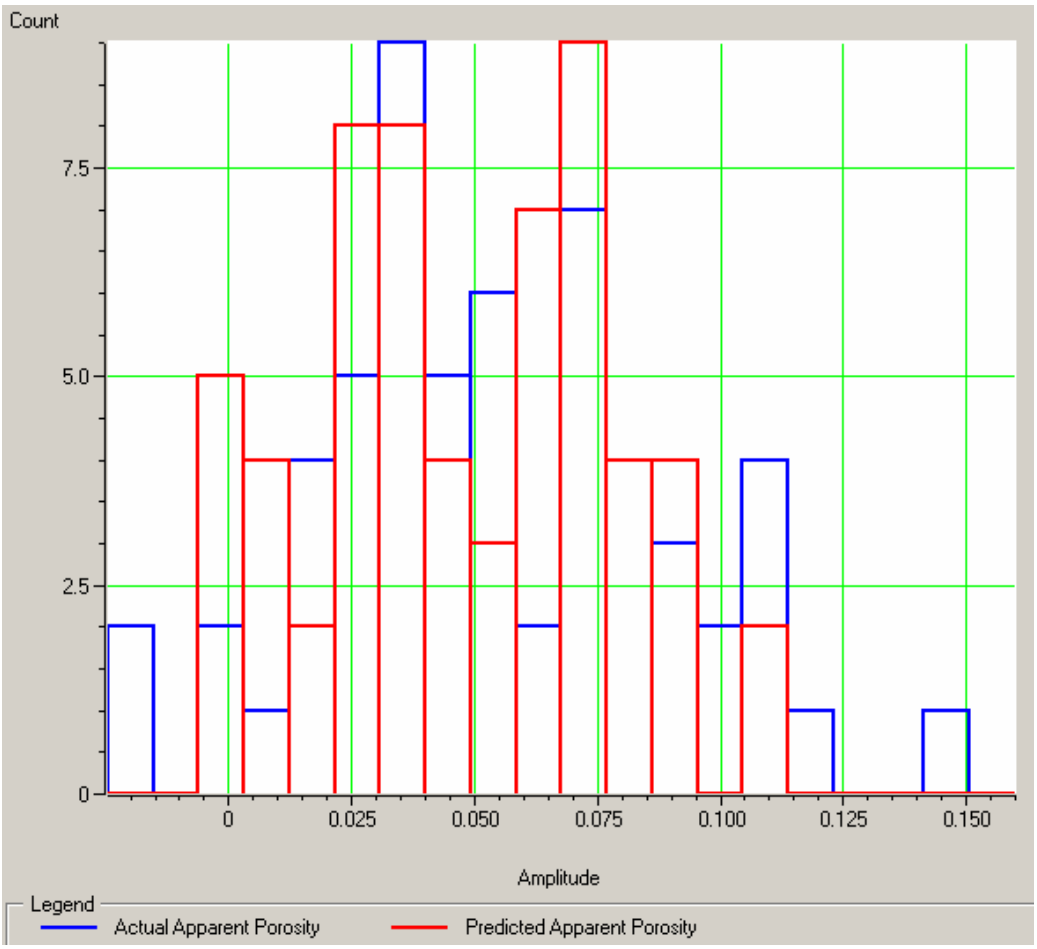

Figure 30: Histogram comparing the actual range of porosity values and those predicted using the MLR trend-cascaded PNN method (statistically and geologically preferred method).

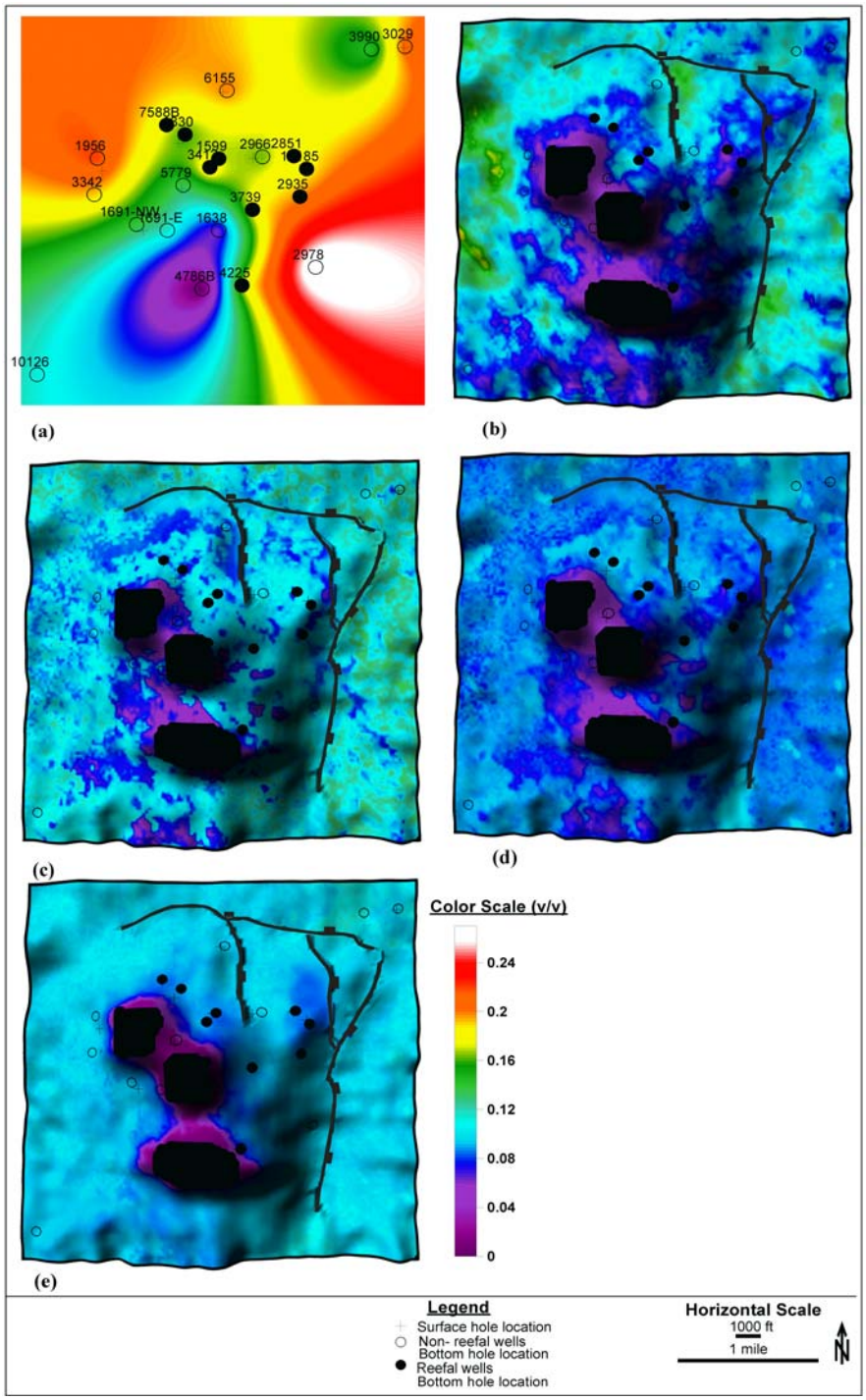

Figure 31: Maps showing the maximum porosity for the Smackover Formation. a) based only on contouring of well data, b) MLR result, c) MLR trend-cascaded PNN result, d) conventional PNN result, e) MLFN result. Note how low these are compared to actual porosity values at well locations.

intervals are very thin. As a result, these zones are "lost" when the logs are converted to time and resampled at 2ms (same as seismic data) by the Hampson-Russell software. The relatively high velocity of the rocks in this area (velocity of the Smackover Formation approximately 19,000 ft/s) acts to decrease the resolution (wavelength = velocity/frequency).

- Sampling bias: We could only use 6 of the 22 wells in the study area because only these six wells could be adequately tied to the seismic data (Section 3.2). These six wells did not capture the full range of porosity in the study area. For example, the well with the highest apparent porosity, 2978 (>27%) and that with the thickest porosity, 3739, were not used in the analysis. Accordingly, we anticipate that sampling bias could have affected the nature of the empirical relationships (MLR or neural networks) that were established between porosity and seismic attributes.
- Method of calculation: Because PhiH is calculated for the Smackover Formation, discrepancies in seismic picks (compare Figs. 32a & b) or log picks are bound to introduce some degree of error in the calculated thickness maps. We note that the base of the Smackover was not picked in some wells (1599, 2966, 4786B, and 7588B) although examination of the logs suggest that it may have been present. Some other wells (2966, 3990 and 3412) TD in the Smackover and so a true value of PhiH cannot be calculated for them.

Powers (1990) suggested that the distribution of porosity in the Smackover at Vocation Field resembles a 'halo', with non-productive wells in the supratidal deposits immediately surrounding paleohighs; productive wells spanning the lagoonal to supratidal areas, and more non-productive wells in the deeper basin away from paleohighs. The trend-cascaded PNN thickness map most closely models this trend (Fig. 29c).

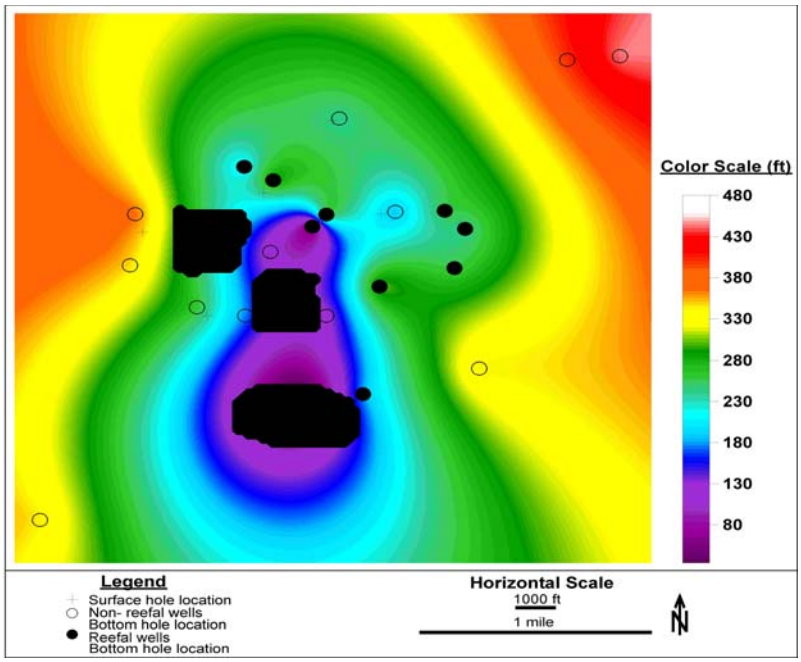

(a)

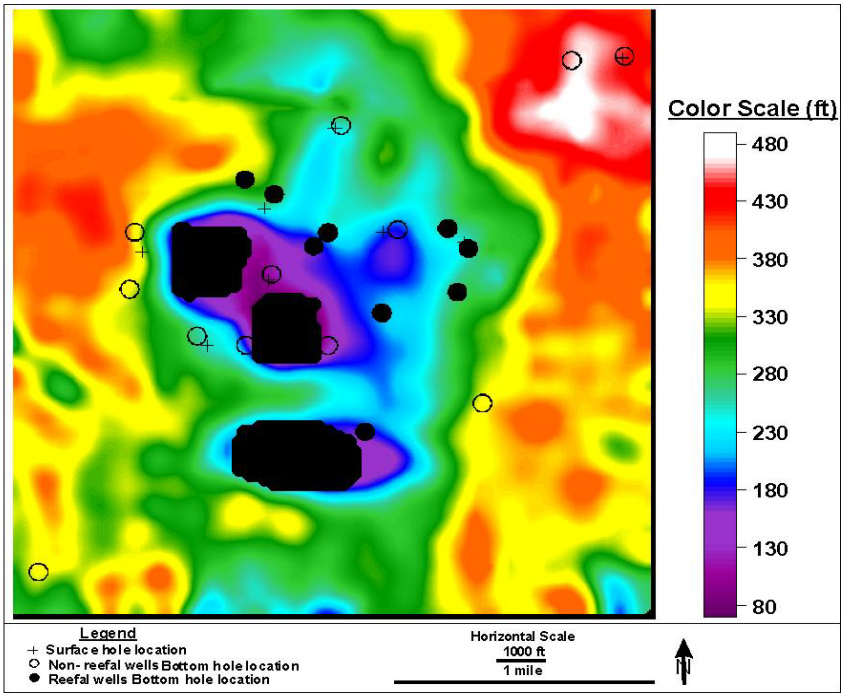

(b)

Figure 32: a) Well-based and b) 3-D seismic-based isopach maps for the Smackover. This thickness maps shows that the Smackover Formation thickens away from paleohighs, a trend most closely followed by Figure 29c. See Figure 17 for identification of wells.

Slices at 2ms intervals into the Porous Smackover (microbial reef) show that reef growth in this field, and as in the Appleton Field (see Section 2), is governed primarily by water depth and the presence of paleostructure. These slices depict reef growth from near basinal depth, at lower sea levels, to progressively shallower water depths as sea level rose in the Oxfordian (10 ms to 0 ms). This trend is most observed at wells 3739 and 11185 that are structurally lowest and highest respectively (Fig. 33). Furthermore, well 11185 is presently the only producing well at the Vocation Field (Mancini, 2002) due its location on the crest of low relief structure, high porosity thickness, and being surrounded by thick porous intervals. Reef growth and porosity development in the Smackover at Vocation Field is further highlighted by W-E transects through both the seismic and PNN trend-cascaded porosity volume, which also show the presence of shoal-derived porosity in the upper Smackover directly beneath the Buckner/Smackover horizon and microbial reefs flanking the paleohighs (e.g., Fig. 34).

The relationships seen between zones of high porosity and faults in all thickness maps might indicate that faults served as conduits for dolomitizing fluids (Figs. 29 & 31). Although none of the wells used in the Emerge analysis penetrate these areas, the 2978 well, which has the highest porosity of the wells available to us, is in or adjacent to one of these zones (Figs. 29 and 31). More significantly, this well has no reefal facies (Table 4) and so porosity must not be associated with this primary depositional facies. Hydrothermal dolomitization, which produced porosity and permeability in tight basinal limestones of units like the Trenton-Black River interval of the Appalachian Basin, could be present in this area. Whatever its origin, we consider the presence of high porosity in the 2978 well as supporting the attribute-based porosity prediction.

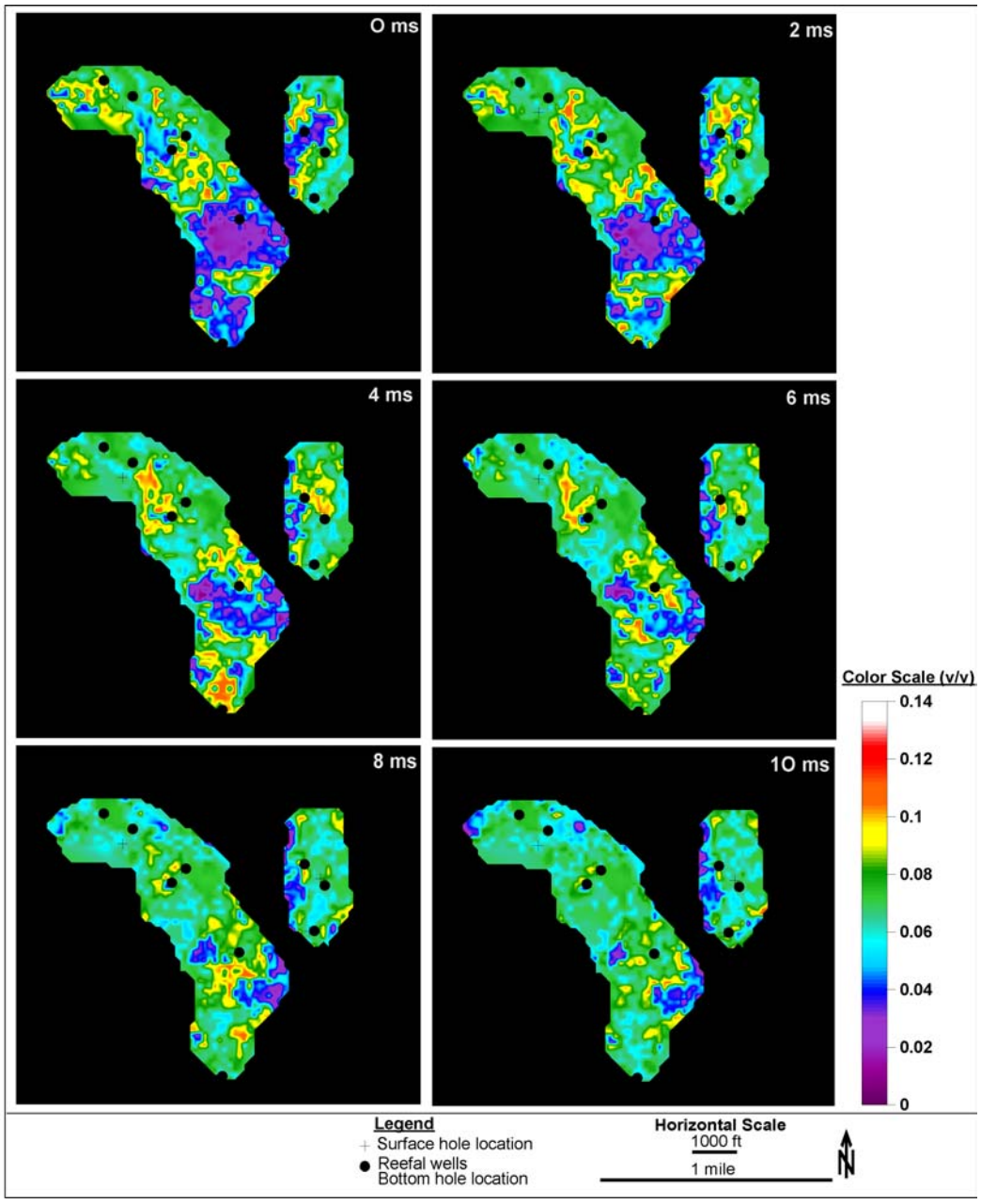

Figure 33: Slices through the porosity volume (porosity values are in decimals, v/v), starting at the porous Smackover pick. Porosity above this pick was attributed to shoal grainstone facies, which constitute the other major reservoir facies in the Vocation and Appleton Fields. The overall distribution of porosity in this interval is intricately related to structure (see Figure 21b), which we have attributed primarily to conditions related to reef growth. See Figure 17 for well permit numbers.

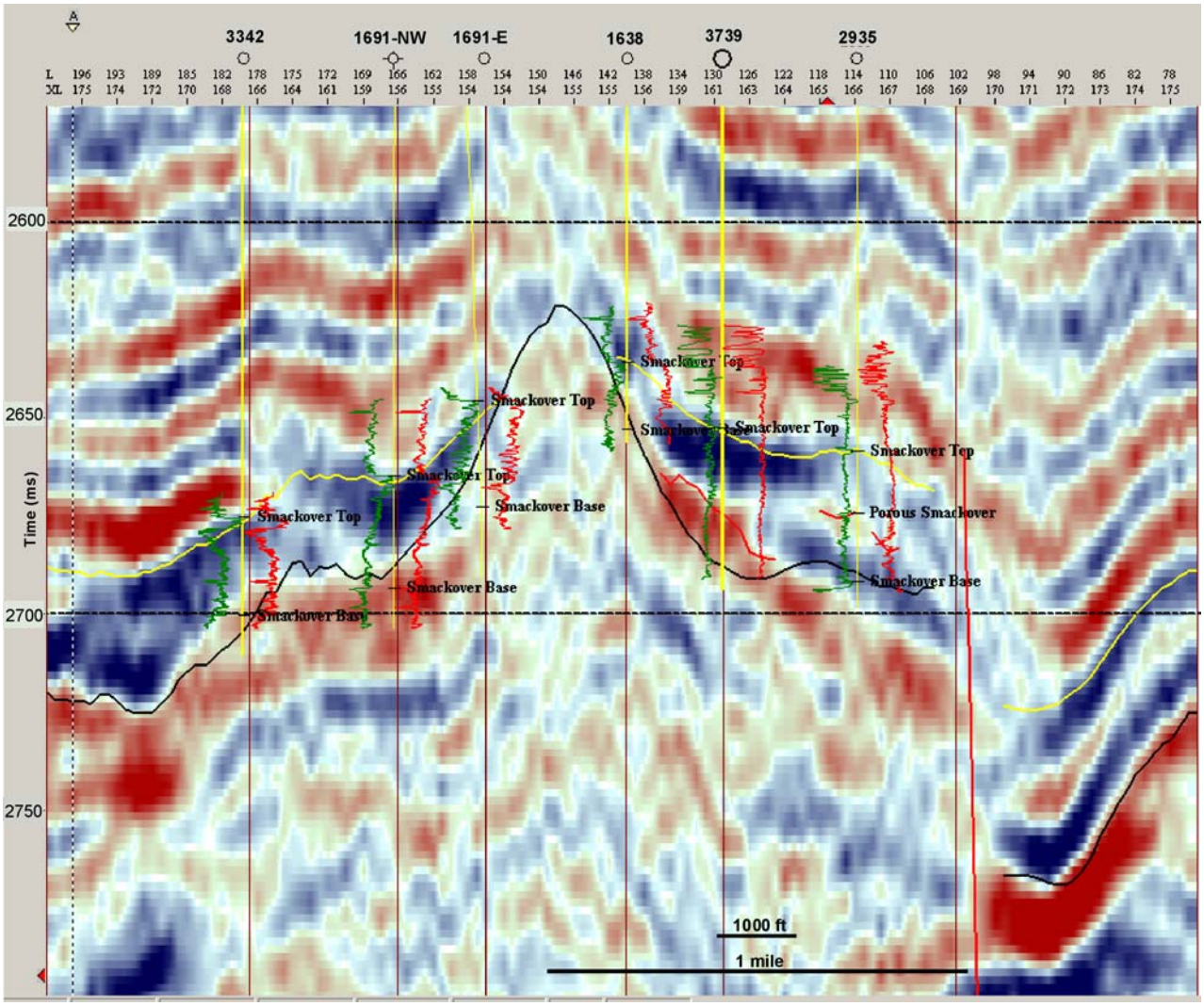
3342
1691-NW
1691-E
1638
3739
2935
2600
2650
2700
2750
Time (ms)
Smackover Top
Smackover Base
Porous Smackover
1000 ft
1 mile

(a)

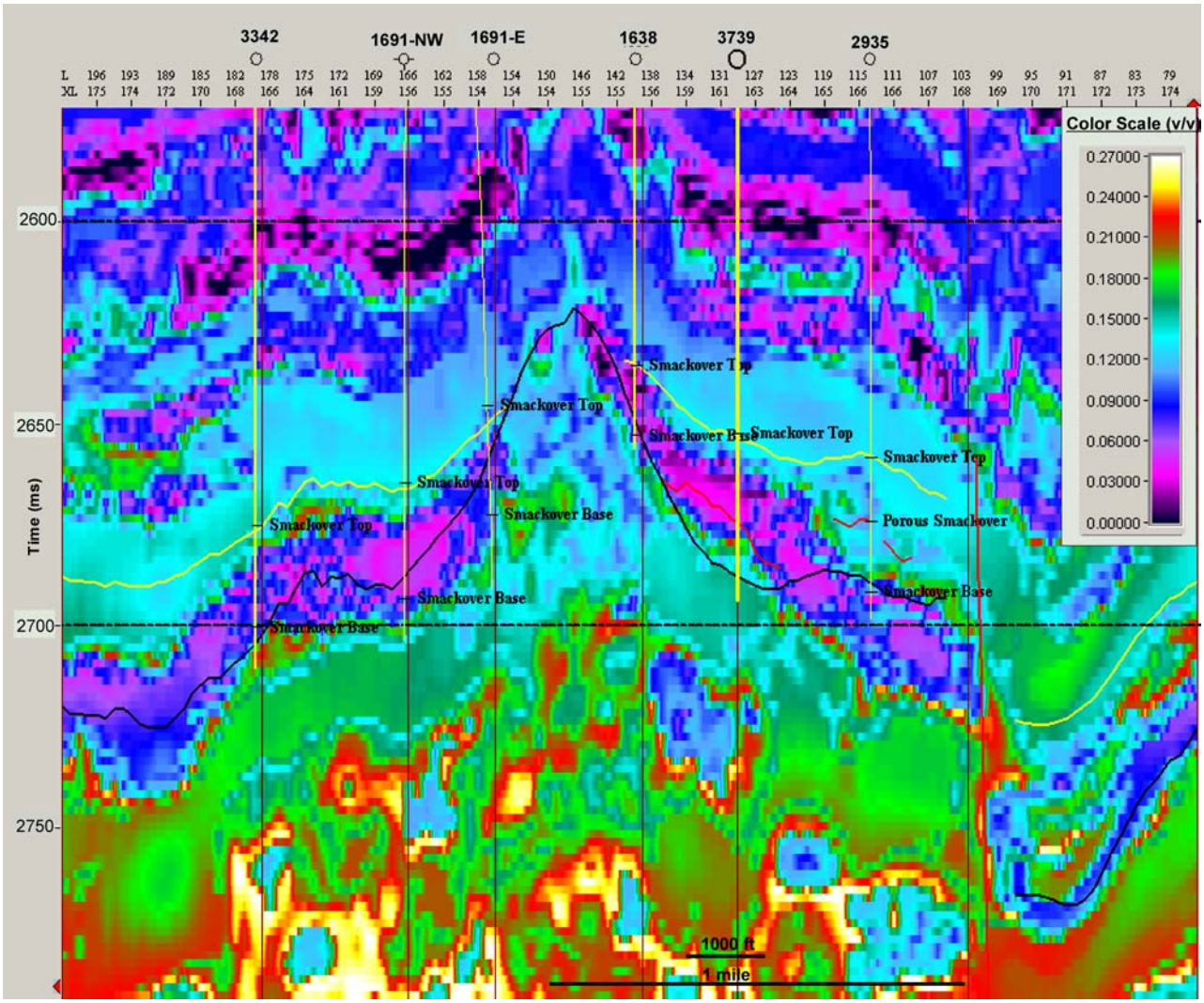

(b)

Figure 34: W-E transects across Vocation Field (A-A'). a) Original amplitude data shows horizon picks and seismic character of the mapped formations (red = trough, blue = peak). Note location of porous (reef) Smackover on flanks of paleostructure. b) Section through the MLR trend-cascaded PNN porosity volume shows a preference for higher porosities (hot colors) to be on the seaward flanks of structure, and also around faults. High porosity directly below the Buckner/Smackover pick is attributed to the shoal grainstone facies. Note porosity predictions are valid only within the Smackover Formation. Transect location shown in Figure 21a.

Conclusions

- As with Appleton Field, porosity and porosity thickness in the Smackover Formation at Vocation Field can be determined using attribute studies.
- Data availability and quality issues prevented us from generating a porosity volume that captures all of the variability observed in wells. Nevertheless, the porosity predictions appear geologically reasonable and have a good statistical basis. There are reasonable physical bases for the empirically derived relationships we established between the three attributes used and porosity.
- A trend-cascaded probabilistic neural network, a new addition to the Hampson-Russell software, best captured fine-scale vertical variations in porosity and gave the most geologically reasonable result.
- Reef growth, and porosity development in general, is primarily a function of water depth, which is in turn governed by sea level fluctuation and height of paleobasement structure.
- Faulting in the east and north of Vocation Field may have served as conduits for dolomitizing fluids. This suggestion is supported by data from the 2978 well, a well not included in the seismic attribute analyses.

Task 3—Reservoir Characterization (Petrophysical).--The mapping and ranking of flow units in the reservoirs at Appleton and Vocation Fields have been done by Morgan and Ahr at Texas A&M. The work described below is from Morgan's (2003) thesis at Texas A&M University.

Flow units in the Smackover Formation at Vocation and Appleton Fields were identified, mapped, and ranked. Pore categories by origin, pore and pore throat geometries, pore-scale

diagenetic history, and core-scale depositional attributes were logged using conventional petrographic and lithological methods and advanced techniques. Resulting data were combined with core descriptions, mercury-injection capillary pressure data, and wireline log data to produce flow unit maps at the field scale.

Appleton and Vocation Fields produce from grainstone buildups and microbial reefs. Specific microbial fabrics were found to have significant influence on pore facies and flow unit quality rankings and ultimately on reservoir quality in these fields. Microbial reefs are composed of five fabric categories and growth forms that reflect variations in water geochemistry, energy level, sedimentation rate and substrate type. They include Type I layered thrombolite with characteristic mm/cm-scale crypts, Type II reticulate and "chaotic" thrombolite, Type III dendroidal thrombolite, Type IV isolated stromatolitic crusts, and Type V oncoidal packstone/grainstone dominated by oncoids that grew on soft to firm substrates in high-energy conditions. Types I, II and III buildups are the most productive reservoirs. Of these, Type III thrombolite buildups contain the highest quality reservoir rocks, which consist of extensively dolomitized dendroidal fabrics that have well-connected intercrystalline dolomite and vuggy porosity. Types IV and V microbialites make poor reservoir rocks because Type IV fabrics are not conducive for communication throughout this facies, and Type V oncoidal facies exhibit isolated moldic and vuggy porosity with low to moderate permeability.

Relationships Between Porosity, Permeability and Median Pore Throat Sizes

The correlation of median pore aperture size (MPA) (Tables 9 and 10) to mercury permeability (K) (Fig. 35) is moderately strong ($R^2 = 0.91$). This correlation suggests that pore aperture size has a direct link to permeability distribution. One observation from Figure 35 is that reef and solution enhanced pore types tend to have larger pore apertures and higher permeability

values. A second observation is that multiple pore types tend to increase pore throat size and permeability, suggesting that there may be more than one mechanism which controls pore throat size and permeability. Combining these observations, one can see that the pore type has significant impact on permeability distribution.

Table 9. Common pore type associations in the MICP sample set, with the average porosity and MPA.

Common pore type associations	Average sample porosities (%)	Average MPA (μm)
interparticle (IP), intraparticle (IPA)	9.65	14.9
interparticle, intraparticle, moldic (M)	7.2	30
interparticle, cement reduced intercrystalline (CRIC)	4.3	1.19
reef (R), solution enhanced intercrystalline (SEIC)	20.0	12.6
reef, solution enhanced interparticle (SEIP), moldic, solution enhanced intercrystalline	12.0	8.09
reef, intercrystalline, cement reduced intercrystalline	4.1	8. 39
reef, solution enhanced interparticle, solution enhanced intercrystalline, moldic, vuggy (V)	15.4	20.63

Table 10. MICP data set: plugs chosen for MICP and measurements.

Well permit #	Core depth	Pore types	Facies type	Hg median pore aperture (mm)	Hg % porosity	Hg permeability (md)
1599	13,987.0	IP, IPA, M	oolitic gs	30	7.2	210
2935	14,078.0	IP, CRIC	peloidal gs	1.19	4.3	0.396
3986	12,970.0	R, SEIP, SEIC, M, V	Type III reef	21.9	14.4	280
3986	12,999.0	R, SEIP, SEIC, M, V	Type II reef	26.10	15.1	410
3986	13,024.0	R, IC, CRIC	Type I reef	8.93	4.1	17.6
4633-B	12,948.0	R, SEIP, M, SEIC	Type III reef	8.09	12.0	44.8
4633-B	12,969.0	R, SEIC	Type I reef	12.6	20.0	196
4633-B	12,984.0	R, SEIP, SEIC, M, V	Type II reef	13.9	16.7	225
5779	13,946.0	IP, IPA	oolitic gs	14.9	9.65	86.7

The correlation of mercury (Hg) permeability (K) to core analysis (CA) permeability (Fig. 36), shows a moderate correlation ($R^2 = 0.62$). The difference in correlation values likely is due to the difference in data sampling since the core analysis is taken at one point every half foot and the mercury derived sample is from plugs at exact depths selected from thin section observations. Since there is a higher variability in the core analysis permeability values that were sampled, a

range of permeability values within a two-foot interval of the mercury-injection capillary pressure (MICP) data depth is shown in the graph.

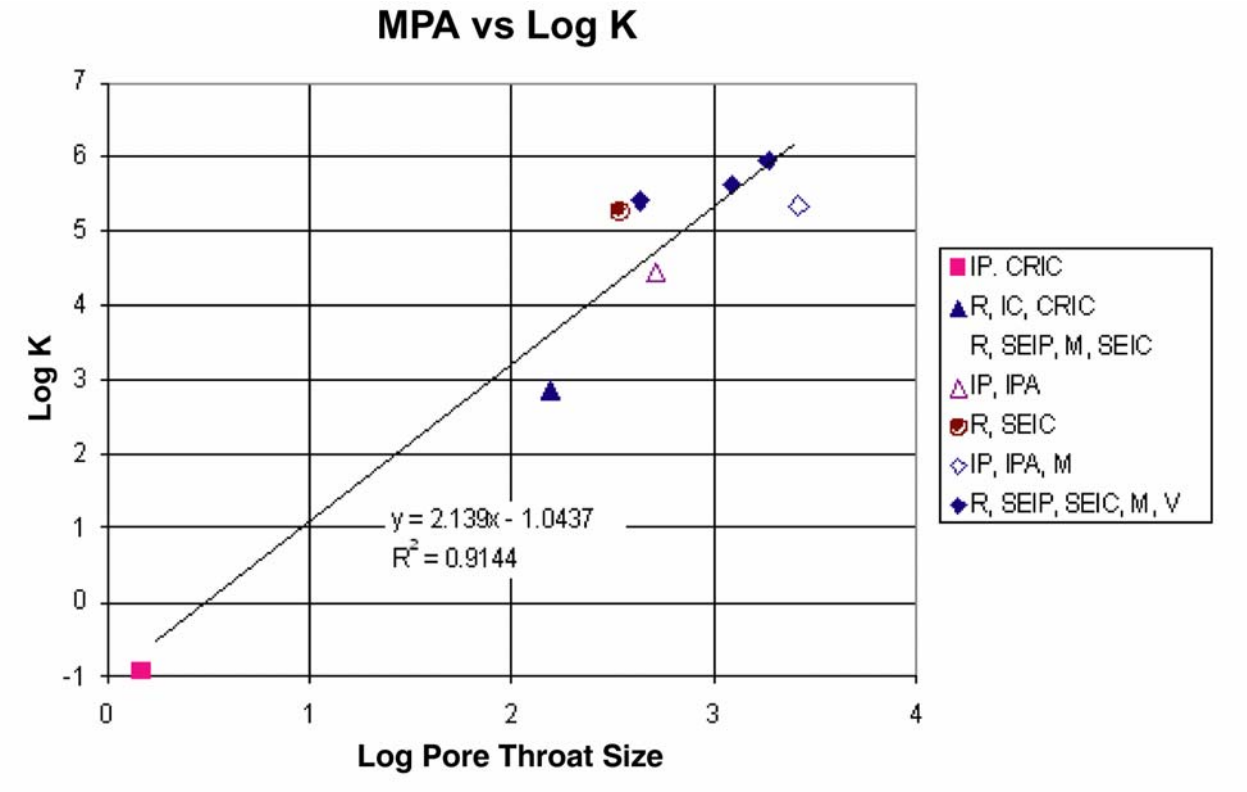

Figure 35. Comparison of median pore aperture size (MPA) and permeability (K).

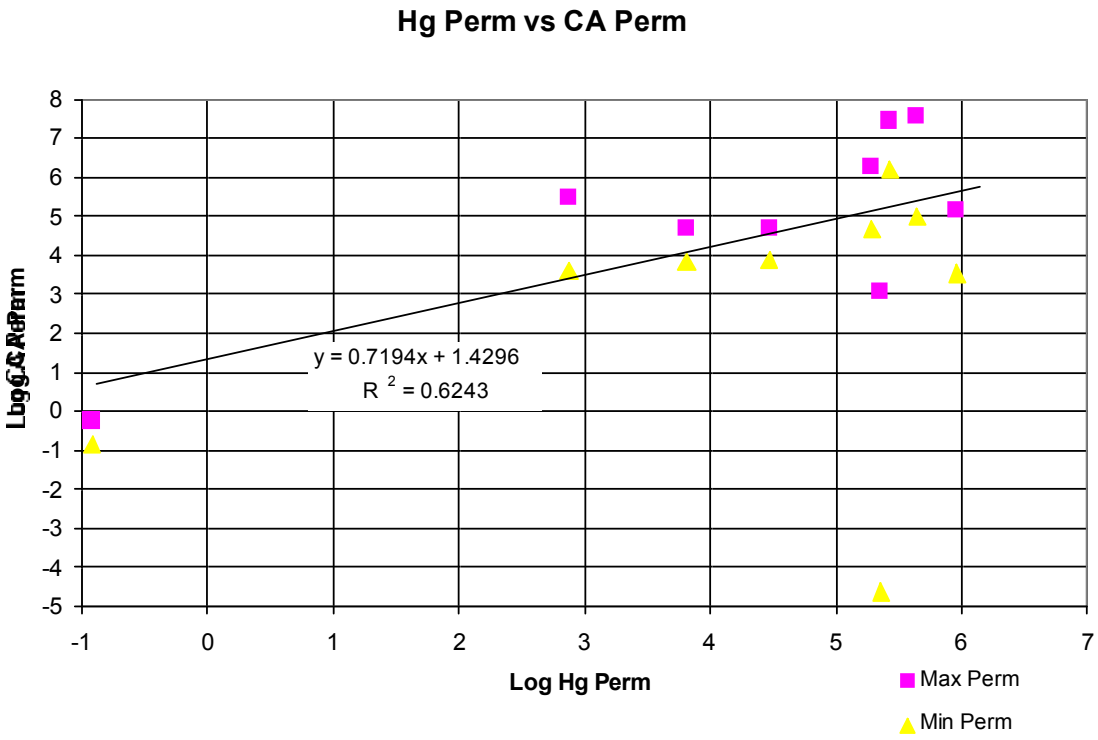

Figure 36. Comparison of mercury derived (Hg) permeability and core analysis (CA) derived permeability. It should be noted that there are two core analysis data points per mercury derived point to account for variability encountered in the interval sampled.

Core analysis porosity and mercury derived porosity was correlated (Fig. 37). This correlation had a moderate correspondence, not quite as strong as the permeability data. The correlation coefficient is due to the difference in sampling intervals.

Results of the MICP data and the corresponding pore types are shown in Table 10. Rocks that contained a combination of reef, solution enhanced interparticle, solution enhanced intercrystalline, moldic and vuggy porosities had the highest reservoir porosities, followed closely by those which also had a combination of some of these types but lacking the solution enhanced interparticle and vuggy porosity. The rocks with the lowest porosities and MPA values contained more than one pore type, but included cement reduced intercrystalline porosity. This

observation suggests that porosity and pore throat size decrease as cement forms in the pore space.

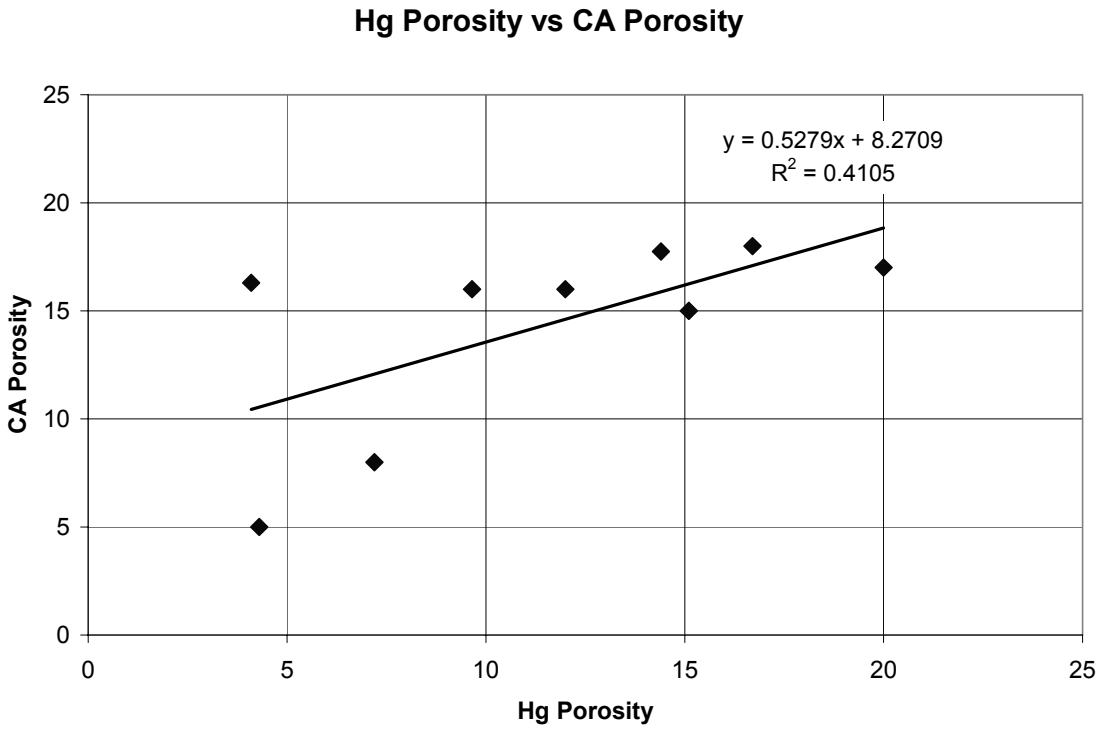

Figure 37. Comparison of mercury (Hg) derived porosity and core analysis (CA) derived porosity.

Using porosity as a predictor for MPA, permeability, or rock type would not be a robust method This is mainly due to the high degree of variability in porosity ranges that correspond to rock types and MPA. The main impact on the variability is the diagenetic overprint in the reservoir which contributes to the wide range of porosities that can be associated with a given MPA or rock type. In order to be able to use porosity as a predictor for MPA and rock type, more samples are required so that a range of porosities and their corresponding MPA and rock types can be established.

Relationship of Petrographic Data to Petrofacies

Porosity and permeability data from core analysis were compared to thin section descriptions to enable the correlation of petrophysical data with the petrologic information. Triaxial (x-y-z) plots were made to establish relationships between porosity-permeability (reservoir quality) and texture, pore types, and diagenetic attributes.

Diagenesis was observed to have had the greatest effect on reservoir quality. The main variable that effects permeability distributions was observed to be pore types in Figure 35. Pore types and porosity were controlled by lithology and grain types. The ranges of porosity and permeability that are associated with the various pore types are shown in Figures 38 and 39.

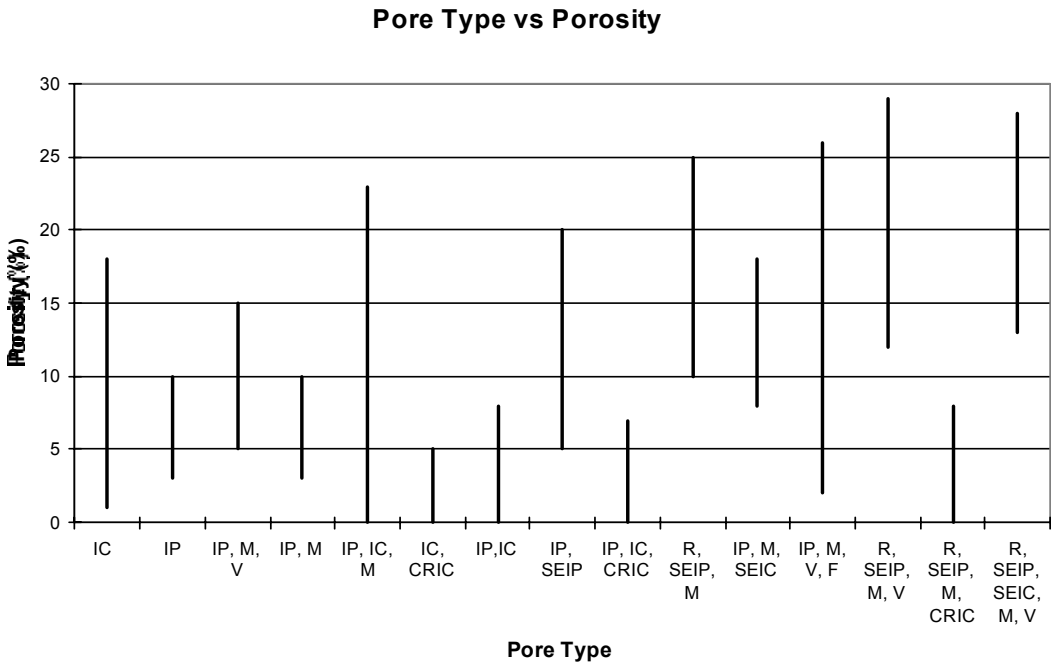

Figure 38. Graph of pore type versus porosity. It should be noted that no one pore type has a porosity range which is distinctive.

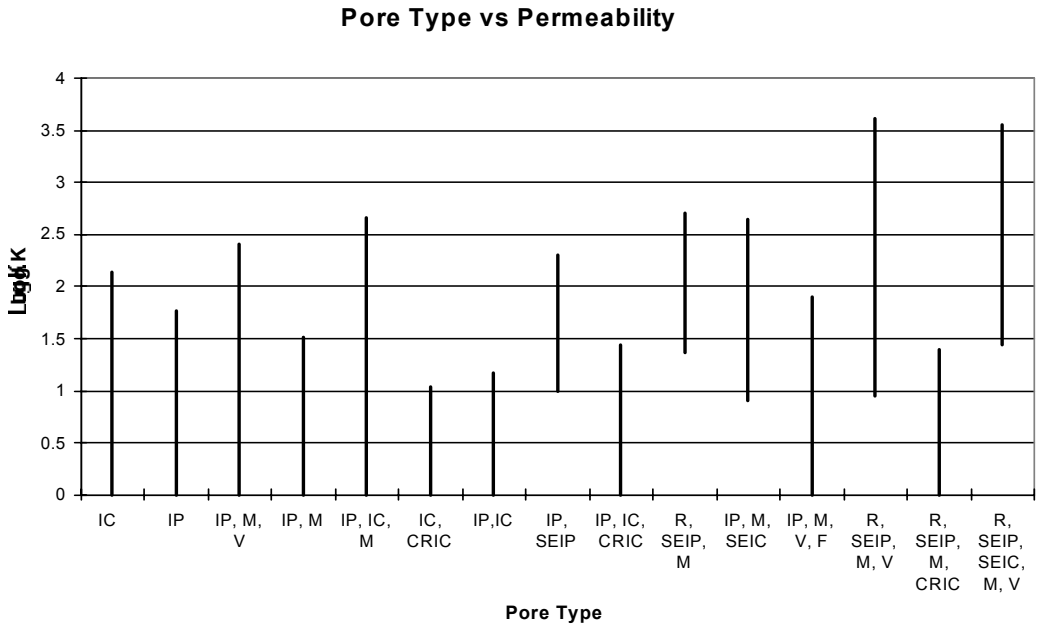

Figure 39. Graph of pore type versus permeability.

One of the advantages of having a set of data such as illustrated in Figures 38 and 39 is that trends can be identified where certain pore types are absent or present. For example, where the process of CRIC was active, porosity and permeability are greatly reduced even though other pore types in the same rock type may be a high-quality reservoir where the CRIC was not active. In some cases, the presence of moldic and vuggy porosity may increase the quality of the reservoir, but permeability may not be increased. A second benefit to graphing pore type versus porosity and permeability is that the graphs can be used as a "proxy" to predict porosity and permeability where no core analysis is available.

Reservoir quality rocks with intercrystalline dolomite porosity tend to be muddier rocks, such as mudstone and wackestone which are in the Vocation Field. The dominant grain type in these lithologies is peloids (if there are any visible grains). Typically there is little to no depositional porosity in these rocks. Thus, for these rocks to have reservoir quality, they must

undergo dissolution and diagenesis. Where these rocks were significantly dolomitized, porosities can be as high as 15 to 20%, with permeabilities of up to 180 md.

Porosity and permeability in grainier carbonates, such as packstone and grainstone, commonly have higher depositional porosity. Grainstone is dominantly oolitic, with some bioclast and oncoid grains. Packstone normally is composed of peloids and oncoids, with ooids as a minor component. These rocks have good depositional interparticle porosities with inter- and intraparticle porosity through dissolution. Moldic and vuggy porosity was also observed in the more diagenetically altered rocks, which exhibited higher porosity. Reservoir grade grainstone and packstone can have porosities that range from 10 to 23% with permeabilities that range from 1 to 620 md.

In nearly all microbial reef rocks, well-interconnected intercrystalline dolomite and vuggy porosity preferentially occurs in association with microbial growth patterns. In general, the porosity and permeability in surrounding mudstone-wackestone are of a high quality because the original lime mud was more densely packed than the microbialite. The thrombolite fabrics (Types I, II, III) produce well connected, intercrystalline porosity. Growth forms also factor into the ultimate reservoir quality. Type I (layered thrombolite) produce medium to coarse intercrystalline dolomite porosity. Core porosity values for Type I microbialite from wells at Appleton and Vocation Fields range from 6 to 23% and permeability values range from 1 to 2000 md. Although these values appear high, the degree of interconnectivity of pores depends on the microbial growth fabric associated with individual horizontal laminae. Individual laminae may have lateral permeability, but this microbial type is only of fair reservoir quality because of poor vertical connectivity. Type II (reticulate-“chaotic”) thrombolite boundstone also produces medium to coarse intercrystalline dolomite porosity, but pore interconnectivity is random, which

is a reflection of the original "chaotic" growth pattern of the microbialite. Porosity values for Type II thrombolites range from 3 to 23% and permeability values range from 0 to 1060 md. There are good reservoir quality zones in Type II buildups, but a predictable pattern is not readily distinguishable. Type III dendroidal thrombolites are characterized by medium to coarse intercrystalline dolomite porosity and vuggy porosity. Porosity values for Type III thrombolites range from 4 to 30% and permeability values range from 0 to 4000 md. The pore interconnectivity in these buildups is very good in both lateral and vertical dimensions because of the branching growth pattern of Type III microbialite. These buildups have the highest reservoir quality of all five types; but as stated earlier, Type III thrombolite buildups only develop on low relief basement structures (e.g., Appleton Field area).

Mapping and Ranking of Flow Units

Contoured "slice maps" of averaged porosity values from core analysis were constructed for each 10-foot stratigraphic interval in the Smackover Formation (Figs. 40-51). Where core analysis was not present, porosity values were calculated from NPHI and DPHI logs. Permeability values corresponding to the porosity values were also averaged and mapped in the same fashion (Figs. 52-63). These maps were then overlain in corresponding depth intervals, and were combined into ranked pairs.

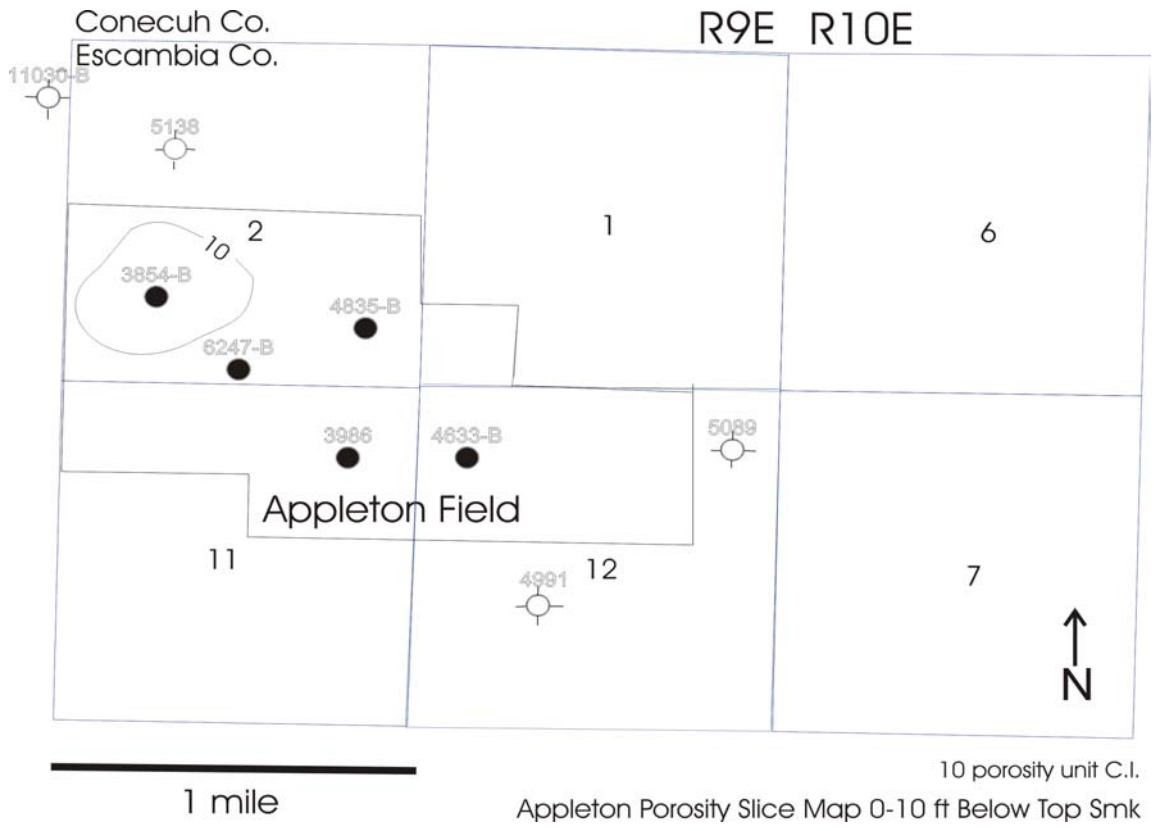

Figure 40. Appleton Porosity Slice Map 0 to 10 ft below Top of Smackover.

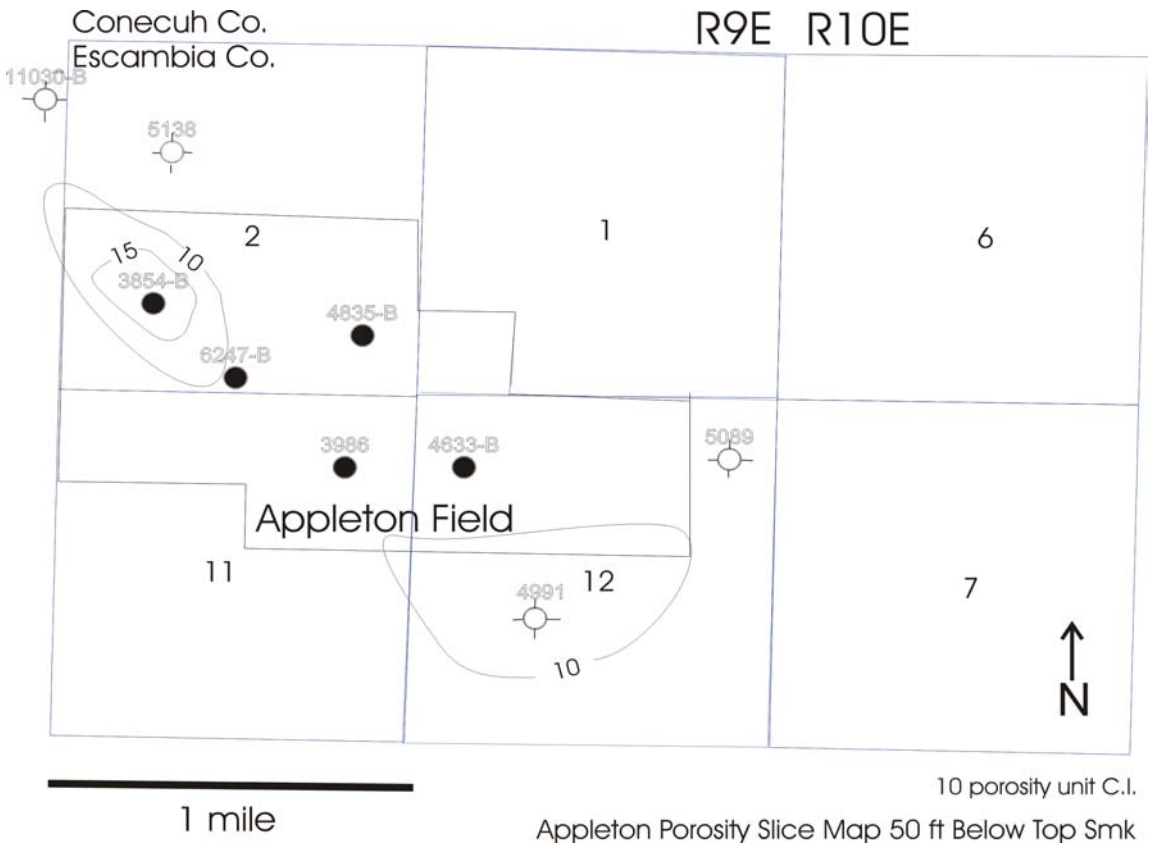

Figure 41. Appleton Porosity Slice Map 50 ft below Top of Smackover.

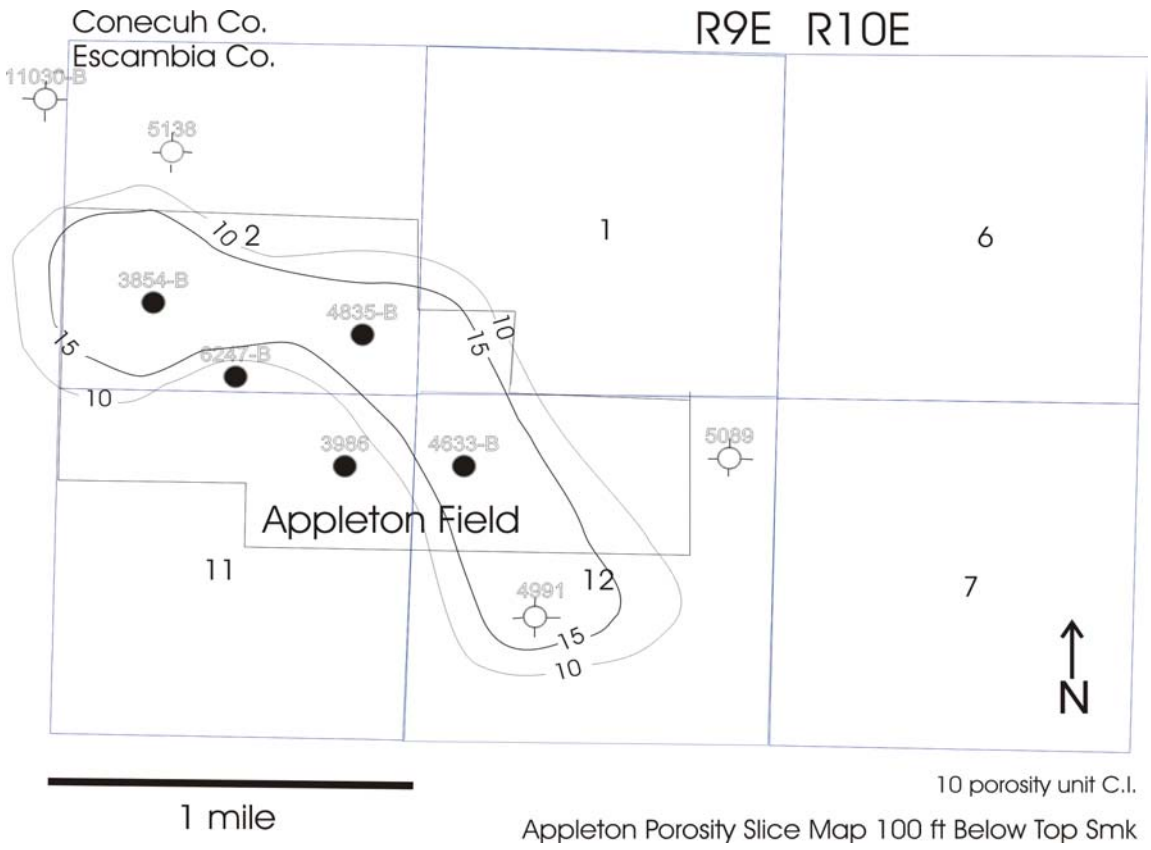

Figure 42. Appleton Porosity Slice Map 100 ft below Top of Smackover.

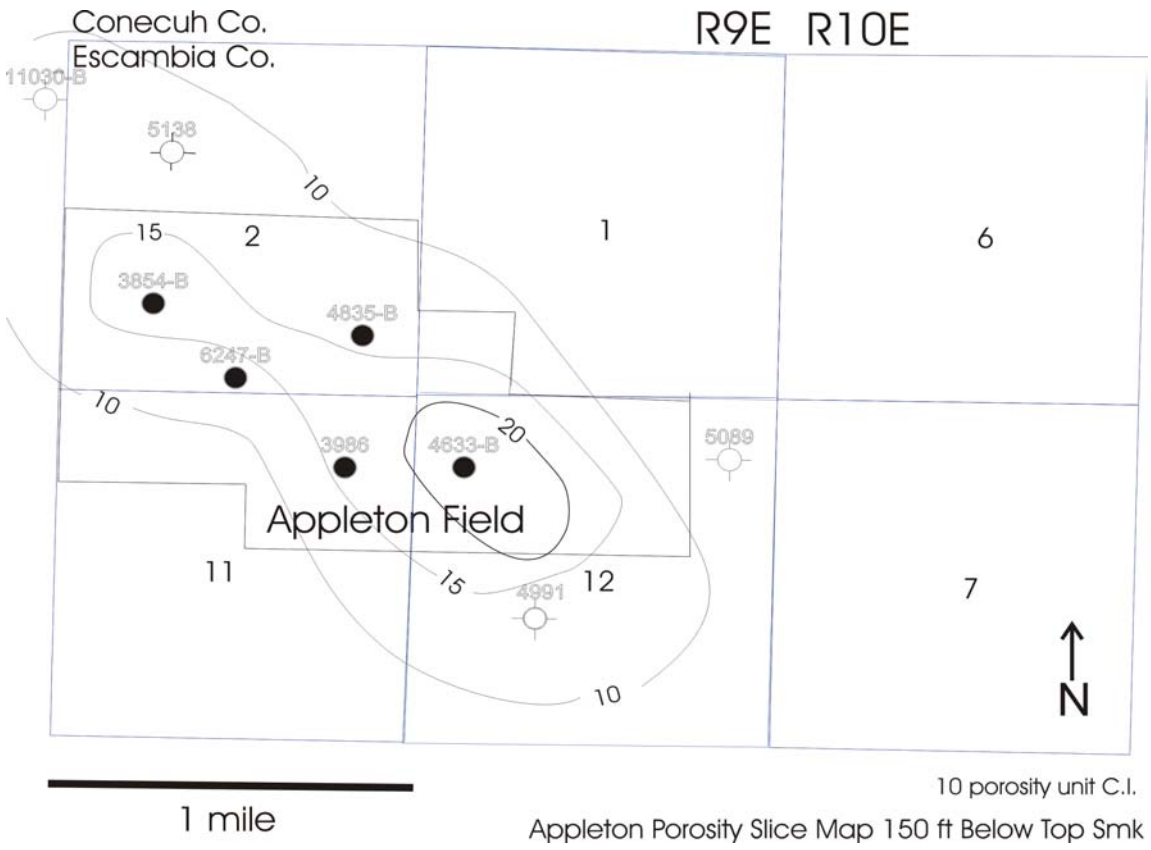

Figure 43. Appleton Porosity Slice Map 150 ft below Top of Smackover.

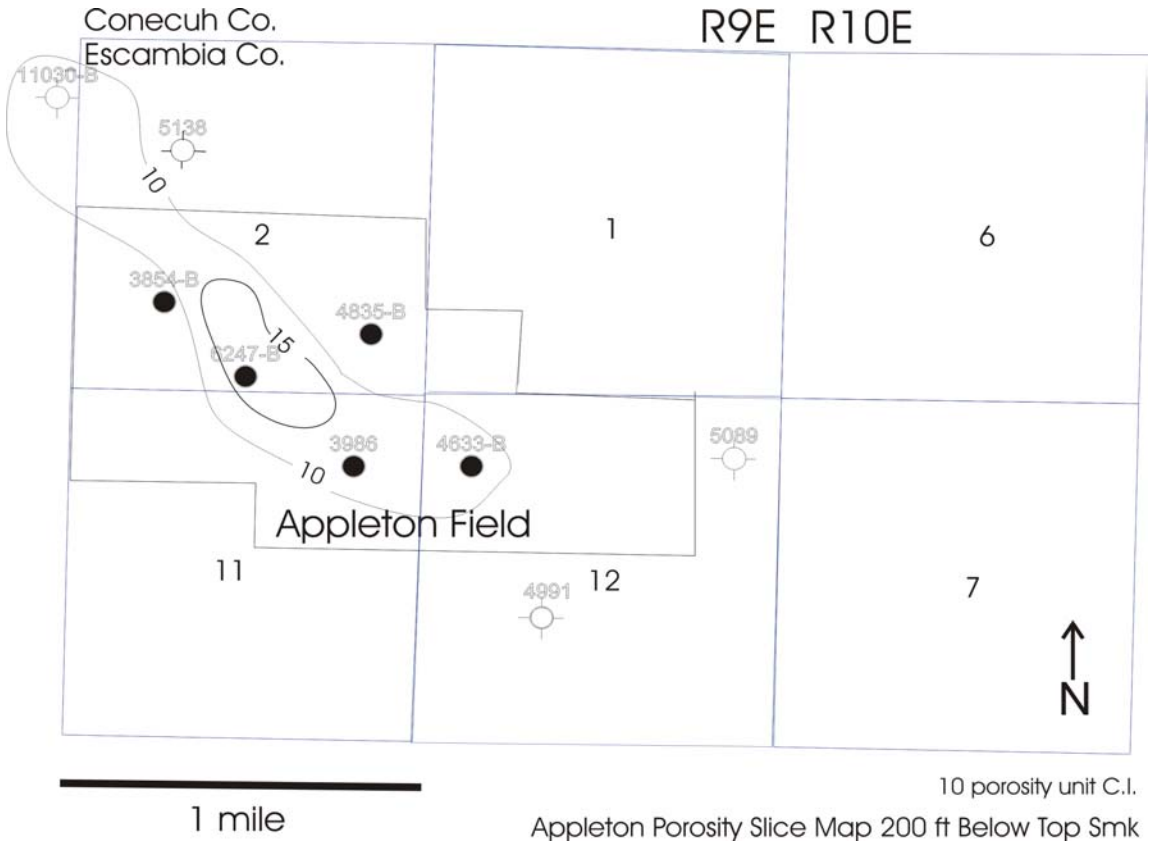

Figure 44. Appleton Porosity Slice Map 200 ft below Top of Smackover.

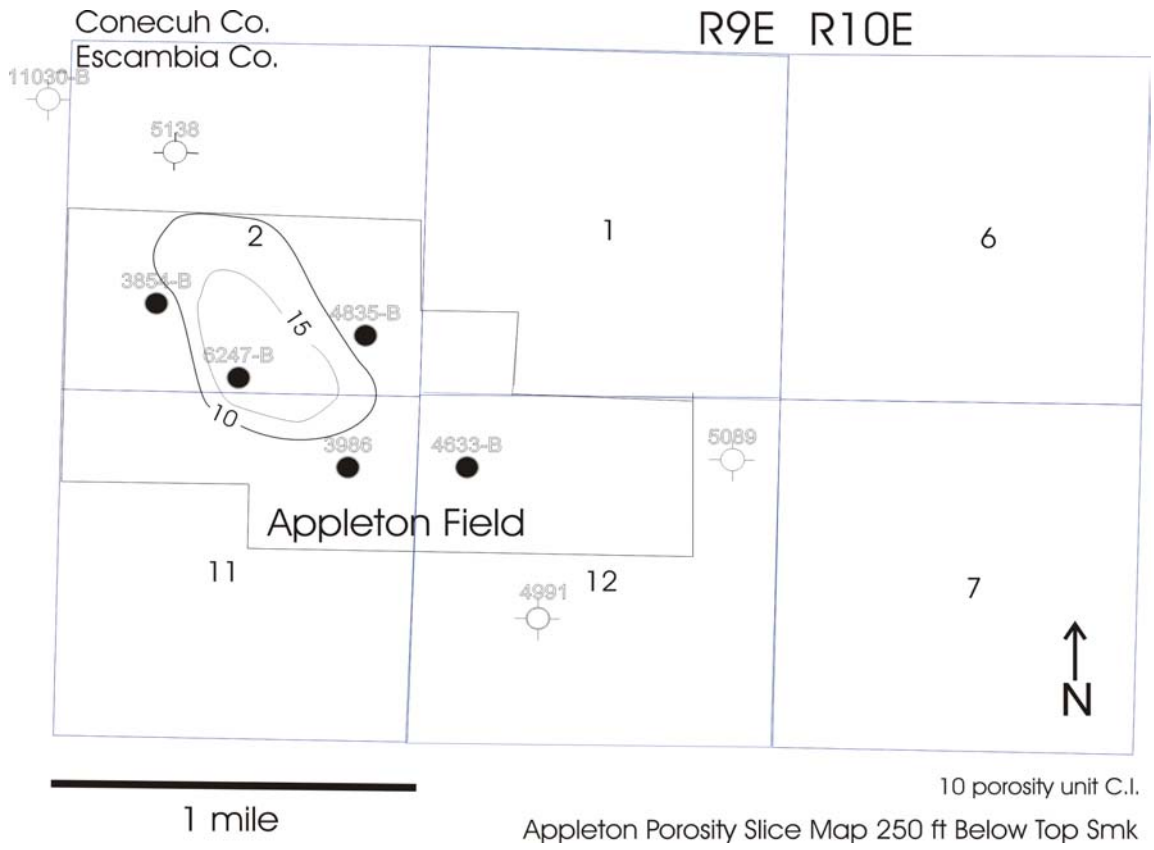

Figure 45. Appleton Porosity Slice Map 250 ft below Top of Smackover.

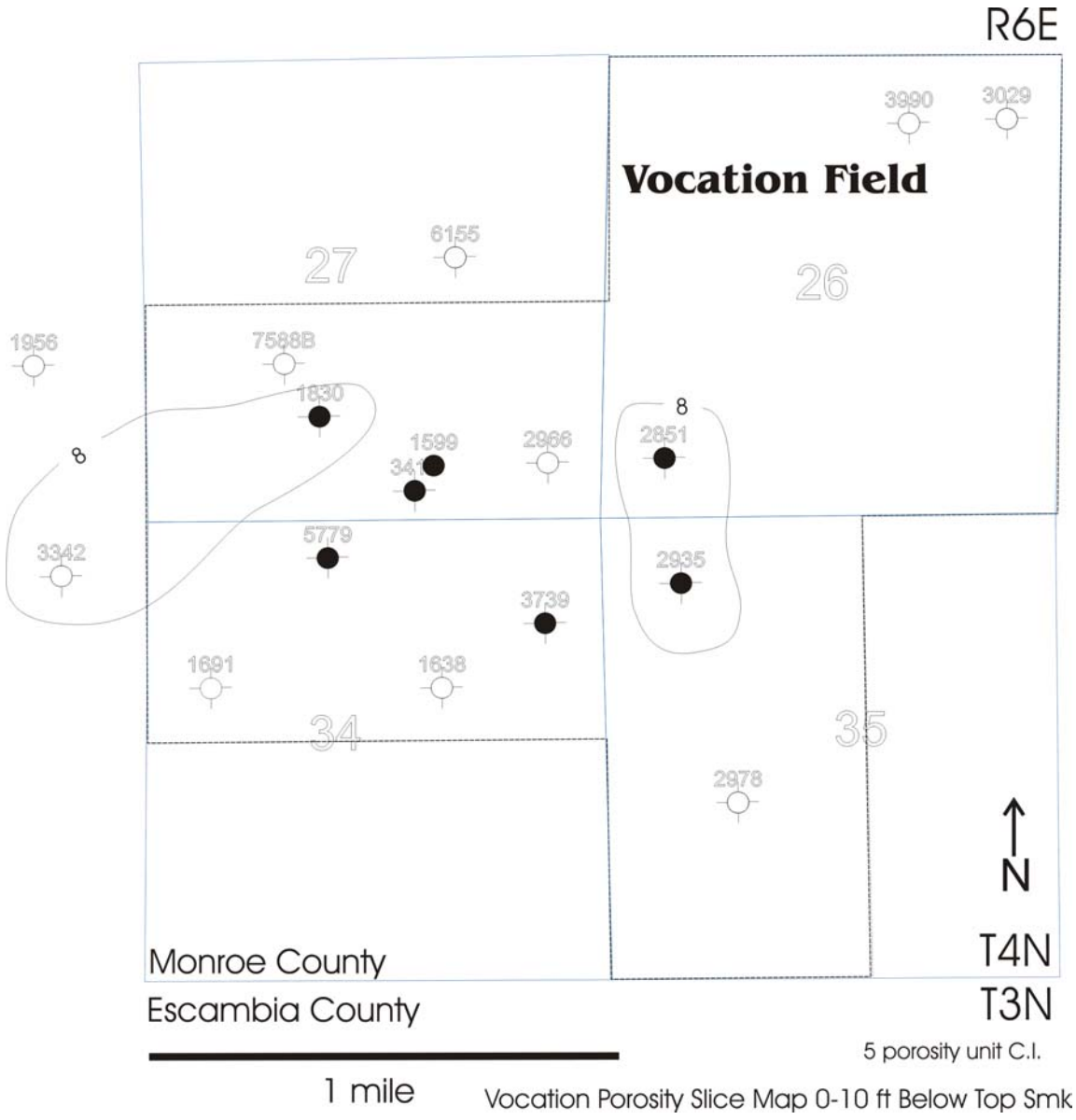

Figure 46. Vocation Porosity Slice Map 0-10 ft below Top of Smackover.

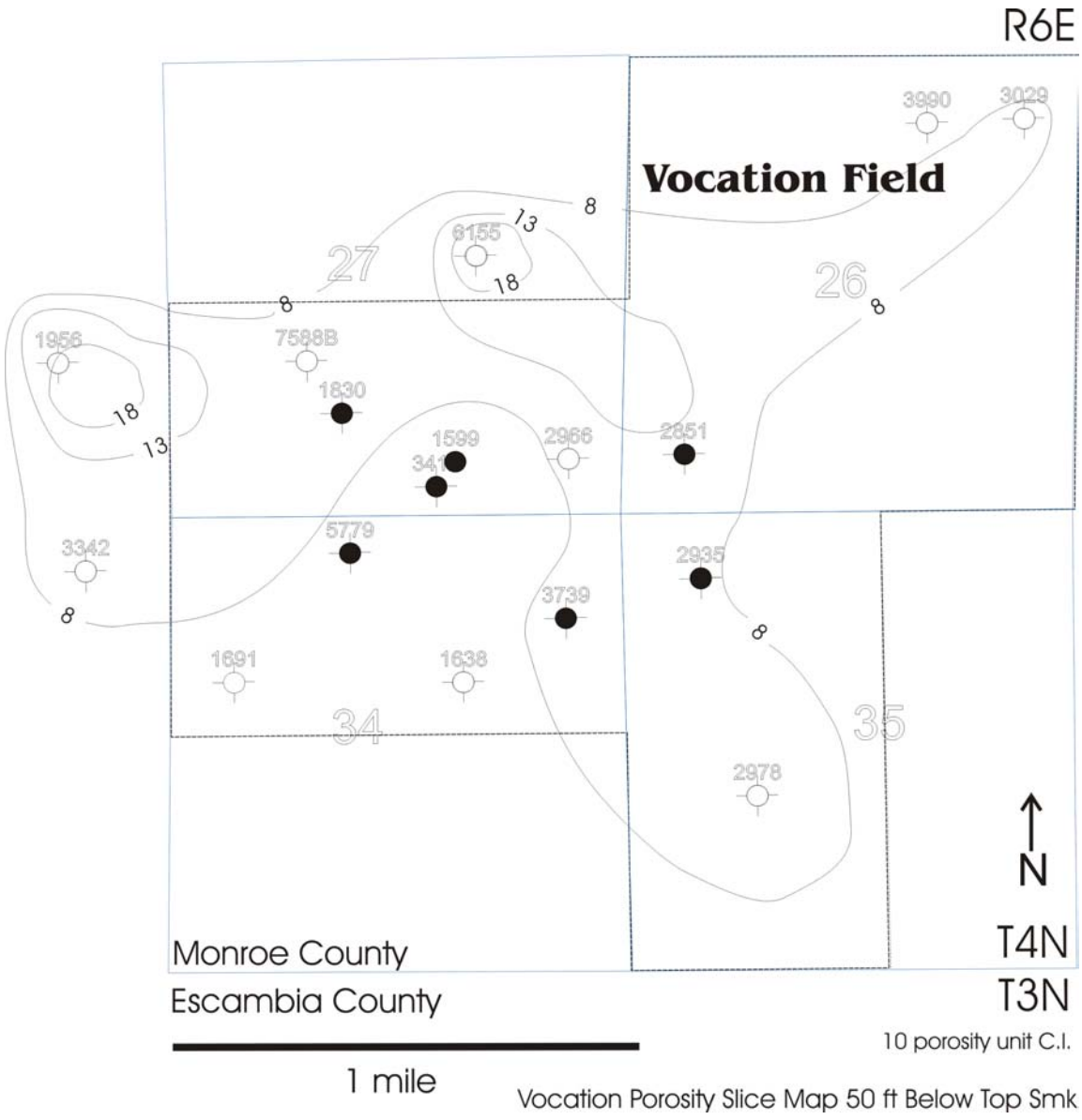

Figure 47. Vocation Porosity Slice Map 50 ft below Top of Smackover.

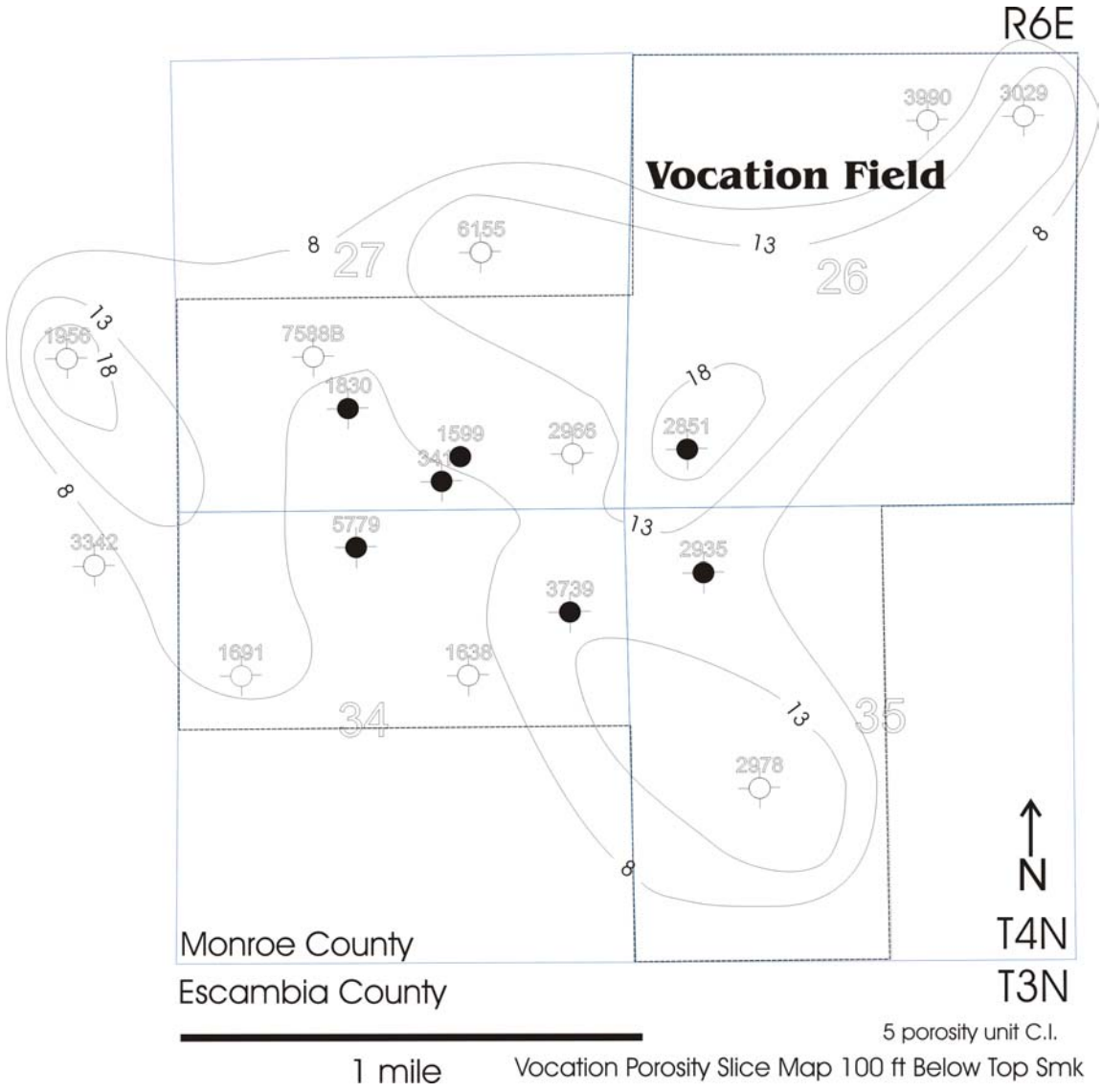

Figure 48. Vocation Porosity Slice Map 100 ft below Top of Smackover.

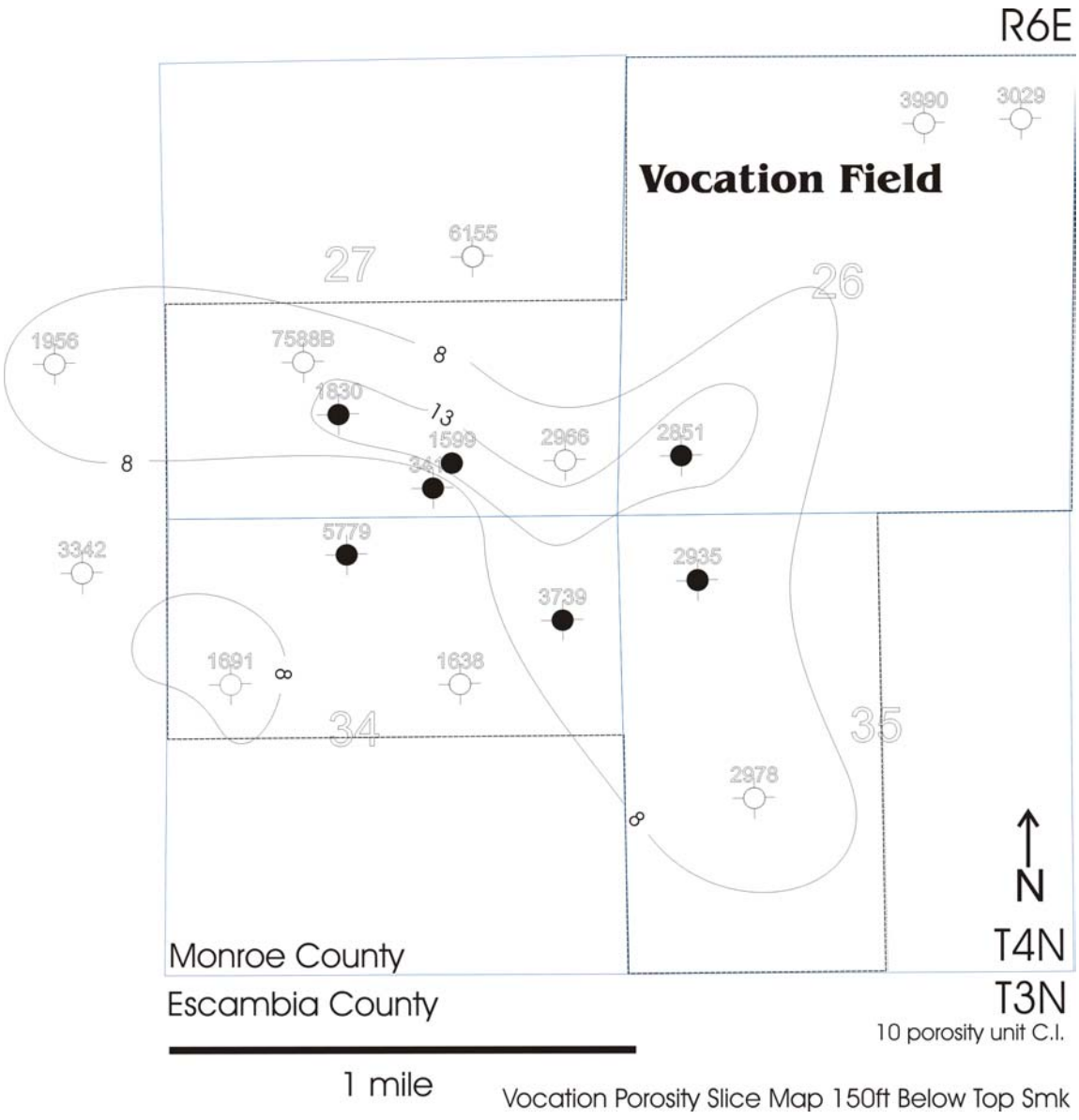

Figure 49. Vocation Porosity Slice Map 150 ft below Top of Smackover.

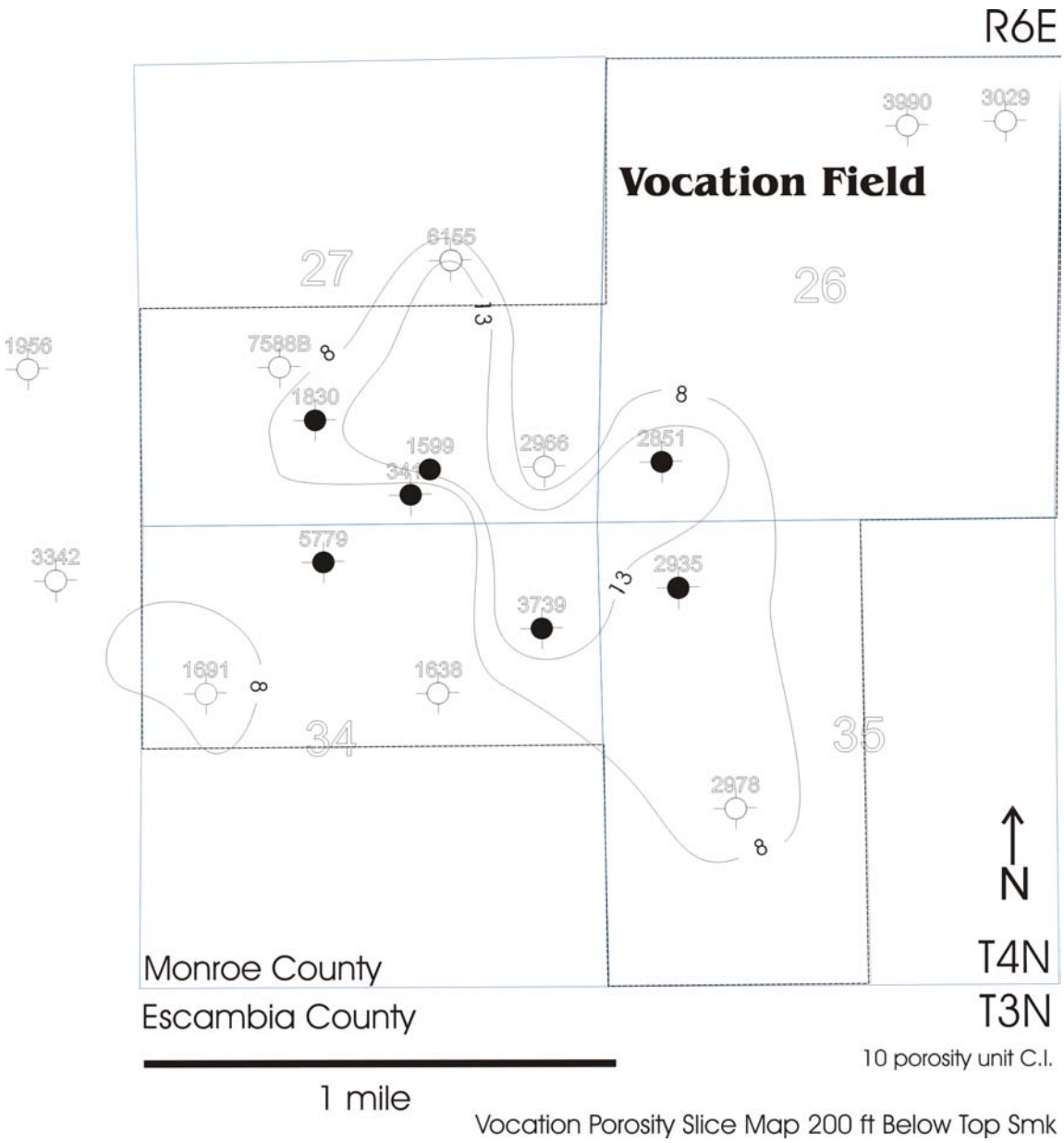

Figure 50. Vocation Porosity Slice Map 200 ft below Top of Smackover.

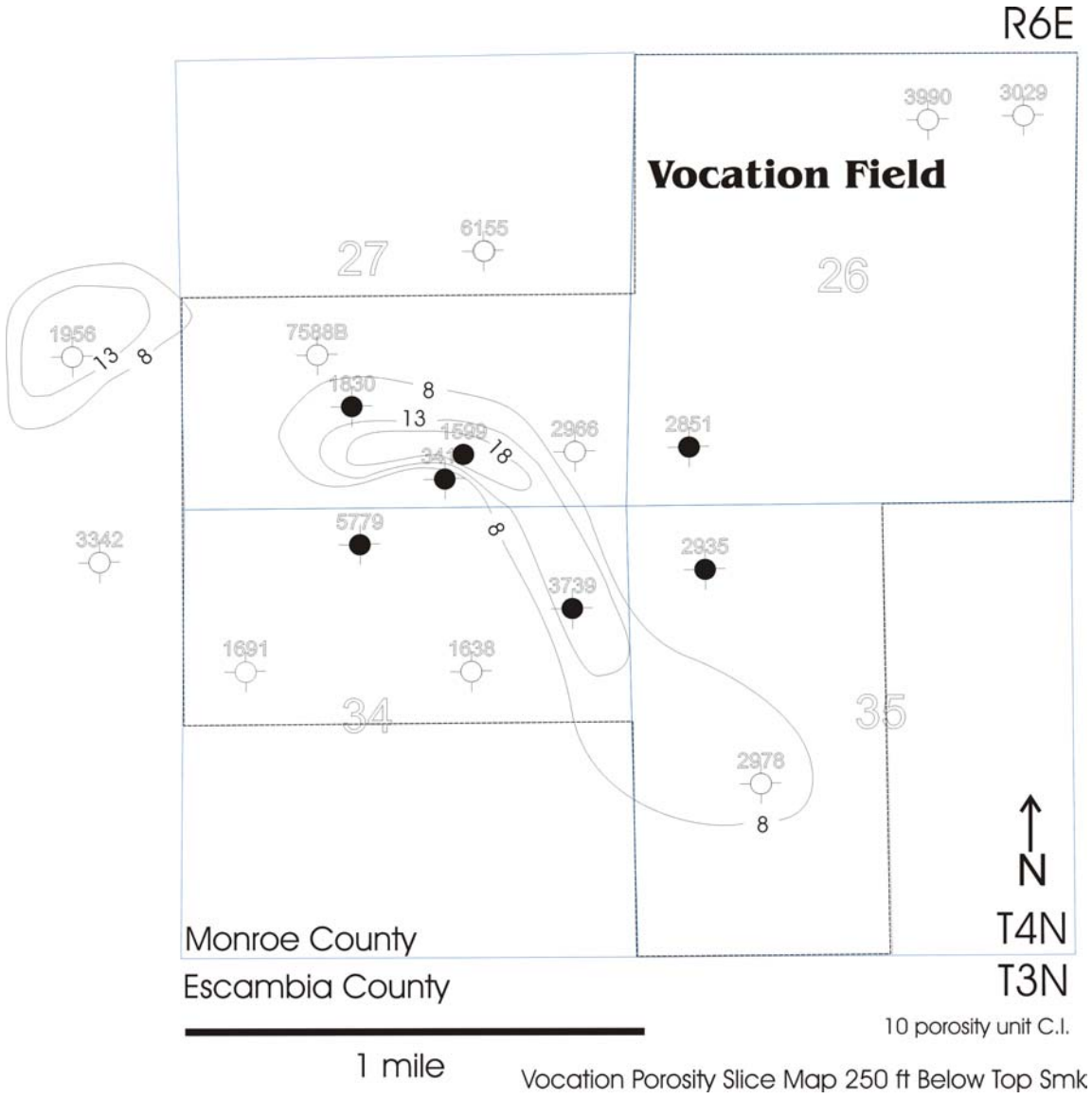

Figure 51. Vocation Porosity Slice Map 250 ft below Top of Smackover.

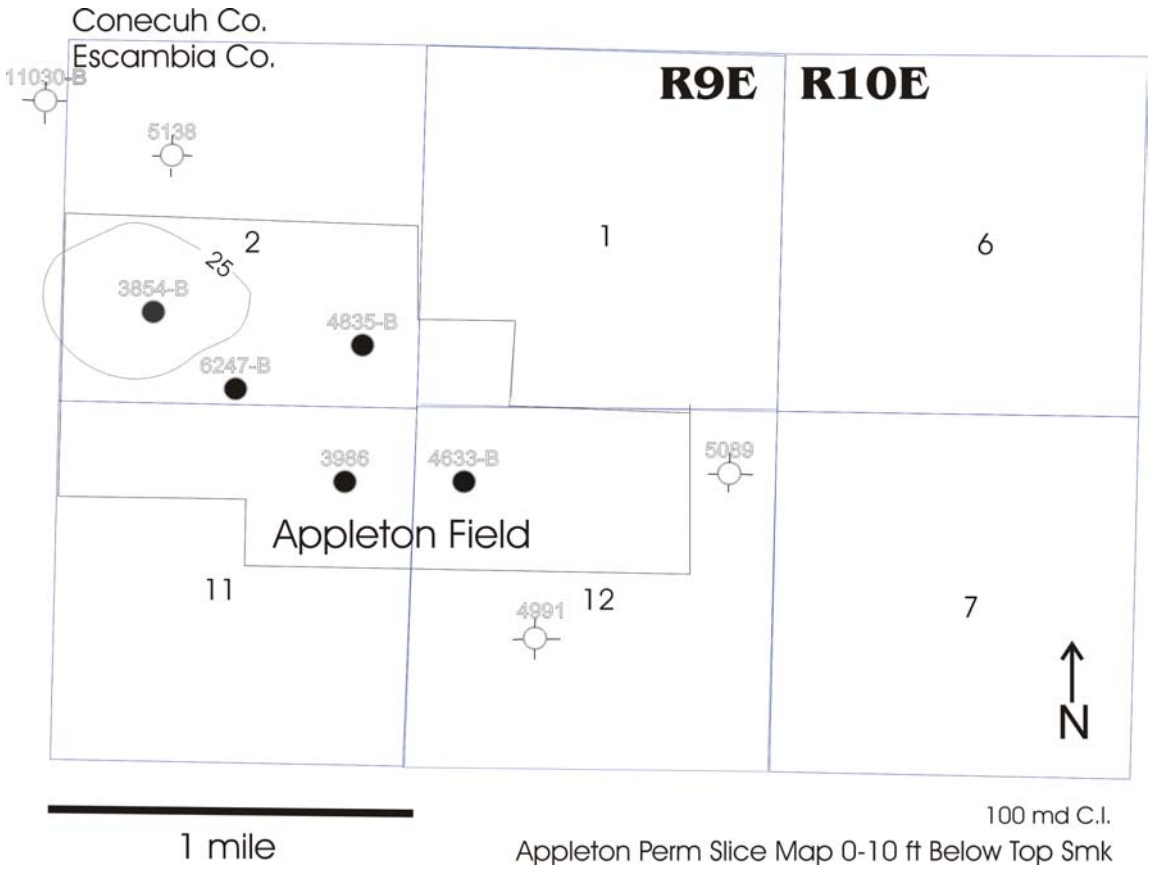

Figure 52. Appleton Permeability Slice Map 0-10 ft below Top of Smackover.

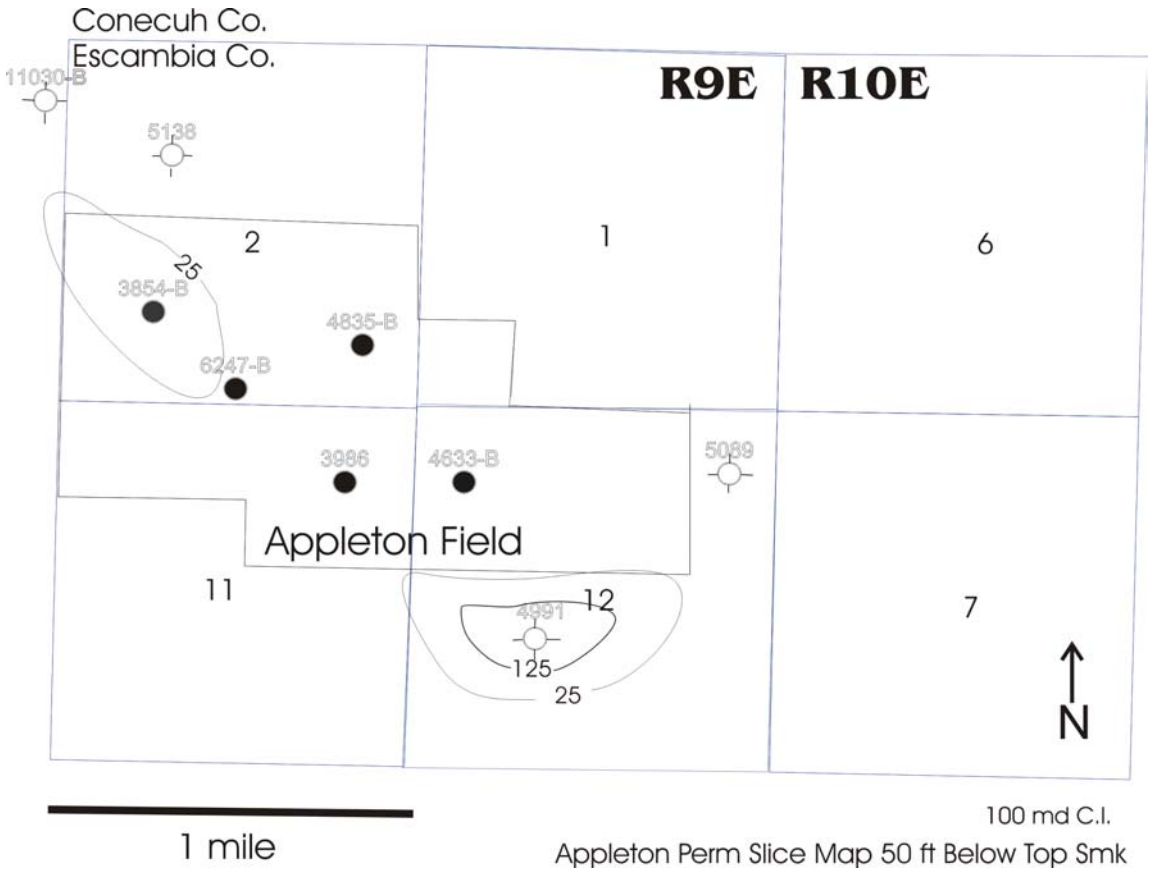

Figure 53. Appleton Permeability Slice Map 50 ft below Top of Smackover.

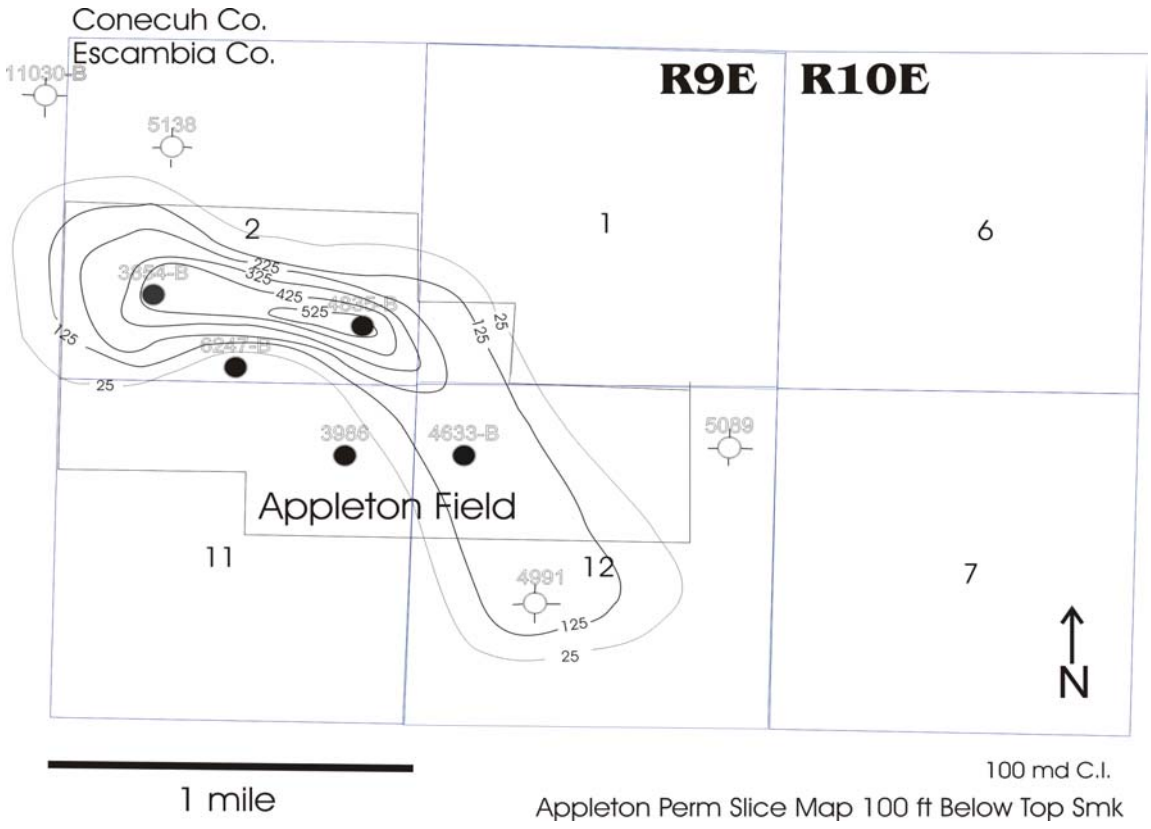

Figure 54. Appleton Permeability Slice Map 100 ft below Top of Smackover.

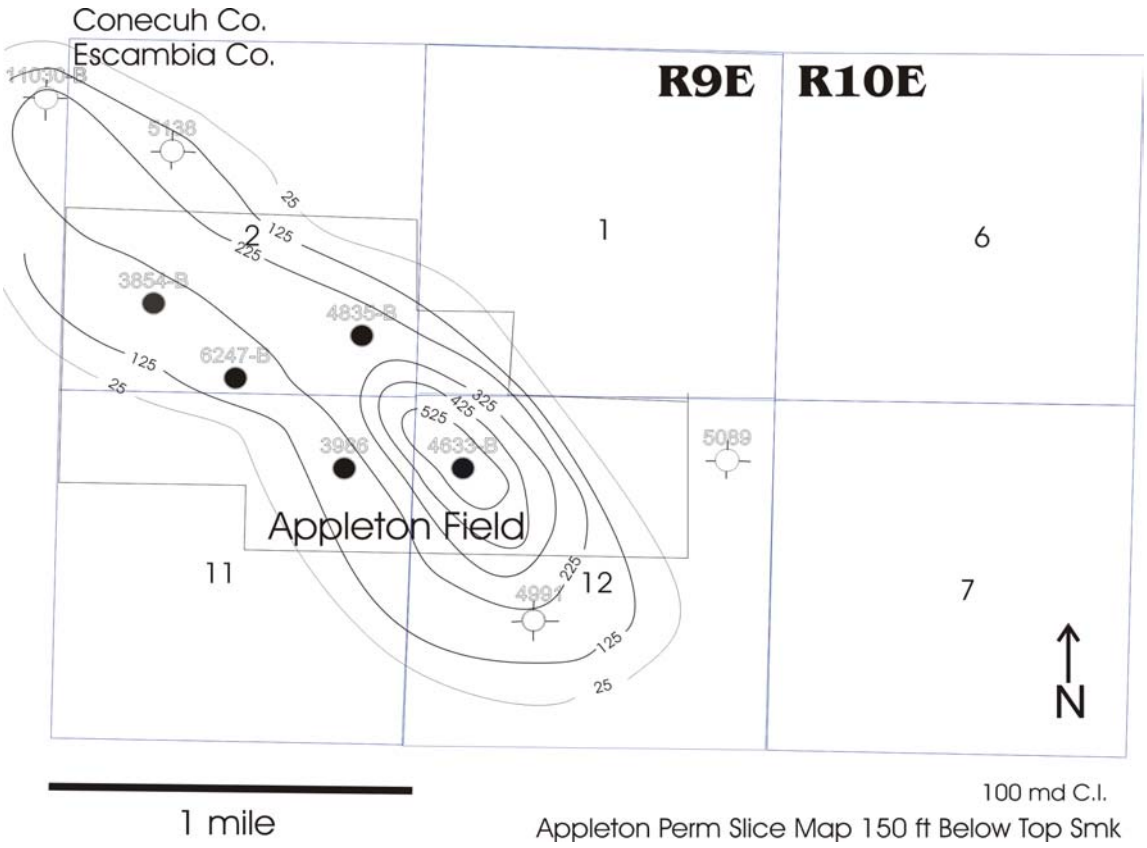

Figure 55. Appleton Permeability Slice Map 150 ft below Top of Smackover.

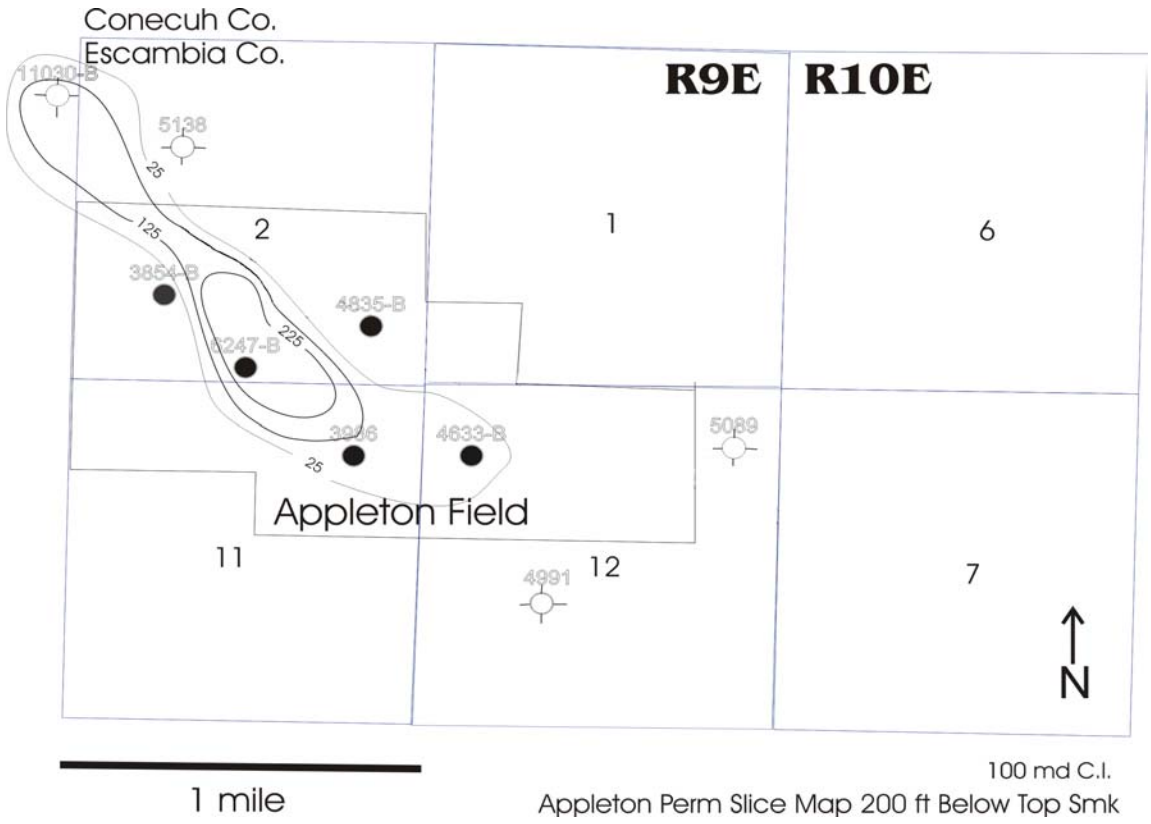

Figure 56. Appleton Permeability Slice Map 200 ft below Top of Smackover.

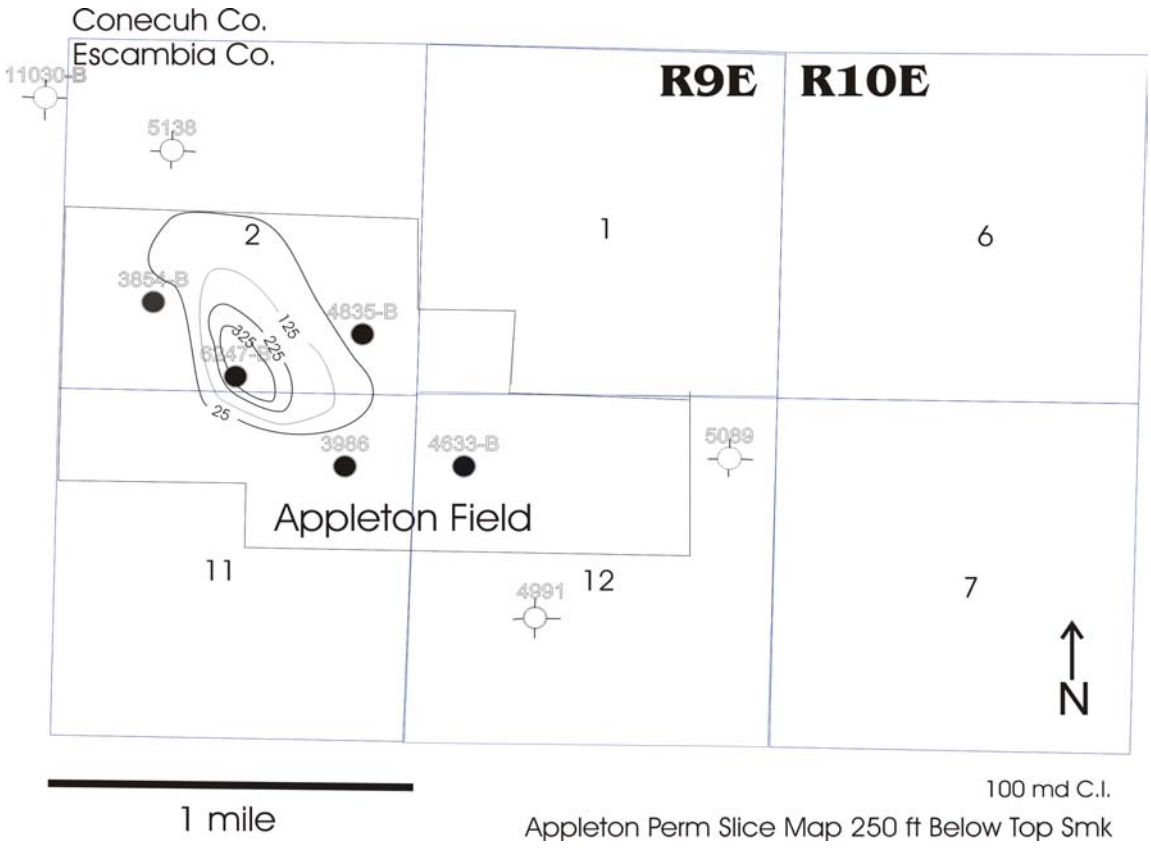

Figure 57. Appleton Permeability Slice Map 250 ft below Top of Smackover.

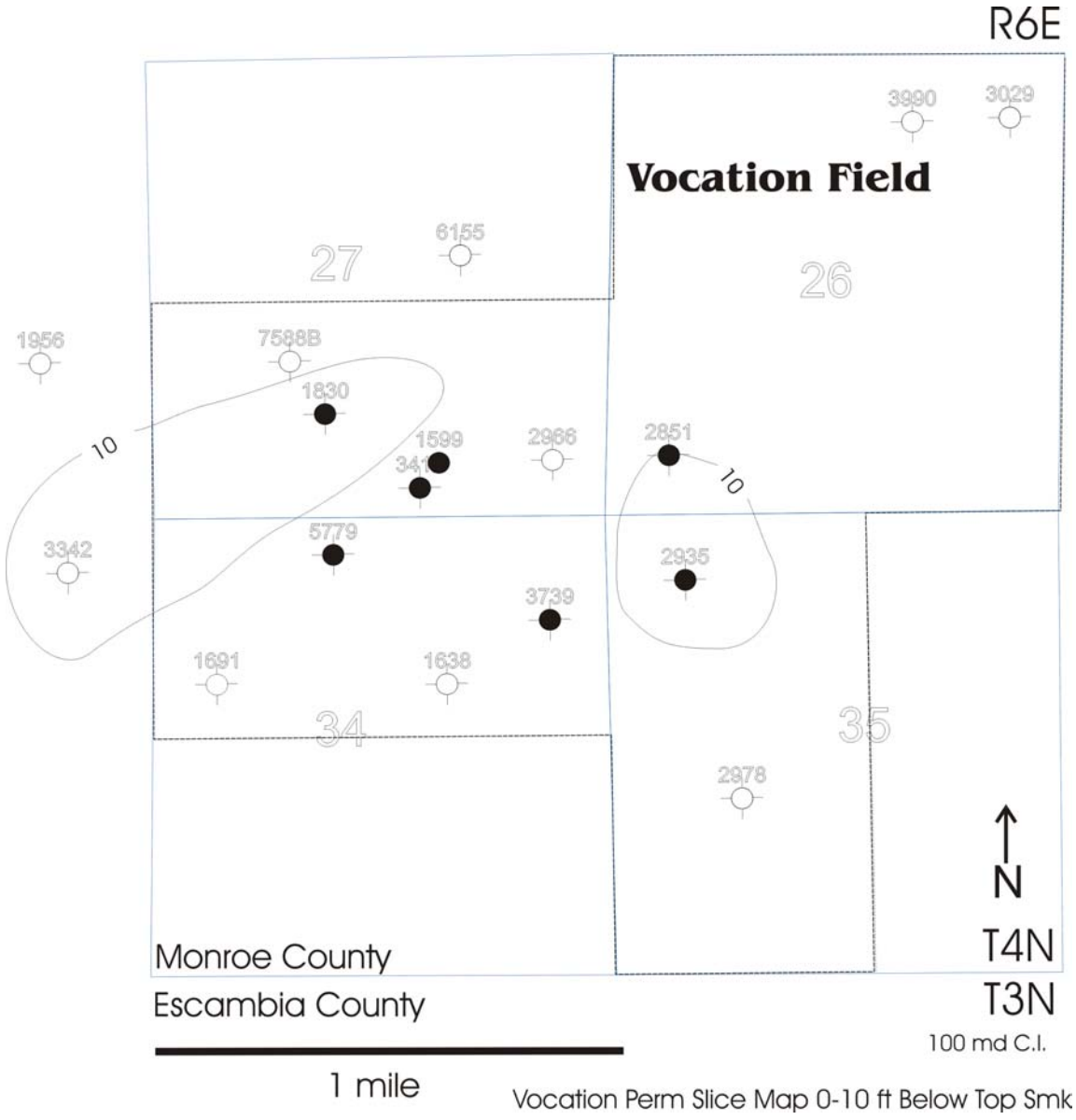

Figure 58. Vocation Permeability Slice Map 0-10 ft below Top of Smackover.

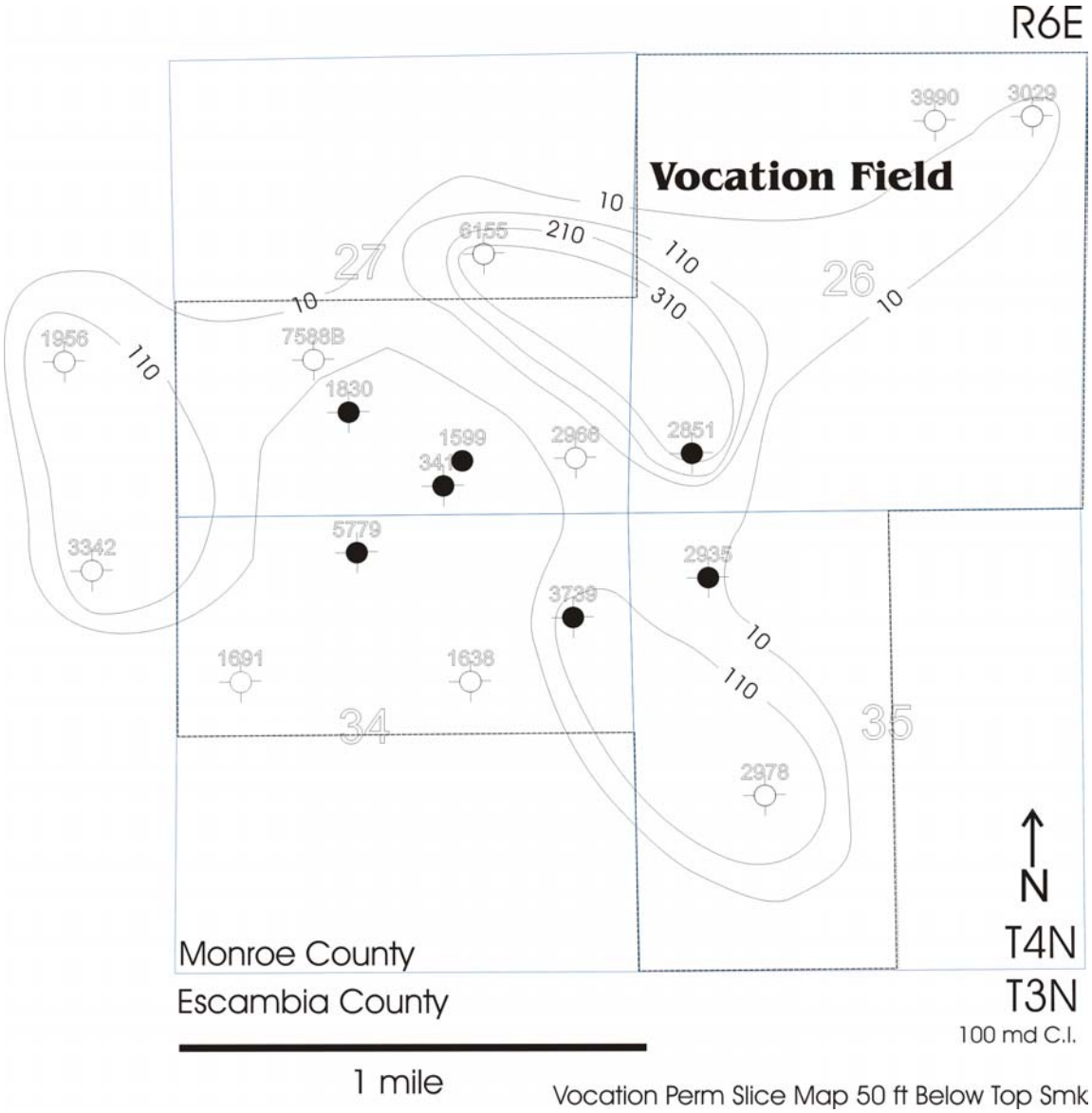

Figure 59. Vocation Permeability Slice Map 50 ft below Top of Smackover.

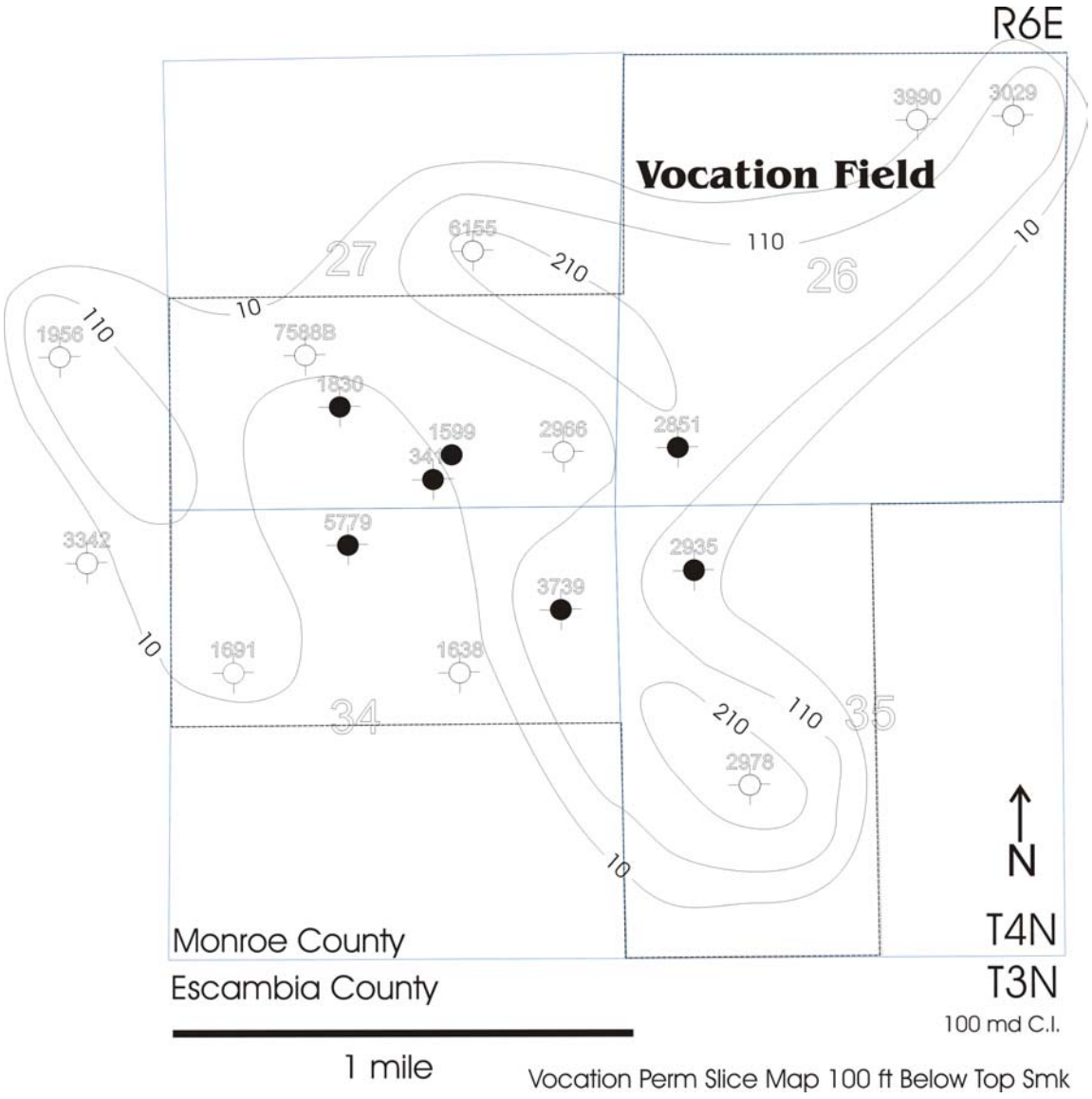

Figure 60. Vocation Permeability Slice Map 100 ft below Top of Smackover.

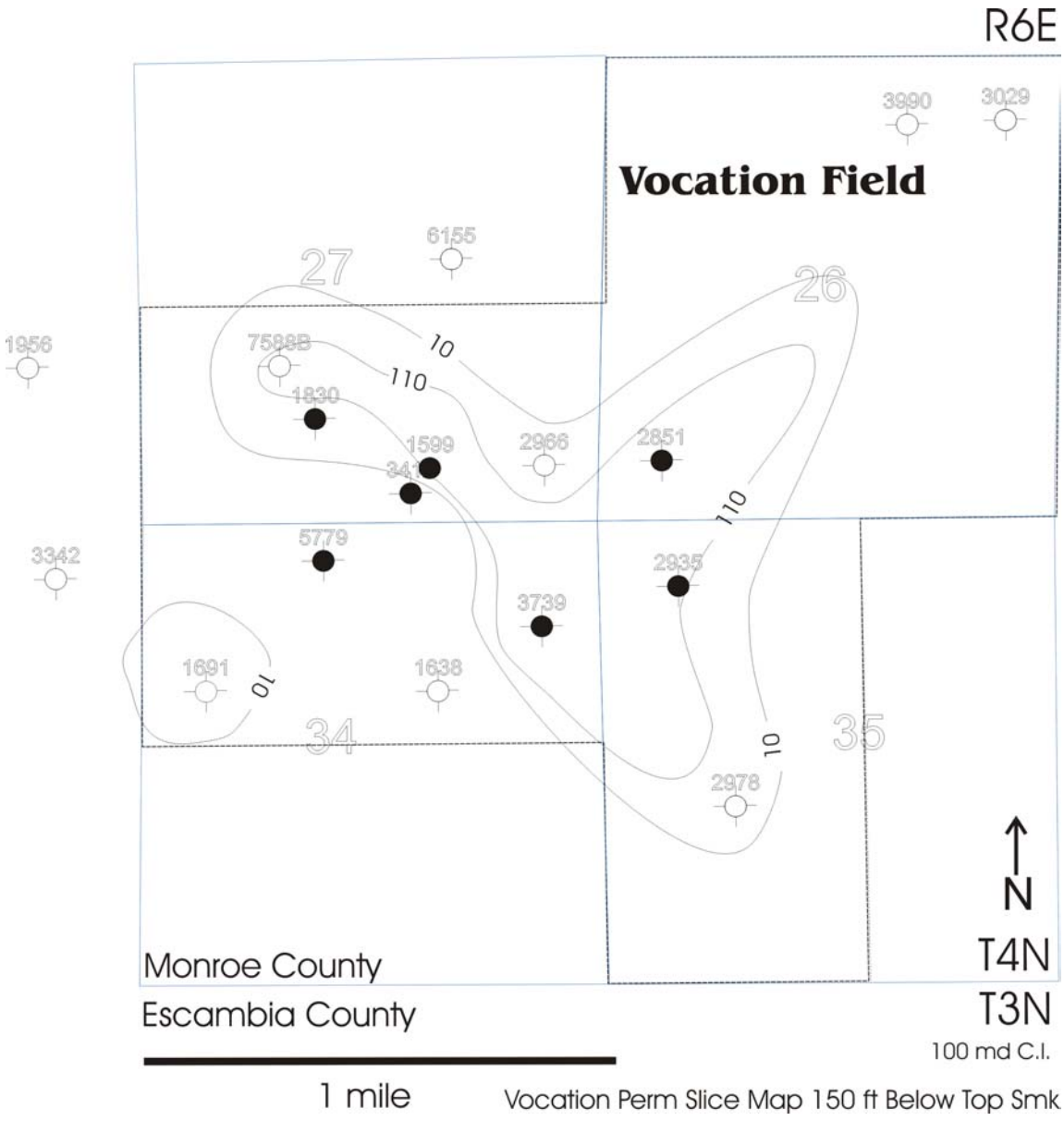

Figure 61. Vocation Permeability Slice Map 150 ft below Top of Smackover.

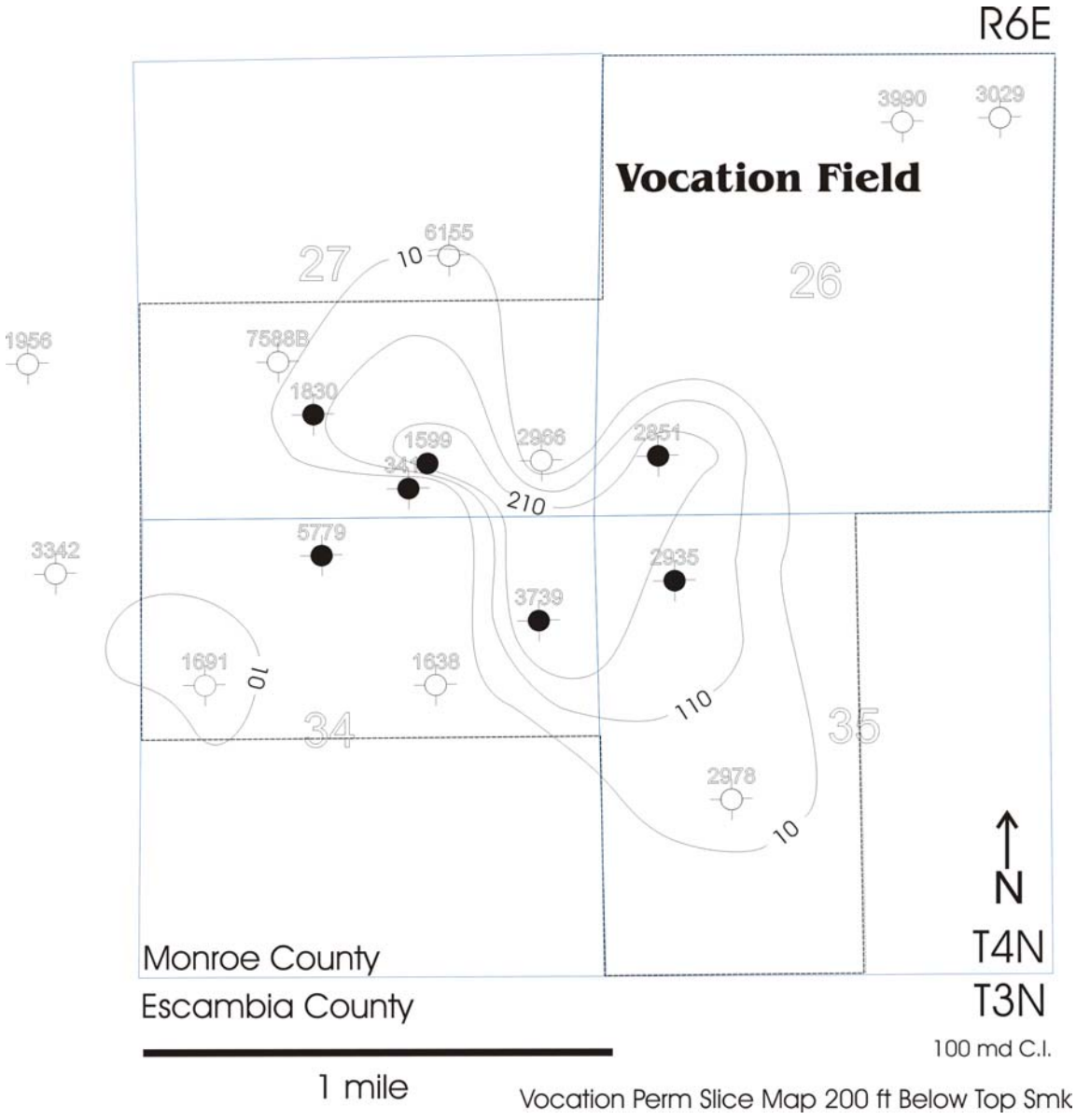

Figure 62. Vocation Permeability Slice Map 200 ft below Top of Smackover.

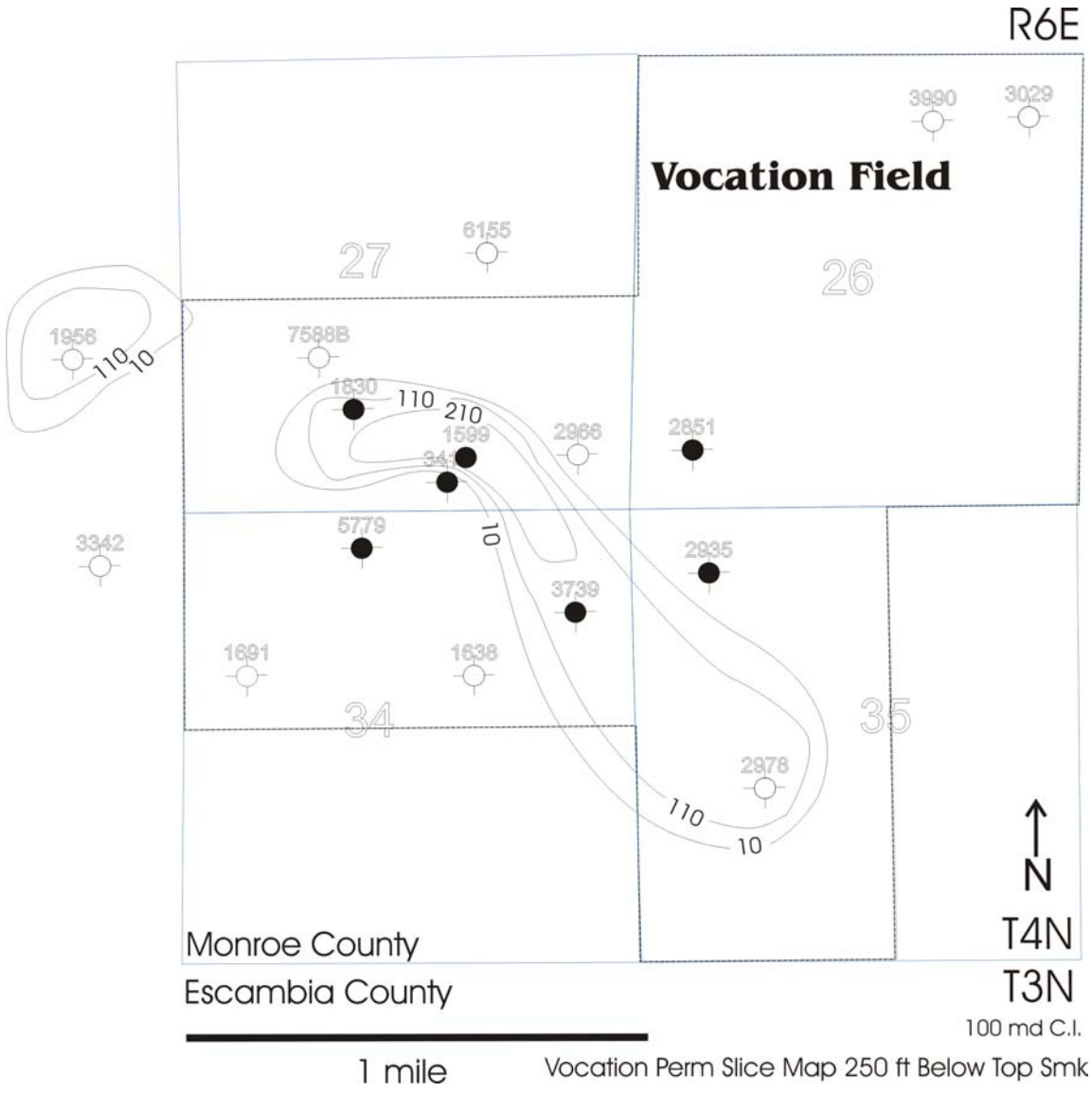

Figure 63. Vocation Permeability Slice Map 250 ft below Top of Smackover.

From the porosity and permeability pairings, nine classes (RQ) (Fig. 64) were developed based on histograms of porosity and permeability trends in the fields. These ranges were also given a corresponding pattern for mapping. Rocks that were not reservoir quality, porosity values < 8% and permeability values < 10 md, were not mapped as a pattern since they are recognized as any area in which the pattern was not present. This decision allows for finer

delineation of the flow units without adding more patterns. Superimposed on the patterns are MPA values from

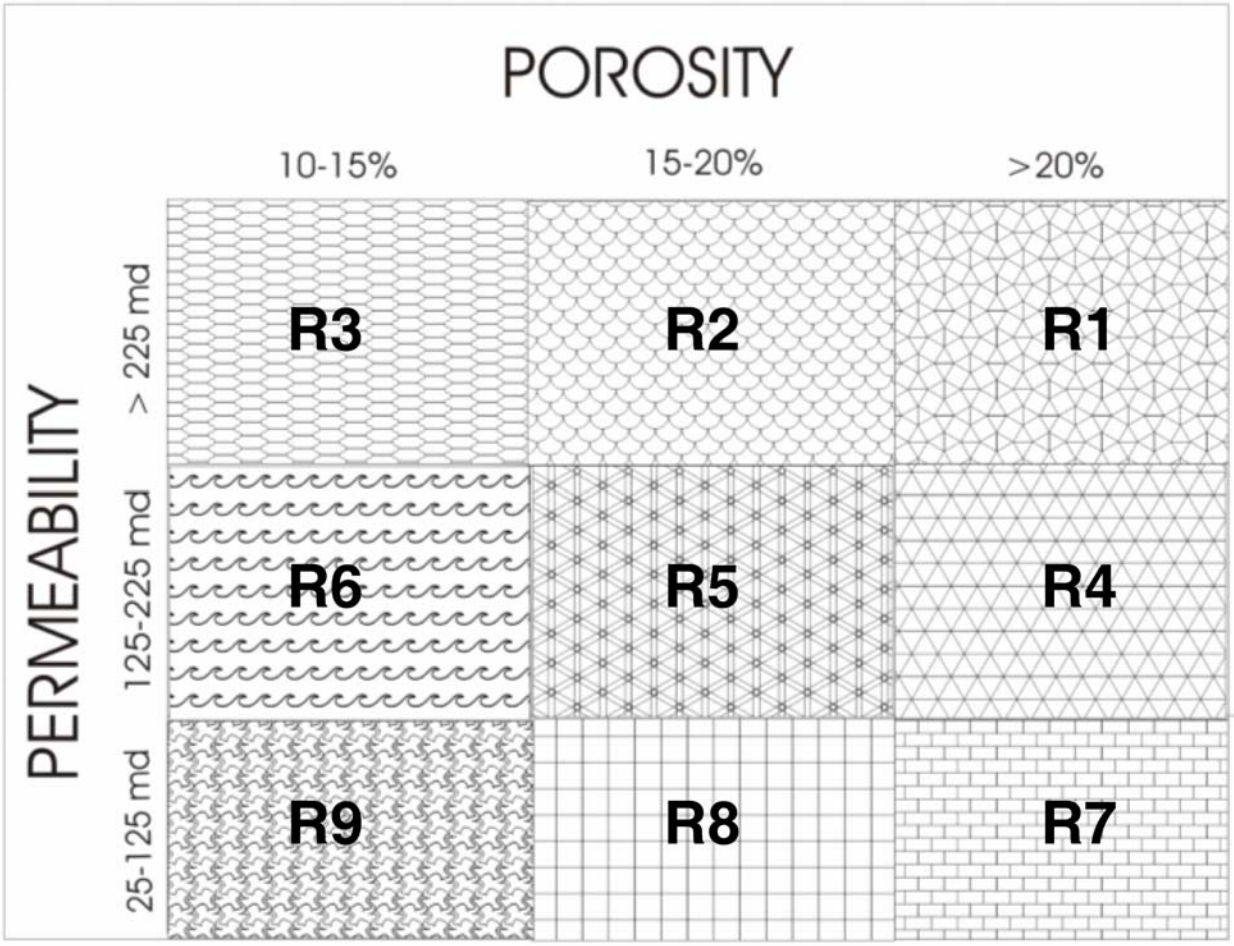

Figure 64. Vocation Reservoir Quality Map Key.

MICP which correspond to the various pairs. In two cases, more than one MPA value corresponded to a poroperm pair. This is because in most samples there are vugs of various sizes- with another range of varying sizes of connecting throats. These pairs were then contoured and mapped over 10-foot stratigraphic interval. (Figs. 65-76). It should be noted here that only the maps drawn every 50 feet are illustrated due to the large number (180) of maps created for both fields.

The better reservoir quality classes such as RQ1, RQ2, and RQ3 are encountered where are combinations (R in reef facies and IP and SEIP-SEIC in non-reef facies) of pore types are predominant. Groups RQ4, RQ5, and RQ6 correspond to IP dominated pores accompanied by IPA, M, and IC. Reservoir groups RQ7 and RQ9 vary in the pore types associated with them, but it is noted that no SEIP or SEIC is associated with the pore types, and CRIC is unique to these groups.

The results of these comparisons are shown in Table 11 and Figure 79.

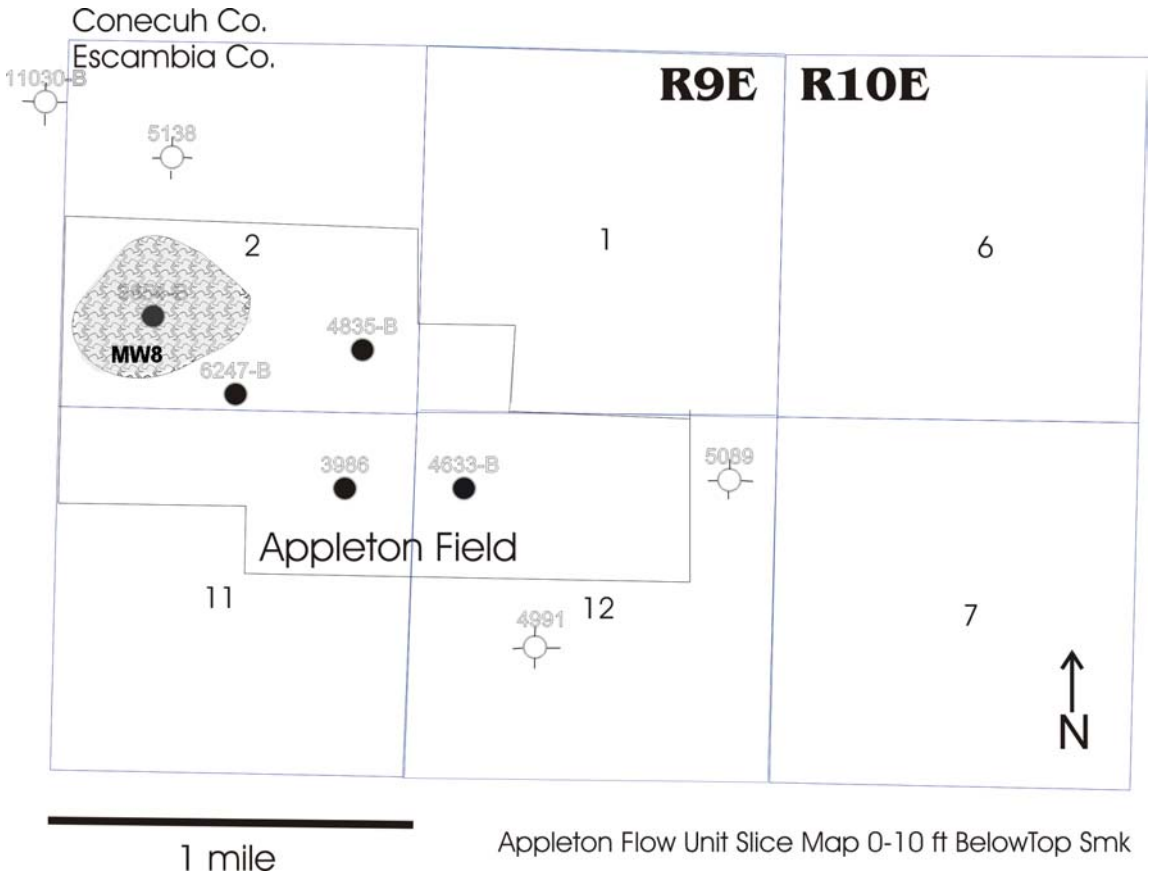

Figure 65. Appleton Flow Unit Slice Map 0-10 ft below Top of Smackover.

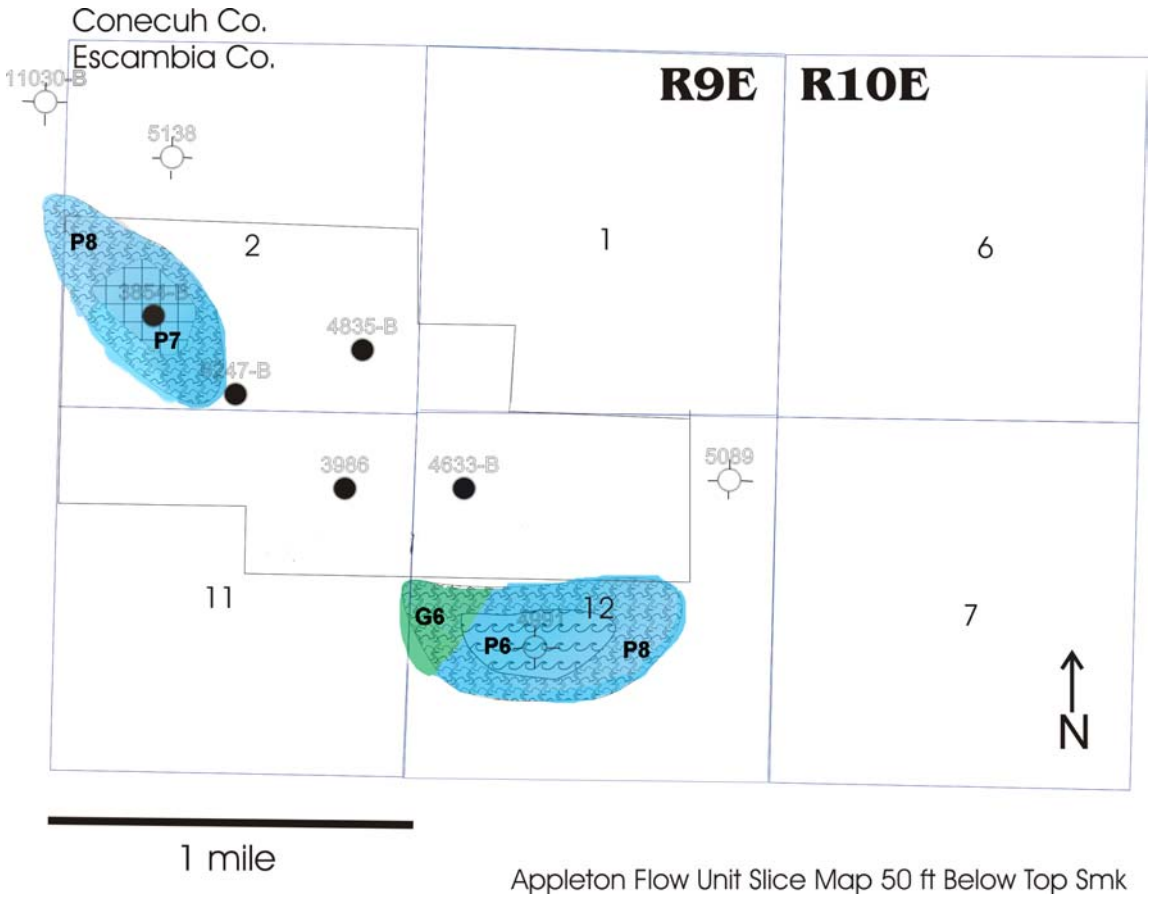

Figure 66. Appleton Flow Unit Slice Map 50 ft below Top of Smackover.

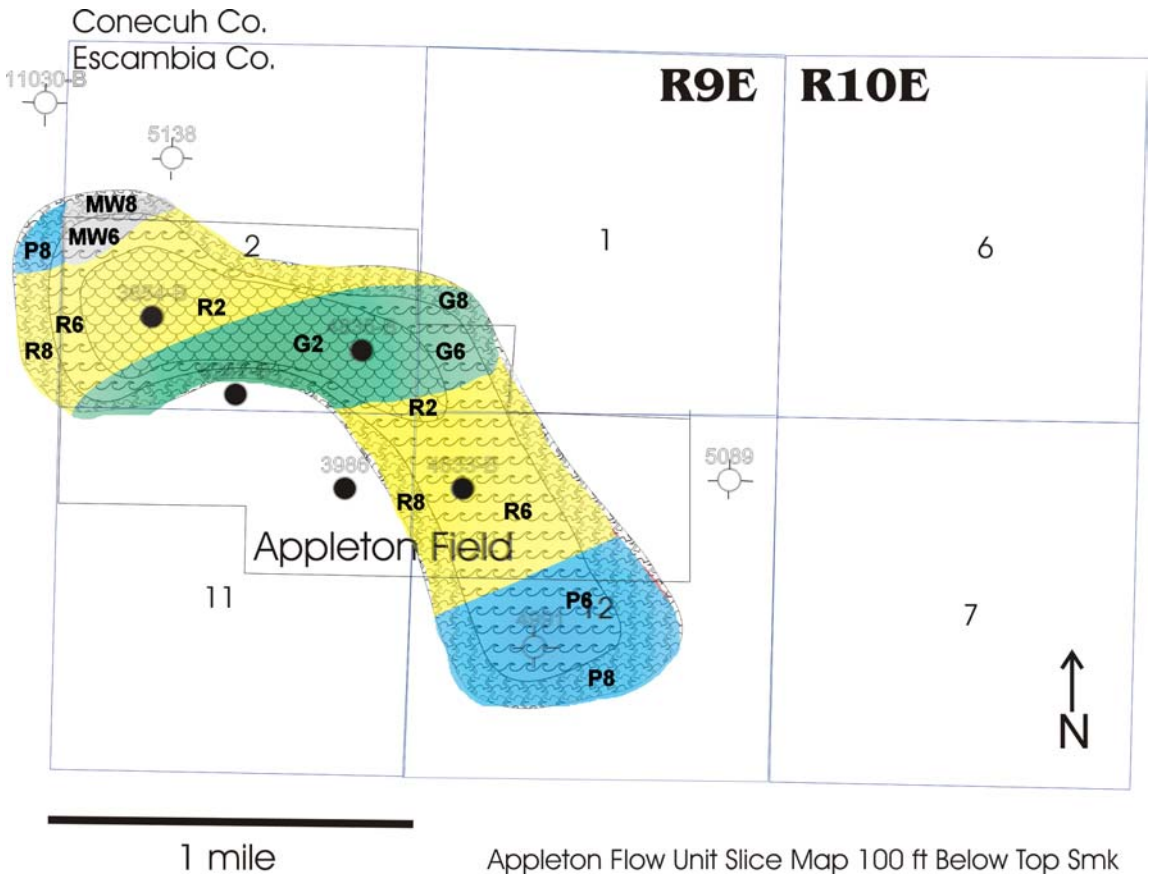

Figure 67. Appleton Flow Unit Slice Map 100 ft below Top of Smackover.

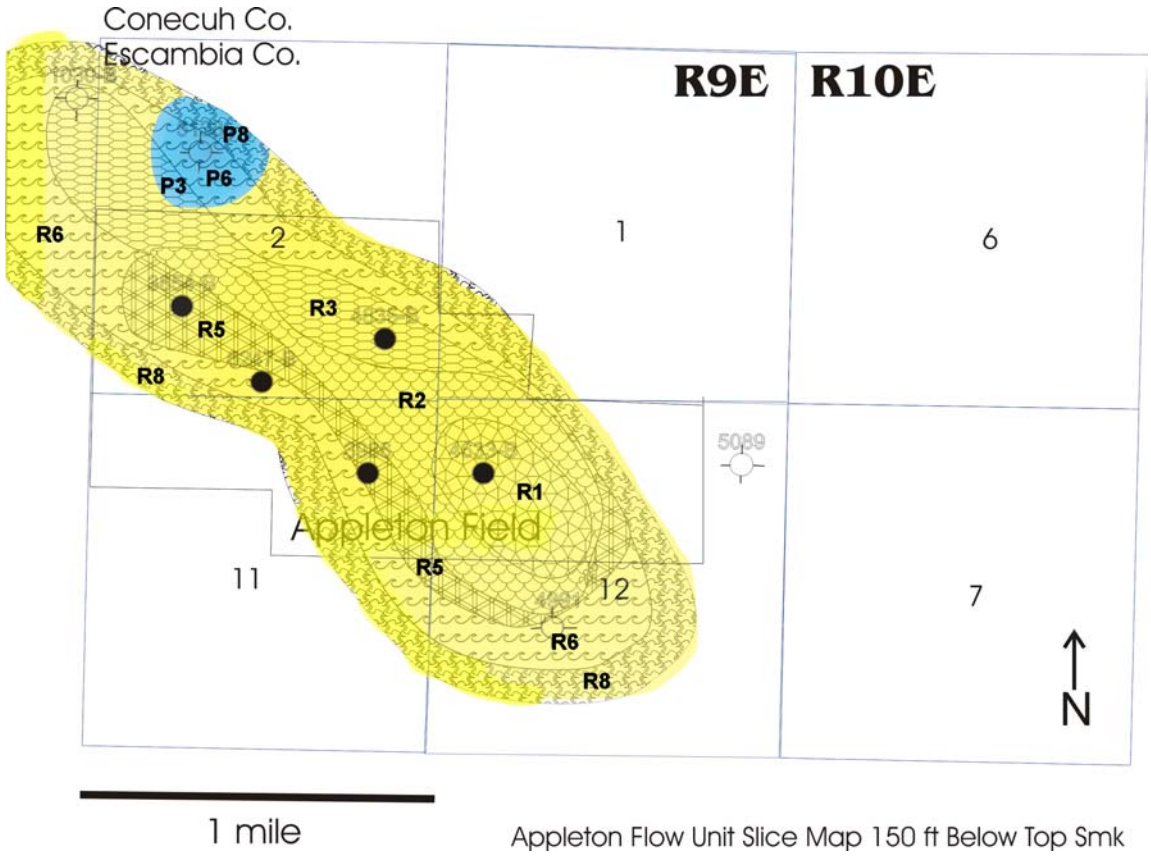

Figure 68. Appleton Flow Unit Slice Map 150 ft below Top of Smackover.

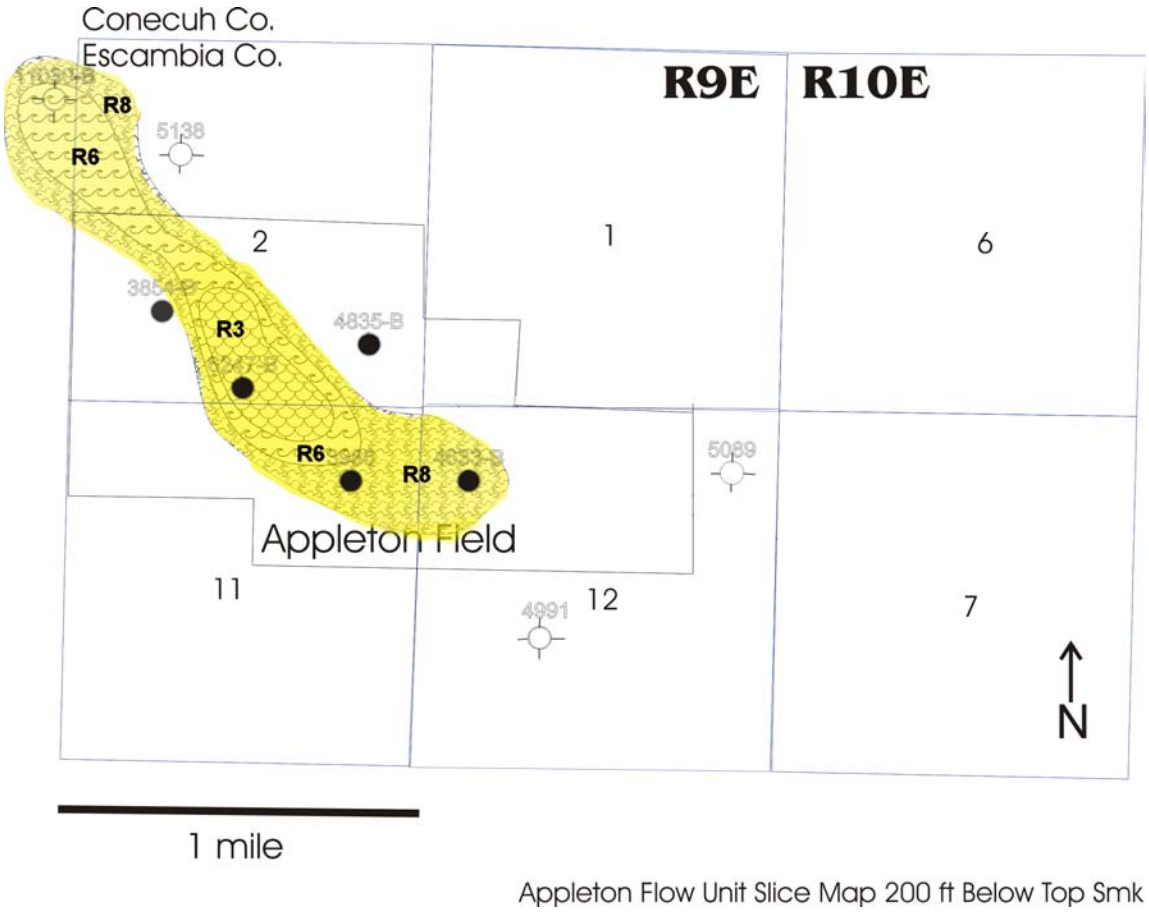

Figure 69. Appleton Flow Unit Slice Map 200 ft below Top of Smackover.

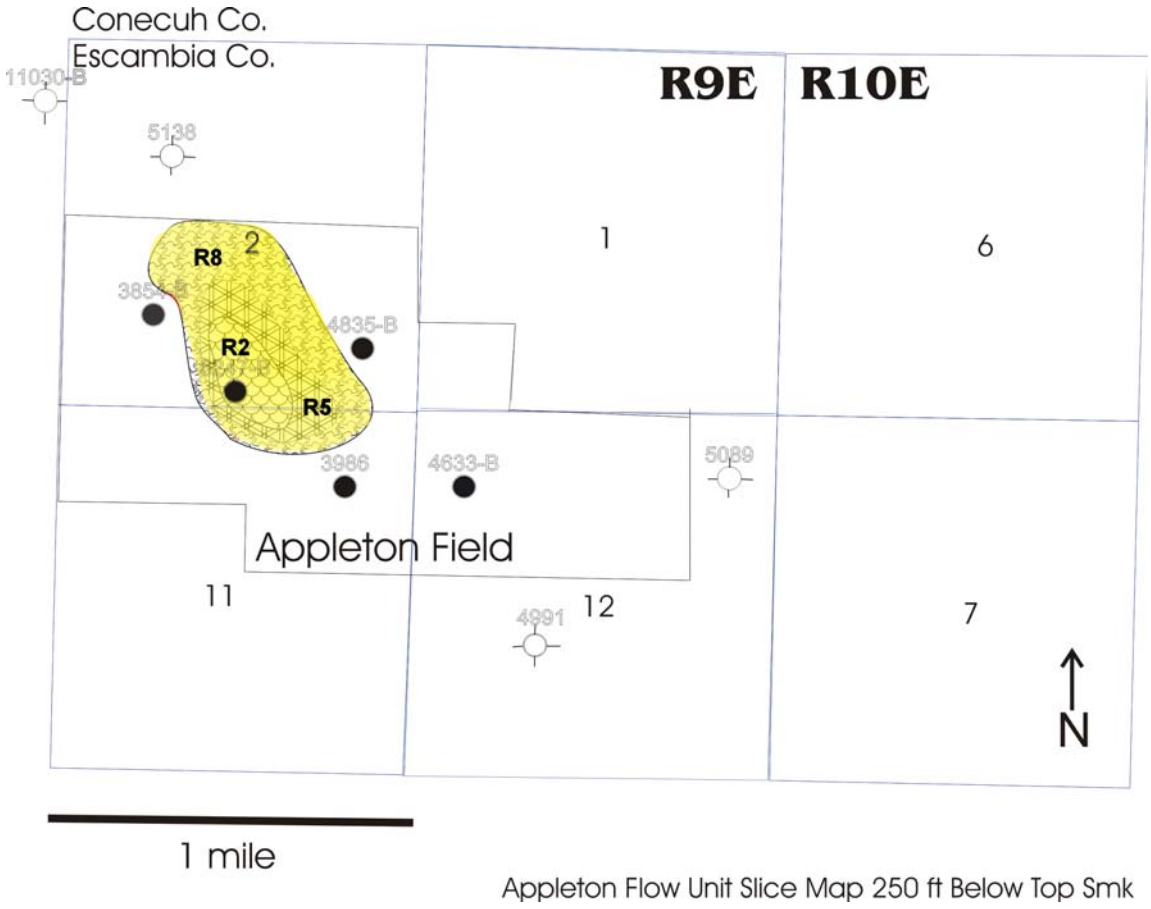

Figure 70. Appleton Flow Unit Slice Map 250 ft below Top of Smackover.

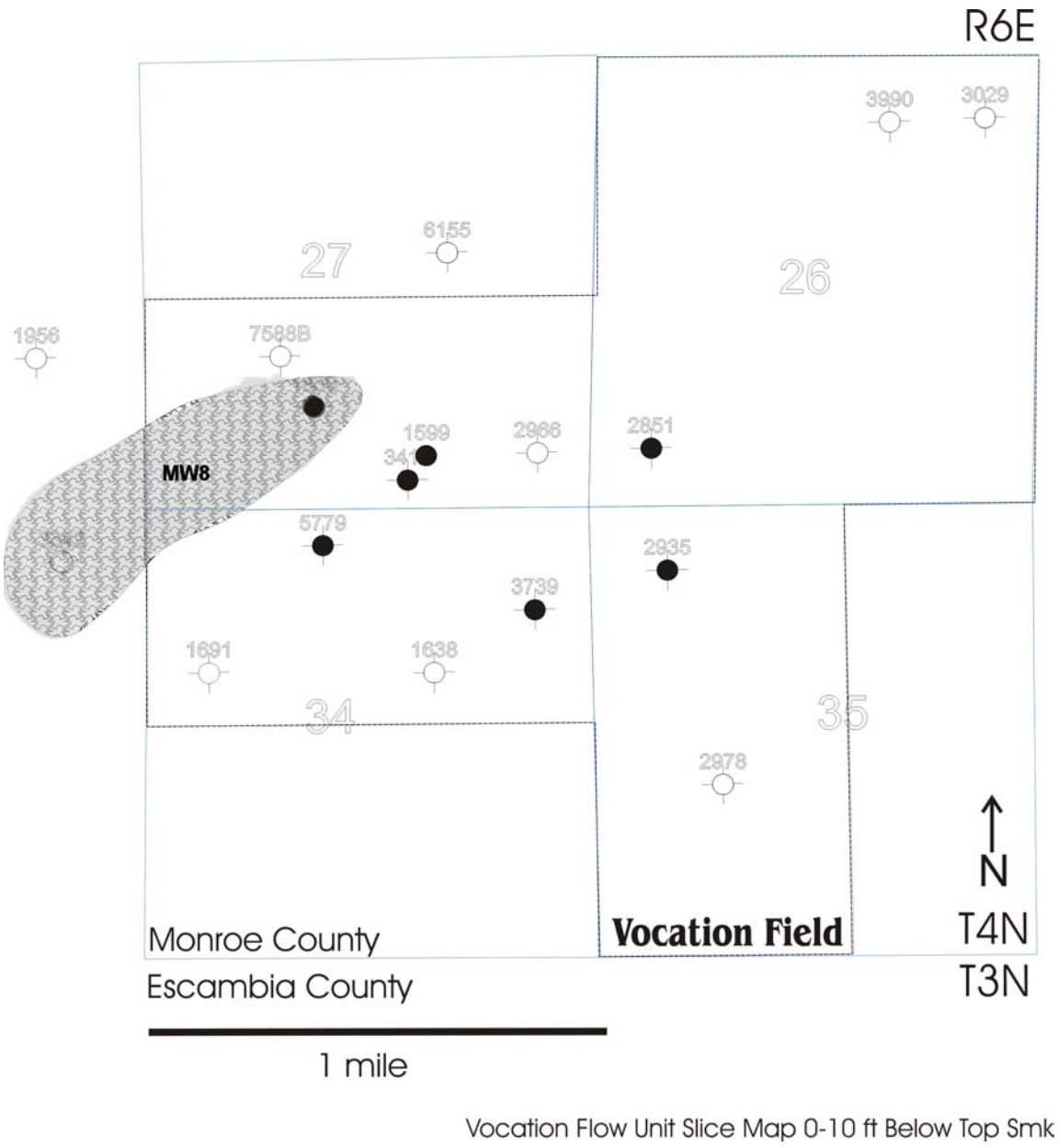

Figure 71. Vocation Flow Unit Slice Map 0-10 ft below Top of Smackover.

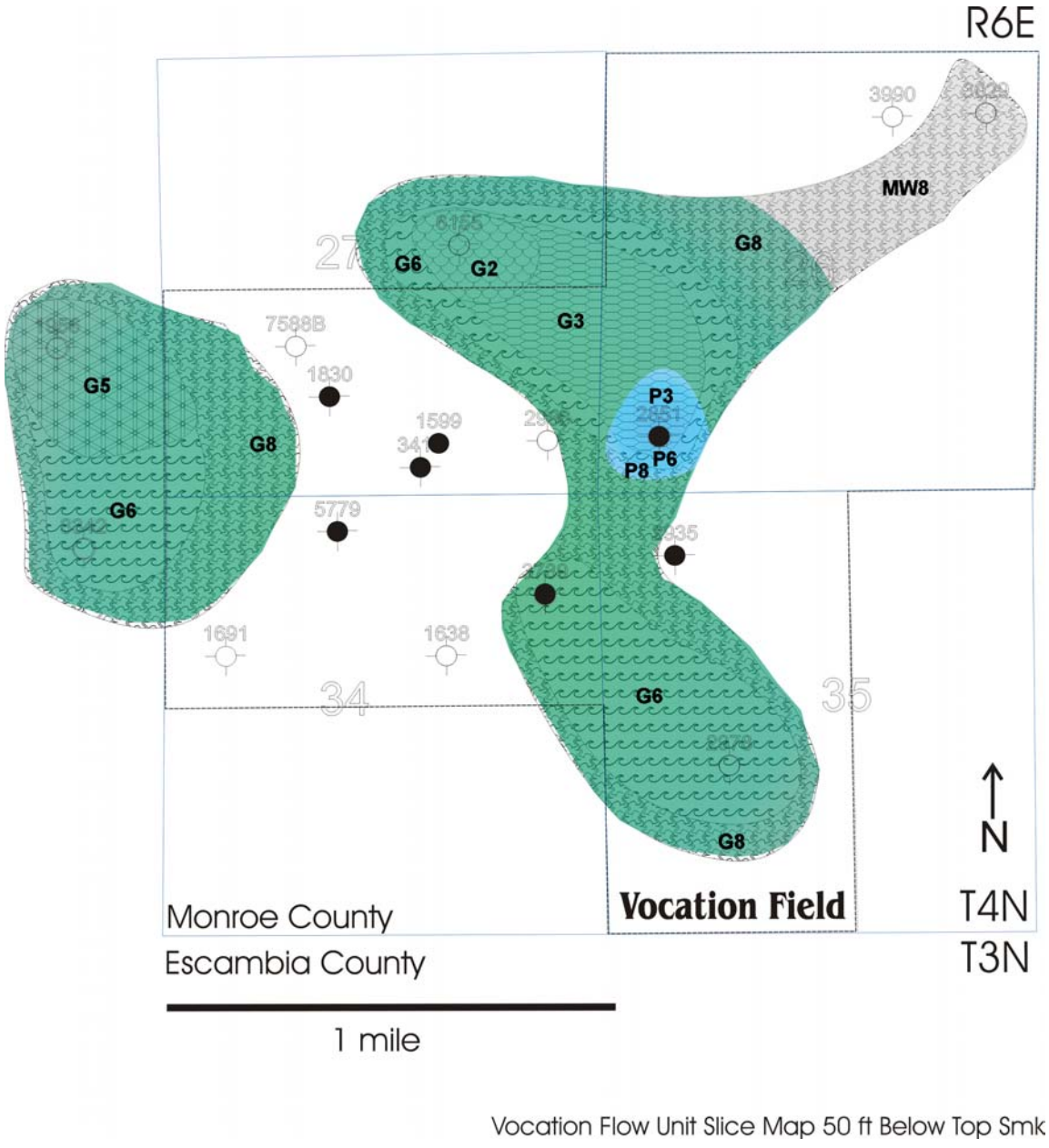

Figure 72. Vocation Flow Unit Slice Map 50 ft below Top of Smackover.

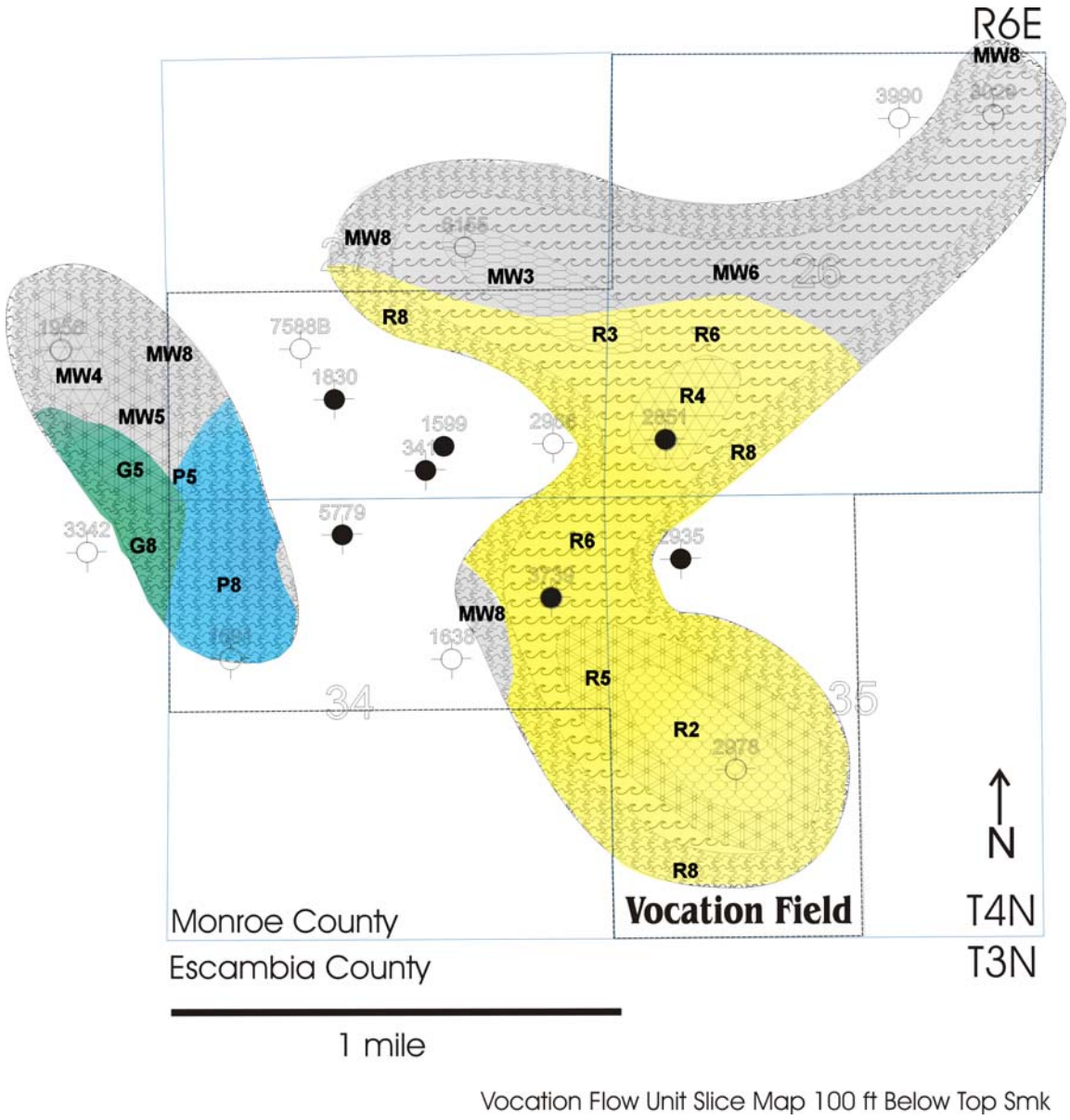

Figure 73. Vocation Flow Unit Slice Map 100 ft below Top of Smackover.

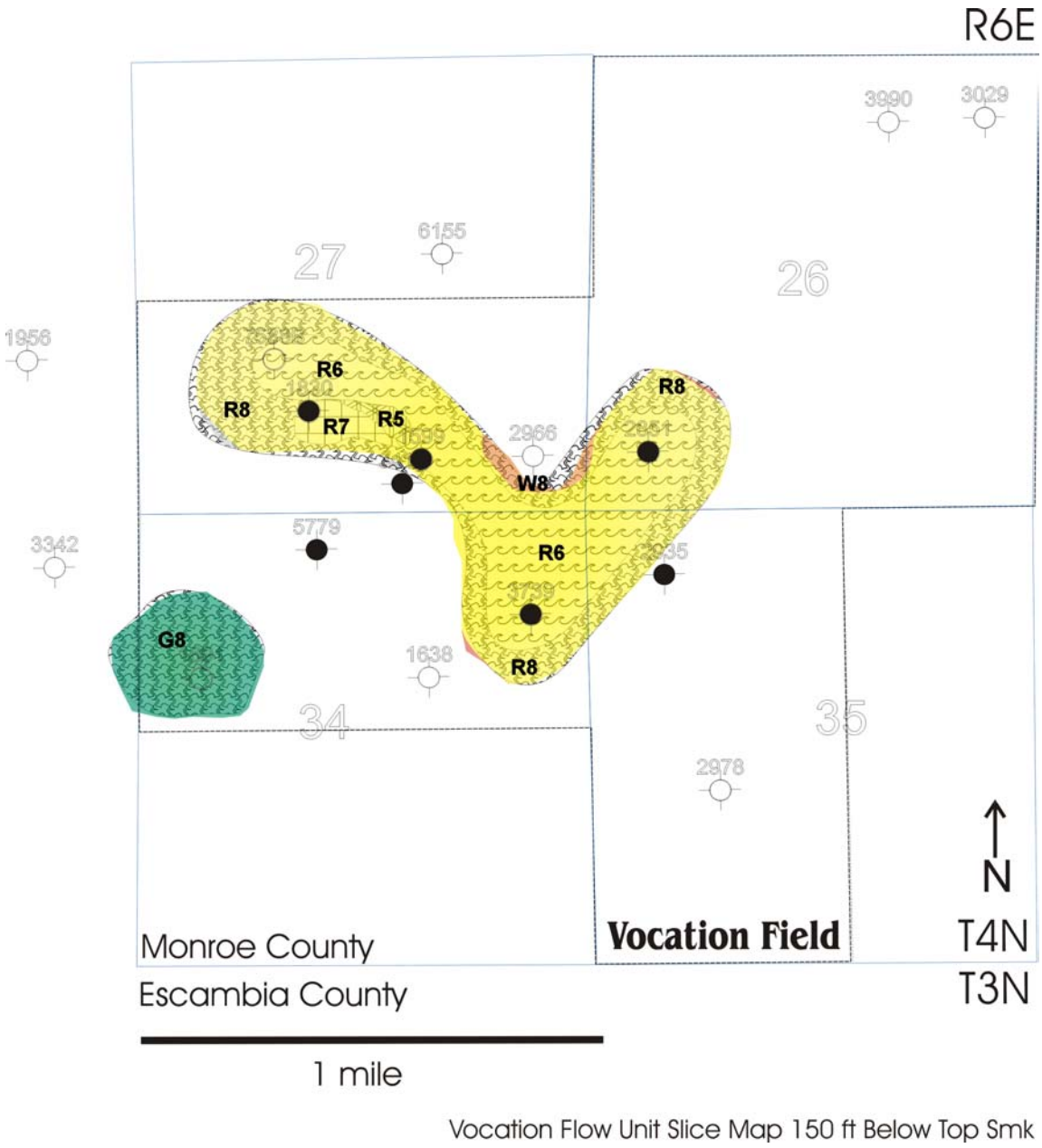

Figure 74. Vocation Flow Unit Slice Map 150 ft below Top of Smackover.

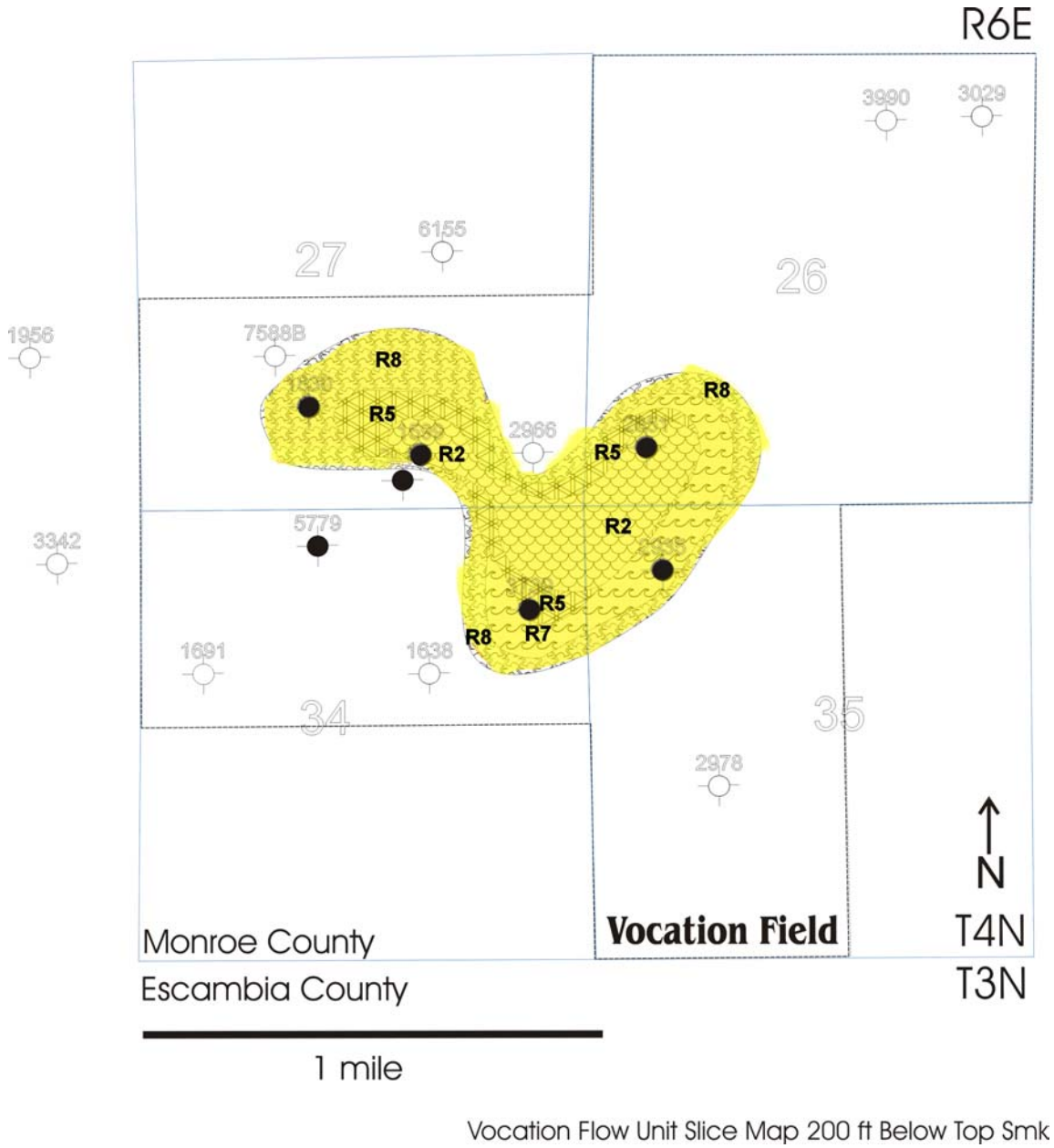

Figure 75. Vocation Flow Unit Slice Map 200 ft below Top of Smackover.

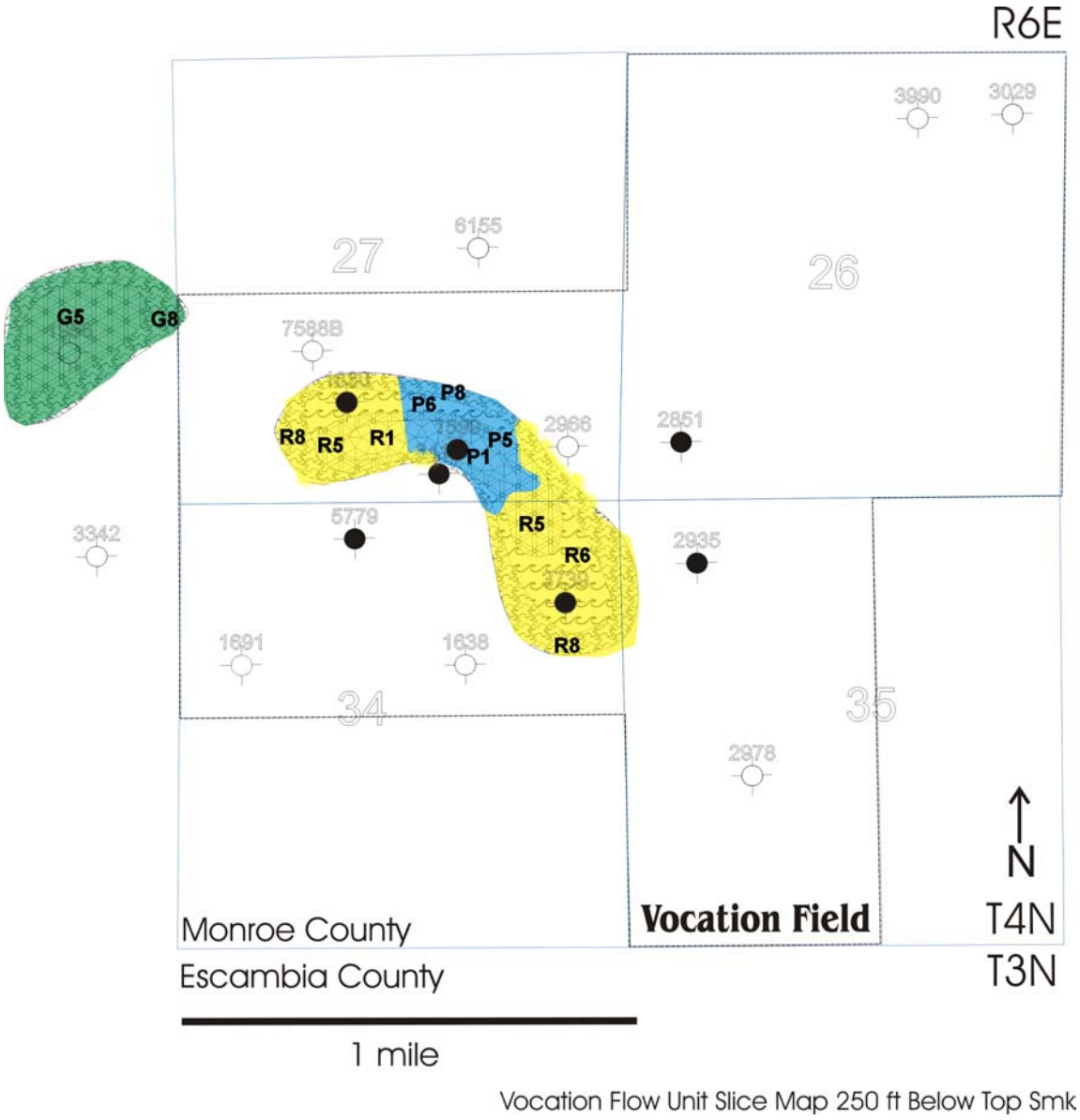

Figure 76. Vocation Flow Unit Slice Map 250 ft below Top of Smackover.

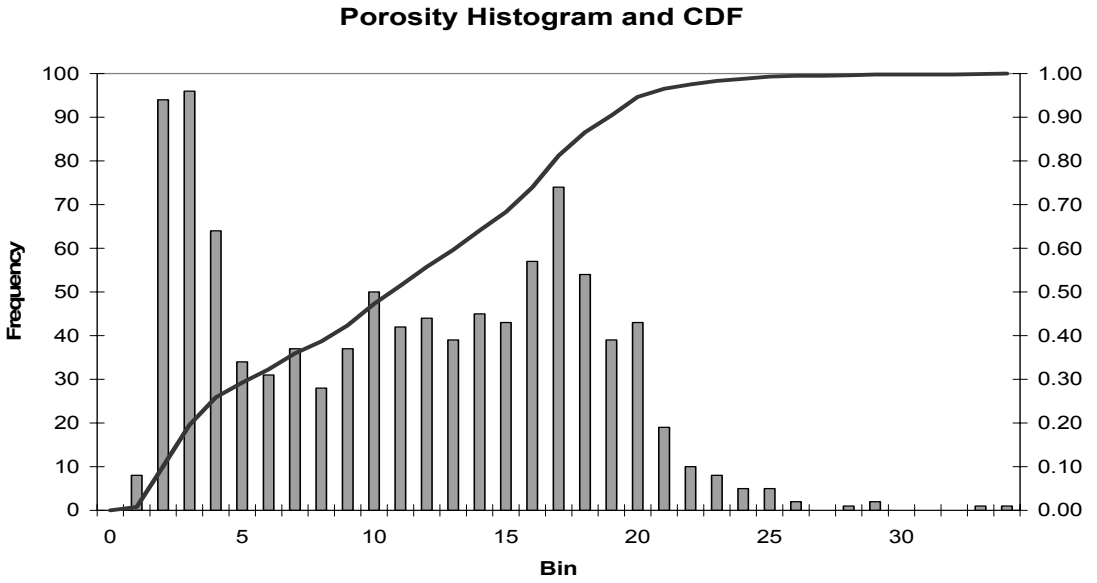

Figure 77. Histogram of porosity distribution and cumulative distribution frequency (CDF) in Appleton and Vocation fields.

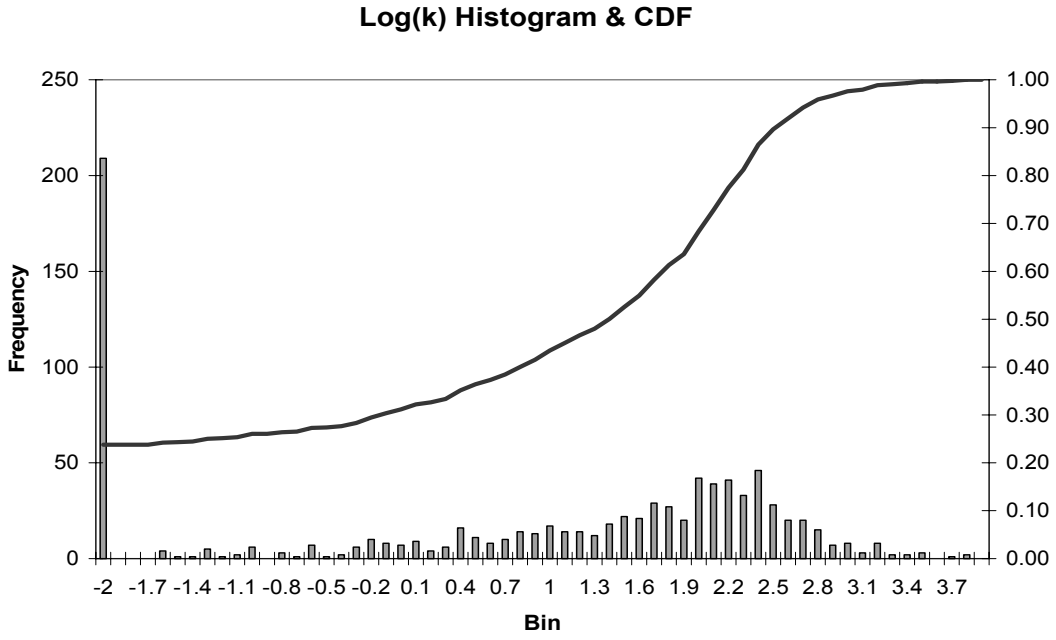

Figure 78. Histogram of permeability distribution and cumulative distribution frequency (CDF) in Appleton and Vocation fields.

Table 11. Typical petrologic characteristics of the various reservoir rankings.

Reservoir quality	Porosity range	Permeability range
RQ1	>19%	>400 md
RQ2	13-19%	>400 md
RQ3	>19%	80-400 md
RQ4	13-19%	80-400 md
RQ5	8-13%	80-400 md
RQ6	13-19%	10-80 md
RQ7	8-13%	10-80 md

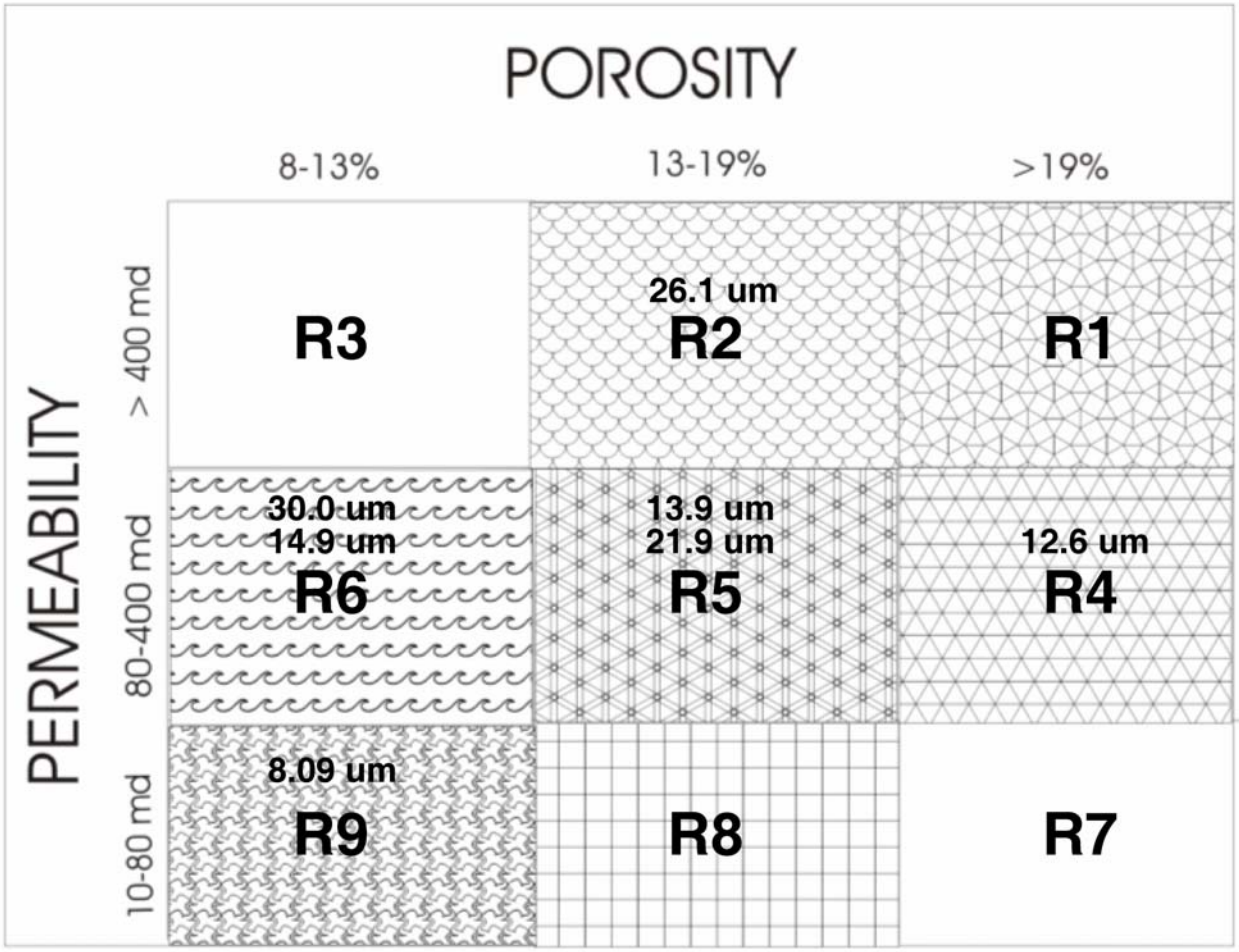

Figure 79. Reservoir quality pairs showing averaged porosity and permeability values along with corresponding MPA values over stratigraphic intervals for flow unit delineation.

Flow units are defined as the mappable portion of the total reservoir within which geological and petrophysical properties that affect the flow of fluids are consistent and are predictably

different from the properties of other reservoir rock volumes. There are no set rules as to how to identify flow units, although they do have five common characteristics.

1. A flow unit is an internally consistent (not necessarily homogeneous) volume of reservoir rock which is composed of one or more reservoir quality lithologies.
2. A flow unit has a consistent range of porosity and permeability values.
3. A flow unit is correlative and mappable between wells.
4. Flow units are recognizable on wireline logs.
5. Flow units may be in communication with other flow units.

In this work, we define flow units, baffles, and barriers. Flow units are those segments of the reservoir that exhibit good, intermediate, or poor connectivity as determined by combined porosity/permeability pairs and by median pore throat sizes. Baffles are poor quality zones that extend and can be correlated across an area of two or more well locations. Barriers are those rocks with very low mercury recovery efficiency, low poroperm pairs, and usually have mud supported or cemented fabrics that can be correlated over one-fourth or more of the reservoir area. These rock types are usually but not always easily identifiable on wireline logs.

Results of Flow Unit Mapping at Appleton and Vocation Fields

Flow units within Appleton and Vocation fields do not conform to facies boundaries or specific depths in the formation. Rather, they correlate with a combination of depositional and diagenetic attributes that are not readily identifiable as stratigraphic units; consequently, they are not always easily correlated between wells. Graphs of porosity-permeability versus rock types are illustrated in Figures 80-87. Seven flow units were identified and coded by reservoir quality (RQ1-7 and superimposed on top of lithofacies (MW—mudstone/wackestone, W—wackestone, P—packstone, G—grainstone and R—reef boundstone). The lithofacies code corresponds with

the first letters of the rock type. Reservoir quality is dependent upon different genetic pore types that have resulted from different styles and degrees of diagenesis that have overprinted depositional rock types and which are not consistently related to simple stratigraphic units within the field. This is evidenced by comparing structural maps in the field to porosity and permeability maps and noting which porosity and permeability trends more closely follow structure than lithofacies, indicating that diagenesis played a large role in porosity and permeability development.

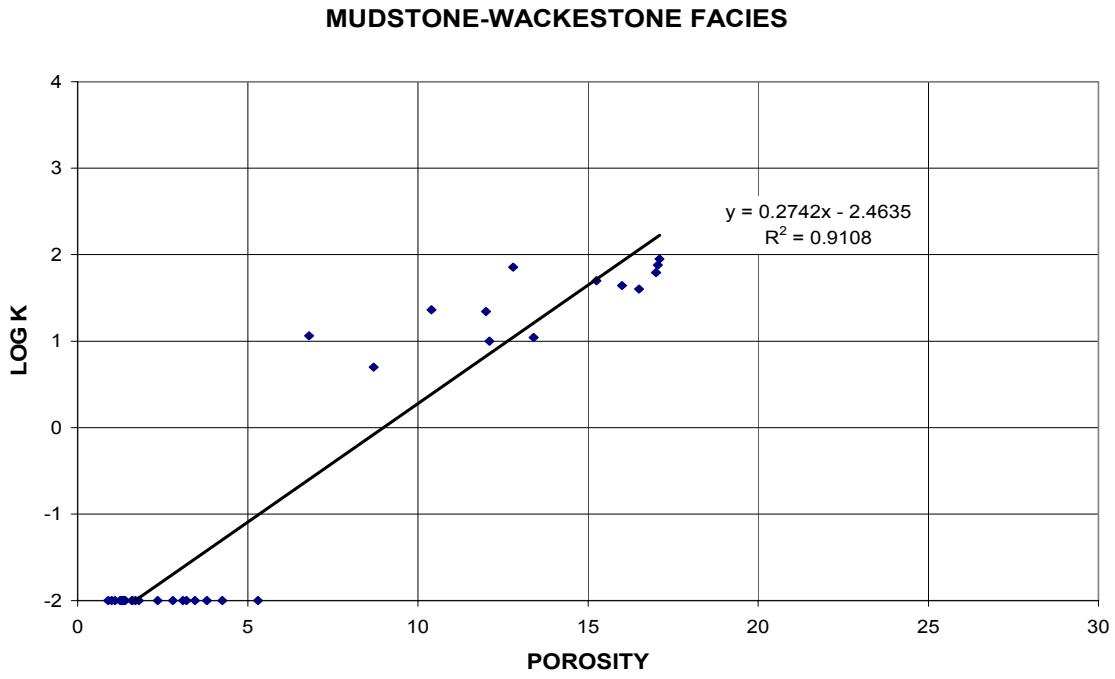

Figure 80. Porosity-permeability plot showing correlation to rock type in Appleton field.

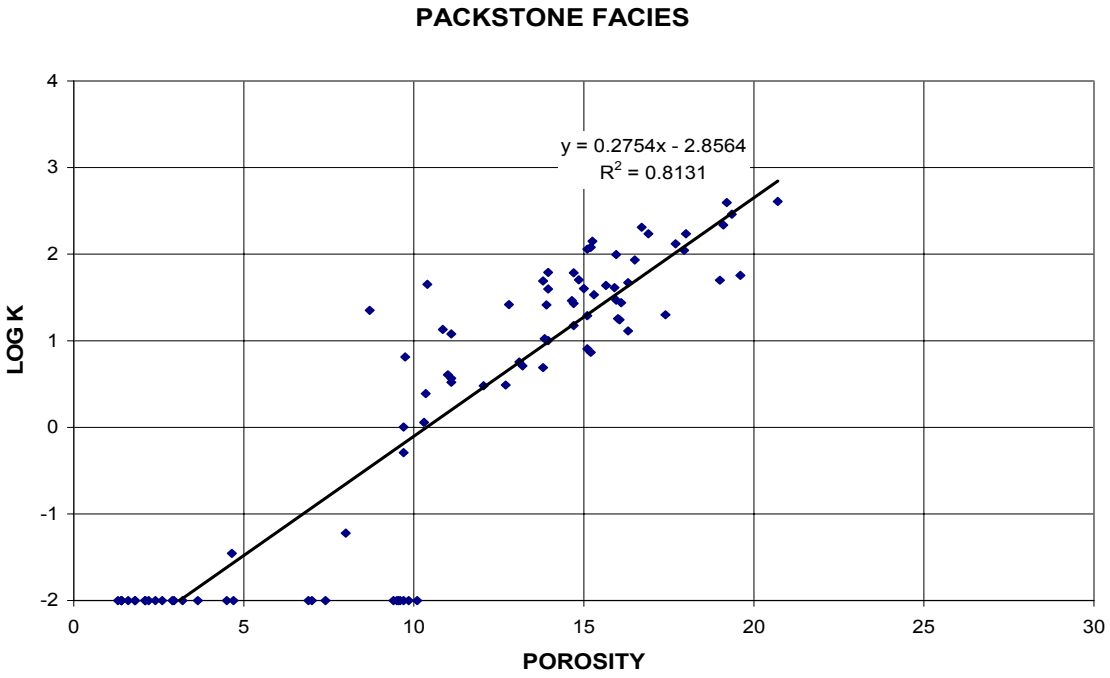

Figure 81. Porosity-permeability plot showing correlation to rock type in Appleton field.

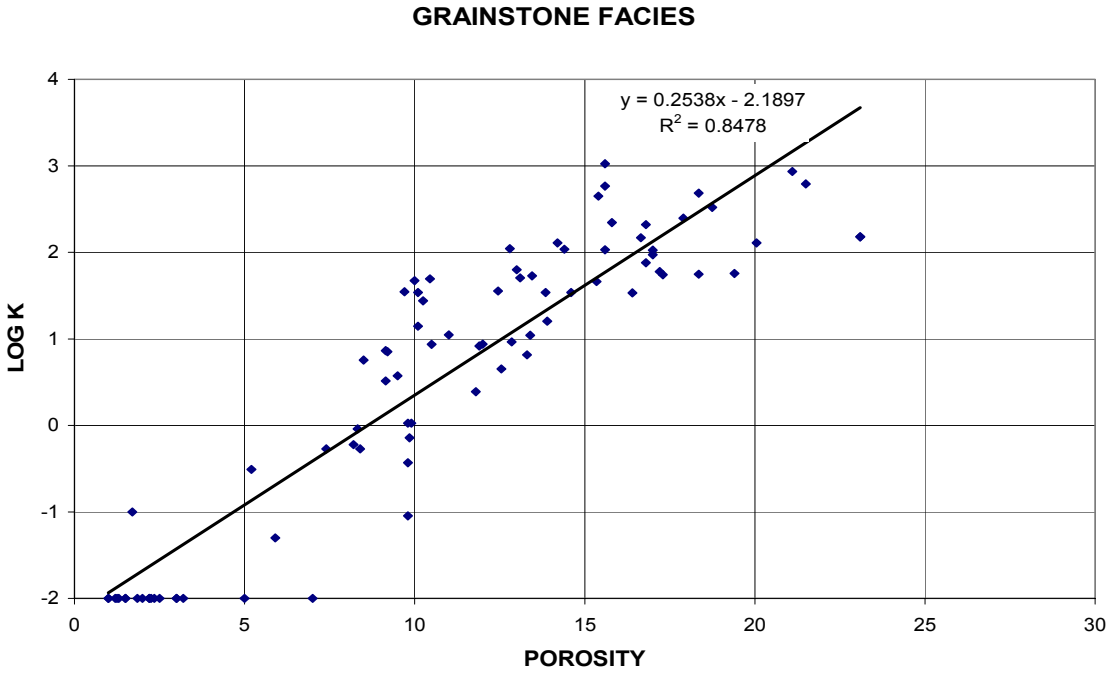

Figure 82. Porosity-permeability plot showing correlation to rock type in Appleton field.

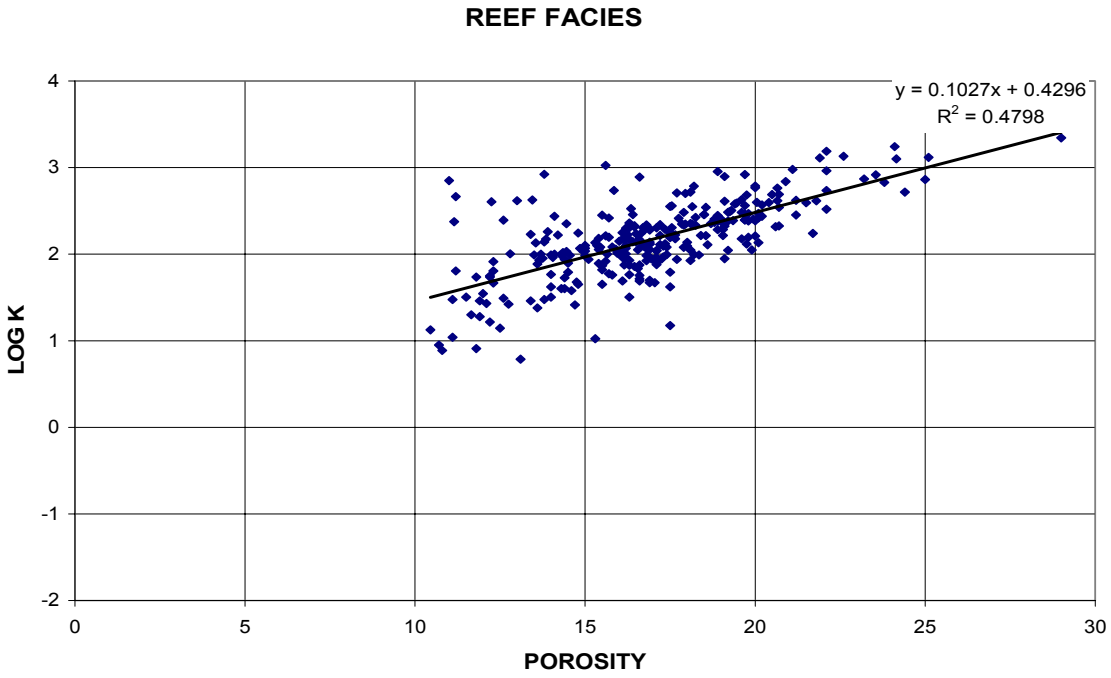

Figure 83. Porosity-permeability plot showing correlation to rock type in Appleton field.

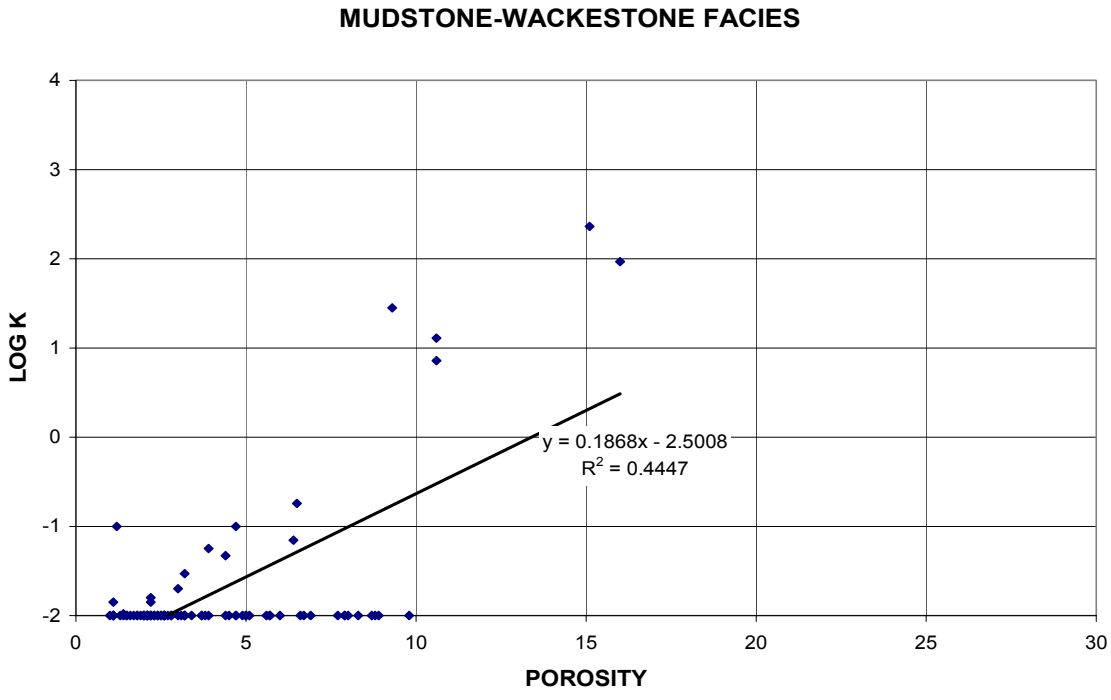

Figure 84. Porosity-permeability plot showing correlation to rock type in Vocation field.

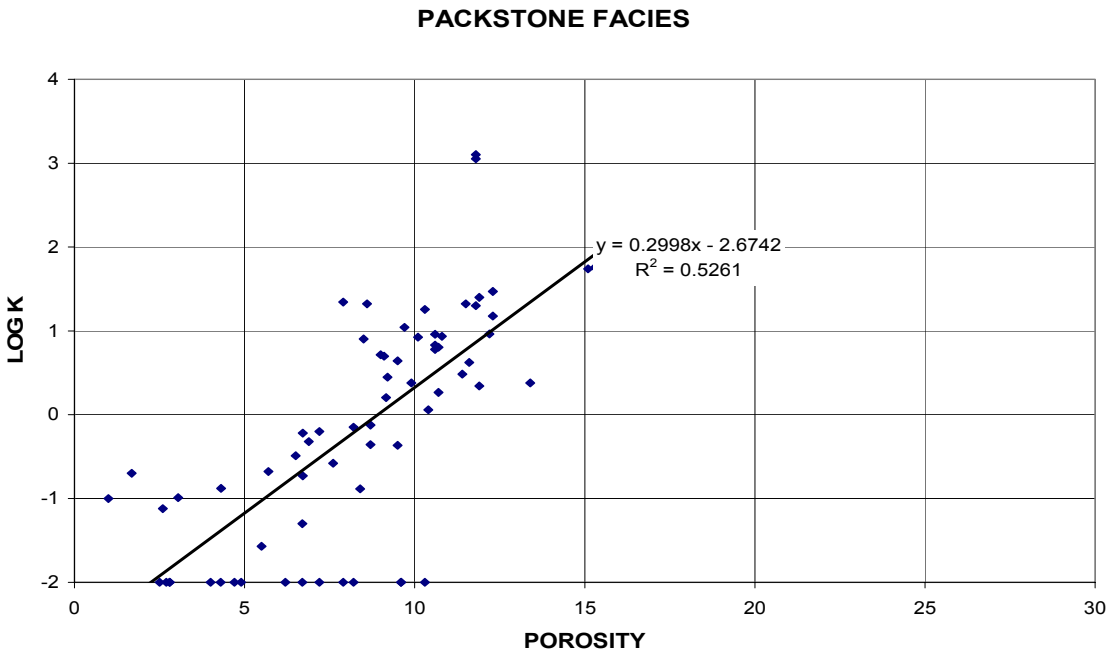

Figure 85. Porosity-permeability plot showing correlation to rock type in Vocation field.

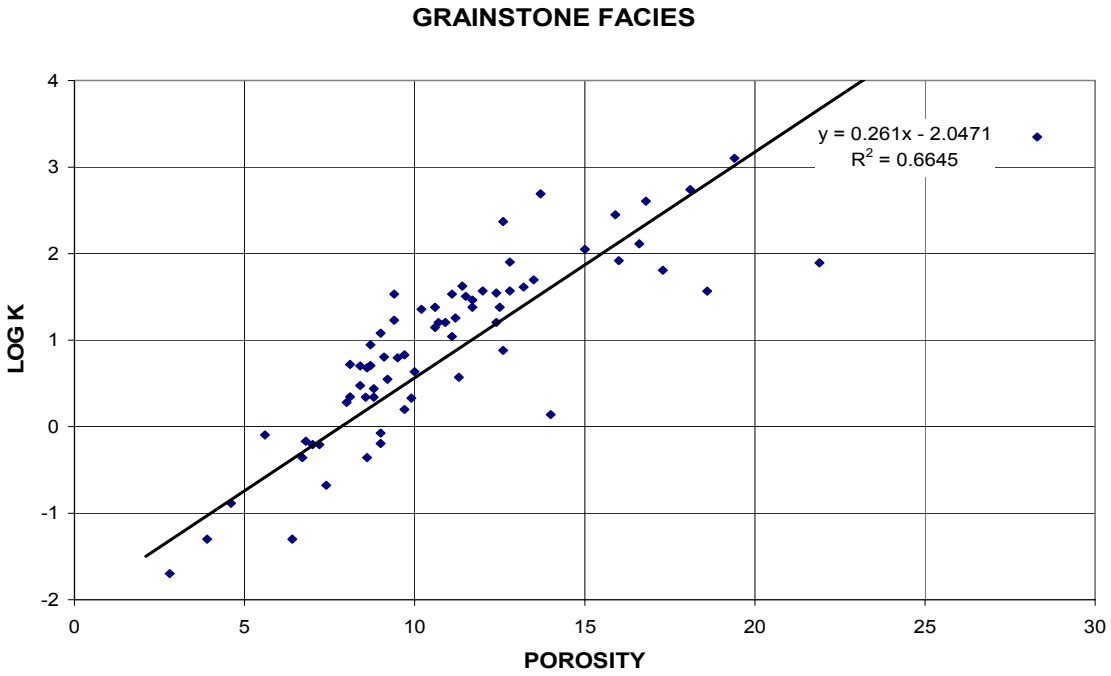

Figure 86. Porosity-permeability plot showing correlation to rock type in Vocation field.

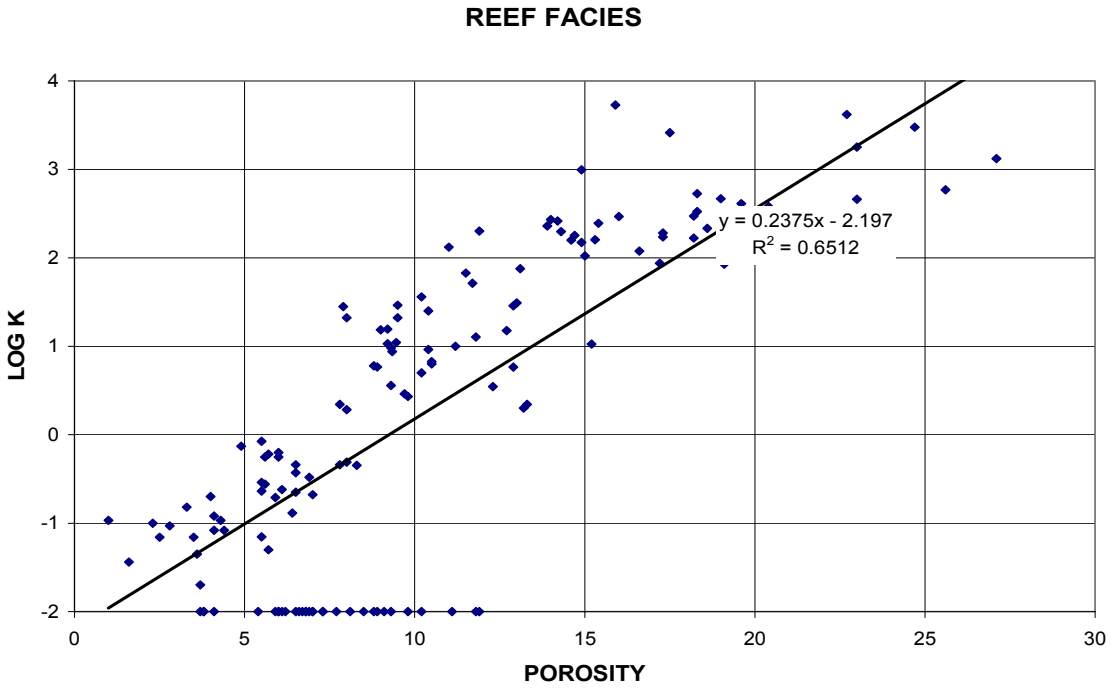

Figure 87. Porosity-permeability plot showing correlation to rock type in Vocation field.

The uppermost interval (0-80 feet below the top of the Smackover) at Appleton Field is dominated by muddier lithologies and RQ5-RQ7 quality flow units. These flow units are discontinuous both laterally and vertically. Reef boundstone facies dominate the lower part of the Smackover in this field and RQ1-RQ4, RQ5 and RQ7 are the more prevalent flow units in this reservoir interval. The highest poroperm values in the reservoir of Appleton Field are well developed beneath the structural culminations of the composite paleotopographic feature. The thickest zones (up to 80 ft) are developed near the crest of the paleostructures. Flow units in the field trend NW-SE throughout the entire Smackover interval which correspond to the same NW-SE paleotopographic trend in the field, implying a diagenetic impact to the porosity-permeability trend. In the lower portion of the reservoir at Appleton Field, flow units do closely tract lithofacies and in this case, log correlation based on lithofacies can be an excellent predictor of the distribution of reservoir quality rocks.

The uppermost interval (0-60 ft below the top of the Smackover) at Vocation Field is dominated by packstone and grainstone with reservoir quality values of RQ3-RQ7. A barrier between flow units is present in the center of the field separating reservoir flow units in the eastern and western parts of the field. This barrier in the flow units is due to different lithologies located in the center of the field that form a communication barrier between flow units. Deeper in the Smackover interval (greater than 100 ft below the top of the Smackover), reef boundstone and grainstone become the dominant lithofacies with reservoir quality ranging from RQ3-RQ7, with the reef boundstone having the highest reservoir quality. An increase in reservoir quality is observed at approximately 200 feet below the top of the Smackover. At this depth, the reservoir in the center of the field has the highest quality reservoir facies while the rocks in the eastern and western portions of the field do not include high quality reservoir rock. This high reservoir quality zone is due to the reef boundstone facies encountered in the reservoir in the center of the field which provides good lateral and vertical continuity. As in Appleton Field, there is a diagenetic overprint that is evident as flow units cut across lithofacies.

Task 7—3-D Geologic-Engineering Model.--The integration of the reservoir characterization information has been done by Mancini and Llinas at the University of Alabama. The work described below is from Llinas' dissertation at the University of Alabama and a paper submitted for publication in the Transactions of the Gulf Coast Association of Geological Societies (2003) by Llinas.

The first discovery of oil in Smackover carbonate sediments deposited over a pre-Jurassic basement high in southwest Alabama was Toxey field in 1967, located in Choctaw County. Since then, the search for similar fields has become an important exploratory objective. The result is that more than 40 Smackover oil fields have been discovered to date along the updip

basement ridge play as defined by Mancini *et al.* (1991). Reservoir grade rocks in these fields have been identified in microbial buildups and shoal/shoreface facies. Nonetheless, characterization of reservoirs in shallow marine carbonate settings is difficult, because of their high susceptibility to the complex interaction of biological, chemical and physical processes. The geometry and irregular topography of the paleohighs on which the Smackover was deposited contribute to complicate the prediction of the distribution and heterogeneity of the reservoir facies. Kerans and Tinker (1997) suggest that depositional topography is the most important variable controlling the nature of the rock record in a shallow marine carbonate setting. Greater depositional topography results in more lithofacies variability, greater reservoir heterogeneity, and increased difficulty in correlating between wells at any spacing (Kerans and Tinker, 1997).

The objective of this paper is to illustrate with examples from the Vocation and Appleton fields the distribution of the depositional/reservoir facies found in the Smackover Formation, and to identify the diverse factors controlling the occurrence of reservoir facies in this particular shallow marine setting. In addition, the importance of integrating geological and geophysical data with geologic concepts in order to improve the knowledge of the dynamics and resulting fabric of Smackover facies associated with basement paleohighs will be shown.

Geologic Setting

The onset of the deposition of the Smackover Formation began in the late Oxfordian with the accumulation of an extensive carbonate succession across the northern margin of the Gulf of Mexico Basin during a third order eustatic sea level rise and subsequent highstand. Benson (1988) correlated this event to the J3.1 cycle of the global sea level curve published by Vail *et al.* (1984). In the Eastern Gulf Coastal Plain, the Smackover Formation is interpreted as being deposited on a carbonate ramp (Ahr, 1973; Benson, 1988; Tew *et al.* 1993). Within this geologic

scenario, Smackover accumulation was controlled by antecedent topography generated by salt tectonics, subsidence and basement highs.

In southwest Alabama the Smackover Formation is the most prolific oil-producing unit in the updip basement ridge play. The play area is bounded downdip by the regional peripheral fault trend, and updip by the pinchout of the Smackover Formation in the Manila and Conecuh Sub-basins area (Fig. 88). In this geologic setting, carbonates of the Smackover Formation unconformably overlie either the Norphlet Formation in low elevated areas, or crystalline rocks on basement highs. The Buckner Anhydrite Member of the Upper Jurassic Haynesville Formation conformably overlies the Smackover Formation and serves as a regional seal rock (Fig. 89). The play is characterized by the onlap of shallow marine carbonate deposits of the Smackover Formation against the flanks and crests of basement paleohighs formed by differential tectonic-thermal subsidence and erosion of large horst blocks formed during the Late Triassic-Early Jurassic rifting event. The traps are structural, formed by anticlines and faulted anticlines developed over the basement highs, and combination traps formed by porosity and/or permeability terminations on the flanks of the anticlines (Mancini *et al.*, 1991).

Benson *et al.* (1991) and Mancini *et al.* (1998) made a subdivision of the basement ridge play into high relief and low relief structures (Fig. 90). In the high relief model, the basement structure was not completely covered during sea level rise due to its high topographic relief, while in the low relief model the structure was completely submerged during Smackover times. In both conceptual models the Smackover is characterized by a symmetric distribution of shallow marine facies around the paleotopographic high. basement paleohighs at Appleton and Vocation

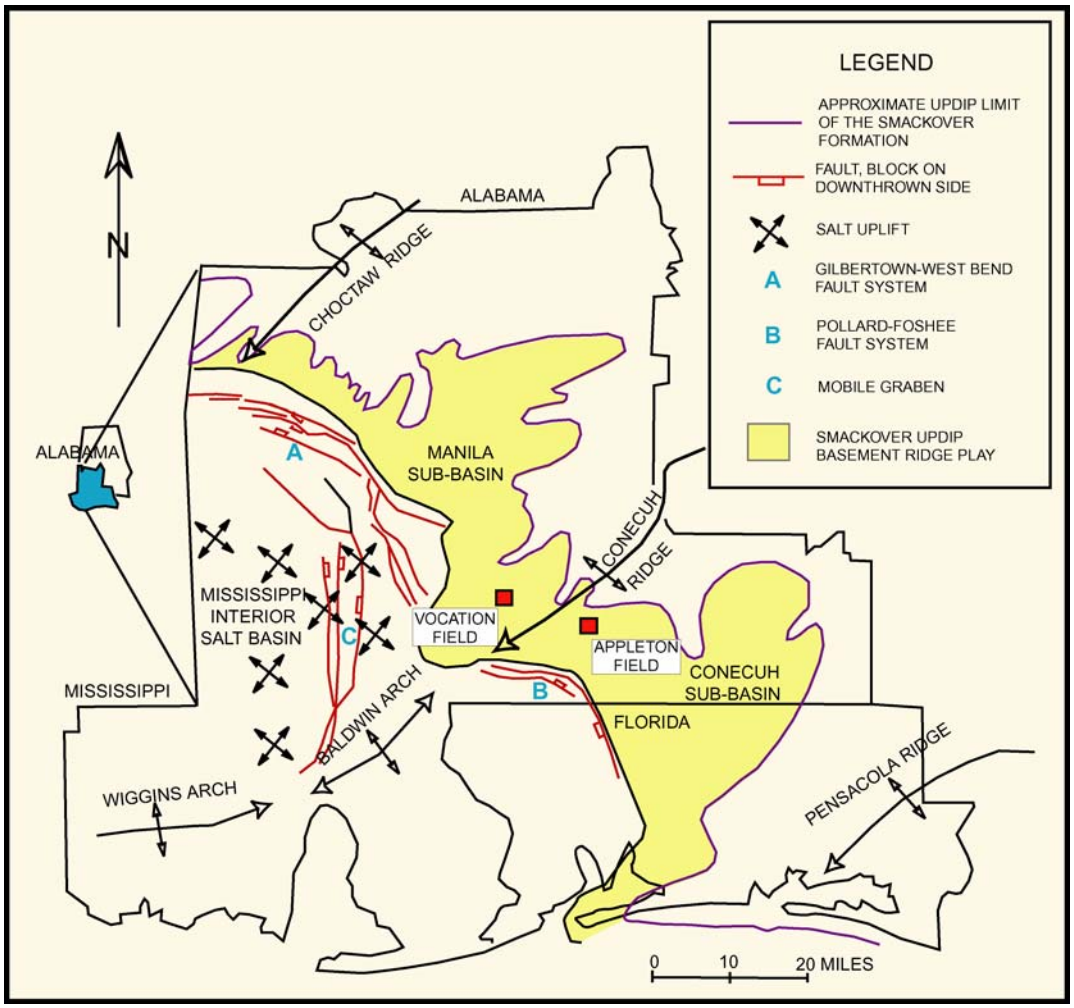

Figure 88: Major tectonic features and the geographic distribution of the updip basement ridge play in southwest Alabama. Location of Vocation and Appleton field is included.

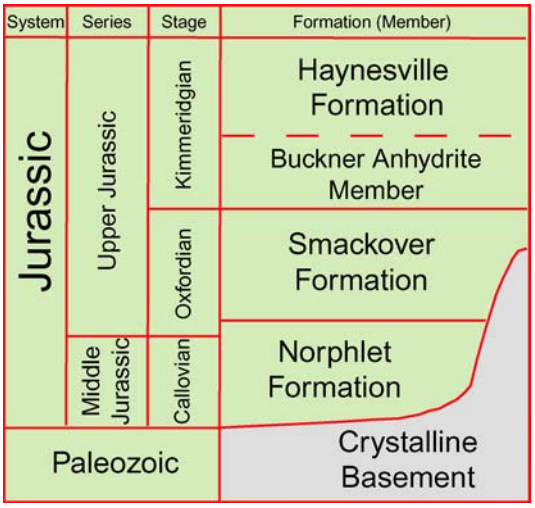

Figure 89: Jurassic stratigraphy in the study area.

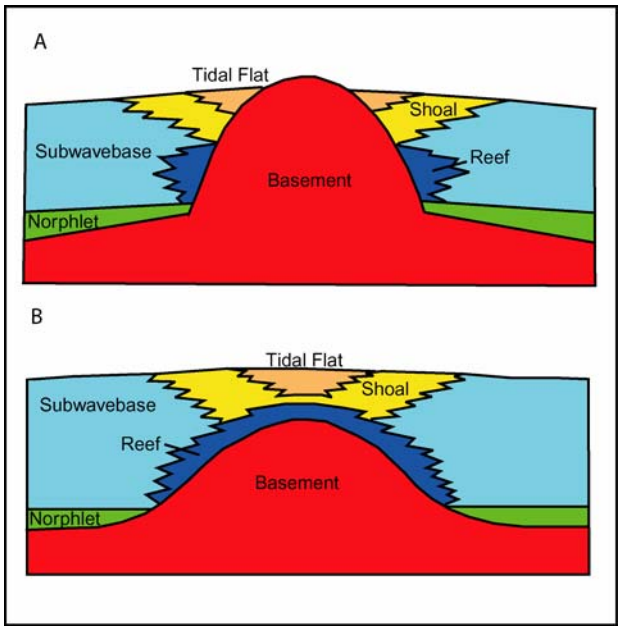

Figure 90: Conceptual models of Smackover plays in updip basement ridge play. High relief (A) and low relief (B) paleotopographic features (modified from Mancini *et al.*, 1998).

fields, located in southwestern Alabama, have been identified as low and high relief structures, respectively (Benson *et al.*, 1991).

Vocation Field

Vocation field was discovered in Monroe County by Getty Oil Co. in 1971. It is located in the southeastern margin of the Manila Sub-basin and along the eastern flank of the Conecuh Ridge. Twenty wells have been drilled with a success ratio of about 50%. The field has produced approximately 2.3 MMBO and 4.9 BCFG from dolograinstone-dolopackstone facies in the upper part of the Smackover Formation. Currently only one well, the Strago-Byrd 26-13 #2 (well permit 11185) is active, while the other oil wells in the field have been abandoned over time as their productivity rates declined.

The well dataset in Vocation field consisted of 1100 feet (including 205 thin sections) of core segments distributed in 11 wells and corresponding to the Smackover-Buckner interval. Conventional petrophysical analyses were also available for each core. Core data were calibrated and integrated with wireline logs in order to characterize the well log response for each depositional facies identified from the core study. This procedure allowed for an extrapolation of depositional environment interpretation from core study to wells lacking core data.

The result of the well data analyses was the identification of six shallow marine depositional facies, which include shallow subwave base, microbial reefal buildup, shoreface, shoal, lagoon and tidal flat covered by sabkha/salina sediments of the Buckner Anhydrite Member. The well log correlation in Figure 91 shows a symmetrical distribution of the depositional facies as predicted in the conceptual model (Fig. 90A) with the exception of the microbial buildups, which are only present in wells located on the eastern and northern flanks of the Vocation basement

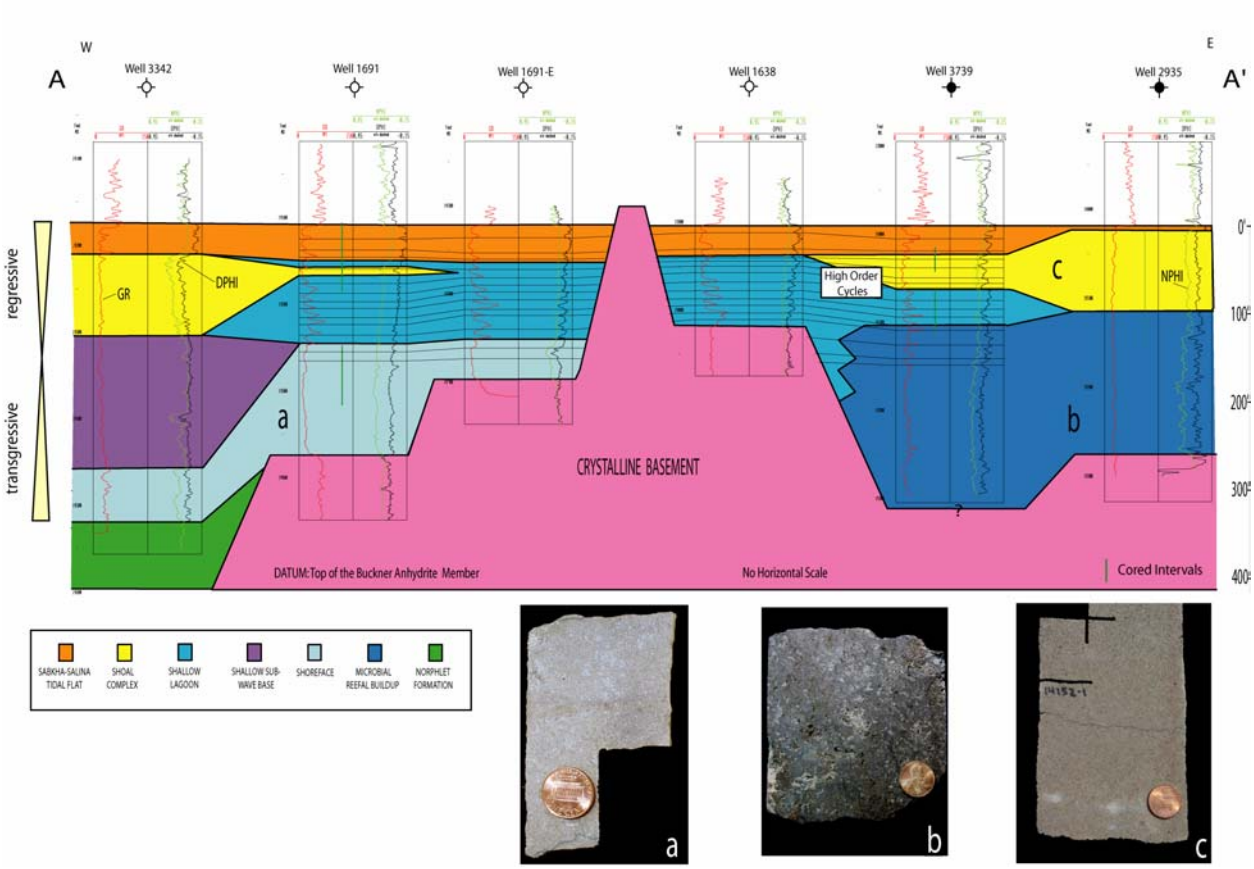

Figure 91: (A) W-E stratigraphic cross section in the Vocation Field area on top of the Buckner Anhydrite Member and showing distribution of depositional facies (see Figure 6 for its location). Main potential reservoir grade rocks include: sucrosic dolostone-shoreface (photo a), thrombolitic doloboundstone-microbial reefal buildup (photo b), and ooid dolograinstone-shoal complex (photo c).

paleohigh defined at this point solely on well data. On the eastern flank, higher energy deposits represented by sucrosic dolostone accumulated contemporaneously with the reefal facies. These rocks were interpreted to represent upper shoreface deposits based on the common presence of ooid-peloid ghosts observed in thin sections and the overall texture of the rock that suggests a homogeneous and grainy depositional fabric.

Despite the long history of diagenetic events that affected the Smackover Formation in the Vocation filed area, the primary depositional texture controls the distribution of the reservoir grade rocks (Llinás, 2002a). The reservoir quality rocks consist of sucrosic dolostone from the shoreface facies (photograph a, Fig. 91), of thrombolitic reticulate doloboundstone from the microbial reefal complex (photograph b, Fig. 91), and of ooid-oncoid dolograinstone/ dolopackstone from the shoal complex (photograph c, Fig. 91). The most important diagenetic events that generated secondary porosity and improved permeability of the pore network include extensive dolomitization of the entire Smackover section in the field, selective leaching of aragonite allochems expressed mainly in the shoal grainstone facies, and the late stage non-selective dissolution event that created cavernous and vuggy porosity widely developed in the reefal facies (Llinás, 2002a). Tectonic and compactional fracturing is also an important mechanism for the enhancement of the porosity and permeability with increasing depth.

A 3-D seismic dataset was used in order to define the geometry of the Vocation paleohigh and the distribution of the Smackover section in the area. The criteria described by Hart and Balch (2000) for the identification of the main horizons were applied in this seismic interpretation.

The time slice at 2.7 sec shown in Figure 92 provides a very good first approximation of the geometry of the basement structure in the area. The high amplitudes (warm colors in the image)

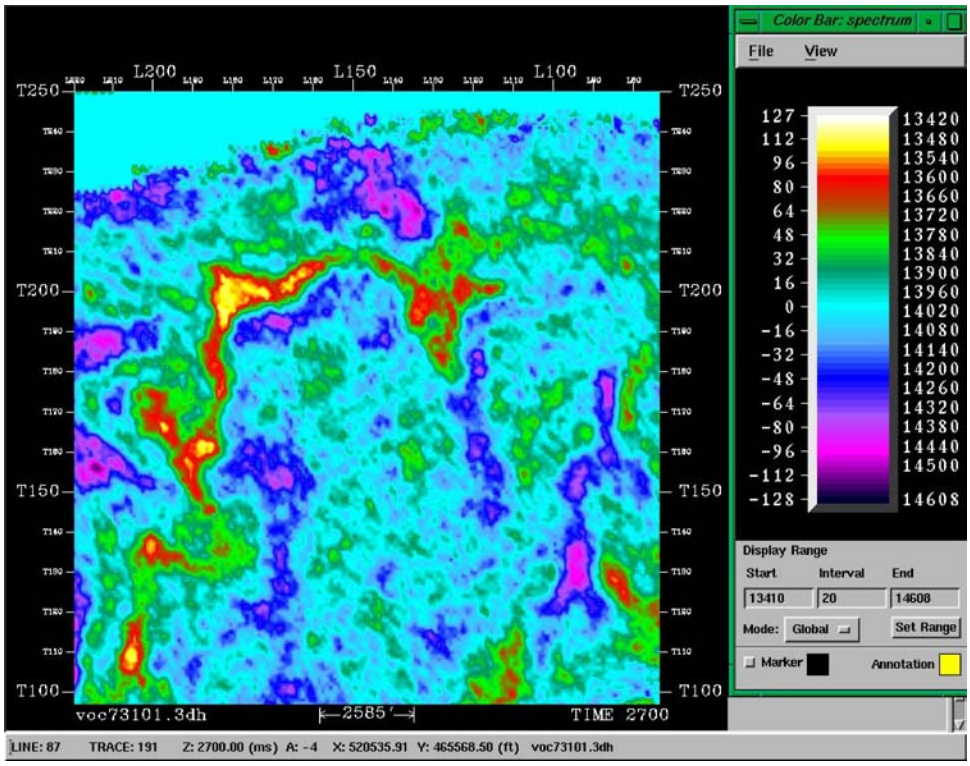

Figure 92: Time slice at 2.7 sec. The high amplitude values (yellow, red and light green) delineate the Vocation paleohigh (compare with Figure 6).

produced by the strong contrast in the acoustic impedance between the Norphlet Formation and Paleozoic crystalline basement define the approximate updip limit of the Norphlet Formation. The Vocation structure is a composite feature consisting of one main north-south elongated paleohigh with three crests that remained subaerially exposed until the end of Smackover time (Fig. 93), and a smaller and lower elevated feature to the northeast, which was completely inundated during that time. These paleohighs are bounded to the east and north by high angle normal faults (Figs. 93 and 94) that formed prior to Smackover accumulation and continued to be active during Smackover time. Figure 94 is an interpreted W-E seismic line showing the main and smaller basement features and the onlap and pinchout of the Norphlet and Smackover formations on the flanks of the paleohighs. The transition from the low velocity siltstone beds of the Haynesville Formation to the dense anhydrite layers of the Buckner is expressed by a peak (positive reflection coefficient) in the seismic trace. The reefal facies was detected as subtle mounded geometries (Fig. 94) formed by a trough in the seismic trace (negative reflection coefficient) generated as the seismic signal enters into this more porous medium. The lower contact of the Smackover Formation is manifested as a trough when it rests directly upon the more dense rocks of the crystalline basement or as a peak when it overlies the Norphlet Formation (Fig. 94). This seismic interpretation confirmed that the presence of microbial buildups is limited to the eastern and northern flanks of the structure as illustrated in Figure 95. The crest of the lower elevated feature to the northeast was completely colonized by these organisms as predicted in the low relief paleotopographic conceptual model (Fig. 90).

Considering that porosity logs (together with the GR curve) proved to be the best logs for the definition of depositional facies, the NPHI and DPHI log curves were used to generate a

single porosity curve adjusted to approximate the porosity results from the core analysis. This porosity

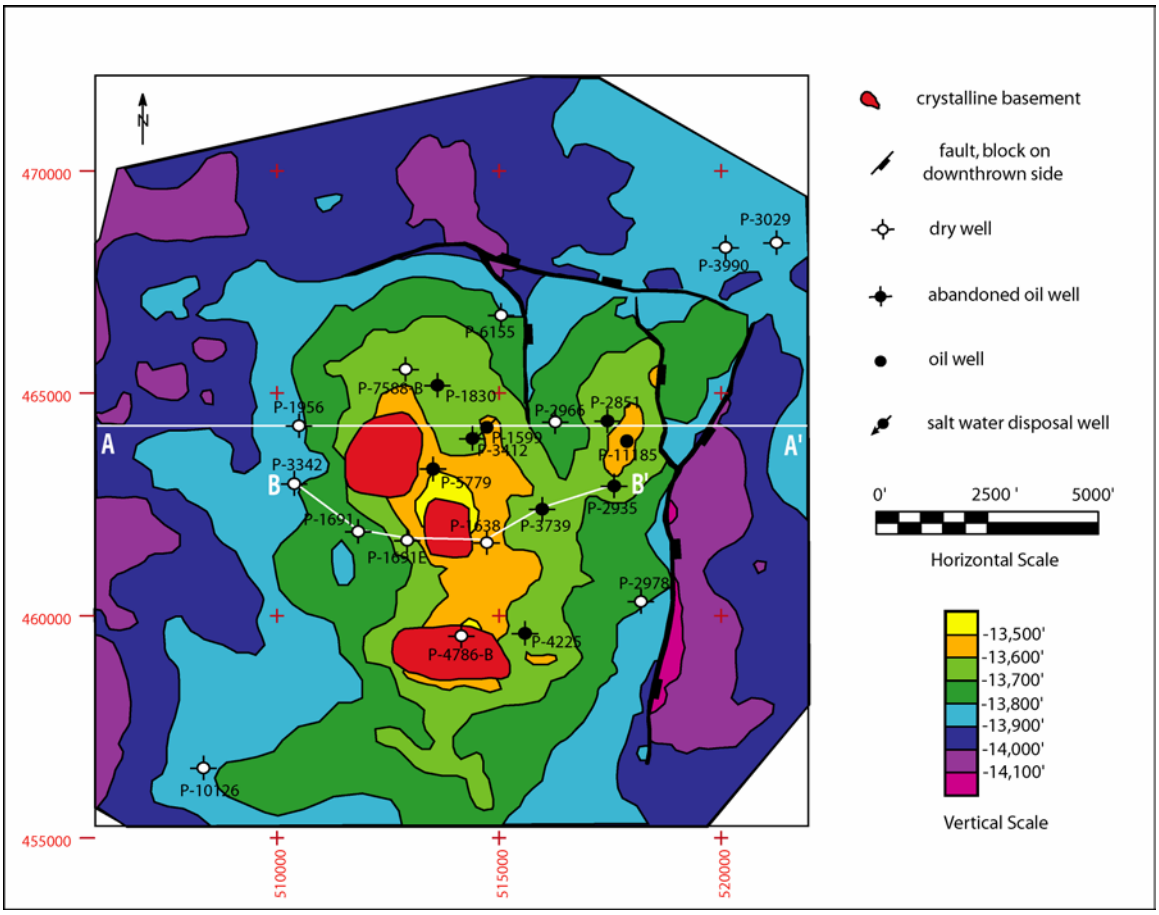

Figure 93: Structure contour map in depth based on 3-D seismic interpretation of the top of the Buckner-Smackover Formation at Vocation Field.

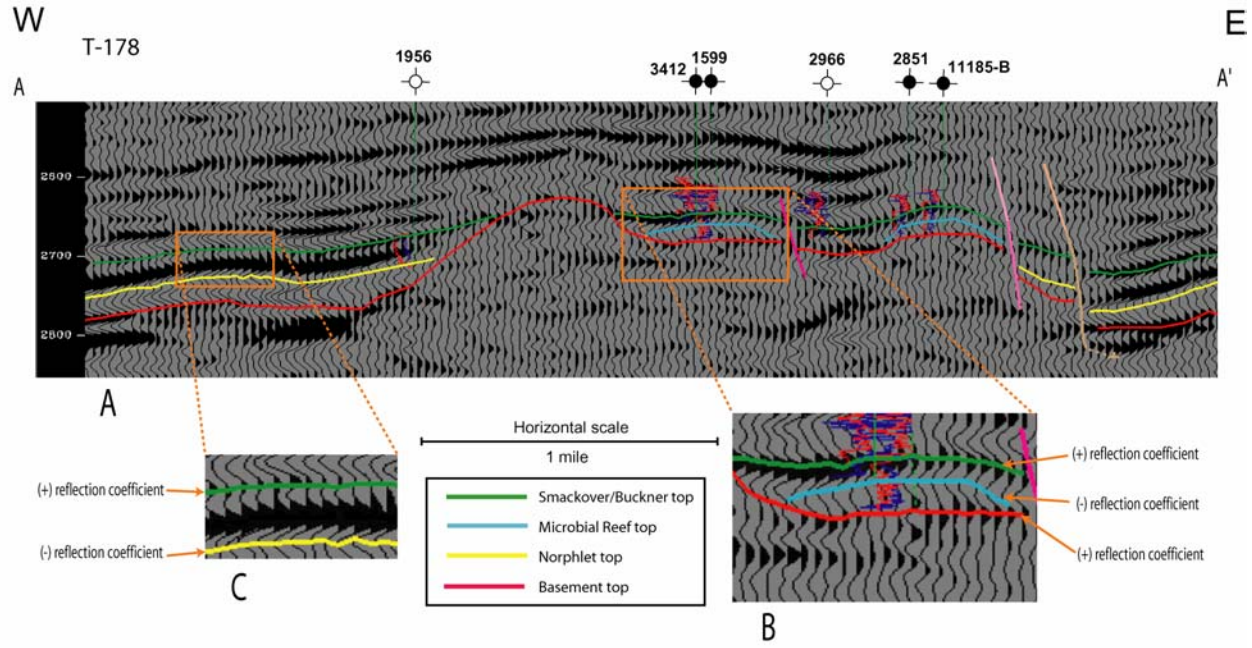

Figure 94: (A) W-E interpreted seismic line along Vocation Field (see Figure 6 for its location), (B) Close-up of the Smackover microbial reefal buildup on top of crystalline rocks, and (C) Close-up of the Smackover Formation on top of the Norphlet Formation.

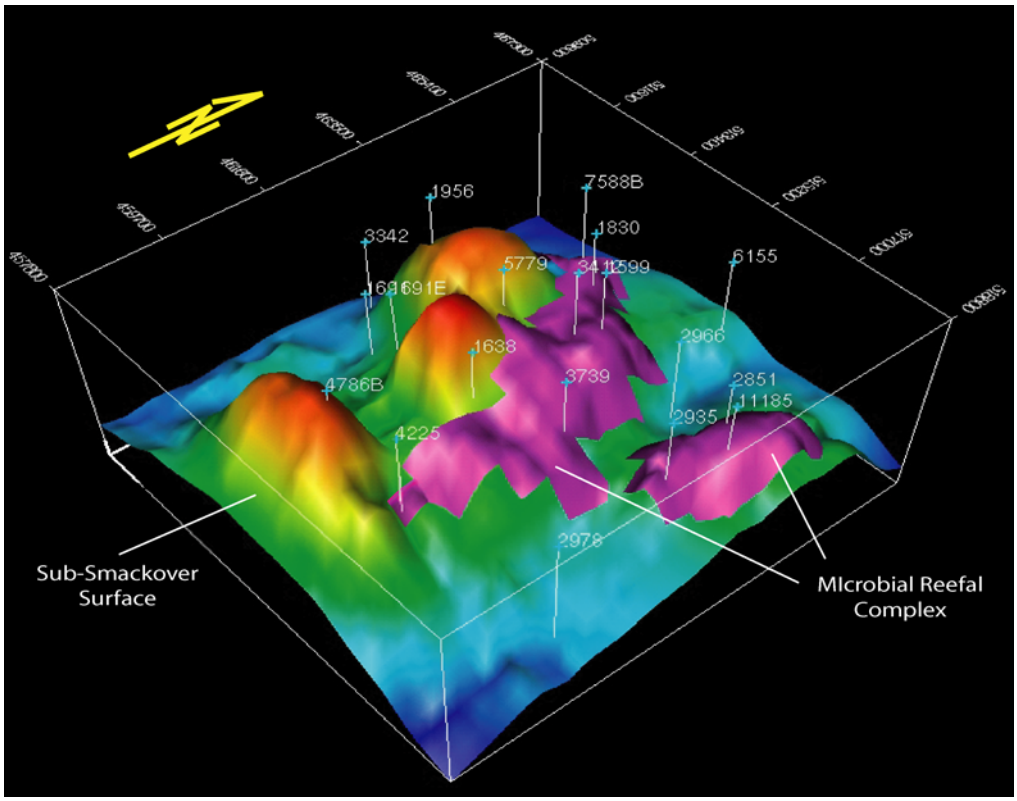

Figure 95: Distribution of the Smackover microbial reef buildups base on the seismic interpretation and constrained by well control.

curve was integrated into the seismic framework interpretation. The result was the generation of the three dimensional model illustrated in Figure 96, which delineates the depositional facies and reservoirs not resolvable by the use of the seismic data alone.

Sediments of the Smackover Formation in the Vocation field area accumulated as part of a transgressive-regressive cycle (Llinás, 2002b) The transgressive phase is driven by the combined effect of a rapid eustatic sea level rise and tectonic/thermal subsidence. It is characterized by the development of microbial buildups and moderate energy shoreface deposits in shallower areas on-structure, and deposition of subwave base sediments in a seaward direction. The particular distribution of significant microbial reefal deposits is explained by paleotopography and differences in the paleoenvironmental conditions (Llinás, 2002b). The establishment of a more restricted and quiet marine environment, in addition to gentler slopes of the depositional surface, favored the development of the microbial buildups on the eastern and northern flanks of the Vocation paleohigh. These deposits followed a retrogradational to aggradational stacking pattern during the “start-up” and “catch-up” phases of the Smackover carbonate system (Figs. 97A, B, and C). The upper part of the Smackover section represents the regressive phase caused by the continuing decrease and eventual stillstand in the rate of sea level rise during Smackover time accompanied by an increase in carbonate productivity due to the continued evaporation of marine water saturated in calcium carbonate (Llinás, 2002b). This change in the depositional setting resulted in variations in the paleoenvironmental conditions that led to the demise of the microbial reefal growth and the progradation of shoal, lagoon and tidal flat deposits that represent the “keep up” phase of the carbonate system (Figs. 97C and D). This progradational succession, including the Buckner evaporites, is characterized by minor sea level fluctuations expressed by fifteen

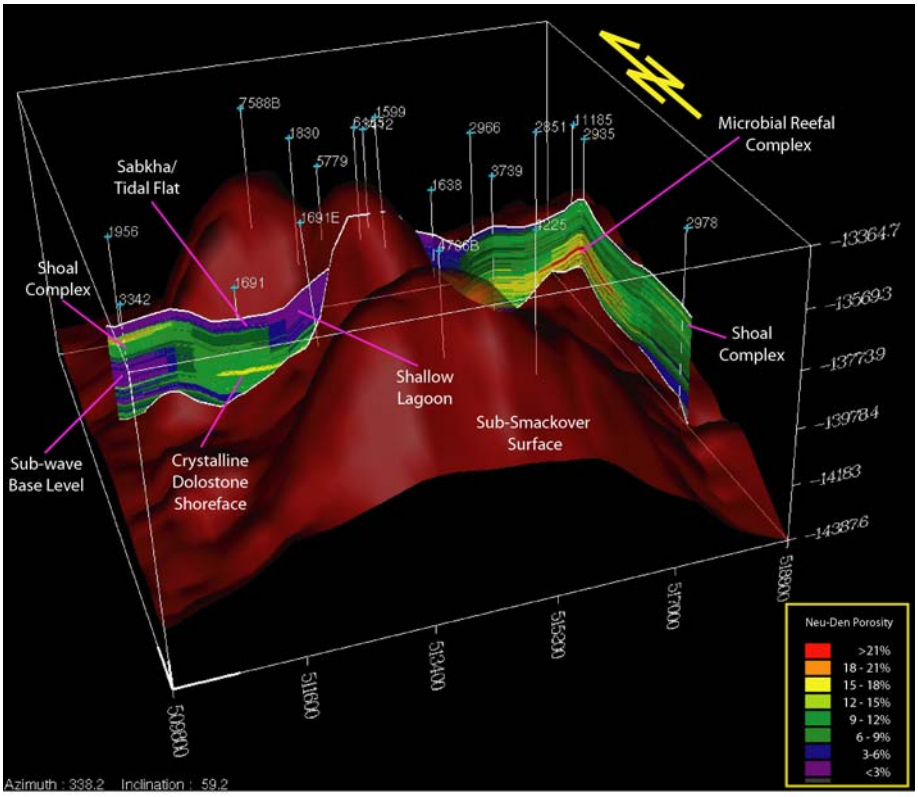

Figure 96: 3-D geologic model of the Vocation Field area showing the spatial distribution of depositional facies based on well log porosity and core data.

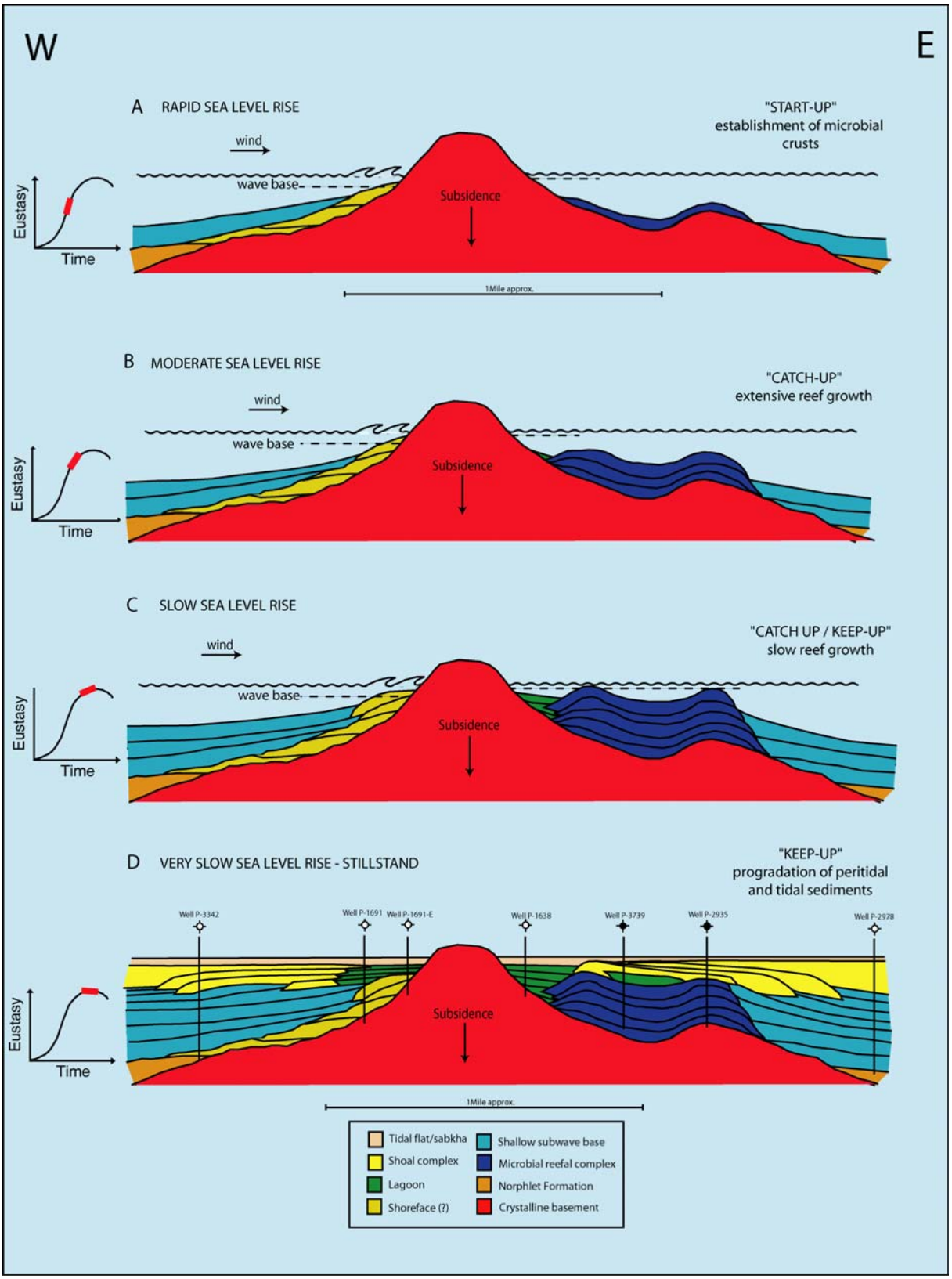

Figure 97: Depositional history of the Smackover Formation in Vocation Field.

higher order shallowing-upward cycles identified and correlated in wells located in proximal areas of the structure (Fig. 91).

Appleton Field

Appleton field, discovered in Escambia County by Texaco in 1982, is located on the western margin of the Conecuh Sub-basin and on the eastern flank on the Conecuh Ridge (Fig. 88). The reservoirs consist of doloboundstone and dolograinstone that represent microbial reefal and shoal /shoreface facies of the Smackover Formation. The field has eleven wells, seven of which are oil producers. Only four wells are currently active. Appleton field has produced approximately 2.7 MMBO (52°API) and 4.7 BCFG.

The interpretation of wireline logs in the field, supported by detailed well core descriptions made by Markland (1992), indicates an overall depositional sequence for the Smackover Formation comparable to the one described in the Vocation field area. The lower Smackover consists of shallow subwave base deposits in off-structure positions and microbial reefal facies accumulated on the structure as described previously by other authors (Markland, 1992: Benson *et al.*, 1996; Mancini *et al.*, 2000). The upper part of the Smackover section consists of ooid-oncoid-peloid dolograinstone to dolopackstone of an upper shoreface environment, and dolowackestone that accumulated in a tidal flat environment (Fig. 98). This succession is covered by supratidal sabkha/salina evaporites of the Buckner Anhydrite Member. There is a noticeable increase in the grain/mud ratio in the shoreface facies from northwest to southeast (Fig. 98). This variation is probably due to the presence of higher energy environments in the windward side (south and southeast) of the paleohigh than on the leeward side (north and northwest) behind the basement structure.

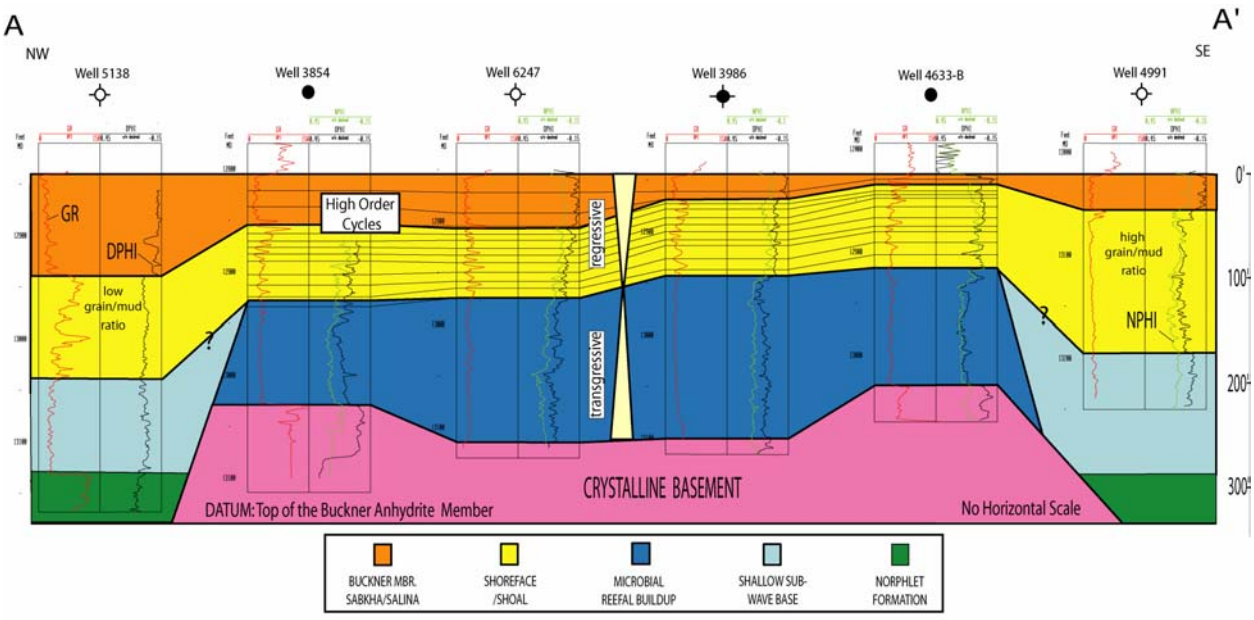

Figure 98: NW-SE stratigraphic cross section in the Appleton Field area on top of the Buckner Anhydrite Member and showing distribution of depositional facies (see Figure 12 for its location).

As in the Vocation field area, the Smackover Formation has been affected by various diagenetic processes including extensive dolomitization that modified the original texture of the rock and consequently its reservoir properties (Mancini *et al.*, 2000). However, as in Vocation field, the distribution of significant reservoir intervals is a function of depositional processes (Mancini *et al.*, 2000).

The seismic model for the Buckner-Smackover horizon published by Mancini *et al.* (2000) shows the Appleton basement structure as a northwest-southeast trending paleotopographic ridge comprised of several local paleohighs (Fig. 99). Figure 100 shows an interpreted W-E seismic line along the Appleton structure. The interpretation uses the criteria for horizon identification described by Hart and Balch (2000) and is constrained by well data. The seismic line shows the Norphlet Formation onlapping the flanks of a major composite local basement paleohigh, which was later covered by Smackover sediments. The interpretation also shows the extensive development of laterally continuous microbial reefal buildups on the crest of the local paleohigh.

Deposits of the Smackover/Buckner section in the Appleton field area accumulated as part of a transgressive-regressive cycle, as in Vocation field. The transgressive phase is generated by a rapid sea level rise that flooded the Appleton structure. During this time, sedimentation is characterized by subwave base sediments in deeper waters off-structure, and microbial reefal buildups on the upper parts of the paleohigh. Similar to Vocation field, microbial buildups were established on stable depositional surfaces with a gentle slope and began to grow in a predominantly aggradational pattern as a "catch–up" response of the carbonate system. The regressive phase is characterized by twelve shallowing-upward higher order cycles, which can correlated in wells drilled in on-structure locations. These cycles consist of aggradational and

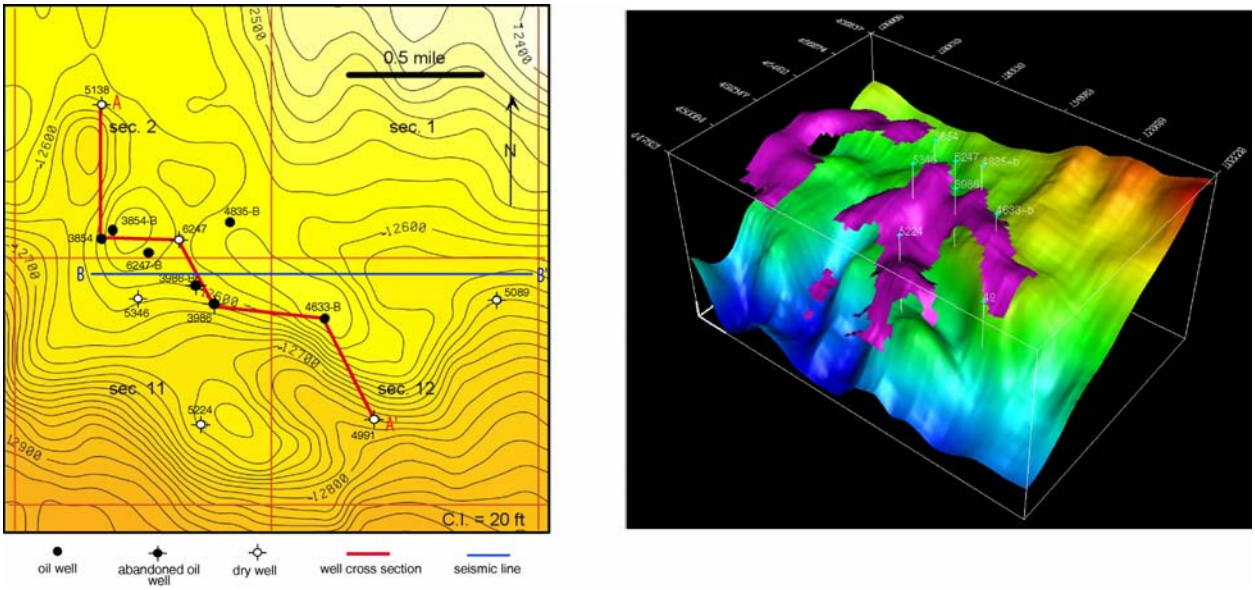

Figure 99: (A) Structure contour map in depth of the top of the Buckner-Smackover Formation in Appleton Field based on seismic interpretation (modified from Mancini *et al.*, 2000). (B) 3-D model showing the distribution of the reefal facies.

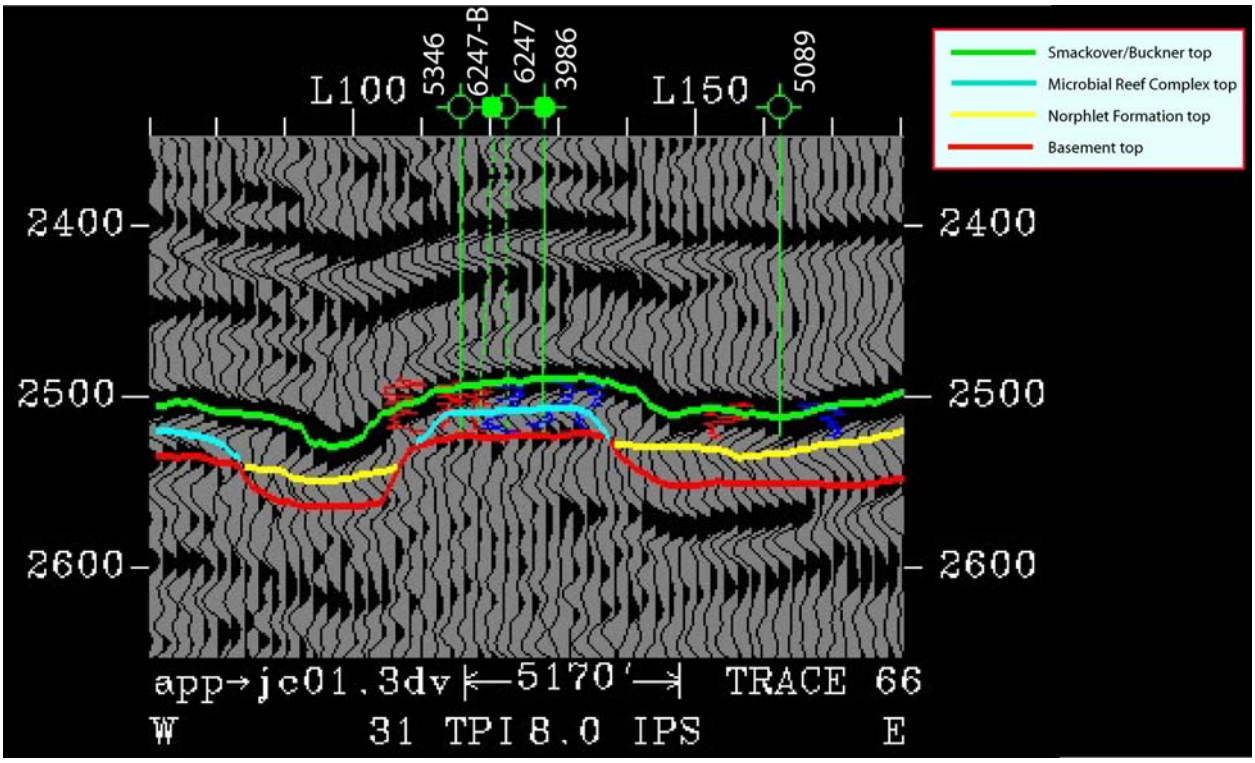

Figure 100: NW-SE interpreted seismic line showing two local basement paleohighs at Appleton Field (see Figure 12 for its location).

later progradational shoreface and tidal flat sediments of the upper Smackover Formation and evaporite deposits of the Buckner Anhydrite Member (Fig. 98). The change from a transgressive phase to a regressive phase occurred, like in Vocation field, when carbonate productivity and accumulation began to outpace the generation of accommodation space as a result of a decrease in the rate of sea level rise combined with variations in the environmental conditions that supported carbonate precipitation.

Conclusions

Smackover sediment accumulation and depositional facies distribution associated with basement paleohighs are part of a transgressive-regressive cycle controlled by the complex interaction of eustasy, subsidence, paleotopography, carbonate productivity and paleoenvironmental conditions.

The conceptual models for the basement ridge play cited in this paper are good first approximations as a general exploration strategy. However, it is necessary to look at each case individually in order to evaluate the possible impact of the variables mentioned above in the distribution and quality of the reservoirs.

Reservoir grade rocks within the Smackover Formation are controlled by the primary depositional texture of the rock despite the overprint of several diagenetic events. Main Smackover reservoirs rocks consist of doloboundstone associated with microbial reefal buildups and dolograinstone-dolopackstone that accumulated in shoal and shoreface environments. Extensive dolomitization led to the formation of sucrosic dolostone, which is a third type of reservoir in the updip basement ridge play.

The study of Vocation and Appleton fields showed the importance of 3-D seismic as a valuable tool in the basement ridge play for two main reasons. With the use of 3-D seismic

datasets, it is possible to accurately define the geometry of the basement structure, which controls depositional facies distribution and consequently the location of the reservoirs. The second reason is that the microbial reefal facies, which comprises high quality reservoir grade rocks, is seismically resolvable. Additionally, seismic data can be further utilized in multi-attribute studies to detect porous zones.

Vocation and Appleton field case studies are good examples to demonstrate the importance of the integration of well core and log data with 3-D seismic data for the interpretation of carbonate depositional facies distribution in association with basement paleohighs.

Task 10—Technology Transfer.--Researchers have presented papers on project results at the following meetings for this reporting period: 2003 AAPG meeting in Salt Lake City, Utah (Morgan and Ahr; Mancini, Parcell, Llinas; Llinas), 2002 GCAGS meeting in Austin, Texas (Llinas), 2002 GCS-SEPM Research Conference in Houston, Texas (Llinas), 2003 AAPG Eastern Section Meeting in Pittsburgh, Pennsylvania (Mancini), and 2003 International AAPG Conference in Barcelona, Spain (Mancini, Parcell, Llinas; Llinas).

Researchers have prepared a short course, Microbial Reef Characterization and Modeling: Reservoir Detection and Development, based on the results of this project to date for the 2003 International AAPG Conference in Barcelona, Spain. Mancini and Parcell prepared the short course notes. Because of lower enrollment for the course than expected, it was canceled.

The contents of the course are as follows: biology of microbial buildups, classification of microbial facies and growth forms, factors controlling microbial buildups and the modeling of these factors, microbial buildups in outcrops, conceptual models from outcrop studies, microbial buildups in the subsurface of the Gulf of Mexico, geophysical expression of microbial strata, case studies (Appleton and Vocation fields) of microbial reservoirs, diagenesis and petrophysical

properties of microbial facies, simulation of microbial reservoirs, conceptual models from subsurface studies, and exploration and development strategies for microbial facies and reservoirs. Instructors for the course were scheduled to be Mancini, Hart, Llinas, Parcell and Aurell.

Biology of Microbes

The following discussion on the biology of microbes was prepared for the short course.

The following discussion about the biology of microbes is from Kalkowsky (1908), Aitken (1967), Kennard and James (1986), Riding (1991), Leinfelder *et al.* (1993), Braga *et al.* (1995), Kruse *et al.* (1995), Monty (1995), Pratt (1995), Leinfelder *et al.* (1996), Decho (2000), Golubic *et al.* (2000), Knorre and Krumbein (2000), Merz-Preiss (2000), Riding and Awramik (2000), Seong-Joo *et al.* (2000), Stolz (2000), Mancini and Parcell (2001), Batten *et al.* (2002), Dupraz and Strasser (2002), Ginsburg (2002), and James and Narbonne (2002).

Microbes are abundant and widespread in sediments, carbonate and siliciclastic. They are microscopic and include bacteria, algae, fungi and protozoans. These organisms stabilize grains and provide for mineral nucleation, thus they modify and create sediment. They range in geologic age from the Proterozoic to today.

Microbites or microbialites are organosedimentary deposits that are the result of the activity of microbes. Microbes can stabilize loose sediment and microbial coatings on sediment surfaces protect the sediment from erosion. Microbes are prokaryotic cells, cells lacking a cell nucleus and specialized organelles such as mitochondria and plastids. Microbes include cyanobacteria (once called blue-green algae) that are photosynthetic. Other microbes are chemosynthetic and anaerobic heterotrophic. Microbes became diminished in the fossil record with the rise of eukaryotic cells. Eukaryotic cells are larger, have a membrane-bounded nucleus with genetic

material, utilize sexual reproduction and contain mitochondria and plastids. Most are multicellular and aerobic, thereby requiring free oxygen. Gastropods live and graze on microbial (stromatolite or algal) mats; therefore, it is assumed microbes thrived under abnormal marine conditions, oxygen depleted, high or low salinities or fluctuating nutrients. These conditions provided an ecological edge to microbial communities in niche competition with metazoans and eliminated metazoan grazing.

Microbial mats and biofilms consist of microbial communities, primarily prokaryotes but can include foraminifera that colonize a surface. There is interaction between the microbes, the colonized surface, and the surrounding environment. These microbial communities form laminated sedimentary structures referred to as stromatolites. Stromatolites are the result of the episodic trapping, binding and precipitation of sediment by the extracellular polymeric matrix produced by microbes. Lamination records temporal oscillations in microbial activities of sedimentation. Filamentous cyanobacteria and their responses to sedimentation typically characterize conditions of fluctuating sedimentation rates, while coccoid cyanobacteria colonize and stabilize sediments during periods of sedimentary stasis. Stromatolites are dominated by colonies of filamentous microbes, but clusters of microbes can also be present.

The microbial mats are considered complex biofilms. Biofilms consist of micro-organisms and their extracellular products that are bound to a solid surface. Biofilms differ from microbial mats in that they form on solid substrates such as rock. Beneath the surface layer of a microbial mat, a layer composed of cyanobacteria is found. This layer is where photosynthesis occurs. Underlying this layer, a transition to anoxic conditions occurs. Anoxygenic phototrophs occur in this layer. Heterogeneity is common within these distinct layers. Thus, a biofilm is viewed as a mass of microcolonies surrounded by a matrix of extracellular polymeric molecules (EPS) which

is honeycombed with water channels. The water channels and the associated convective flow facilitates nutrient delivery and waste removal.

Microbial structures characterized by a mesoscopic clotted internal fabric are called thrombolites. The clots are interpreted as primary features produced by calcified microbes. Thrombolites are interpreted as microcolonies of coccoid-dominated calcimicrobes such as *Girvanella* and *Renalcis*. The clotted fabric is primarily a microbial feature and not a disrupted or modified laminated fabric; however, the clotted fabric can be enhanced by physical damage in high-energy conditions and by bioerosion. Calcium carbonate precipitation can be facilitated by an increase in carbonate alkalinity. Increased carbonate alkalinity can be induced by microbes as a by-product of physiological activities. Cyanobacterial photosynthesis, thus, can promote carbonate precipitation of micrite. In situ, microbial calcification has been associated commonly with thrombolites, while agglutination of allochthonous grains has been associated with stromatolites. However, both organosedimentary deposits can be produced by either process. Sediment trapping can be accomplished by thrombolites and calcification can be achieved by stromatolites. Episodic sediment trapping has been shown to produce either fabric with an uneven pattern of accretion favoring a clotted fabric and an even pattern of accretion favoring a laminated fabric. Leiolites (microbial structureless or dense macrofabric) formed where a steady uniform supply of well-sorted sediment was provided to the area colonized by the microbes.

Microbial Classification

The following discussion on microbial classification was prepared for the short course.

Aitken (1967)

Aitken (1967) proposed a field classification for carbonates which included four types of cryptalgal biolithites, oncolites, stromatolites, thrombolites and cryptalgalaminates. Cryptalgal

was defined as sedimentary rocks or structures originating through sediment-binding and/or carbonate-precipitating activities of non-skeletal algae. He used the term thrombolite to describe cryptalgal structures related to stromatolites that lacked lamination but were characterized by a macroscopic clotted fabric.

Kennard and James (1986)

Kennard and James (1986) proposed a tripartite field classification of lower Paleozoic microbial structures based on the dominant type of constructive mesoscopic (centimeter to millimeter-size features visible with the naked eye or hand lens) constituent. The three end members are stromatolites, thrombolites and undifferentiated microbial boundstones. Microbial communities are commonly dominated by procaryotic cyanobacteria (formerly called cyanophytes or "blue-green algae"), rather than algae that are eucaryotic photosynthetic organisms.

Stromatolites of Kalkowsky (1908) are laminated organosedimentary structures built by episodic sediment-trapping, sediment-binding and/or carbonate-precipitating activity of microbial communities. The diagnostic component of stromatolites is the "stromatoid" or individual layers or laminae within stromatolites. Stromatoids (stromatolites) are constructed by laterally continuous, internally well-layered, mat-like microbial communities that are dominated by filamentous microbes.

Thrombolites lack lamination and are characterized by a mesoscopic clotted fabric. They have a distinct internal mesostructure consisting of millimeter and centimeter-size clots separated by patches of mud and sand-size sediment or calcite cement. The individual clots or mesoclots are typically dark in color and have a micritic, microcrystalline structure. They display a variety of shapes (subrounded, amoeboid, grape-like, arborescent, digitate, prostrate, pendent,

cerebral) and different spatial arrangements (isolated, interconnected, coalesced) and generally make up more than 40% of the thrombolite. Mesoclots have a complex internal structure consisting of the following microstructure types: lobate, cellular, microspherulotic, grumous, corpuscular, peloidal, vermiform, mottled, massive, variegated. The microstructures were attributed to in-situ calcification of coccoid or coccoid-dominated microbial communities (cyanobacteria) rather than sediment-trapping. Detrital particles (silt, sand, peloids, ooids, bioclastic debris) are absent or sparse in the mesoclots. The unbound-sediment pockets between the mesoclots are composed of detrital particles. The mesoclots and interstitial unbound-sediment pockets may be extensively burrowed and/or bored.

The mesoclots are the diagnostic constituent of thrombolites and represent discrete colonies or growth forms of calcified coccoid or coccoid-dominated microbial communities. The penecontemporaneous growth and calcification of the microbes resulted in the construction of a rigid framework of variable architecture and significant microrelief (several millimeters or greater), between which unbound detrital particles accumulated. An abundant and diverse skeletal and/or soft-bodied metazoan fauna are commonly associated with the thrombolites resulting in a complex microbial-metazoan community. Laminoid fenestrae generally are not found within thrombolites, they can be prevalent in stromatolites. Tubular voids generated by burrowing/boring and irregular cavities occur in thrombolites.

Thrombolites commonly grade vertically and laterally to stromatolite caps. Stromatolites can grade vertically into thrombolites.

Cryptomicrobial (crytalgal of Aitken, 1967) fabrics are poorly differentiated. They are mottled, patchy or vague sediment fabrics that are attributable to constructional microbial activities, but their architecture has been obscured by other organic or inorganic processes.

Disruptive processes include: oxidation and bacterial decay of the microbial community producing nonlaminated massive sediments or irregular voids that are subsequently filled to form patches of detrital sediment or carbonate cement; bioturbation of the microbial community and associated trapped and precipitated sediments; dehydration, desiccation, compaction and/or displacive growth of diagenetic minerals; and late diagenetic processes (neomorphism, solution, stylolitization, dolomitization and silicification). Thrombolites which are constructed by calcified microbial communities are probably less susceptible to disruption by other organisms than are non-calcified stromatote-forming communities.

In this classification, structures composed mainly of mesoclots are designated thrombolites, and structures composed mainly of stromatoids are stromatolites. Structures composed of a combination of stromatoids and mesoclots are designated stromatolitic thrombolites if the mesoclots are most abundant.

Braga, Martin and Riding (1995)

Braga *et al.* (1995) used a classification of laminated (stromatolite), clotted (thrombolite) and structureless and dense (leiolite) to describe the macrofabric of late Miocene microbial biostromes and bioherms. Stromatolitic lamination can form by regular espisodic accretion, involving particle trapping, microbial growth and/or precipitation. The lamination is recognized as a primary feature. Thrombolites can form by microbial calcification and/or agglutination of particles. The clots of the thrombolites can be primary features produced by calcified microbes or they can be a result of an alteration or disturbance of stromatolite fabrics. Both stromatolites and thrombolites in the late Miocene were basically created by similar combined processes of agglutination of sediment grains together with microbial calcification. Both also can be

subdivided into distinct, crude and diffuse varieties depending on the degree of development of the fabric (variations in microfabric components and their relative abundance).

Schmid (1996)

Schmid (1996) recognized three basic fabrics of microbolites. Schmid (1996) uses the term microbiolite rather than microbialite as per the recommendation of Riding (1991). The fabrics include thrombolites (clotted), stromatolites (laminated) and leiolites (unstructured). Using these basic fabric types, a tripartite classification of Upper Jurassic microbolites at the microscopic scale (millimeters) based on the end members of peloidal microstructure, laminated particle microstructure and dense microstructure was proposed. He recognized thrombolites that were layered. He published a compilation of growth forms at the macroscopic scale (centimeters to kilometers), which included bioherms, patch reefs, conical patch reefs, biostromes, isolated crusts, and oncoids, and at the mesoscopic scale (centimeters), which included massive, columnar, dendroid, flat, platy, reticulate, hemispheroid, and basal cover crust.

Parcell (2000)

Parcell (2000) used a classification of microbial fabrics to study Upper Jurassic microbiolites in the subsurface. He used the following end members, thrombolite, stromatolite and leiolite. He used a microbial growth form classification at the centimeter scale to recognize five dominant growth forms: laminated (layered) thrombolite, reticulate/chaotic thrombolite, dendritic thrombolite, encrusting stromatolite and oncoidal cortexes. The laminated (layered) thrombolites are characterized by dark-colored, horizontal microbial laminae with abundant crypts (millimeter to centimeter scale) and are bioturbated. The reticulate/chaotic and dendritic thrombolites have a vertical growth component (stronger in the dendritic form) and much interstitial sediment associated with these forms. The encrusting stromatolite form represents

essentially horizontal growth. Oncoids served as stable nucleation points for the development of the microbial oncoidal cortexes.

Badali (2002)

Badali (2002) differentiated Lower Cretaceous microbial deposits based on their microstructure. Microstructures utilized included peloidal-clotted, alveolar, laminated, micritic massive and micritic irregular. A sixth microstructure identified was related to the encrusting calcareous red alga, *Pseudolithotamnium album*. Mesostructures identified were oncolitic, patchy, micritic, micritic massive, and laminated. The term "micritic massive" was used to identify a mudstone-wackestone structure, and the term "micritic" was used to indicate a packstone-rudstone structure.

Outcrops from Spain

The outcrops of microbial buildups in Portugal and Spain were found to be the best analogs for the microbial buildups in the Gulf of Mexico. The following discussion on these outcrops was prepared for the short course.

The discussion on the outcrops from Spain is from the following publications: Fezer (1988), Leinfelder *et al.* (1993), Leinfelder *et al.* (1994), Nose (1995), Aurell and Badenas (1997), and Badenas (1999).

The Upper Jurassic (Kimmeridgian to Tithonian) outcrops of the Jabaloyas, Tormon and Arroyo Cerezo areas are located southeast of Teruel in northeast Spain. They occur in the west central part of the Iberian Chain. Reefs observed in these outcrops were developed in marginal areas of the Iberian Basin. Late Jurassic marine sedimentation in this basin occurred in a carbonate ramp setting. The carbonate ramp was open to the Tethys Sea to the east, but during major flooding episodes connection with the Boreal realm was possible.

The stratigraphic section for the area is as follows. The Upper Oxfordian to Lower Kimmeridgian Sot de Chera Formation is a marly unit which grades offshore into rhythmic bedded mudstone and marl of the Loriguilla Formation. The Kimmeridgian sandstones and oolitic grainstones of the Pozuel Formation prograde over these units. The Upper Kimmeridgian Torrecilla Formation, which contains reefal deposits, overlies the Pozuel Formation. The Torrecilla Formation attains a thickness of 72 m. To the west, the upper part of this formation is partly eroded and is unconformably overlain by Albian fluvial sandstones of the Utrillas Formation. The lower part of the Torrecilla Formation consists of marls and burrowed sandstones containing plant remains. These deposits probably accumulated in lagoonal environments. Two cyclic parasequences have been identified in this formation. The lower parasequence, including pinnacle reefs, is exposed in the Jabaloyas area.

The pinnacle reefs have a height/width ratio of approximately 1 and have very steep slopes, greater than 45 degrees. They can attain a thickness of 16 m. These coral-microbial and coral-bearing thrombolitic patch reefs occur as irregularly spaced, cylindrical to conical shaped buildups on a continuous ramp gradient of 15 km chiefly in proximal to distal middle carbonate ramp settings. The reef fabric consists of colonial corals (5-6%), microbial crusts (10-80%) and internal sediment (15-40%). Two types of internal cavities occur: cavities resulting from the growth of colonial corals and microbial crusts and cavities originating from bioerosion and boring. The internal sediment filling the cavities consists mostly of silty mudstones and wackestones. Bivalves, gastropods and echinoids are common in the reef facies. Essentially, the reefs can be classified as coral-microbial (where the coral percent is greater than the microbial content) and microbial (thrombolite) bearing corals (where the microbial content is greater than the reef macrofauna).

The coral reefs have been described as coral-chaetetid-stromatoporoid-microbial reefs. Solenoporarean algae and sponges are present. The corals include massive, hemispherical and branching forms. The dominant taxa are *Thamnasteria* and *Microsolena*.

The microbial crusts consist of a dense micrite to peloidal composition. The fabric is primarily clotted with a domal morphology. *Tubiphytes*, serpulids and bryozoans are common.

Associated reef facies include pre-reef and inter-reef (oncoidal, ooid, peloidal and bioclastic grainstone and packstone to skeletal wackestone, from proximal to distal areas) and post-reef (ooid and bioclastic grainstone and packstone in middle ramp areas). The facies distribution overall shows a retrogradational stacking pattern in the lower part of the section and a progradational stacking pattern in the upper part.

Reef growth is initiated on a cemented and encrusted surface (sediment starvation surface). Reef growth occurred chiefly during a time of sea-level rise. During sea level highstand conditions, the relative proportion of microbial crusts to corals decreased and the growth of the reef was diminished. Coral-microbial reefs are more common in the proximal portion of this middle ramp setting, while coral-bearing thrombolites of up to 12 m in height developed on the distal portion of this middle shelf setting.

Outcrops in Portugal

The discussion regarding outcrops in Portugal is from the following publications: Ramalho, 1988; Leinfelder, 1993; Leinfelder *et al.*, 1993; Leinfelder and Wilson, 1998; Mancini and Parcell, 2001.

The eastern part of the Algarve Basin of Portugal has been interpreted as the northern shelf of the western Tethyan Ocean. The western part of the Algarve Basin is a transition area between the Tethys shelf and the central Portuguese Lusitanian Basin, which is a marginal basin

associated with the opening of the North Atlantic Ocean. Tectonic events are as follows: Triassic to Callovian rifting and thermal subsidence, Middle Oxfordian to Early Berriasian ocean spreading, Valanginian to Early Aptian rifting, and Late Aptian to Campanian ocean spreading. Sedimentation in the Algarve and Lusitanian Basins began with an initial graben rift phase that resulted in the deposition of upper Triassic and lower Jurassic red beds, volcanics and evaporites. Shallow water and hemipelgic carbonates and muds accumulated in the early to middle Jurassic. The Callovian to Oxfordian transition is marked by a subaerial unconformity in these basins. Upper Jurassic sediments in the eastern part of the Algarve Basin and the central part of the Lusitanian Basin consist of mixed carbonate and siliciclastic shallowing upwards succession.

In the eastern Algarve Basin, a shallowing upward succession is developed. The Kimmeridgian Peral deposits (200 m) represent a shallowing upward alteration of ammonite-rich marls and bedded marly limestones. The Jordanna beds (20 to 160 m) include intraclastic and bioclastic grainstones, packstones and wackestones. The Cabeca deposits (150 to 200 m) consist of a reefal coral facies associated with bioclastic debris. The Tavira beds occur locally as detrital floatstones, rudstones and wackestones associated with brecciated boundstones. The Kimmeridgian Sa Romao deposits are a local unit of up to 400 m of coral rich shallow water ramp carbonates. These beds are similar lithologically to the Cabeca deposits.

At Rocha, Portugal, thrombolites with a thickness of 30 m occur between the Peral and Jordanna units. This microbial buildup (bioherm) is underlain by the marly to micritic Peral unit that contains abundant ammonites (transgressive systems tract deposits). The top of these beds (Peral) is characterized by a marly, encrusted limestone bed, rich in glauconite, bioclastic debris, and highly bioturbated with *Planolites* burrows (sediment starvation surface). Cauliflower and

pillow-type thrombolites containing glauconite constitute the majority of the buildup (highstand systems tract deposits). *Tubiphytes*, serpulids and siliceous sponges occur throughout the bioherm with an interval rich in cup-shaped dictyid sponges in the middle part of the bioherm section. Layered thrombolite is common in the middle and near the lower top of the section, reflecting changes in rates of sea-level rise and water energy. The bioherm encompasses an area of 7 km^2. Transgressive systems tract sponge spicule packstones and wackestones of the Jordanna beds overlie the microbial bioherm. Typically, the Jordanna deposits consist of intraclastic and bioclastic grainstones. The intraclasts include reworked thrombolitic limestones.

The stratigraphic succession in the central part of the Lusitanian Basin (Arruda Subbasin) is similar to the section in the eastern part of the Algarve Basin. Synsedimentary tectonics and sea-level fluctuations played a major role in the development of the stratigraphic succession in the overall shallowing upward section of the Arruda Subbasin. The Cabacos beds (middle Oxfordian) consist of 200 to 400 m of lacustrine to marginal marine carbonates. The Montejunto deposits (Middle to Upper Oxfordian) represent a succession of 400 to 1200 m of deeper water hemipelagic lime muds and shallow water bioclastic packstones, grainstones and coral patch reef boundstones. The Upper Oxfordian to Lower Kimmeridgian Abadia deposits are associated with a second rifting phase that resulted in siliciclastic sediments being deposited in the Lusitanian Basin. The Abadia beds (800 m) include clays and marls locally rich in ammonites. The Abadia section shallows upwards to microbial and coral limestones (Serra Isabel unit). The overlying Amaral beds consist of a lower unit of bioclastic wackestones and packstones and coral boundstones and an upper oolitic grainstone and packstone unit. Marine sandstones and marls occur in the upper unit. The Upper Kimmeridgian Sobral beds include prodelta and delta marls and clays.

In the Arruda area of the Arruda Subbasin, north of Arruda dos Vinhas, a condensed section (sediment starvation surface) in the Abadia beds is exposed at Serra Isabel. The Serra Isabel horizon occurs 30-40 m below the Abadia-Amaral contact. The Serra Isabel marly limestones and bindstones are up to 10 m thick and consist of a basal iron-stained, burrowed sediment starvation surface, which includes numerous steinkern of ammonites, gastropods and bivalves and encrusting bryozoans. This marly limestone is overlain by up to 7 m of thrombolite bindstone containing corals, siliceous sponges and *Tubiphytes*. Abadia marls locally rich in ammonites (transgressive systems tract) underlie the Serra Isabel unit, and Abadia marls, locally containing wood debris (early highstand systems tract) overlie the Serra Isabel unit. The Amaral beds, coral/microbial bafflestone and bioclastic wackestones/packstones with coral boundstones, and oolitic grainstones/packstones with sandstones, have been interpreted as late highstand systems tract deposits or as parts of two overlying depositional sequences.

Biology of Microbes

References

Aitken, J.D., 1967, Classification and environmental significance of cryptalgal limestones and dolomites, with illustrations from the Cambrian and Ordovician of southwestern Alberta: Journal of Sedimentary Petrology, v. 37, p. 1163-1178.

Batten, K.L., Narbonne, G.M., and James, N.P., 2002, Tonian microbial buildups and sea-level change: Neoproterozoic Little Dal Group, Northwest Territories, Canada: Abstracts with Programs, Geological Society of America Meeting, v. 34, no. 6, p. 65.

Braga, J.C., Martin, J.M., and Riding, R., 1995, Controls on microbial dome fabric development along a carbonate-siliciclastic shelf-basin transect, Miocene, SE Spain: Palaios, v. 10, p. 347-361.

Decho, A.W., 2000, Exopolymer microdomains as a structuring agent for heterogeneity within microbial biofilms, *in* Riding, R.R., and Awramik, S.M., eds., Microbial Sediments: Springer-Verlag, Berlin, p. 9-15.

Dupraz, C., and Strasser, A., 2002, Nutritional modes in coral-microbialite reefs (Jurassic, Oxfordian, Switzerland): evolution of trophic structure as a response to environmental change: Palaios, v. 17, p. 449-471.

Ginsburg, R.N., 2002, a compound Holocene stromatolite/thrombolite from the Bahamas: Abstracts with Programs, Geological Society of America Meeting, v. 34, no. 6, p. 491.

Golubic, S., Seong-Joo, L., and Browne, K.M., 2000, Cyanobacteria: architects of sedimentary structures, *in* Riding, R.R., and Awramik, S.M., eds., Microbial Sediments: Springer-Verlag, Berlin, p. 57-67.

James, N.P., and Narbonne, G.M., 2002, Proterozoic reef evolution: Abstracts with Programs, Geological Society of America Meeting, v. 34, no. 6, p. 64.

Kalkowsky, E., 1908, Oolith and stromatolith im norddeutschen Bundsandstein: Deutschen Geologischen Gesellschaft, v. 60, p. 68-125.

Kennard, J.M., and James, N.P., 1986, Thrombolites and stromatolites: two distinct types of microbial structure: Palaios, v. 1, p. 492-503.

Knorre, H.V., and Krumbein, W.E., 2000, Bacterial calcification, *in* Riding, R.R., and Awramik, S.M., eds., Microbial Sediments: Springer-Verlag, Berlin, p. 25-31.

Kruse, P.D., Zhuravlev, A.Y., and James, N.P., 1995, Primordial metazoan-calcimicrobial reefs: Tommotian (Early Cambrian) of the Siberian Platform: Palaios, v. 10, p. 291-321.

Leinfelder, R.R., Nose, M., Schmid, D.U., and Werner, W., 1993, Microbial crusts of the Late Jurassic: composition, paleoecological significance and importance in reef construction: Facies, v. 29, p. 195-230.

Leinfelder, R.R., Werner, W., Nose, M., Schmid, D.U., Krautter, M., Laternser, R., Takacs, M., and Hartman, D., 1996, Paleoecology, growth parameters and dynamics of coral, sponge and microbolite reefs from the Late Jurassic: Gottinger Arb. Geol. Palaont., Sb2, p. 227-248.

Mancini, E.A., and Parcell, W.C., 2001, Outcrop analogs for reservoir characterization and modeling of Smackover microbial reefs in the northeastern Gulf of Mexico area: Gulf Coast Association of Geological Societies Transactions, v. 51, p. 207-218.

Merz-Preiss, M., 2000, Calcification of cyanobacteria, *in* Riding, R.R., and Awramik, S.M., eds., Microbial Sediments: Springer-Verlag, Berlin, p. 50-56.

Monty, C.L.V., 1995, The rise and nature of carbonate mud-mounds: an introductory actualistic approach, *in* Monty, C.L.V., Bosence, D.W.J., Bridges, P.D., and Pratt, B.R., eds., Carbonate Mud-Mounds: Their Original Evolution: International Association Sedimentology Special Publication, v. 23, p. 11-48.

Pratt, B.R., 1995, The origin, biota and evolution of deep-water mud-mounds, in Monty, C.L.V., Bosence, D.W.J., Bridges, P.D., and Pratt, B.R., eds., Carbonate Mud-Mounds: Their Origin and Evolution: International Association Sedimentology Special Publication, v. 23, p. 49-123.

Riding, R., 1991, Classification of mirobial carbonates, *in* Riding, R., ed., Calcareous Algae and Stromatolites: Springer-Verlag, Berlin, p. 21-51.

Riding, R.R., and Awramik, S.M., 2000, Preface, *in* Riding, R.R., and Awramik, S.M., eds., Microbial Sediments: Springer-Verlag, Berlin.

Seong-Joo, L., Browne, K.M., and Golubic, S., 2000, On stromatolite lamination, *in* Riding, R.R., and Awramik, S.M., eds., Microbial Sediments: Springer-Verlag, Berlin, p. 16-24.

Stolz, J.F., 2000, Structure of microbial mats and biofilms, *in* Riding, R.R., and Awramik, S.M., eds., Microbial Sediments: Springer-Verlag, Berlin, p. 1-8.

Microbial Classification

References

Aitken, J.D., 1967, Classification and environmental significance of cryptalgal limestones and dolomites, with illustrations from the Cambrian and Ordovician of southwestern Alberta: Journal of Sedimentary Petrology, v. 37, p. 1163-1178.

Badali, M., 2002, Sequence and seismic stratigraphy of the Lower Cretaceous strata in the northeastern Gulf of Mexico area: Ph.D. dissertation, University of Alabama, Tuscaloosa, 214 p.

Braga, J.C., Martin, J.M., and Riding, R., 1995, Controls on microbial dome fabric development along a carbonate-siliciclastic shelf-basin transect, Miocene, SE Spain: Palaios, v. 10, p. 347-361.

Kalkowsky, E., 1908, Oolith and stromatolith im norddeutschen Bundsandstein: Deutschen Geologischen Gesellschaft, v. 60, p. 68-125.

Kennard, J.M., and James, N.P., 1986, Thrombolites and stromatolites: two distinct types of microbial structure: Palaios, v. 1, p. 492-503.

Parcell, W.c., 2000, Controls on the development and distribution of reefs and carbonate facies in the Late Jurassic (Oxfordian) of the eastern Gulf Coast, United States and eastern Paris Basin, France: Ph.D. dissertation, University of Alabama, Tuscaloosa, 226 p.

Riding, R., 1991, Classification of mirobial carbonates, *in* Riding, R., ed., Calcareous Algae and Stromatolites: Springer-Verlag, Berlin, p. 21-51.

Schmid, D.U., 1996, Marine mikrobolithe und mikroinkrustierer aus dem Oberjura: Profil, v. 9, p. 101-251.

Outcrops from Spain

References

Aurell, M., and Badenas, B., 1997, The pinnacle reefs of Jabaloyas (Late Kimmeridgian, NE Spain): vertical zonation and associated facies related to sea level changes: Cuadernos de Geologia Iberica, no. 22, p. 37-64.

Badenas, B., 1999, La sedimentacion en las rampas carbonatadas de Kimmeridgiense en las cuencas del este de la pleca Iberica: Ph.D. dissertation, University of Zaragoza, Zaragoza, Spain, 189 p.

Fezer, R., 1988, Die oberjurassische karbonatische regressionsfazies im sudwestlichen Keltiberikum zwischen Grigos und Aras de Alpuente (Prov. Teruel, Cuenca, Velencia; Spanien): Arb. Inst. Geol. Palaont., University of Stuttgart, 84, 119 p.

Leinfelder, R.R., Krautter, M., Laternser, R., Nose, M., Schmid, D., Scheigert, G., Werner, R., Rehfeld-Kiefer, U., Schroeder, R., Reinhold, C., Kock, R., Zeiss, A., Schweizer, V., Christmann, H., Menger, G., and Luterbacher, H., 1994, The origin of Jurassic reefs: Current research and development results: Facies, v. 31, p. 1-56.

Leinfelder, R.R., Nose, M., Schmid, D.U., and Werner, W., 1993, Microbial crusts of the Late Jurassic: composition, palaeoecological significance and importance in reef construction: Facies, v. 29, p. 195-230.

Nose, M., 1995, Vergleichende faziesanalyse und palokologie korallenreicher verflachungsabfolgen des iberischen objerjura: Profil 8, University of Stuttgart, 237 p.

Outcrops from Portugal

References

Leinfelder, R.R., 1993, A sequence stratigraphic approach to the Upper Jurassic mixed carbonate-siliciclastic succession of the central Lusitanian Basin, Portugal: Profil 5, p. 119-140.

Leinfelder, R.R., Krautter, M., Nose, M., Ramaho, M.M., and Werner, W., 1993, Siliceous sponge facies from the Upper Jurassic of Portugal: Neus Jahrbuch fur Geologie and Palaontologie, Abhandlugen 189, p. 199-254.

Leinfelder, R.R., and Wilson, R.C.L., 1998, Third-order sequences in an Upper Jurassic rift-related second order sequence, central Lusitanian Basin, Portugal, *in* de Graciansky, P-C., Hardenbol, J., Jacquin, T., and Vail, P.R., eds., Mesozoic and Cenozoic Sequence Stratigraphy of European Basins: SEPM Special Publication 60, p. 507-525.

Mancini, E.A., and Parcell, W.C., 2001, Outcrop analogs for reservoir characterization and modeling of Smackover microbial reefs in the northeastern Gulf of Mexico area: Gulf Coast Association of Geological Societies Transactions, v. 51, p. 207-218.

Ramalho, M., 1988, Sur la decouverte de biomermes stromatolithiques a spongiaires siliceux dans le Kimmeridgien de l'Algarve (Portugal): Communicoes dos Servicos Geologicos de Portugal, 74, p. 41-55.

Work Planned for Continued Year 3

Task 6—3-D Reservoir Simulation Model.--The simulation modeling of the reservoirs at Appleton and Vocation Fields will be refined by incorporating the geophysical data and interpretations of Tebo and Hart and the petrophysical data and interpretation of Morgan and Ahr.

Task 7—Geologic-Engineering Model.--The geologic-engineering model of the reservoirs of Appleton and Vocation Fields will be revised to include the results from the continuation of the simulation modeling of these reservoirs.

Task 8—Testing Geologic-Engineering Model.--The seismic data and well logs and core obtained from the drilling of a well northwest of Appleton Field will be examined with regard to reservoir facies, architecture, pore systems and petrophysical characteristics.

Task 9—Applying the Geologic-Engineering Model.--The geologic-engineering model will be used to evaluate the potential for new improved or enhanced oil recovery operations to implement in Appleton and/or Vocation Fields.

Task 10—Technology Transfer.--A technology workshop will be held at the conclusion of the project to transfer the project results to the petroleum industry. Technical presentations on the project results will be presented at professional meetings and conferences.

RESULTS AND DISCUSSION

3-D seismic attribute studies are useful for predicting the distribution of physical properties in the subsurface. Using a data set consisting primarily of digital logs and seismic data, it can be shown how correlations may be identified between seismic attributes and physical properties (porosity), and how those relationships may be exploited to predict the distribution of the property of interest in three dimensions. The results of these studies: a) provide quantitative, site-

specific 3-D models of physical properties that are of more use for applied studies than qualitative 2-D models commonly derived from facies modeling or sequence stratigraphic analysis, b) are generally more geologically reasonable than studies based on geostatistics alone, c) can provide sedimentary geologists with fundamental insights into depositional and/or diagenetic controls on the distribution of properties of interest, d) need to be rigorously evaluated by integrating other types of data and analyses, and e) are best thought of as supplementing, rather than replacing, conventional geologic analyses. The concepts and methods we illustrate may have application in various branches of sedimentary geology. The study of Appleton and Vocation Fields in Alabama focused on predicting the 3-D distribution of porosity in carbonates of the Upper Jurassic Smackover Formation using a probabilistic neural network and a combination of four attributes. The results suggest that porosity was best developed, and preserved, in thrombolite facies of a reef.

We have demonstrated the usefulness of seismic attribute studies for predicting porosity in reef and carbonate shoals associated with paleohighs. Specifically, we integrated 3-D seismic and wireline log data from two separate Smackover Fields (Appleton and Vocation) and generated porosity volumes for the Smackover Formation at each location. Data availability and quality play an important role in ensuring the success of an attribute study. In both cases, the short length of the digital logs available to us prevented us from generating adequate synthetic seismograms for all wells in the study area. Seismic data quality was also a problem in at least parts of both study areas. We used various techniques for generating porosity volumes, including multivariate linear regression (MLR), probabilistic neural networks (PNN) and a multi-layer feed-forward network (MLFN). Each of these methods provided a solution that was different, to a variable degree, from the other methods. As a general rule, neural networks provided better

solutions than the MLR because the former were better able to capture non-linear relationships between attributes and physical properties. A trend cascaded probabilistic neural network gave better results at Vocation Field than other types of neural networks or MLR. The option of using a trend cascaded PNN was not available during the analyses of Appleton Field. Given the differences in the predictions of each method, the results emphasize the importance of evaluating the results of an attribute study from a geological perspective. In so doing, the reservoir characterization team uses geologic judgment to assess the results of the attribute study. At the same time, the team can gain insights into the controls on the distribution of physical properties that may not be otherwise obtainable. Porosity at Appleton and Vocation Fields appears to be primarily related to depositional facies. In particular, the results suggest that the thrombolite reef facies is associated with the best porosity, and best production, in the porosity volumes. At Vocation Field, an observed relationship between porosity and faulting suggests that the faults may have acted as conduits for the movement of dolomitizing fluids. The results suggest that similar studies could provide important results in other carbonate or clastic reservoirs, thus helping producers to maximize production.

Flow units in the Smackover Formation at Vocation and Appleton Fields were identified, mapped, and ranked. Pore categories by origin, pore and pore throat geometries, pore-scale diagenetic history, and core-scale depositional attributes were logged using conventional petrographic and lithological methods and advanced techniques. Resulting data were combined with core descriptions, mercury-injection capillary pressure data, and wireline log data to produce flow unit maps at the field scale. Appleton and Vocation Fields produce from grainstone buildups and microbial reefs. Specific microbial fabrics were found to have significant influence on pore facies and flow unit quality rankings and ultimately on reservoir quality in these fields.

Microbial reefs are composed of five fabric categories and growth forms that reflect variations in water geochemistry, energy level, sedimentation rate and substrate type. They include Type I layered thrombolite with characteristic mm/cm-scale crypts, Type II reticulate and "chaotic" thrombolite, Type III dendroidal thrombolite, Type IV isolated stromatolitic crusts, and Type V oncoidal packstone/grainstone dominated by oncoids that grew on soft to firm substrates in high-energy conditions. Types I, II and III buildups are the most productive reservoirs. Of these, Type III thrombolite buildups contain the highest quality reservoir rocks, which consist of extensively dolomitized dendroidal fabrics that have well-connected intercrystalline dolomite and vuggy porosity. Types IV and V microbialites make poor reservoir rocks because Type IV fabrics are not conducive for communication throughout this facies, and Type V oncoidal facies exhibit isolated moldic and vuggy porosity with low to moderate permeability.

The first discovery of oil in Smackover carbonate sediments deposited over a pre-Jurassic basement high in southwest Alabama was Toxey field in 1967, located in Choctaw County. Since then, the search for similar fields has become an important exploratory objective. The result is that more than 40 Smackover oil fields have been discovered to date along the updip basement ridge play as defined by Mancini *et al.* (1991). Reservoir grade rocks in these fields have been identified in microbial buildups and shoal/shoreface facies. Nonetheless, characterization of reservoirs in shallow marine carbonate settings is difficult, because of their high susceptibility to the complex interaction of biological, chemical and physical processes. The geometry and irregular topography of the paleohighs on which the Smackover was deposited contribute to complicate the prediction of the distribution and heterogeneity of the reservoir facies. Kerans and Tinker (1997) suggest that depositional topography is the most important variable controlling the nature of the rock record in a shallow marine carbonate setting. Greater

depositional topography results in more lithofacies variability, greater reservoir heterogeneity, and increased difficulty in correlating between wells at any spacing (Kerans and Tinker, 1997). The objective of this work has been to illustrate with examples from the Vocation and Appleton fields the distribution of the depositional/reservoir facies found in the Smackover Formation, and to identify the diverse factors controlling the occurrence of reservoir facies in this particular shallow marine setting. In addition, the importance of integrating geological and geophysical data with geologic concepts in order to improve the knowledge of the dynamics and resulting fabric of Smackover facies associated with basement paleohighs will be shown.

CONCLUSIONS

The University of Alabama in cooperation with Texas A&M University, McGill University, Longleaf Energy Group, Strago Petroleum Corporation, and Paramount Petroleum Company are undertaking an integrated, interdisciplinary geoscientific and engineering research project. The project is designed to characterize and model reservoir architecture, pore systems and rock-fluid interactions at the pore to field scale in Upper Jurassic Smackover reef and carbonate shoal reservoirs associated with varying degrees of relief on pre-Mesozoic basement paleohighs in the northeastern Gulf of Mexico. The project effort includes the prediction of fluid flow in carbonate reservoirs through reservoir simulation modeling which utilizes geologic reservoir characterization and modeling and the prediction of carbonate reservoir architecture, heterogeneity and quality through seismic imaging.

The primary objective of the project is to increase the profitability, producibility and efficiency of recovery of oil from existing and undiscovered Upper Jurassic fields characterized by reef and carbonate shoals associated with pre-Mesozoic basement paleohighs.

The principal research effort for Year 3 of the project has been reservoir characterization, 3-D modeling, testing of the geologic-engineering model, and technology transfer. This effort has included six tasks: 1) study of seismic attributes, 2) petrophysical characterization, 3) data integration, 4) building the geologic-engineering model, 5) the testing of the geologic-engineering model, and 6) technology transfer.

Progress on the project is as follows: Geoscientific reservoir characterization is completed. The architecture, porosity types and heterogeneity of the reef and shoal reservoirs at Appleton and Vocation Fields have been characterized using geological and geophysical data. All available whole cores have been described and thin sections from these cores have been studied. Depositional facies were determined from the core descriptions and well logs. The thin sections studied represent the depositional facies identified. The core data and well log signatures have been integrated and calibrated on graphic logs. The well log and seismic data have been tied through the generation of synthetic seismograms. The well log, core, and seismic data have been entered into a digital database. Structural maps on top of the basement, reef, and Smackover/Buckner have been constructed. An isopach map of the Smackover interval has been prepared, and thickness maps of the Smackover facies have been prepared. Cross sections have been constructed to illustrate facies changes across these fields. Maps have been prepared using the 3-D seismic data that Longleaf and Strago contributed to the project to illustrate the structural configuration of the basement surface, the reef surface, and Buckner/Smackover surface. Seismic forward modeling and attribute-based characterization has been completed for Appleton and Vocation Fields. Petrographic analysis has been completed and a paragenetic sequence for the Smackover in these fields has been prepared.

The study of rock-fluid interactions is completed. Thin sections (379) have been studied from 11 cores from Appleton Field to determine the impact of cementation, compaction, dolomitization, dissolution and neomorphism has had on the reef and shoal reservoirs in this field. Thin sections (237) have been studied from 11 cores from Vocation Field to determine the paragenetic sequence for the reservoir lithologies in this field. An additional 73 thin sections have been prepared and studied for the shoal and reef lithofacies in Vocation Field to identify the diagenetic processes that played a significant role in the development of the pore systems in the reservoirs at Vocation Field. The petrographic analysis and pore system studies have been completed. A paragenetic sequence for the Smackover carbonates at Appleton and Vocation Fields has been prepared.

Petrophysical and engineering property characterization is completed. Petrophysical and engineering property data have been gathered and tabulated for Appleton and Vocation Fields. These data include oil, gas and water production, fluid property (PVT) analyses and porosity and permeability information. Porosity and permeability characteristics of Smackover facies have been analyzed for each well using porosity histograms, permeability histograms and porosity versus depth plots. Log porosity versus core porosity and porosity versus permeability cross plots for wells in the fields have been prepared.

Well performance studies through type curve and decline curve analyses have been completed for the wells in Appleton and Vocation Fields, and the original oil in place and recoverable oil remaining for the fields has been calculated.

3-D geologic modeling of the structure and reservoirs at Appleton and Vocation Fields has been completed. The models represent an integration of geological, petrophysical and seismic data.

3-D reservoir simulations of the reservoirs at Appleton and Vocation Fields have been completed. The 3-D geologic models served as framework for these simulations.

Data integration is up to date, in that, geological, geophysical, petrophysical and engineering data collected to date for Appleton and Vocation Fields have been compiled into a fieldwide digital database for development of the geologic-engineering model for the reef and carbonate shoal reservoirs for each of these fields.

The geologic-engineering models of the Appleton and Vocation Field reservoirs have been developed. These models are being tested. The geophysical interpretation for the paleotopographic feature being tested has been made, and the study of the data resulting from the drilling of a well on this paleohigh is in progress.

Numerous presentations on reservoir characterization and modeling at Appleton and Vocation Fields have been made at professional meetings and conferences and a short course on microbial reservoir characterization and modeling based on these fields has been prepared.

REFERENCES

Ahr, W.M., 1973, The carbonate ramp: an alternative to the shelf model: Gulf Coast Association of Geological Societies Transactions, v. 23, p. 221-225.

Ahr, W.M., and Hammel, B., 1999, Identification and mapping of flow units in carbonate reservoirs: an example from Happy Spraberry (Permian) field, Garza County, Texas USA: Energy Exploration and Exploitation, v. 17, p. 311-334.

Baria, L.R., Stoudt, D.L., Harris, P.M., and Crevello, P.D., 1982, Upper Jurassic reefs of Smackover Formation, United States, Gulf Coast: American Association of Petroleum Geologists Bulletin, v. 66, p. 1449-1482.

Benson, D.J., 1985, Diagenetic controls on reservoir development and quality, Smackover Formation of southwest Alabama: Gulf Coast Association of Geological Societies Transactions, v. 35, p. 317-326.

Benson, D.J., 1988, Depositional history of the Smackover Formation in southwest Alabama: Gulf Coast Association of Geological Societies Transactions, v. 38, p. 197-205.

Benson, D.J., Mancini, E.A., Groshong, R.H., Fang, J.H, Pultz, L.M., and Carlson, E.S., 1997, Petroleum Geology of Appleton Field, Escambia County, Alabama: Transactions, Gulf Coast Association of Geological Societies, v. 47, p. 35-42.

Benson, D.J., Markland, L.A., and Powers, T.H., 1991, Paleotopographic control on Smackover reservoir evolution: southwest Alabama. (Abstract): American Association of Petroleum Geologists, v. 75, p. 540-541.

Benson, D.J., Pultz, L.M., and Bruner, D.D., 1996, The influence of paleotopography, sea level fluctuation, and carbonate productivity on deposition of the Smackover and Buckner Formations, Appleton Field, Escambia County, Alabama: Gulf Coast Association of Geological Societies Transactions, v. 46, p. 15-23.

Brown, A.R., 1996, Interpretation of Three-Dimensional Seismic Data, 4th ed.: American Association of Petroleum Geologists Memoir 42, 424p.

Carr, M., Cooper, R., Smith, M., Taner, M.T., and Taylor, G., 2001, The generation of rock and fluid properties volume via the integration of multiple seismic attributes and log data: First Break, v. 19, no. 10, p. 567-571.

Chen, Q., and Sidney, S., 1997, Seismic attribute technology for reservoir forecasting and monitoring: The Leading Edge, v. 16, no. 5, p 445-456.

Dubrule, O., 1998, Geostatistics in petroleum Geology: American Association of Petroleum Geologists Continuing Education Course Note Series, no. 38, 52p.

Gastaldi, C., Biguenet, J-P., and DePazzis, L., 1997, Reservoir characterization from seismic attributes: An example from the Peciko Field (Indonesia): The Leading Edge, v. 16, no. 3, p. 263-266.

Hampson, B., Schuelke, J. and Quirein, J., 2001, Use of Multi-attribute Transforms to Predict Log Properties from Seismic data: Geophysics, v. 66, no. 1, p. 3-46.

Hart, B.S., 1999, Geology plays key role in seismic attribute studies: Oil & Gas Journal, p. 76-80.

Hart, B.S., 2000, 3-D seismic interpretation: A primer for geologists. SEPM Short Course Notes #48, Tulsa, OK, 124p.

Hart, B.S., 2002, Validating seismic attribute studies: Beyond statistics: The Leading Edge, 21, no. 10, p. 1016-1021.

Hart, B.S., and Balch, R.S., 2000, Approaches to defining reservoir physical properties from 3-D seismic attributes with limited well control: an example of the Jurassic Smackover Formation, Alabama: Geophysics, v.65, p.368-376.

Haywick, W.D., Brown, M.B., and Pfeiffer, L., 2000, Smackover Reservoir diagenesis in the Appleton Field, Escambia County, Alabama (Extended Abstract): American Association of Petroleum Geologists Bulletin, v. 84, no. 10, p. 1680.

Hirsche, K., Boerner, S., Kalkomey, C., and Gastaldi, C., 1998, Avoiding pitfalls in geostatistical reservoir characterization: A survival guide: The Leading Edge, v. 17, no. 4, p. 493-504.

Jansa, L.F., Pratt, B.R., and Dromart, G., 1989, Deepwater thrombolite mounds from Upper Jurassic of Offshore Nova Scotia, *in* Geldsetzer, H.H., James, N.P., and Febbutt, G.E. (eds.),

Reefs, Canada and Adjacent Areas: Canadian Society of Petroleum Geologists Memoir, no. 13, 1989, p. 725-735.

Kalkomey, C.T., 1997, Potential risks when using seismic attributes as predictors of reservoir properties: The Leading Edge, v. 16, no. 3, p. 247-251.

Kerans, C., and Tinker, S.W., 1997, Sequence stratigraphy and characterization of carbonate reservoirs: SEPM Short Course No. 40, 130 p.

Kopaska-Merkel, D.C., Mann, S.D., and Schmoker, J.W., 1994, Controls on reservoir development in a shelf carbonate: Upper Jurassic Smackover Formation of Alabama: American Association of Petroleum Geologists Bulletin, v. 78, no. 6, p. 938-959.

Leinfelder, R.R., 1993, Upper Jurassic reef types and controlling factors: A preliminary report: Profil 5, p. 1-45.

Leinfelder, R.R., Werner, W., Nose, M., Schmid, D.U., Krautter, M., Laternser, R., Takacs, M., and Hartmenn, D., 1996, Paleoecology, Growth Parameters and Dynamics of Coral, Sponge and Microbolites Reefs from the Late Jurassic, *in* Reitner, J., Neuweiler, F., and Gunkel, F. (eds.), Global and Regional Controls on Biogenic Sedimentation. I. Reef Evolution: Research Reports - Göttinger Arb. Geol. Paläont., SB2, p., 227-248, Göttingen.

Leiphart, D.J., and Hart, B.S., 2001, Comparison of linear regression and probabilistic neural network to predict porosity from 3-D seismic attributes in Lower Brushy Canyon channeled sandstones, southeast New Mexico: Geophysics, v. 66, no. 5, p. 1349-1358.

Llinás, J.C., 2002a, Diagenetic history of the Upper Jurassic Smackover Formation and its affect on reservoir properties. Vocation Field, Manila Sub-basin, Eastern Gulf Coastal Plain: Gulf Coast Association of Geological Societies Transactions, v. 52, p.631-644.

Llinás, J.C., 2002b, Carbonate sequence stratigraphy. Influence of paleotopography, eustasy, and tectonic subsidence: Upper Jurassic Smackover Formation, Vocation field, Manila Sub-basin (Eastern Gulf Coastal Plain): Sequence Stratigraphic Models for Exploration and Production: Evolving Methodology, Emerging Models and Application Histories. 22nd Annual Gulf Coast Section SEPM Foundation Bob F. Perkins Research Conference, p. 383-401.

Mancini, E.A. 2002, Integrated geologic-engineering model for reef and carbonate shoal reservoirs associated with paleohighs: upper Jurassic Smackover Formation, NE Gulf of Mexico: Annual Report Year 2. Online Report retrieved Oct. 3, 2002, from Petroleum Technology Transfer Council Web site: http://egrpttc.geo.ua.edu/reports/geo_eng _model2/title.html.

Mancini, Ernest A., Badali, M., Puckett, T.M., Parcell, W.C., and Llinas, J.C., 2001, Mesozoic carbonate petroleum systems in the northeastern Gulf of Mexico, Petroleum Systems of Deep-Water Basins: Global and Gulf of Mexico Experience, Proceedings of the 21st Annual Research Conference, Gulf Coast Section, SEPM Foundation, p. 423-451.

Mancini, E.A., and Benson, D.J., 1998, Upper Jurassic Smackover carbonate reservoir, Appleton Field, Escambia County, Alabama: 3-D seismic case history, 3-D Case Histories of the Gulf of Mexico, p. 1-14.

Mancini, Ernest A., Benson, D.J., Hart, B.S., Balch, R.S., Parcell, W.C., and Panetta, B.J., 2000, Appleton field case study (eastern Gulf Coastal Plain): field development model for Upper Jurassic microbial reef reservoirs associated with paleotopographic basement structures: American Association of Petroleum Geologists Bulletin, v.84, no. 11, p.1699-1717.

Mancini, Ernest A., Benson, D. Joe, Hart, Bruce S., Chen, Hannah, Balch, Robert S., Parcell, William C., Yang, Wen-Tai, and Panetta, Brian J., 1999, Integrated geological, geophysical and computer modeling approach for predicting reef lithofacies and reservoirs: Upper Jurassic Smackover Formation, Appleton Field, Alabama, Advanced Reservoir Characterization for the Twenty-First Century, Proceedings of the 19th Annual Research Conference, Gulf Coast Section, SEPM Foundation, p. 235-247.

Mancini, E.A., Hart, B.S., Chen, H., Balch, R.S., Parcell, W.C., Wang, W., and Panetta, B.J., 1999, Integrated geological, geophysical, and computer approach for predicting reef lithofacies and reservoirs: Upper Jurassic Smackover Formation, Appleton Field, Alabama. GCS-SEPM Foundation 19th Annual Research Conference: Advanced Reservoir Characterization. December 5-8, 1999, p. 235-247.

Mancini, E.A., Mink, R.M., Tew, B.H., Kopaska-Merkel, D.C., and Mann, S.D., 1991, Upper Jurassic Smackover oil plays in Alabama, Mississippi and the Florida panhandle: Gulf Coast Association of Geological Societies Transactions, v. 41, p. 475-480.

Mancini, Ernest A., and Panetta, B.J., 2002, Reservoir characterization and modeling of Upper Jurassic Smackover carbonate shoal complex reservoirs, Womack Hill oil field, Choctaw and Clarke Counties, Alabama: Gulf Coast Association of Geological Societies Transactions, v. 52 (in press).

Mancini, Ernest A., and Parcell, W.C., 2001, Outcrop analogs for reservoir characterization and modeling of Smackover microbial reefs in the northeastern Gulf of Mexico area: Gulf Coast Association of Geological Societies Transactions, v. 51, p. 207-228.

Mancini, E.A., Parcell, W.C., Benson, D.J., Chen, H., and Yang, W.T., 1998, Geological and computer modeling of Upper Jurassic Smackover reef and carbonate shoal lithofacies,

Eastern Gulf Coastal Plain: Gulf Coast Association of Geological Societies Transactions, v. 48, p. 225-233.

Mancini, Ernest A., Puckett, T.M., and Parcell, W.C. (eds.), 2000, Carbonate Reservoir Characterization and Modeling for Enhanced Hydrocarbon Discovery and Recovery, AAPG/EAGE International Research Conference, Program and Abstracts Volume, 68 p.

Mancini, E.A., Tew, B.H., and Mink, R.M., 1990, Jurassic sequence stratigraphy in the Mississippi Interior Salt Basin: Gulf Coast Association of Geological Societies Transactions, v. 40, p. 521-529.

Marhaendrajana, T., and Blasingame, T.A., 1997, Rigorous and semi-rigorous approaches for the evaluation of average reservoir pressure from pressure transient tests: Paper 38725 presented at the 1997 Annual SPE Technical Conference and Exhibition, San Antonio, TX, October 6-8.

Markland, L.A., 1992, Depositional history of the Smackover Formation, Appleton field, Escambia County, Alabama: unpublished Masters Thesis, The University of Alabama, 145 p.

Masters, T., 1994, Signal and image processing with neural networks: John Wiley and Sons (publ.)

Mukerji, T., Avseth, P., Mavko, G., Takahashi, I., and Goree, W.S., 2001, Statistical rock physics: Combining rock physics, information theory, and Geostatistics to reduce uncertainty in seismic reservoir characterization: The Leading Edge, v., 20, no. 3, p. 313-319.

Parcell, W.C., 2000, Controls on the development and distribution of reefs and carbonate facies in the Late Jurassic (Oxfordian) of the eastern Gulf Coast, United States and eastern Paris Basin, France (PhD Thesis): University of Alabama. 226p.

Partyka, G., Gridley, J. and Lopez, J., 1999, Interpretational applications of spectral decomposition in reservoir characterization: The Leading Edge, v. 18, no. 3, 353-360.

Pearson, R.A., and Hart, B.S., *in press*, 3-D seismic attributes help define controls on reservoir development: case study from the Red River Formation, Williston Basin. *In:* G.P. Eberli, J.L. Masaferro, and J.F. Sarg (eds.), Seismic Imaging of Carbonate Reservoirs and Systems: American Association of Petroleum Geologists Memoir.

Petyon, L., Bottjer, R. and Partyka, G., 1998, Interpretation of incised valleys using new 3-D seismic techniques: A case history using spectral decomposition and coherency: The Leading Edge, v. 17, no. 9, 1294-1298.

Powers, T.J., 1990, Structural and depositional controls on petroleum occurrence in the Upper Jurassic Smackover Formation, Vocation Field, Monroe County, Alabama: Tuscaloosa, Alabama, University of Alabama, Masters Thesis, 171p.

Prather, B.E., 1992, Origin of dolostone reservoir rocks, Smackover Formation (Oxfordian), Northeastern Gulf Coast, U.S.A: American Association of Petroleum Geologists Bulletin, v. 76, no. 2, p. 133-163.

Pratt, B.R., 1995, The origin, biota, and evolution of deep-water mud-mounds, *in* Monty, C.L.V., Bosence, D.W.J., Bridges, P.H., and Pratt, B.R. (eds.) Carbonate Mud Mounds: Their Origin and Evolution: International Association of Sedimentologists Special Publications, v. 23, p. 49-123.

Pratt, B.R., James, N.P., and Bourque, P., 1992, Reefs and Mounds, *in* Walker, R.G and N.P. James (eds.), Facies Models - Response to Sea Level Change: Geological Association of Canada, p. 323-348.

Raeuchle, S.K., Hamilton, D.S., and Uzcátegui, M., 1997, Case history: Integrating 3-D seismic mapping and seismic attribute analysis with genetic stratigraphy: Implications for infield reserve growth and field extension, Budare Field, Venezuela: Geophysics, v. 62, no. 5, p. 1510-1523.

Robertson, J.D., and Nogami, H.H., 1984, Complex seismic trace analysis of thin beds: Geophysics, v. 49, no. 4 (April 1984), p. 344-352.

Russell, B., Hampson, D., Schuelke, J., and Quirein, J., 1997, Multi-attribute Seismic Analysis: The Leading Edge, v. 16, no. 10, p. 1439-1443.

Saller, A.H., and Moore, B.R., 1986, Dolomitization in the Smackover Formation, Escambia County, Alabama: Transactions, Gulf Coast Association of Geological Societies, v. 36, p. 275-282.

Schultz, P.S, Ronen, S., Hattori, M., and Corbett, C., 1994a, Seismic-guided estimation of log properties: Part 1: A data-driven interpretation methodology: The Leading Edge, v. 13, no. 5, p. 305-315.

Schultz, P.S., Ronen, S., Hattori, M., and Corbett, C., 1994b, Seismic-guided estimation of log properties: Part 2: Using artificial neural networks for nonlinear attribute calibration: The Leading Edge, v. 13, no. 6, p. 674-678.

Taner, M.T., 2001, Seismic attributes: CSEG Recorder, September 2001, 49-56.

Taner, M.T., Koehler, F., and Sheriff, R.E., 1979, Complex seismic trace analysis: Geophysics, v. 44, no. 6 (June 1979), p. 1041-1063.

Tebo, J.M., 2003, Use of volume-based 3-D seismic attribute analysis to characterize physical property distribution: A case study to delineate reservoir heterogeneity at the Appleton Field, SW Alabama (M.Sc Thesis): McGill University, 181p.

Tew, B.H., Mink, R.M., Mancini, E.A., Mann, S.D., and Kopaska-Merkel, D.C., 1993, Geologic framework of the Jurassic (Oxfordian) Smackover Formation, Alabama and Panhandle Florida coastal waters area and adjacent federal waters area: Gulf Coast Association of Geological Societies Transactions, v. 43, p. 399-411.

Vail, P.R., Hardenbol, J., and Todd, M.G., 1984, Jurassic unconformities, chronostratigraphy and sea-level changes from seismic stratigraphy and biostratigraphy; in W.P.S. Ventress, D.G. Bebout, B.F. Perkins and C.H. Moore, eds., The Jurassic of the Gulf Rim: Proceedings of the Third Annual Research Conference Gulf Coast Section. Society of Economic Paleontologists and Mineralogists Foundation, p. 347-364.